AD_____

AWARD NUMBER DAMD17-93-V-3018

TITLE: Georgetown Institute for Cognitive and Computational Sciences

PRINCIPAL INVESTIGATOR: Dr. Robert S. Ledley

CONTRACTING ORGANIZATION: National Biomedical Research Foundation
Washington, DC 20007

REPORT DATE: November 1998

TYPE OF REPORT: Final

PREPARED FOR: U.S. Army Medical Research and Materiel Command
Fort Detrick, Maryland 21702-5012

DISTRIBUTION STATEMENT: Approved for public release;
distribution unlimited

The views, opinions and/or findings contained in this report are those of the author(s) and should not be construed as an official Department of the Army position, policy or decision unless so designated by other documentation.

DTIC QUALITY INSPECTED 3

REPORT DOCUMENTATION PAGE

Form Approved
OMB No. 0704-0188

Public reporting burden for this collection of information is estimated to average 1 hour per response, including the time for reviewing instructions, searching existing data sources, gathering and maintaining the data needed, and completing and reviewing the collection of information. Send comments regarding this burden estimate or any other aspect of this collection of information, including suggestions for reducing this burden, to Washington Headquarters Services, Directorate for Information Operations and Reports, 1215 Jefferson Davis Highway, Suite 1204, Arlington, VA 22202-4302, and to the Office of Management and Budget, Paperwork Reduction Project (0704-0188), Washington, DC 20503.

1. AGENCY USE ONLY *(Leave blank)*	2. REPORT DATE	3. REPORT TYPE AND DATES COVERED
	November 1998	Final (30 Sep 93 - 30 Sep 98)

4. TITLE AND SUBTITLE
Georgetown Institute for Cognitive and Computational Sciences

5. FUNDING NUMBERS
DAMD17-93-V-3018

6. AUTHOR(S)
Dr. Robert S. Ledley

7. PERFORMING ORGANIZATION NAME(S) AND ADDRESS(ES)
National Biomedical Research Foundation
Washington, DC 20007

8. PERFORMING ORGANIZATION REPORT NUMBER

9. SPONSORING / MONITORING AGENCY NAME(S) AND ADDRESS(ES)
U.S. Army Medical Research and Materiel Command
Fort Detrick, MD 21702-5012

10. SPONSORING / MONITORING AGENCY REPORT NUMBER

19990209 109

11. SUPPLEMENTARY NOTES

12a. DISTRIBUTION / AVAILABILITY STATEMENT
Approved for public release; distribution unlimited

12b. DISTRIBUTION CODE

13. ABSTRACT *(Maximum 200 words)*

GICCS is a multidisciplinary neuroscience research institute whose mission is to understand higher cognitive function—both under normal and pathological conditions. Its major focus areas are: higher auditory processing and language; brain injury and plasticity; computational neuroscience; and drug discovery.

GICCS faculty have continued to elucidate the complex mechanisms of higher auditory processing in experimental animals, from bats to primates. Parallel research in humans, using functional brain imaging and cognitive psychology, examines how the human brain deals with complex sounds, particularly those relating to speech. These studies address not only normal language processing but also examine disorders of speech/language, including developmental and acquired dyslexias.

Investigators also use tools from cellular/molecular neurobiology and from systems neuroscience to study plasticity after acute or chronic brain injury, as well as after early vision or hearing loss. This includes development of novel pharmacological strategies to limit brain damage and to enhance cognitive function after injury or neurodegeneration. Brain magnetic resonance techniques (including functional imaging) are also used. Computational methods are employed to model sensory processing based upon experimental studies. Predictions based upon mathematical modeling are evaluated in subsequent laboratory experiments.

14. SUBJECT TERMS
Visual cortex, Brain injury, Metabotropic glutamate receptors, Apoptosis, Caspases, Huperzine, Compensatory Plasticity, fMRI experiments, Dyslexia, Alzheimer's Disease, Language, Auditory processing, Neuroprotective drug development.

15. NUMBER OF PAGES
140

16. PRICE CODE

17. SECURITY CLASSIFICATION OF REPORT	18. SECURITY CLASSIFICATION OF THIS PAGE	19. SECURITY CLASSIFICATION OF ABSTRACT	20. LIMITATION OF ABSTRACT
Unclassified	Unclassified	Unclassified	Unlimited

FOREWORD

Opinions, interpretations, conclusions and recommendations are those of the author and are not necessarily endorsed by the U.S. Army.

N/A Where copyrighted material is quoted, permission has been obtained to use such material.

N/A Where material from documents designated for limited distribution is quoted, permission has been obtained to use the material.

✓ Citations of commercial organizations and trade names in this report do not constitute an official Department of Army endorsement or approval of the products or services of these organizations.

✓ In conducting research using animals, the investigator(s) adhered to the "Guide for the Care and Use of Laboratory Animals," prepared by the Committee on Care and use of Laboratory Animals of the Institute of Laboratory Resources, national Research Council (NIH Publication No. 86-23, Revised 1985).

✓ For the protection of human subjects, the investigator(s) adhered to policies of applicable Federal Law 45 CFR 46.

N/A In conducting research utilizing recombinant DNA technology, the investigator(s) adhered to current guidelines promulgated by the National Institutes of Health.

N/A In the conduct of research utilizing recombinant DNA, the investigator(s) adhered to the NIH Guidelines for Research Involving Recombinant DNA Molecules.

✓ In the conduct of research involving hazardous organisms, the investigator(s) adhered to the CDC-NIH Guide for Biosafety in Microbiological and Biomedical Laboratories.

Robert J Talley 1/26/99

PI - Signature Date

Cooperative Agreement No. DAMD17-93-V-3018

TABLE OF CONTENTS

INTRODUCTION

The Georgetown Institute for Cognitive and Computational Sciences (GICCS) is a neuroscience research institute whose mission is to understand higher cognitive function through interactive collaborative efforts among scientists using multidisciplinary investigative strategies. Its major focus areas are: higher auditory processing and language; brain injury and plasticity; computational neuroscience; and drug discovery.

GICCS faculty are working to elucidate the complex mechanisms of higher auditory processing. Species with specialized hearing, such as bats, are used as models for complex sound processing and compared to those using cats and primates, which also use acoustic signals as a primary means of communication. Parallel research in humans using functional brain imaging and cognitive psychology examine how the human brain deals with complex sounds, particularly those relating to speech. These studies address not only normal language processing but also examine disorders of speech/language, including developmental and acquired dyslexias. One goal is to develop treatments for these disorders through specialized training.

Understanding and modifying brain plasticity represents another major research area. Investigators use tools from cellular/molecular neurobiology and from systems neuroscience to study plasticity after acute or chronic brain injury as well as after early vision or hearing loss. This includes development of novel pharmacological strategies to limit brain damage and to enhance cognitive function after injury or neurodegeneration. Brain magnetic resonance techniques (including functional imaging) are also used, employing a high field (7T) animal research magnet as well as a human 1.5T magnet, to clarify mechanisms of tissue damage and plasticity and the response to targeted treatments. In addition to advanced brain imaging, computational neuroscience is an important experimental area that serves to integrate these multidisciplinary research efforts. Sophisticated computational methods are used to model sensory processing based upon experimental studies. Predictions based upon mathematical modeling are evaluated in subsequent laboratory experiments.

Together, the goal of this diverse but complementary research team is to better understand cognitive processes in order to address important clinical problems including deafness, language disorders, traumatic and ischemic brain injury, and Alzheimer's Disease.

Faculty include three at the professorial level, 1 associate professor, 12 assistant professors, 6 research associates, and 1 research instructor. A total of 26 postdoctoral fellows and 20 research technicians have also been recruited to date. The faculty are divided into 5 sections: cognitive neuroscience (human); cognitive neuroscience (animal); computational neuroscience; drug discovery and design; and molecular neurobiology and plasticity. There are numerous collaborative connections within and across these sections. For example, all members of the human cognitive group and several members of the animal cognitive group share a common interest in the use of magnetic resonance imaging technology to address fundamental questions. Magnetic resonance technology also links the animal cognitive group with the group in molecular biology and plasticity. The drug development and design group has extensive collaborations both within the Institute as well as involving other departments at the Medical Center. Additional projects have been funded through the Institute with other neuroscience faculty in areas of complementary interest. Research developments during the past year are divided into 5 parts, one relating to each institute section.

HUMAN COGNITIVE NEUROSCIENCE: There are five faculty members who are grouped into this area. Dr. Bavelier examines neural bases of visual cognition. Dr. Eden uses functional neuroimaging to study the pathophysiology of developmental dyslexia. Dr. Friedman examines the neuropsychology of language. Dr. Liu's research focuses on both the development and application of functional Magnetic Resonance Imaging (fMRI) of human brain. Dr. Ullman investigates neural bases of language and memory. In addition, Drs. Pekar and Rauschecker conduct research projects in Human Cognitive Neuroscience using fMRI.

DAPHNE BAVELIER, Ph.D.

Dr. Bavelier's research focuses on visual scene analysis and its underlying neural bases in humans. We use behavioral techniques to characterize the processing stages of visual analysis, and imaging techniques (functional magnetic resonance imaging (fMRI)) to investigate their neural implementation. With the support of the Otolaryngology department at Georgetown, we have been setting up a vision laboratory to test visual abilities of deaf individuals. We have also developed in collaboration with Dr. Liu, an assistant professor at Georgetown expert in fMRI, a series of fMRI experiments. Two independent but complementary lines of research have been supported by Institutional funds.

PROJECT 1. VISUAL FUNCTIONS IN NORMAL HUMAN ADULTS

Our present line of research focuses on the processes at play when viewing a complex visual scene. How do we find the phone when entering the cluttered office of a friend? We study the mechanisms responsible for directing our visual attention and selecting a few objects of interest amongst several irrelevant objects. In the last year, we have pursued our investigation of the negative consistency effect. This has led to a revision of the paper by Bavelier, Deruelle and Proksch and to a series of new experiments.

PROJECT 2. COMPENSATORY PLASTICITY IN VISUAL FUNCTIONS

Our broad goals are to characterize the role of altered sensory and language experience on the cerebral organization of visual functions by studying deaf individuals who acquire at birth American Sign Language, a visuo-spatial language. To separately assess the effects of deafness and ASL acquisition, we also study hearing individuals who are born to deaf parents and native signers.

The working hypothesis is that there is considerable variability in the degree to which different visual functions are modified by early experience. We have been testing the hypothesis that experience-dependent changes are (i) functionally specialized, i.e. they affect only certain aspects of visual processing such as visual attention, and (ii) limited to specific critical periods, i.e. the amount of compensatory plasticity observed in congenitally deaf individuals is expected to be greater than that observed in later deafened individuals.

Project 2A. Cerebral Organization for Visual Attention

While there is anecdotal evidence that the deaf 'see' better than the hearing, evidence supporting this claim is limited and controversial. Interestingly, most investigations have focused on the assessment of psychophysical thresholds neglecting higher visual functions such as visual attention/selection or object tracking. Since coming to Georgetown, we have directed our efforts to test the hypothesis that some aspects of these functions will be enhanced in congenitally deaf individuals using the fMRI technique.

fMRI EXPERIMENTS:

Experiment 1:

The goal of this experiment was to compare the neural basis of visual motion processing with and without attention in deaf, hearing and hearing native signers. 7 congenitally deaf subjects (from Gallaudet University), 5 hearing native signers and 7 hearing monolingual subjects.

Computer-generated flow fields were downloaded on a videotape, and displayed to the subject through an LCD projector. Subjects were lying on a patient bed viewing a translucent screen at their feet through the means of a mirror. In a first condition, subjects viewed passively an alternation of radially-moving dots and of static random dots. Attention was then manipulated by asking subjects to detect either luminance changes or velocity changes. To assess whether plastic changes are larger in the periphery than the fovea, for some conditions changes occurred only in the periphery while for others they occurred only in the fovea. The material and procedure are summarized in Figure 1.

Spin-echo-2D echo-planar images (TE=40 ms, Flip angle=90 degree) were obtained using a 1.5 SIEMENS Vision MR system fitted with a removeable head receive/transmitter coil. Twenty tilted axial slices were collected during each TR of 4 sec with an in plane resolution of 3.5x3.5 and slice thickness of 5 mm. Each experimental run consisted of 64 images per slice.

Behavior: Subjects accurately detected the changes in luminance or velocity indicating that they paid attention to the stimuli. fMRI: The SPM package was used for analysis

Deaf, hearing and hearing native signers showed similar patterns of activation when passively viewing the alternations of moving and static dots. However, in the attentional condition (monitor luminance or velocity changes), deaf subjects displayed larger activation in the brain areas devoted to motion processing and visual attention than hearing or hearing native signers (Figures 2 to 5) . These results suggested that deaf subjects can recruit more efficiently processing resources when attention is needed suggesting a more efficient attentional system. The finding that hearing native signers were similar to hearing suggest that this plastic changes in deaf subjects is due to early deafness rather than acquisition of American Sign Language. This experiment did not yield differences between fovea and periphery; also the pattern of activation were similar whether subjects were asked to monitor luminance or velocity changes. This experiment was presented at the 5th annual meeting of the Cognitive Neuroscience Society.

Experiments 2 and 3:

Experiment 1 has led us to design two new experiments to test the hypothesis that visual attention undergoes major plastic changes in deaf individuals.

In Experiment 2, we have replicated Experiment 1 but with a design better suited to compare the attention and no attention condition. The no attention condition did not always appear at the beginning of the experiment, but its order was randomized with the attentional conditions. Subjects were always asked to monitor luminance changes. In Experiment 3, we assess whether the attentional difference generalize to the processing of other kind of visual information or is specific to motion processing. Thus, subjects viewed either faces or objects with or without attention. As in Experiment 2, attention was manipulated by asking subjects to monitor luminance changes. Twelve deaf and hearing subjects have participated in these experiments so far. Their data will be presented at the 28th meeting of the Neuroscience Society.

Project 2B. Cerebral Organization for Visuo-Manual Languages such as American Sign Language

We have employed fMRI to compare the brain regions active during sentence processing in English and in ASL. We report that classical language areas within the left hemisphere are recruited by both English and ASL. This suggests a bias of the left hemisphere to process natural languages independently of the modality through which language is perceived. Furthermore, in contrast to English, ASL strongly recruited right hemisphere structures. This was true irrespective of whether the native signers were deaf or hearing. Thus, language modality appears to affect the cortical organization for language. These results show that the processing of fast acoustic transitions is not necessary for recruitment of the left hemisphere structures in the language system. In contrast, the left hemisphere invariance across languages is consistent with the view that grammatical recoding drives the left hemisphere specialization for language. The finding of a different right hemisphere recruitment for English and ASL raises the possibility that some aspects of language processing can also drive a right hemisphere specialization for language.

We have been developing a collaboration with Dr. Cohen (NIH), Dr. Braun (NIDCD) and Dr. Poeppel (U. of Maryland) to test the recruitment of the right hemisphere in ASL using the TMS technique (Transcranial Magnetic Stimulation). The first phase of this study is being carried at NIH.

We are studying the cerebral organization for spoken English. We are investigating the impact of viewing the speaker on right hemisphere recruitment during language processing. This study compare the pattern of brain activation in monolingual right handed subjects when (i) watching a video-tape of a speaker uttering English sentences, (ii) only hearing the sound part of those tapes, (iii) only viewing the video part of those tapes. Four subjects have participated in this study. This work will be presented at the 28th meeting of the Neuroscience Society.

FIGURE LEGENDS

Figure 1: Examples of stimulus sequences used to compare visual processing with and without attention in hearing and congenitally deaf individuals.

Figure 2: Pattern of activation for hearing and deaf when passively looking at an alternation of static and moving dots. Under this no-attention condition, the interaction shows no difference between the two groups of subjects.

Figure 3: Pattern of activation for hearing and deaf when monitoring brightness and velocity changes in alternating frames of static and moving dots. Under this attention condition, the deaf individuals display greater activation bilaterally in MT and in the right parietal cortex.

Figure 4: Pattern of activation for hearing individuals native of ASL and deaf when passively looking at an alternation of static and moving dots. Under this no-attention condition, the interaction shows almost no difference between the two groups of subjects.

Figure 5: Pattern of activation for hearing individuals native of ASL and deaf when monitoring brightness and velocity changes in alternating frames of static and moving dots. Under this attention condition, the deaf individuals display greater activation in MT and in the left parietal cortex.

Figure 6: Pattern of activation in Broca's and Werniske's area when monolingual hearing individuals read English sentences and congenital deaf individuals view ASL sentences.

STIMULI

Passive Looking

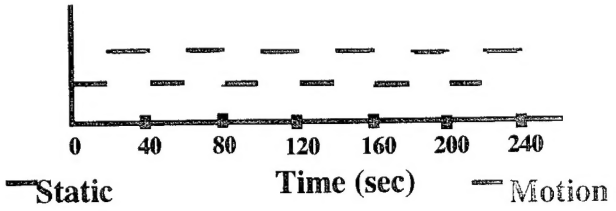

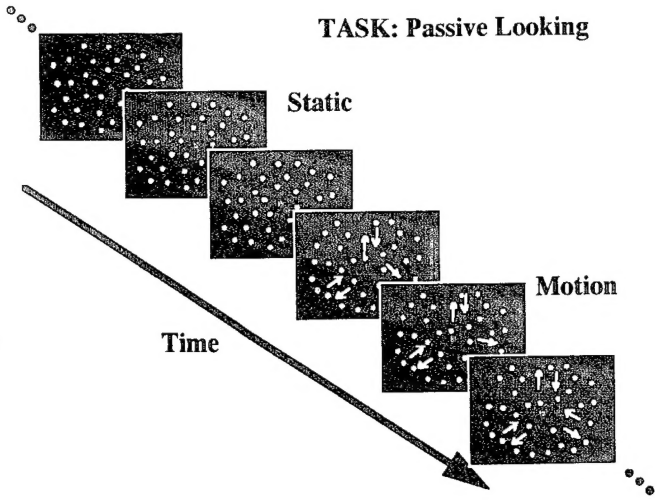

Monitor Brightness Changes

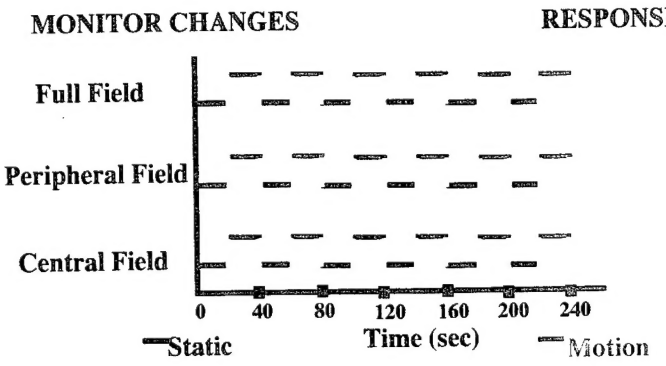

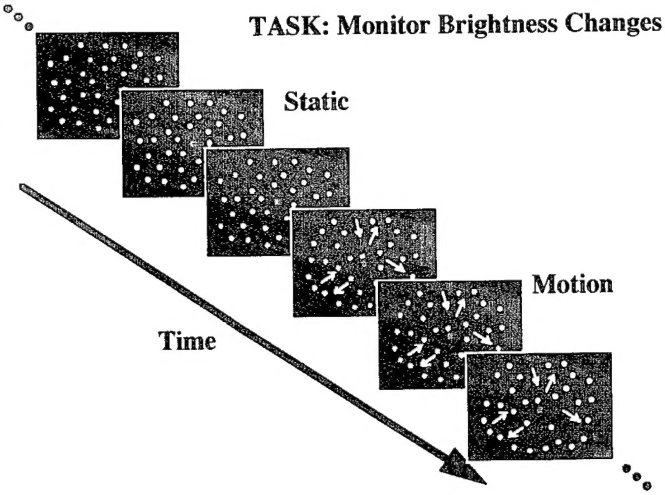

Monitor Velocity Changes

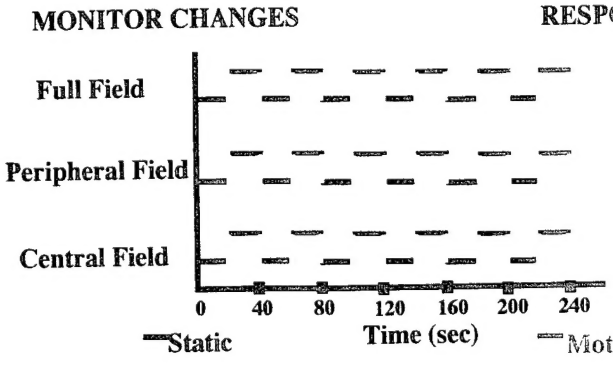

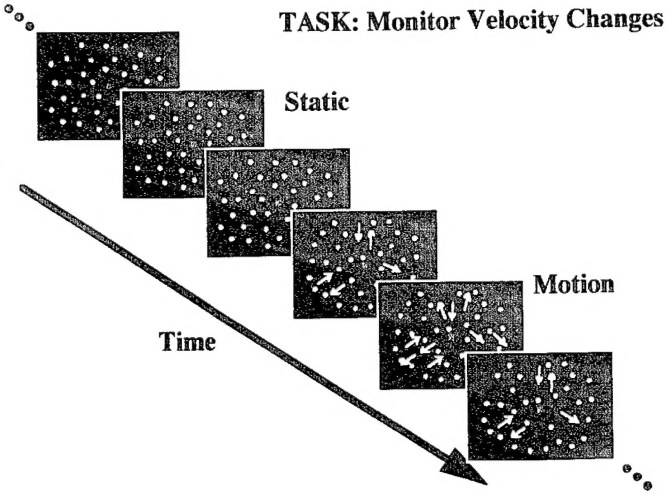

Figure 1

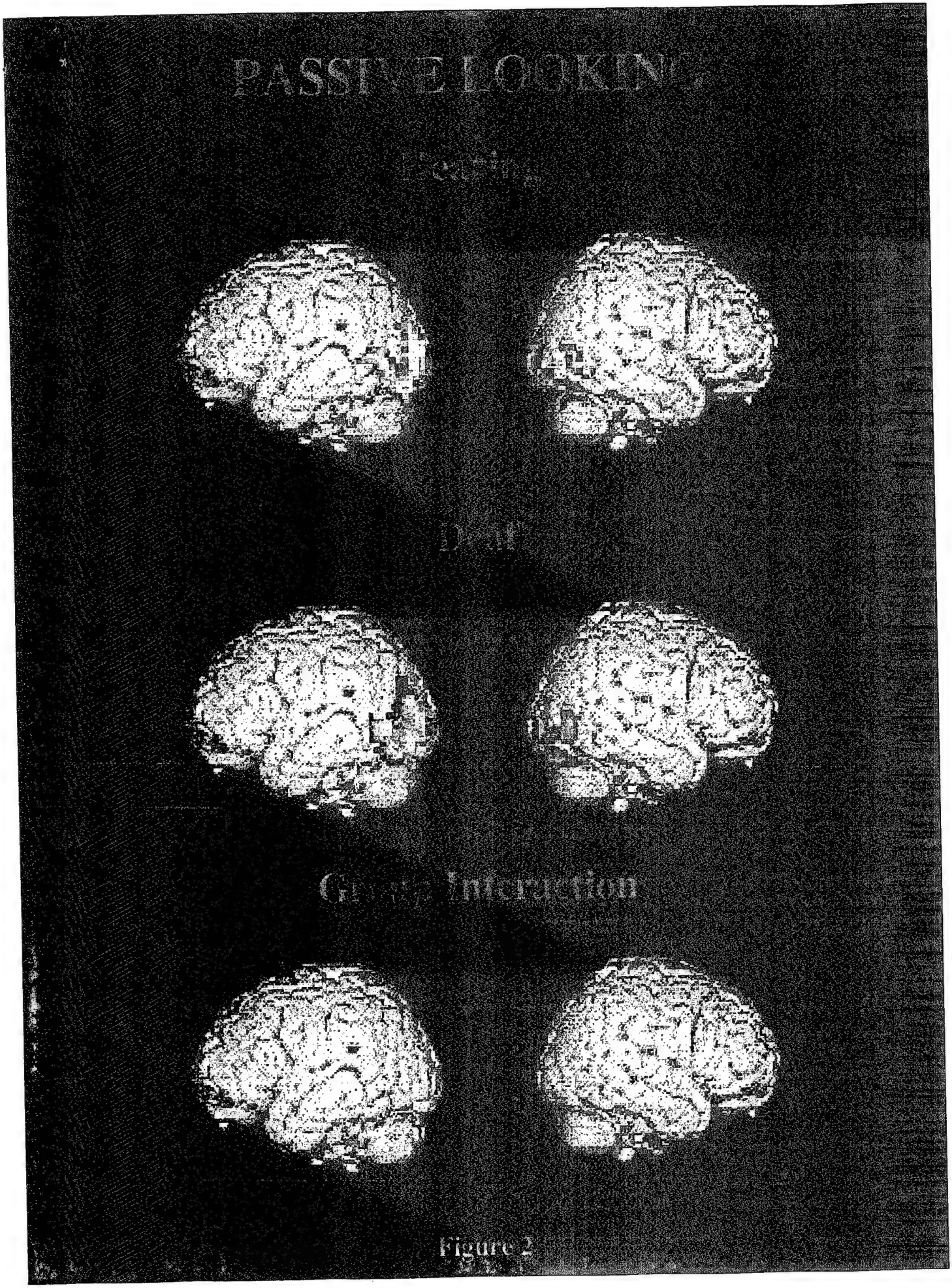

Figure 2

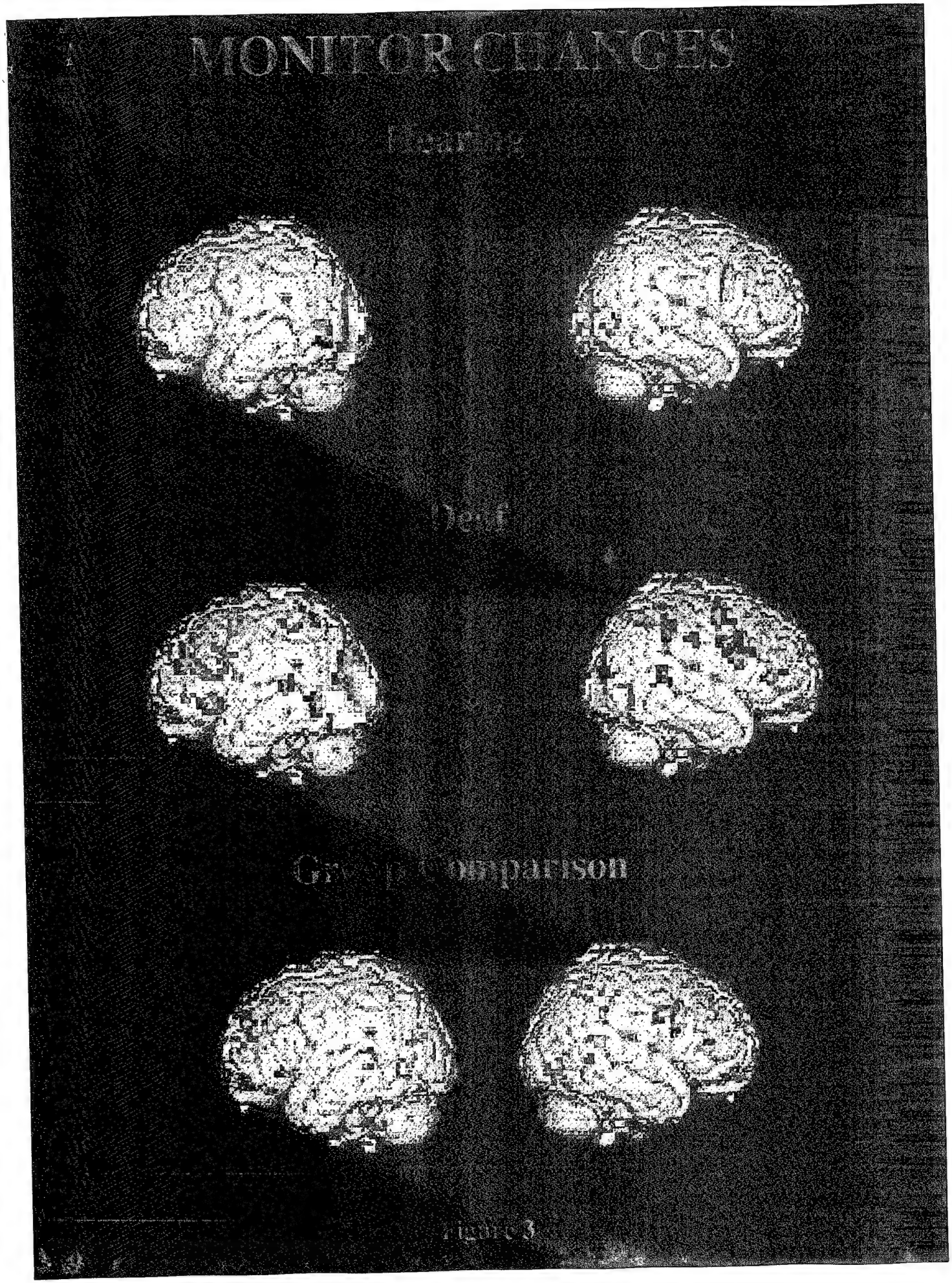

Figure 3

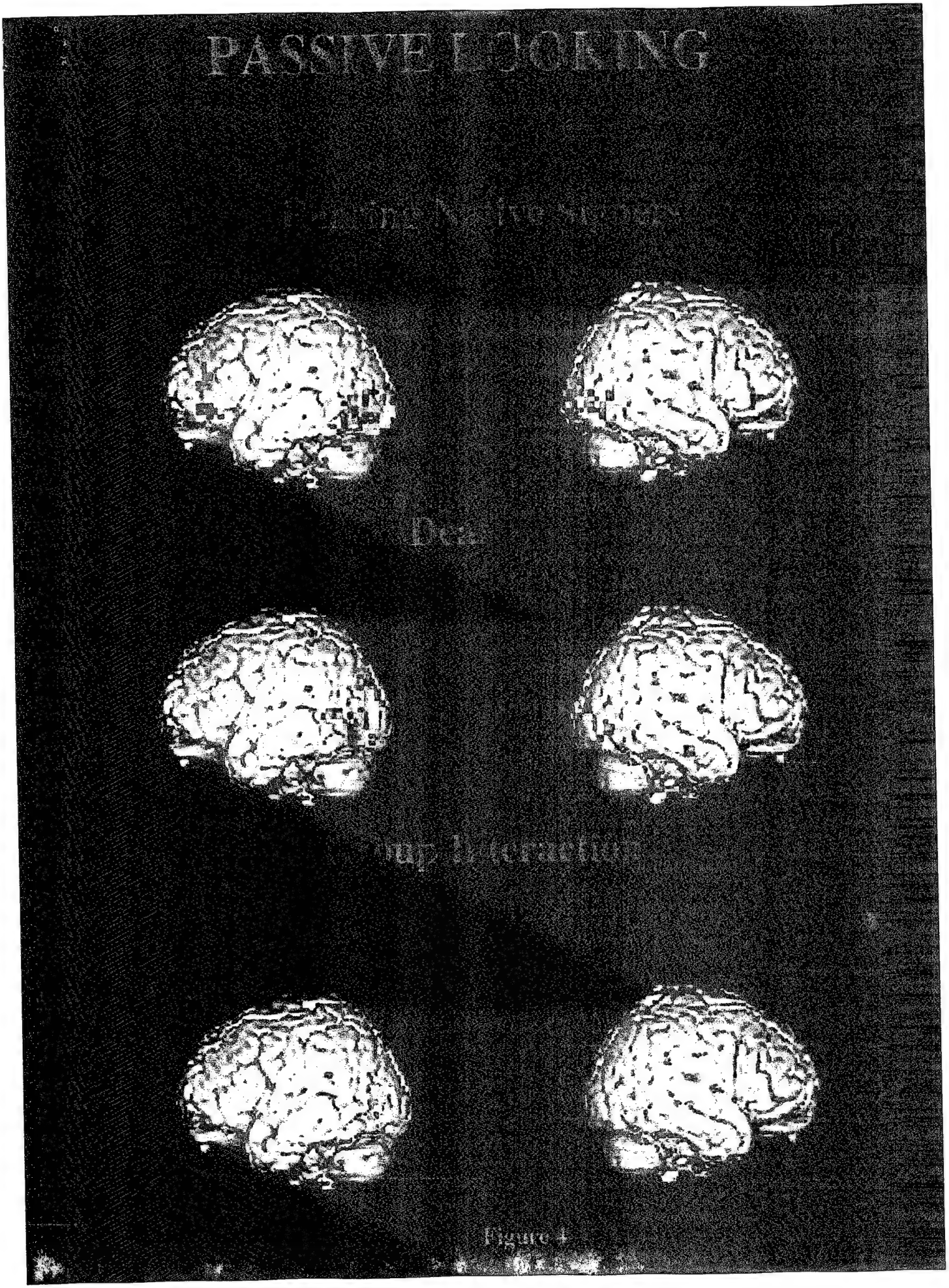

Figure 4

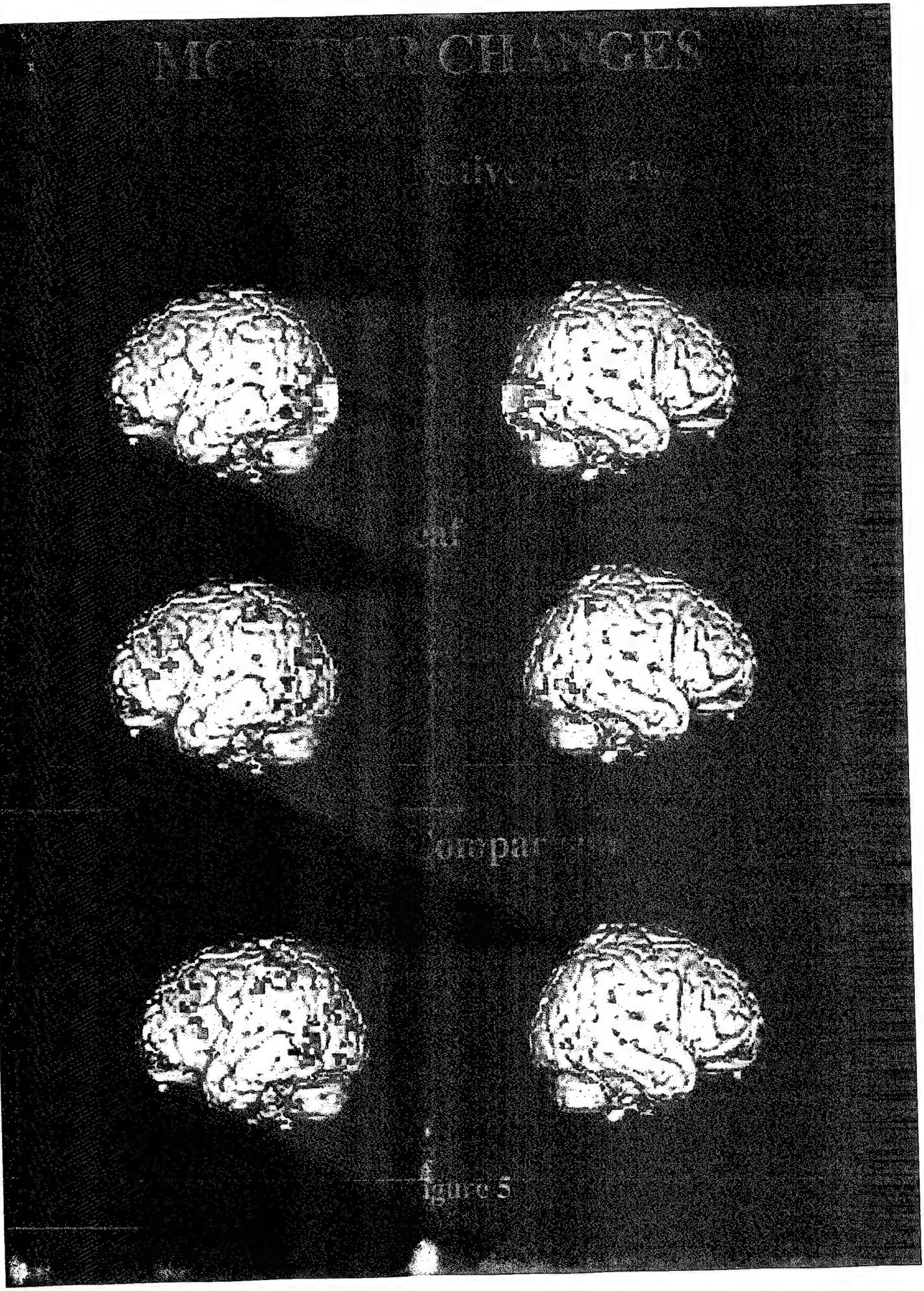

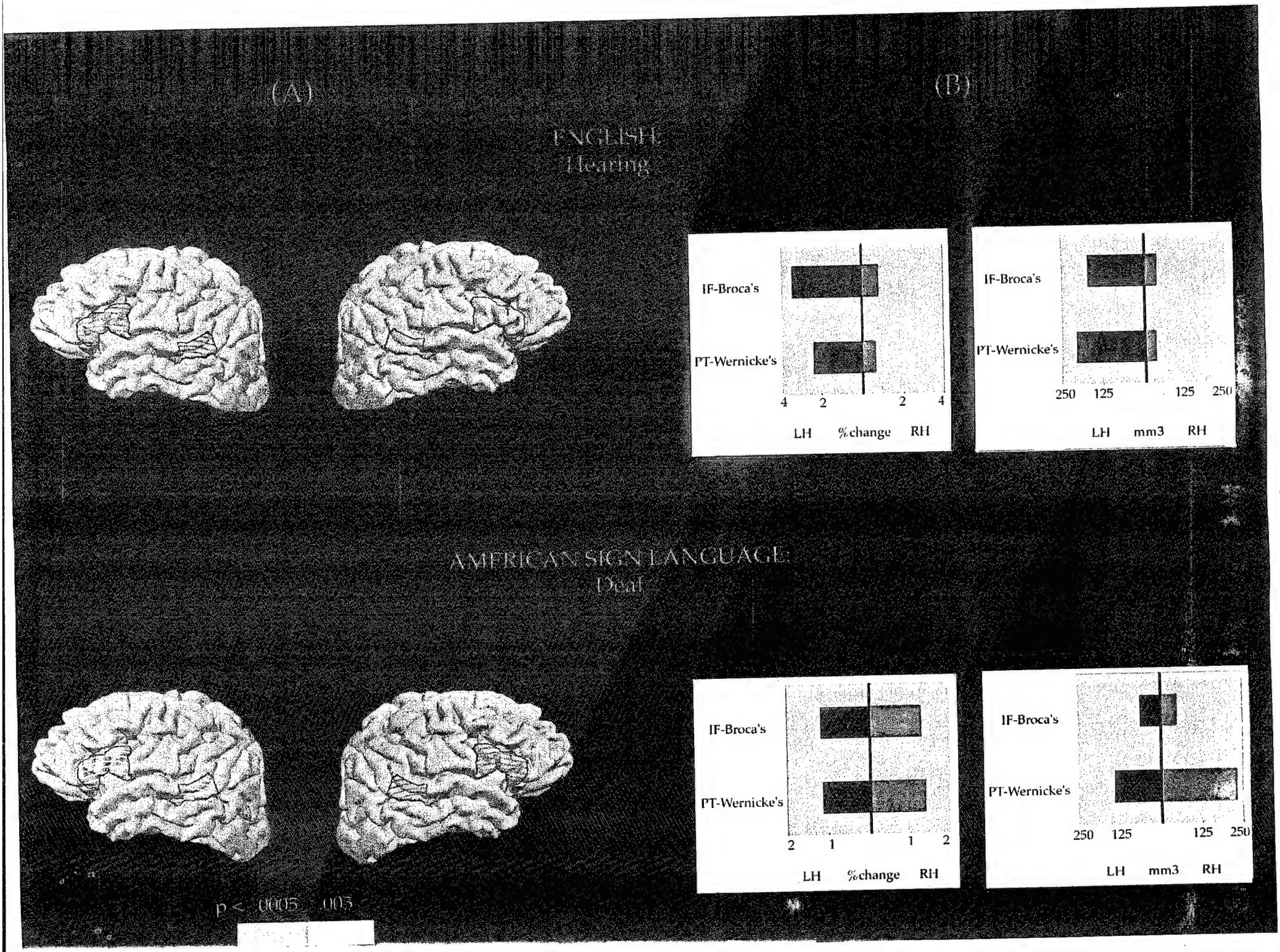
(A)
(B)
ENGLISH:
Hearing
IF-Broca's
PT-Wernicke's
4
2
2
4
LH
%change
RH
IF-Broca's
PT-Wernicke's
250
125
125
250
LH
mm3
RH
AMERICAN SIGN LANGUAGE:
Deaf
IF-Broca's
PT-Wernicke's
2
1
1
2
LH
%change
RH
IF-Broca's
PT-Wernicke's
250
125
125
250
LH
mm3
RH
p < .0005
.005

GUINEVERE EDEN, Ph.D.

Guinevere Eden's laboratory uses behavioral testing and functional magnetic resonance imaging (fMRI) to characterize sensory and cognitive processing in individuals with and without developmental dyslexia. These studies include examinations of rapid visual and auditory processing as well as phonological awareness. Although these processes have been previously shown to be impaired in dyslexics, the nature of their shared contribution and questions concerning a common neocortical etiology are being investigated for the first time.

The clinical manifestations of developmental dyslexia are varied. In addition to their reading difficulties, individuals with developmental dyslexia exhibit impairments in their ability to process the phonological features of written or spoken language. We have demonstrated that these individuals are also impaired on a number of visual tasks, involving visuomotor, visuospatial and visual motion processing. These results suggest that the pathophysiology of dyslexia is more complex than originally thought, extending beyond the classically defined brain language areas. We are currently investigating the existence of a deficit in sensory information processing in dyslexia that is common to multiple sensory modalities. Our approach is to perform analogous behavioral and functional studies in the visual and auditory system and to relate them to phonological awareness skills in dyslexics and controls. The results will further delineate the relationship between psychophysical performance and neuronal processing mechanisms in dyslexia and may suggest new strategies for remediation.

PROJECT 1: DEVELOPMENTAL DYSLEXIA AND THE VISUAL SYSTEM

Functional neuroimaging utilizing positron emission tomography (PET) and functional magnetic resonance imaging (fMRI) have identified a specific motion sensitive area, V5/MT, thought to be dominated by input from the magnocellular stream. Behaviorally, these channels can be distinguished by their spatial frequency preference, their temporal properties and their contrast sensitivity. Both contrast sensitivity and visible persistence has been shown to be varied in reading disabled children, indicating that these children have disturbances in the magnocellular or transient system, which mediates global form, movement, and temporal resolution. We investigated such a motion processing deficit in the visual system of dyslexics and found passive perception of visual motion in dyslexics failed to produce any detectable task-related functional activation in area V5/MT (part of the magnocellular system). In contrast, all control subjects had a robust response in the same region. We concluded that dyslexics suffer from abnormalities of the fast visual processing pathway (magnocellular), whilst the slower form processing system (parvocellular) was unaffected. This profound physiological abnormality was accompanied by a relatively subtle behavioral deficit in visual motion detection. This finding of an V5/MT deficiency in dyslexia has recently been replicated in an fMRI study that showed activity in this area to be directly correlated with reading skill.

These studies have only examined area MT/V5 but not areas in parietal cortex, which receives projections from V5/MT and hence the magnocellular system. Using radial motion, we present a study of the entire brain to investigate radial visual motion processing in posterior parietal cortex. Single-unit recording studies in non-human primates have provided strong evidence for visual motion processing in posterior parietal cortex (PPC). In contrast, human functional neuroimaging studies of visual motion processing have been more inconsistent in their identification of task-related signals in PPC. Both human and non-human primate studies are in good agreement concerning the existence of visual motion

processing centers in the V5/MT complex; however, the role of the PPC in motion processing in humans has received less attention. While some of these inconsistent results may be explained with respect to technical limitations, e.g. the limited field-of-view of PET cameras or anatomical variability compromising intersubject averaging techniques, it is possible that there exists a species difference in regional functional specialization for motion processing. To explore this discrepancy we examined the localization of visual motion processing in PPC utilizing visual stimuli similar to those employed in previous single-unit studies and an experimental design that allowed single-subject statistical map generation.

Ten subjects viewed 3 different visual stimuli: (1) FIXATION: a light gray cross-hair centered on a dark gray background, (2) STATIC: 300 randomly arranged light gray dots on a dark gray background, and (3) RADIAL MOTION: 300 light gray dots radiating centrifugally from the central fixation point. The luminance was the same in all conditions and the stimuli subtended 52 degrees of visual angle. The 24 second epochs were presented in the following order: fixation, static, fixation, motion, etc. for a total of 32 epochs per run. Data were acquired utilizing a multislice echo-planar image (EPI) technique (40 msec TE, 6 sec TR, 64x64 matrix, 50 axial slices and 3 mm cubic voxels). MEDx was used for functional image analysis and visualization. Each EPI time series was corrected for head motion, global intensity variations and local (temporal) intensity variations. Statistical maps were generated by contrasting task and control conditions for each subject. For neuroanatomical localization the functional data were registered with a high-resolution anatomical scan.

In each subject the RADIAL MOTION versus STATIC contrast revealed bilateral task-related increases in striate and extrastriate visual cortex (including area V5/MT), anterior cingulate gyrus, inferior frontal gyrus, anterior superior temporal gyrus, posterior parietal cortex and posterior cerebellum. The PPC response was easily identified in all subjects. Figure 1 shows this activation in one individual subject.

Using radial visual motion stimuli and single-subject analysis techniques we observed task-related signal increases in PPC in all subjects. Inconsistent results in previous functional neuroimaging studies may have resulted from either technical data acquisition limitations or anatomical variability in the regional functional localization of motion processing in the PPC. Reliable identification of PPC motion responses in control subjects will allow studies of clinical populations with presumed dysfunction in this area.

We will be studying visual motion processing in dyslexics and controls with fMRI to investigate whether there are differences in the PPC as might be predicted. Also, we are interested if attention used to compensate for visual motion processing deficits in dyslexia. Behavioral compensation is an important mechanism by which individuals demonstrate recovery after brain injury of various kinds. The aim is to examine the attentional modulation of visual motion processing in dyslexia. If the behavioral compensation hypothesis is correct, dyslexics should show a large attention-related modulation of activation in relation to visual motion in area MT/V5 and the posterior parietal cortex.

PROJECT 2: DEVELOPMENTAL DYSLEXIA AND THE AUDITORY SYSTEM

A visual deficit in dyslexia is associated with abnormal processing in a subsystem specialized for rapid visual information processing. It has been argued that analogous problems may exist in the auditory system and may have a direct effect on phonological processing in dyslexics. These studies have shown that children with dyslexia have difficulties in distinguishing two tones when separated by a short time

period. We have begun neuroimaging studies to allow us to identify the areas that subserve the processing of rapidly presented auditory stimuli in order to investigate whether there might be differences in these areas in dyslexia. Initially we have set out to map tones so that a cortical map of the allrelevant frequencies can be obtained. These studies are currently ongoing (n=7).

fMRI is used to map alterations in activity induced in cortical brain regions by pure-tone stimulation. Tonotopic mapping: We use those tone frequencies previously used for the two-tone discrimination task with additional flanking frequencies. Normal adults are scanned while passively listening to five different tones, 500 ms in duration followed by a 500 ms pause before the onset of the next tone. The frequencies examined are 200, 400, 800, 1600 and 3200 Hz and each tone was randomly presented for a total of 64 times over the course of three, 12 minute runs.

Tone discrimination: Subjects listen to a pure tone-sequence that is one of four different possible combinations of two tones (800Hz and 1600Hz). Each tone sequence consists of two 75 ms tones separated by a 5ms inter-stimulus-interval. Following the presentation of a completed sequence, a 2500 ms response period ensues in which the subject is required to make an appropriate button press response depending on the condition. The subject responds by pressing button 1 if the two tones heard in the tone sequence were the "same" and button 2 if the tones were "different".

Tone sequencing: This time button 1 is to be associated with the 800 Hz tone (the "low" tone) and button 2 with the 1600 Hz tone (the "high" tone). In this condition the subject must press out the order in which they heard the tones presented. Subjects will hear the exact same presentation of sequences for each of these three conditions, the only difference being how they are to respond.

Tonotopic maps were obtained in four of the subjects as demonstrated in Figure 2. Data acquisition and analyses for the tone sequencing and tone discrimination are currently ongoing.

The areas of the brain involved in the rapid processing of tones might be different in individuals with and without dyslexia. In order to relate this type of rapid temporal processing to other rapid processing we wish to invstigate if the motion processing deficit in dyslexia involve both vision and audition. The aim of these experiments is to search for the physiological motion processing mechanisms common to vision and audition. Task-related signal change will be contrasted in individuals with and without dyslexia using functional magnetic resonance imaging (fMRI). Comparison of results across modalities will reveal to what degree dyslexics exhibit functional deficits common to vision and audition, and may suggest the neuroanatomical localization of a common neural substrate.

PROJECT 3: PRESENTING AUDITORY INFORMATION TO STUDY THE AUDITORY AND LANGUAGE SYSTEM

Functional magnetic resonance imaging (fMRI) is currently making a significant contribution to our understanding of the neuronal correlates of sensory and cognitive processing. However, signal detection may be adversely affected by the presence of gradient noise, which is inherent in this imaging technique. Studies involving language or sound processing are especially likely to be polluted by the external noise and few studies have successfully been able to eliminate the noise by insulation or otherwise. Most fMRI studies use the subtraction analysis technique and thereby assume that the physiological changes induced by the gradient disappear as a result of the subtraction. Recently it has become clear that this

assumption is incorrect and noise-induced signal change may be misidentified as task-related signal change. Further, it appears that the noise diminishes certain cortical responses, presumably by inducing decreases (e.g. in visual cortex) and accentuates others. It is also likely that gradient noise distracts the subject from the task at hand. In our study we employed an approach in which the gradients were off during periods of task execution and then immediately switched on to acquire data. Detection of the task-related signal change relied on the presence of a hemodynamic lag of 5-8 seconds between neuronal activity and the resulting BOLD contrast response.

An externally-paced finger movement task known to induce large signal changes in motor areas was used. Six subjects performed an index finger tapping task (dominant hand) at a rate of 2 Hz paced by a large flashing green star. Finger tapping alternated with periods of rest, during which the subject viewed a red star, flashing at the same rate. Multislice echo-planar image (EPI) acquisition was used (43 msec TE, 12 sec TR, 64x64 matrix, 256mm FOV, 40 axial slices, 4 mm thickness, 4 mm cubic voxels, 50 time points per run). Two runs were performed in the following 4 acquisition modes: Acquired after task - Behavior-Interleaved-Gradients (BIG), which consisted of data acquisition after the task involved 8 seconds of tapping during which no data was acquired; this was followed by a 4 second interval during which 1 whole-head volume was acquired. Acquired during task(control) alternates between rest and task as in the previous condition, but the acquisition is begun during the 2nd half of the task period, thereby providing a control for the assumed haemodynamic lag. Acquired concurrently 1 employed the traditional block design of continuous task and rest periods. Acquired concurrently 2 was the same as the previous acquisition, but controlled for differences in the number of movements produced over the total scans by changing the tapping rate. Fifty time points were collected for each condition. Using MEDx the image data were corrected for head motion, global and local intensity variations. Task and rest periods were compared using the t-statistic which was then transformed to a Z-score. The Z-map was then searched for local maxima.

Statistical maps revealed task related changes in primary motor cortex, primary somatosensory cortex, premotor cortex, supplementary motor area, cingulate motor area, thalamus and anterior cerebellum. Contrasting the Z maps generated from the movement minus rest condition between the BIG and the Acquired concurrently 1, Acquired concurrently 2 and Control technique, revealed that activations in primary motor cortex are similar or higher when data acquisition occurred after the task completed, as is the case for BIG. Figure 3 summarizes the experimental procedure and the results.

Interleaving task performance and data acquisition allows task performance under relatively quiet experimental conditions. Eight-second task performance periods were sufficiently long to yield excellent statistical results. Although the total data acquisition period is prolonged using this design, subjects exhibited decreased head motion compared to the conventional block data acquisition approach. We expect this technique to be useful when the experiment requires maximal acoustic isolation of the subject. It is also be advantageous when speech is required, as articulation, with its attendant motion artifacts, will not occur during periods of data acquisition.

We are applying BIG to our fMRI studies on the auditory system to study the mechanisms underlying phonological processing.

PROJECT 4: DEVELOPMENTAL DYSLEXIA AND PHONOLOGICAL AWARENESS

The most widely accepted current explanation for dyslexic's reading difficulties involves abnormal phonological processing. The term "phonological awareness" has been used as an umbrella term for the skill of manipulation and segmentation of the constituent sounds of words. The neuronal mechanisms that subserve the type of rapid phonological retrieval and phonological segmentation impaired in dyslexia are not yet clearly defined. Some of the differences observed in dyslexics during previous functional neuroimaging studies are difficult to interpret due to our incomplete understanding of "normal" language processing. With advancements in neuroimaging technology, it is now possible to study an individual subject's performance during a wider variety of tasks than was previously possible due to radiation dosimetry limits. As a result, an effort has begun in our laboratory to systematically study individuals with normal cognitive development to understand the functional organization of the brain for language. These efforts will allow a deeper understanding of the effects of developmental dyslexia on a range of sensory and phonologically related skills. These studies are currently ongoing (n=12).

We utilized the BIG technique (see above) to investigate phonological awareness skills in 10 adults. The tasks utilized required an awareness of the sound structure of language and an ability to perceive and manipulate both auditory phonemes and written graphemes. The following four tasks were employed, using both written and auditory presentations of single words with equal levels of difficulty, in order to study phonological processing: (1) elision, (2) segmentation, (3) rhyme judgement, and (4) semantic category judgement. fMRI results revealed involvement of inferior frontal gyri, inferior parietal areas, temporal areas and cerebellum. The results suggest that the choice of the phonological task modulates the activation patterns observed. For example, rhyme judgement engages parietal areas more extensively than word elision, which predominantly activated frontal areas. The observed pattern of task-related brain activity varied between subjects and with respect to task or presentation modality. See Figure 4 for results.

These four phonological tasks will be studied in individuals with dyslexia. Differences between dyslexic and control group maps of task-related brain activity will allow neuroanatomical localization of the areas affected by dyslexia. Most importantly, this experiment will reveal the anatomical and functional characteristics of brain areas subserving phonological and rapid naming abilities in relation to those areas subserving visual and auditory temporal processing. The areas altered in dyslexia are predicted to be those engaged during both phonological and rapid temporal task. Co-localization of these two apparently disparate brain functions may explain the co-occurrence of reading disability and sensory abnormalities in dyslexia.

Integration of the resulting behavioral, anatomical and physiological information into structure/function correlations is a principal goal of our research program. Using these techniques we will examine the degree to which these physiological changes correlate with the observed behavioral deficits. Comparison of results across modalities will reveal to what degree dyslexics exhibit functional deficits common to vision and audition, and may suggest the neuroanatomical localization of a common neural substrate. The results of these experiments will provide new information concerning the neural substrates responsible for the visual, auditory and phonological abnormalities characteristic of developmental dyslexia. Moreover, the laboratory is interested in the development of new diagnostic tools that may allow earlier and more accurate identification of individuals with developmental language disorders.

Figure 1.
In each subject the RADIAL MOTION versus STATIC contrast revealed bilateral task-related increases in striate and extrastriate visual cortex (including area V5/MT), anterior cingulate gyrus, inferior frontal gyrus, anterior superior temporal gyrus, posterior parietal cortex and posterior cerebellum. Anatomical areas, Brodmann areas, Talairach coordinates, and statistical significance are shown for each area.

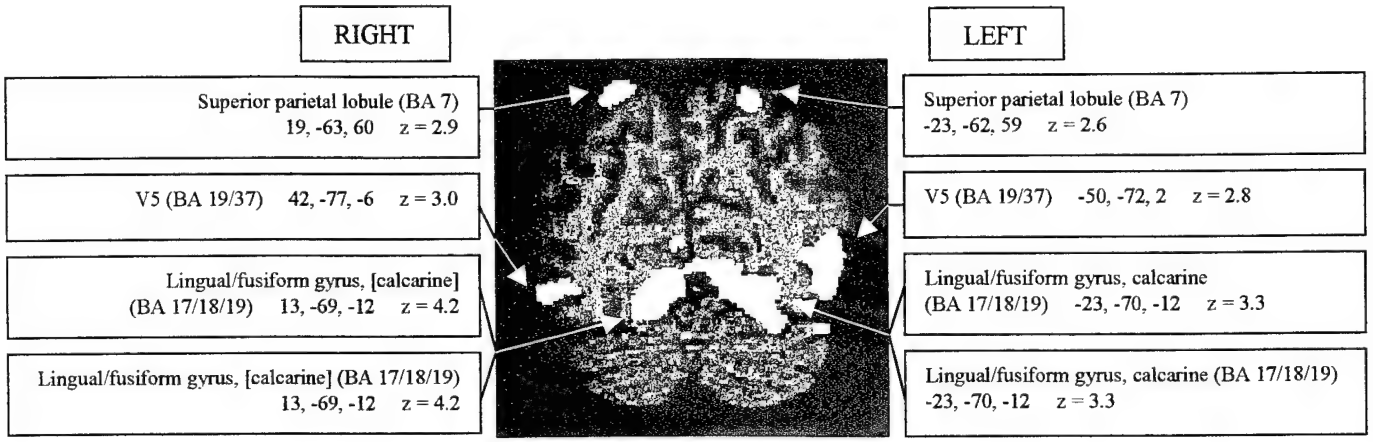

Figure 2a.
Tonotopic representation of 200 Hz (red), 800Hz (yellow) and 200Hz (blue).

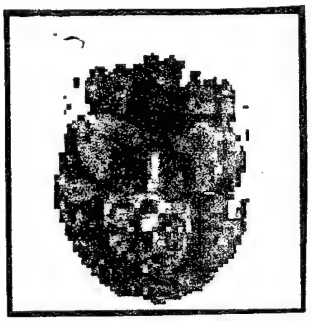

Figure 2b.
Three-dimensional rendering showing the location of primary auditory cortex in Heschl's gyrus.

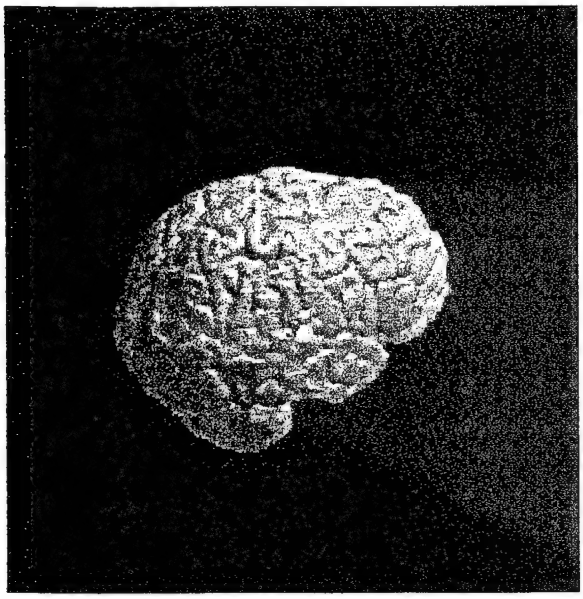

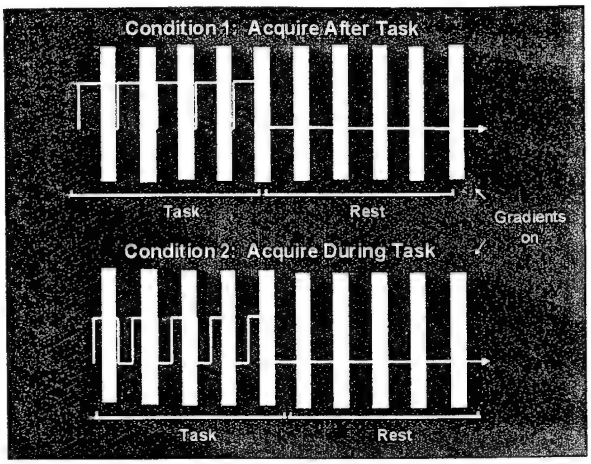

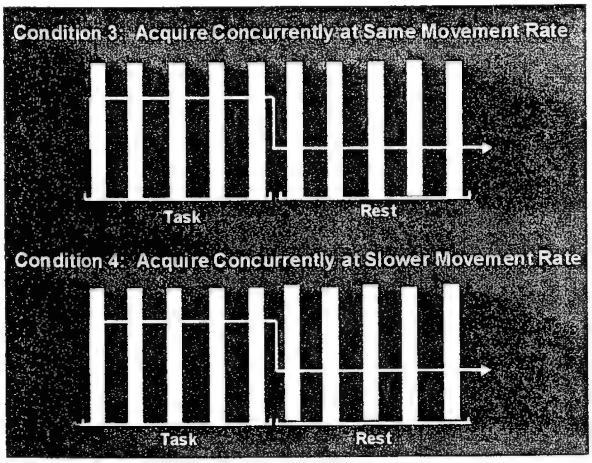

Figure 3a. Task descriptions for Acquire After Task (BIG), Acquire During Task, Acquire Concurrently at Same Movement Rate, and Acquire Concurrently at Slower Movement Rate.

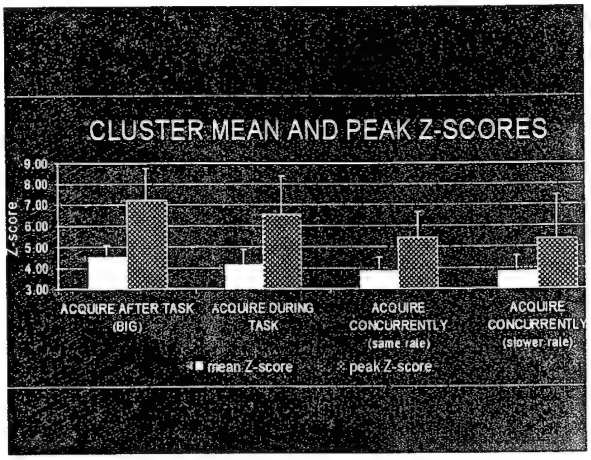

Figure 3b.
Peak and mean Z-score values for MI cluster across the 4 experimental conditions.

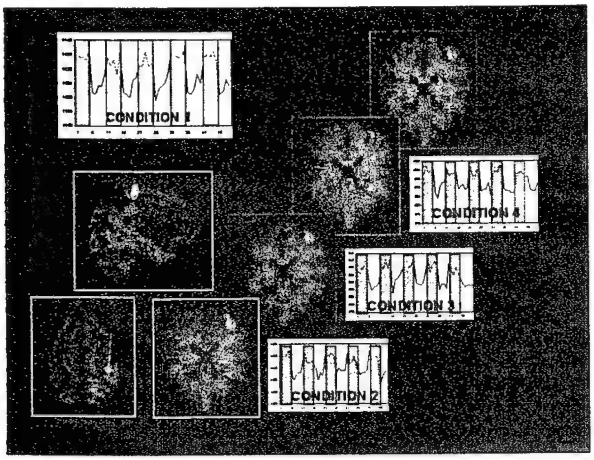

Figure 3c.

Signal change in MI in all task conditions in one individual. Task related signal change is presented in the maximally activated single voxel.

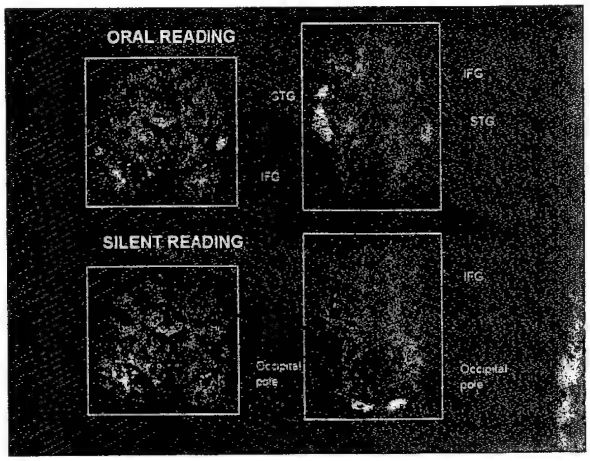

Figure 3d.
Activation in one of the subjects acquired with the behavior interleaved gradients technique. The task in this case is (bottom) silent word reading and (top) reading aloud. Resulting z-maps and task related signal change illustrate the feasibility of utilizing BIG in overt language studies. IFG - inferior frontal gyrus; STG - superior temporal gyrus; IFG- inferior frontal gyrus.

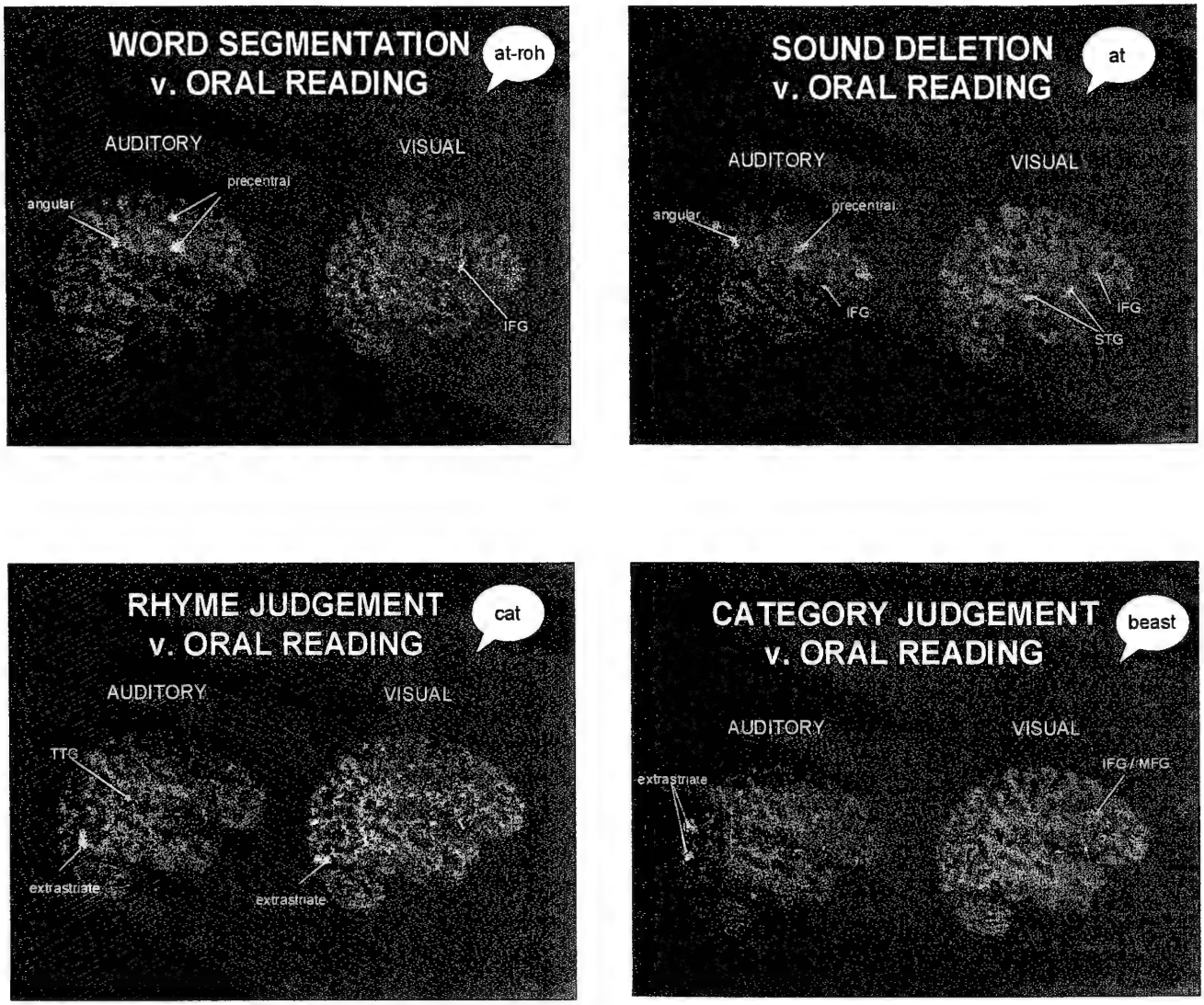

Figure 4.
Activation in single individual, while performing one of three phonological tasks (segmentation, deletion or rhyme judgement) compared to a category judgement task. The tasks were performed during both visual and auditory stimulation. The results show differences in the activation across tasks and across stimulus presentation mode.

DR. RHONDA B. FRIEDMAN, Ph.D.

Dr. Friedman's research encompasses three major projects: (1) Cognitively-based treatments of acquired dyslexias (2) Written language processing in Alzheimer's Disease; and (3) Evaluating cognitive neuropsychological models of language recovery with fMRI.

PROJECT 1: COGNITIVELY-BASED TREATMENTS OF ACQUIRED DYSLEXIAS

The purpose of this project is the development of a set of therapy programs that are shown to be effective in the treatment of acquired disorders of reading (acquired dyslexias, also known as alexias.). This goal is achieved through the development, implementation, and evaluation of several experimental therapies, each targeted for a specific type of reading deficit, based upon a cognitive neuropsychological model of reading. The data obtained from this study are also used to improve our models of normal reading, which may lead to more effective methods of teaching reading to both normal and developmentally dyslexic children.

Patients with acquired reading disorders following stroke are referred to our project by neurologists or speech pathologists for further evaluation. The patient's reading and other cognitive skills are assessed using a battery of screening tests that we have developed over the past several years. Based upon the results of these tests, the patient's alexic disorder is characterized. Patients whose deficits are among those that are the focus of this project are assigned to one of the treatment programs devised specifically for that type of deficit. For many, the question of bypassing an impaired system vs. remediating the disturbance is addressed. When feasible, factors that might predict the success of a particular treatment for a particular patient are examined. The overall structure of the study consisted of single case studies, replicated over several patients, each employing a multiple baseline design.

The following results have been obtained over the past year

Study 1. Pure Alexia

Hybrid Treatment. Hybrid treatment combines the successful elements of the two pure alexia approaches we are examining, rapid word presentation and speeded letter-by-letter reading (described in previous annual reports). The patient is trained to (1) rapidly recognize a set of the most frequently occurring words, (2) quickly read less frequently occurring words in letter-by-letter fashion, and finally (3) combine both strategies when reading sentences. In our previous report, we demonstrated successful sight word reading for subject FT (stage 1). The data also indicated that the sight word treatment effect transferred to speed of sentence reading of the trained words, but not of the untrained words, as we predicted. This year we completed stages 2 and 3.

After speeded training of naming letters in isolation, FT's speed of letter naming improved from 717 msec per letter to 597 msec/letter. At this point word reading speed was only minimally affected, improving from 1890 to 1769 msec/word. Speed of reading both trained and untrained words improved after speeded word treatment (see figure 1). At this point, sentence reading speed was only minimally affected, improving from 10.2 to 9.8 s/sentence. Speed of reading trained and, to a lesser extent, untrained sentences improved after speeded sentence treatment (see figure 2).
Time to read sentences that were tested only twice, before and after treatment, did not change (9.7 to 9.6 s/sentence). Accuracy remained well above 90% for all of these stimuli.

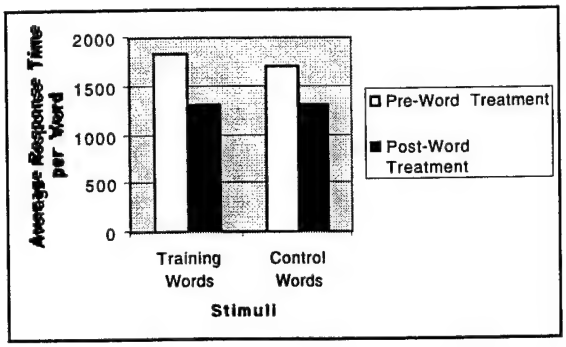

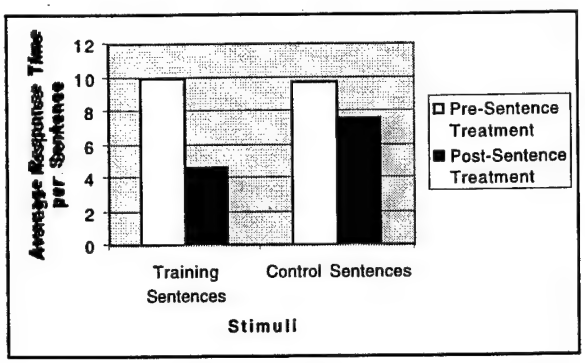

Figure 1. FT's average response time per training and control words before and after word treatment.

Figure 2. FT's average response time per training and control sentences before and after sentence treatment.

Revised Hybrid Treatment. We redesigned the hybrid treatment in order to specifically address whether sight word training (rapid presentation) is more advantageous than speeded letter-by-letter reading training (free vision presentation) in improving single word reading and in transferring this improvement to sentence reading. In this paradigm, a set of words is first presented in free vision and the subject is trained to read them as quickly and accurately as possible. The patient's time to read sentences containing the trained words is recorded before and after treatment. Half of the trained words are then trained in rapid presentation format, while the other half continue to be trained in free vision presentation. Again, the patient's time to read the sentences is recorded. If the sight word treatment is advantageous, the sentences containing words that were trained as sight words should be read faster than those containing words that were only trained in letter-by-letter fashion.

We initiated this treatment with subjects FT and SV. After 6 sessions, SV's reading of words trained in free vision improved from an average of 2446 to 1822 msec, while untrained words improved from an average of 2482 to 1941 msec. After 5 sessions, FT's reading of words trained in free vision improved from an average of 2531 to 2055 msec, while untrained words improved from an average of 2552 to 2251 msec. It is impossible to interpret these results as they stand, because both subjects withdrew from the study in the initial stages of treatment for medical reasons.

Study 2: Phonological/Deep Alexia

Patients with this type of alexia cannot read via a system of assembled phonology (letter - sound conversion). Thus unfamiliar words and pronounceable nonwords are read poorly relative to real familiar words.

Bigraph-Phoneme Conversion Treatment. This therapy is predicated on the premise that grapheme-phoneme conversion is not the most natural way to translate letters into sounds. Our treatment uses the bigraph syllable, which is a more natural and psychologically real unit of language. In this treatment, patients are trained to pronounce syllables by pairing them with key words (e.g. li - lips), and then to sound out words by combining these syllables. The success of this treatment with two subjects to date confirms our prediction. Furthermore, we have shown in previous reports that both patients demonstrated considerable generalization to words that were untrained but composed of trained bigraphs.

After training was completed on all 3 sets, when all stimuli were tested together, our subjects were no longer performing as well on previously trained items. We set up new treatment phases in which all bigraphs, and then all words, were trained simultaneously. Replicating results previously reported with LR, subject KT regained criterion level performance on the bigraphs (see figure 3). The combined bigraph training had only a limited effect on her word reading (see figure 3). Words were then trained in a combined paradigm as well. KT regained criterion level performance reading trained words (see figure 3). LR was unable to regain criterion level word reading performance, improving only from 61% to 63% correct.

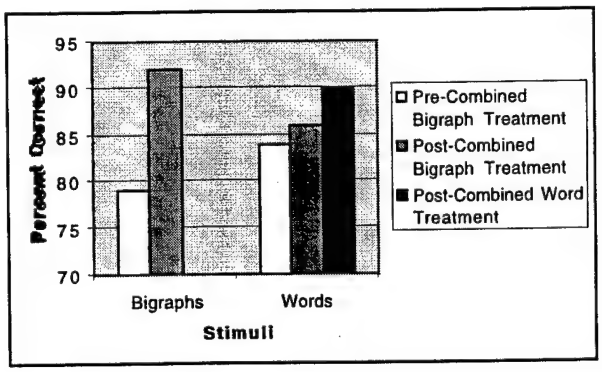

Figure 3. KT's bigraph and word reading before and after the combined bigraph treatment, and then after combined word treatment.

The different results obtained for the two subjects suggest different limitations on learning for these patients. KT had the capacity to learn a large corpus of items, and needed only a change in training paradigm to learn and retain them all successfully. LR appears unable to retain a large corpus, gaining new information at the expense of previously learned items. Possible reasons for these differences will be a focus of future investigations.

Phonological Neighborhood Treatment. This therapy derives from connectionist models of word reading, which hold that the ability to read unfamiliar words is related to the strengths of the connections between the orthographic and phonologic units of which they are composed. These strengths are related to the number of times that words containing those connections have been read, i.e. the number of times that the orthography has been paired with the phonology. In the therapy, the oral reading of two groups of orthographically similar words are trained to criterion. One group is similar in its initial unit (e.g. came, case, cape), while the other is similar in its final unit (e.g. bake, make, lake). The patient is tested on his/her ability to read a target word composed of the two trained orthographic units (e.g. cake). As controls, words containing one trained and one untrained unit and words containing no trained units were also tested. The models predict that the repeated pairing of each of these written words with their pronunciations should strengthen all of the component orthography to phonology connections needed to orally read the target word.

We previously reported that GR's reading of words composed of two trained units improved more than those composed of only one or no trained units, supporting our hypothesis that orthography to phonology connection strengths can be reestablished in an implicit processing task.

We revised this treatment in an attempt to make the task even more implicit. Only one word, instead of groups of three orthographically similar words, was provided for each trained unit. Results were similar to those obtained in the initial treatment (see figure 4).

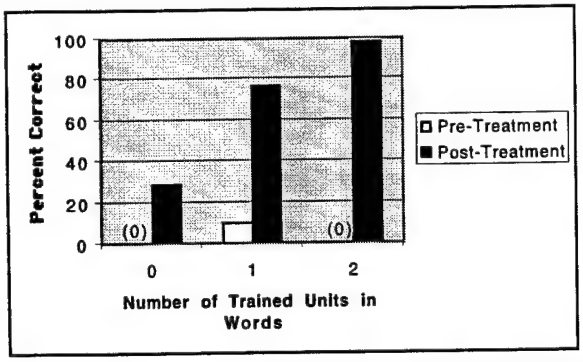

Figure 4. GR's accuracy reading words composed of 0, 1 or 2 trained units.

Semantic Mediation Treatment. While the previous therapy concentrated on "restoring" the damaged route to reading, this therapy takes the "re-organization" approach. It attempts to use the semantic route to circumvent the problems in the phonological reading route. This treatment pairs difficult words low in semantic value (functors and verbs), which are difficult for these patients to read, with homophones (words that are pronounced the same) or near homophones (e.g. in and inn, me and meat) that have high semantic value. The word pairs are trained via flashcards; the front contains the written target word and the back contains the written homophone along with its picture. Three sets of targets were trained sequentially.

As previously reported, both subjects DN and HN improved their reading of the target words, supporting the hypothesis that semantic route reading may be invoked to re-organize impaired phonologic route reading. As with the bigraph treatment, we found that when all stimuli were tested together at the end of treatment, patients did not perform as well as they did on previously trained words. Again, we added a final treatment phase in which all stimuli were trained together. Replicating previously reported results,

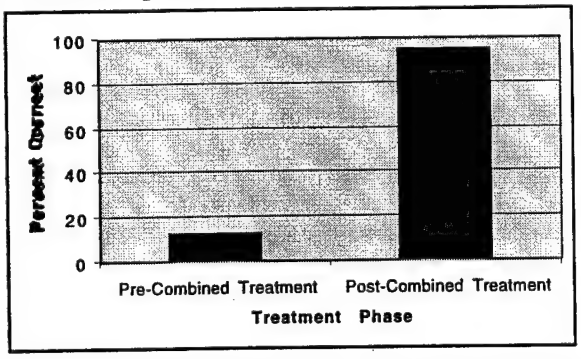

DN also regained criterion level performance after combined treatment (see figure 5).

Figure 5. DN's word reading before and after combined treatment.

To examine whether the use of homophones contributed to the success of this treatment, or whether equal success could be obtained simply with repeated practice with the target words, a second treatment task that did not utilize homophones was administered. The target words for this study consisted of the pre/post stimulus words from the previous study. The target word was printed on one side of a card, and a sentence containing the target word was printed on the other side. Training consisted of presenting the subject with the written target word. If read incorrectly, the stimulus card was turned over to reveal a

simple sentence which included the target word and focused on the meaning of the target word. The sentence was read aloud by the examiner when the written cue was not sufficient.

Neither HN nor DN was able to achieve criterion level performance on this task (see figure 6). At this point, training of the same words reverted to the original paradigm in which a homophone was provided for each target word. Both subjects achieved criterion level performance (see figure 6). These data suggest that the use of homophones is critical to the success of this treatment.

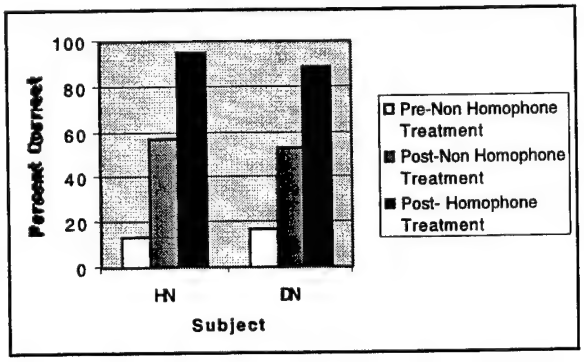

Figure 6. HN's and DN's word reading performance before and after the non-homophone treatment, and then after the homophone treatment.

The semantic mediation treatment was successful in improving the subjects' reading accuracy, but response time remained slow. In order to improve functional reading, treatment focusing on speed and sentence level reading was created. High frequency nouns and 50 of the trained words were used to compose sentences. Prior to sentence training, the 50 trained words were trained in a speeded paradigm. The remaining 30 words from the original paradigm were not trained in this speeded paradigm, but were regularly probed to assess generalization. Words were presented one at a time on a computer screen. The subject was instructed to read the word as quickly and accurately as possible, and his/her response time was recorded. As feedback, the subject was told his/her average response time. Treatment continues until the subject reaches asymptote. To date, both subjects have improved both their speed and accuracy of trained, but not untrained, words (see figures 7 and 8). Athough HN's speed of reading untrained words improved, her accuracy decreased. The treatment effect, therefore, does not appear to be generalizing to untrained words for either subject.

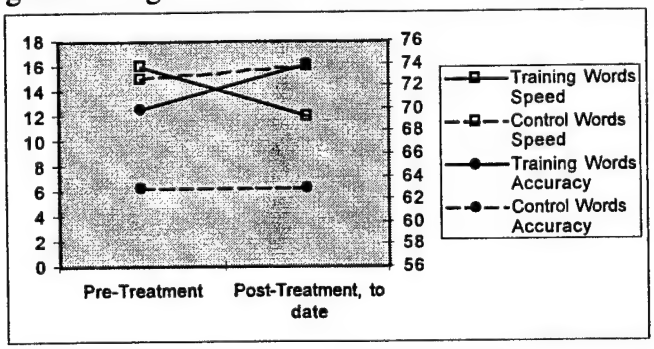

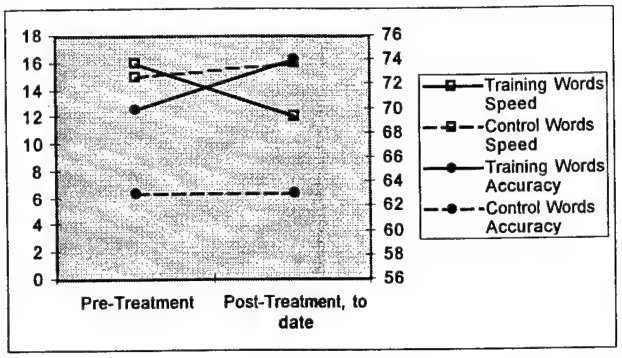

Figure 7. DN's word reading speed and accuracy of training and control words, before and after speeded treatment.

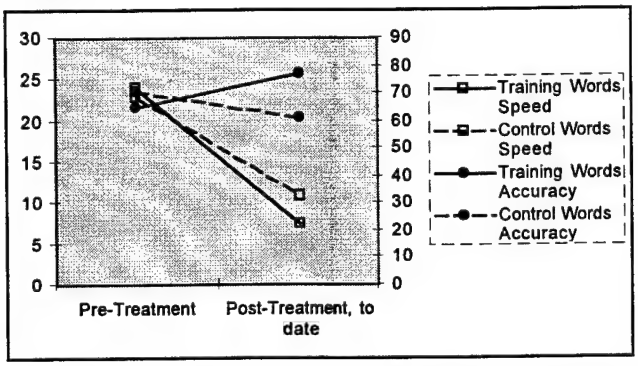

Figure 8. HN's word reading speed and accuracy of training and control words, before and after speeded treatment

PROJECT 2: WRITTEN LANGUAGE PROCESSING IN ALZHEIMER'S DISEASE

Comparing Reading and Spelling in AD

Patients with probable Alzheimer's disease (AD) are reported to show mild, but reliable, difficulties reading aloud and spelling to dictation "exception" words, which have unusual or unpredictable correspondence between their orthography and pronunciation (e.g. "touch"). This finding has been interpreted as indicating an underlying disturbance of lexical orthographic processing, as is seen in patients who develop surface alexia following a stroke. This study tested several predictions that follow from this interpretation.

Patients with AD and normal control subjects were given tasks of single word reading and single word spelling. The words were regular, ambiguous, or irregular. Separate lists were used for reading and spelling, as words that are ambiguous/exceptional for spelling and not necessarily ambiguous/ exceptional for reading, and vice versa.

The following results were obtained.

As expected, AD patients scored lower than normal controls, and showed a greater regularity effect (irregular words worse than regular words).

Contrary to what is seen in surface alexia:

the AD patients did not show difficulty with the ambiguous words relative to the regular words.

the AD patients showed a greater regularity effect for reading than for spelling.

the AD patients did not show a greater tendency to produce "regularization" errors than normals.

These results, taken together, do not support the hypothesis that the written language problems seen in patients with AD stem from a disturbance in orthographic representations. Rather, they appear to be caused by impairments to nonlinguistic functions outside of the central language processing system.

PROJECT 3: EVALUATING NEUROPSYCHOLOGICAL MODELS OF LANGUAGE RECOVERY WITH FMRI

We have scanned a total of 50 different subjects in a series of four related studies aimed at delineating brain regions that mediate learning and plasticity in single word reading. These studies examined: (1) areas that are activated in a short-term memory task using words and word-like strings; (2) areas that are specific to the short-term memory component of processing such strings; (3) Changes in activation patterns that result from repeated exposure to the same, initially novel, stimuli; and (4) Changes that occur after intensive training on novel word-like strings for a period of two to three weeks. All fMRI tasks consisted of one-back matching of four-letter strings alternating with blocks of one-back matching of single symbols.

In the first study we examined the response to visually presented words and word-like strings during a one-back matching task. The stimuli were (1) common words (e.g. boat) (2) pseudowords (PW), which are pronounceable but not real words (e.g. bink), (3) consonant letter strings (LS, e.g. lxwp), and (4) strings made up of letter like symbols that are unfamiliar to the subjects (false fonts, e.g. g, u). We contrasted these tasks with one-back matching of single symbols. The difference between tasks should delineate brain regions that are involved in perceptual processing of strings of varying degrees of familiarity and regions that form the basis of short term memory (on the order of about 1 second) for such strings.

Study 1 results: All subjects were strongly lateralized to the left occipital/fusiform gyrus in the real words task. Posterior areas of activation were consistent among subjects in the words task. Activations in anterior regions, including the prefrontal areas were more variable. A number of subjects showed activation in Broca's area. No significant differences were found between the word and the PW conditions. The LS condition, on the other hand, produced activations that were somewhat more posterior, bilateral, and parietal than the words and pseudowords tasks, while the FF condition resulted in either right sided or bilateral foci of activations in the occipital and fusiform areas. In general the FF condition also showed somewhat more parietal activations than the LS condition.

Several questions were raised by these results. Are the differences in activations for different stimuli mainly due to top-down influences that arise from use of different strategies (e.g. visual vs. pronunciation; scanning vs. whole stimulus processing; focus on a particular spatial location)? Or are they due to stimulus-driven (bottom-up) mechanisms that automatically "filter" different types of stimuli

into separate streams along the perceptual path, such as is the case with visual attributes such as shape and color? In the latter case, it would be expected that this automatic "filtering" is the result of learning, since there are no inherent differences between real words and consonant letter strings, for example, that would explain the results cited above. There are a number of dimensions along which these stimuli vary. 1) visual familiarity of the strings as a whole 2) visual familiarity of the components (letters or symbols) 3) lexical validity 4) pronounceability 5) orthographic regularity and 6) degree of semantics. The degree to which each of these attributes is mediated by either stimulus-driven or top-down effects would be expected to vary, and the observed differences may be the result of varying effects or strategies based on some or all of these dimensions. Factors (1) and (2) might be expected to be reflected mainly as stimulus-driven effects in earlier visual areas, while the other factors most likely are at least partially influenced by top-down effects, influenced by regions that mediate the respective attributes. These issues motivated the following three studies.

In the second study we examined the locations that specifically subserve the short-term memory component of the task for each of the four types of stimuli. This study was designed to test the hypothesis that different anterior association areas and prefrontal regions are involved in maintaining a short-term memory for the different string types. The stimuli and tasks were again the same as in the previous studies, but there were two different conditions in which the interstimulus interval (ISI) was either one second or 2 seconds. Subtraction of the one second ISI condition from the two second ISI condition would then be expected to reveal locations involved in the retention of the stimuli between stimulus presentations. Only anterior visual and some prefrontal regions showed activation differences in this contrast. Moreover, the regions that were activated were specific to the stimulus type, suggesting that the strategies did indeed differ for different stimuli. The reverse contrast, one second ISI minus two second, emphasizes the perceptual components of the task, since proportionately more time is spent in perception when between-stimulus delays are shorter. This subtraction yielded mainly posterior activations.

The third study examined changes that occur as a result of repeated exposure to initially unfamiliar stimuli during a relatively short period of time, on the order of about one hour. The main goal of this study was to attempt to identify brain regions that mediate learning on a temporal scale that corresponds to a typical therapy session during rehabilitation. Each subject was exposed to repetitions of either letter strings or false font strings. The same tasks were used, but each subject was exposed to exactly the same stimulus set a total of nine times during the course of a scanning session. Scans were acquired for every other presentation in order to track any changes that might occur in the course of the study. A preliminary analysis of these data suggests that areas of activation tend to become more focused and somewhat more lateralized with repeated exposure.

The fourth study was designed to examine more long-term effects of prolonged and repeated study of new symbol strings. The goal was to test the hypothesis that differences between word and letter string tasks in the left fusiform /occipital regions are due to familiarity of sequences of symbols in a purely visual modality. Subjects were asked to participate twice a day for half-hour sessions for a period of two or three weeks. They were first trained for 6 sessions over 3 days on symbols in a restricted false front alphabet of 12 symbols. They were then trained on a set of 27 or 54 four- character strings composed of these symbols. All training tasks were designed to be performed on a purely visual basis. fMRI scans were performed before the onset and immediately after the end of training. Stimuli in the fMRI sessions consisted of either the trained " words " or of " consonant" letter strings, made of sequences of symbols never seen during training. This is an ongoing study and the data are still being analyzed.

Dr. Liu's research focuses on both the development and application of functional Magnetic Resonance Imaging (fMRI) of human brain. The general research interests are in a) improved MR methods for functional brain mapping, including the measurement of cerebral blood volume and cerebral blood flow in health and in disease; and b) the development and the uses of diffusion MR methods for the early diagnosis of ischemic stroke and the measurement of the biological activity of experimental stroke therapies.

Additional experience has been acquired in the past several years using the echo-shifting based fMRI technique in human auditory signal processing. We have demonstrated successful applications of this technique in the studies of both tonotopic and phonological organization of human auditory cortices in normal volunteers.

PROJECT 1: DEVELOPMENT OF MOTION-ARTIFACT INSENSITIVE 3D FUNCTIONAL MRI TECHNIQUES

The potential clinical applications of fMRI techniques are relatively unexplored. The successful application of fMRI techniques in the clinical (as opposed to the research) environment requires the implementation of rapid pulse sequences insensitive to motion-induced artifacts and capable of imaging large volumes of the brain. This project focuses on the development of the 3D volume scanning fMRI technique employing fast imaging and motion reduction techniques, with high efficiency and low image distortion for whole brain 3D functional mapping. The project consists of two parts: A) development of fast 3D data acquisition techniques in conjunction with the use of echo-shifting to enhance T2* sensitivity, and segmented k-space trajectory to increase the speed; B) development of 3D navigator echo techniques that directly and accurately measure motion induced phase changes, thus allowing motion corrections for rotations and translations in all three directions.

Methods developed and validated in this project will benefit clinical applications of fMRI to various categories of neuropsychological and pathological processes in patients, through both Blood Oxygenation Level Dependent (BOLD) contrast mechanism and direct measurements of relative cerebral blood volume by the injection of a contrast agent. Further development and application to various categories of patients are slated for study.

PROJECT 2: DEVELOPMENT OF SINGLE-SHOT DIFFUSION MRI FOR ACCURATE DIFFUSION MAPPING OF HUMAN BRAIN AND ITS APPLICATION TO ACUTE HUMAN STROKE

Diffusion MRI is a useful method for visualizing early cerebral ischemia and is proving to be an important tool for monitoring noninvasively the progress and treatment of the disease in animal model. Despite a number of successful human applications of diffusion MRI in stoke patients which demonstrate that ischemic lesion can be detected earlier than conventional MRI, diffusion MRI in clinical environments is hampered by its sensitivity to micrometer displacements, and thus, the resulted motion artifacts. Diffusion-weighted Echo Planner Imaging (EPI) has shown great promise, by demonstrating lesion progression in the penumbra region. However, the expensive instrumental upgrade

required for EPI technique and the severe chemical shift and susceptibility artifacts inherent to this technique limit large clinical trials.

This project combines two approaches to overcome the problems of patient motion: 1) single-shot MRI pulse sequence designed for the measurement of diffusion , and 2) advanced navigator motion correction. The basis of the technique is the use of gradient and spin echoes (GRASE) with a modified k-space trajectory and CPMG phase cycle. This single-shot diffusion MR imaging technique with reduced motion sensitivity will allow accurate diffusion mapping of human brain with potential application to acute stroke, on an unmodified conventional clinical instrument without any special hardware.

PROJECT 3: FUNCTIONAL MRI OF PHONOLOGICAL ORGANIZATION IN AUDITORY CORTEX

It has been well established that specific anatomical areas of the superior temporal and inferior parietal cortex, including primary auditory cortex, adjacent auditory association cortex, such as Wernicke's area, and the planum temporale, play an important role in processing speech. The exact relationship between phonological processing of verbal information and the auditory structure has not yet been determined. Our long-term research plan is to seek evidence concerning the location and organization of the cortical regions that transform the acoustic representations of speech into phonological representations. The theoretical premise of our studies is the hypothesis that these transformations involve a spatial remapping of tonotopic representations into phonological representations within auditory cortices.

As the first step towards our overall objective, this study will address three basic aspects of auditory processing in humans, using fMRI: 1) Initial experiments will use simple auditory stimuli (pure-tones) that vary along the frequency axis to define the tonotopic organization of human auditory cortex. In particular, we will seek evidence of additional tonotopic representations outside the primary auditory cortex, and will evaluate the spatial location and boundaries of these multiple tonotopic areas. 2) In contrast to pure tones, activation associated with more complex stimuli, such as band-passed noise bursts and frequency modulated sweeps with differing center frequencies, will be compared as a function of stimulus complexity, thus allowing a systematic investigation of how these cortical areas participate in the hierarchical processing of auditory signals. 3) Finally, using phonemes and scrambled phonemes that are spectrally identical, we will seek to delineate the acoustic features of speech processing and phonological aspects of auditory representations.

The empirical bases for this project are our preliminary fMRI studies of hierarchical processing within human auditory cortex. Our previous human studies demonstrated frequency-specific activation in the primary auditory cortex. Furthermore, we have demonstrated that secondary auditory cortical fields exhibit stronger activation in response to stimuli having phonetic properties of speech in contrast to spectrally identical stimuli lacking the temporal structure of speech sounds.

PROJECT 4: FUNCTIONAL MRI STUDIES OF NEUROANATOMY OF TINNITUS

Tinnitus refers to auditory sensations that cannot be attributed to any external source. It is a severe psychological and clinical problem for which there is, currently, no realistic animal model or objective measurement tool. Although a recent neuroimaging study of tinnitus using PET has demonstrated

evidence for limbic system links and neural plasticity, little is known about the brain areas involved and there are few indications for a particular therapy. Our recent work on normal subjects using a 3D fMRI technique demonstrated activation of the superior temporal gyrus in the perception and processing of various auditory stimuli, including pure tones, non-speech noise, and speech sounds. Functional MRI techniques could therefore play an important role in the management of patients experiencing tinnitus.

In collaboration with Dr. Kenneth Grundfast, professor and acting chairman of the department of Otolaryngology at Georgetown, the research project intends to evaluate these techniques for the study of cerebrocortical activity in patients with auditory cortex pathologies, in particular tinnitus. A special emphasis will be on the effectiveness for the reduction of motion artifacts and image distortion. Using fMRI, we will pinpoint brain regions associated with the existence of tinnitus. To accomplish this goal, the intensity of tinnitus will be varied, and the corresponding change in brain activity will be measured. Previous studies show that broadband white noise and masking can partially alleviate the ringing sound perceived as tinnitus. The results of this study would aid in understanding the mechanism of tinnitus and more importantly may provide a physiologic correlate to measure changes in tinnitus. This marker could then be used to quantify patient response to medications, biofeedback, habituation therapy and other treatments for tinnitus.

MICHAEL ULLMAN, Ph.D.

Our use of language depends upon a *mental lexicon* of memorized words, and a *mental grammar* of rules that combine lexical forms into larger words, phrases, and sentences. Together, these two capacities provide us with the ability to produce and to comprehend an infinite number of sentences. However, fundamental questions about the brain bases of the two capacities remain unanswered. In particular, two very different theoretical frameworks have been competing for the explanation of their basic functional neuroanatomy. Whereas "dual-system" theories link the lexicon to temporal cortex, and grammar to frontal cortex, "single-system" theories link both capacities to a single network with broad anatomic distribution. Dual-system theories predict dissociations between lexicon and grammar, whereas single-system theories do not. However, testing for lexicon/grammar dissociations has been problematic because tasks probing for lexicon and for grammar usually differ in ways other than their use of the two capacities. We have therefore developed an innovative approach to test the competing views. We will investigate the brain bases of irregular and regular word transformations, in which lexicon and grammar can be contrasted, while other factors are held constant. Irregular transformations are largely arbitrary (e.g., *cling-clung, bring-brought*), and therefore must be memorized in the lexicon, whereas regular transformations (e.g., *look-looked*) can be described by rules of grammar (e.g., an *-ed*-suffixation rule). A dual system view predicts double dissociations between regulars and irregulars, with irregulars (lexicon) linked to temporal cortex, and regulars (grammar) to frontal cortex.

Dual-system theories usually assume components dedicated ("domain-specific") to language, whereas single-system theories assume general-purpose ("domain-general") circuitry. However, the dual-system/single-system issue is logically independent from the domain-specific/domain-general issue. We have proposed a third alternative — that *dual* but *domain-general* systems subserve lexicon and grammar. Specifically, we posit that the lexicon/grammar distinction is tied to a fundamental distinction between two well-studied memory systems in the brain: The memorization and use of words depends upon a temporal-lobe "declarative memory" system previously implicated in the learning and use of facts, whereas the learning and use of grammatical rules depends upon a frontal/basal-ganglia "procedural memory" system previously implicated in the learning and use of motor and cognitive skills.

PROJECT 1: NEUROLOGICAL STUDIES OF LANGUAGE

Double dissociations between irregulars and regulars in our studies of patients with impairments of either declarative or procedural memory support this theory, and suggest that the basal ganglia' well-studied role in motor activity extends to grammatical rule use. Specifically, we asked brain-damaged patients to produce the past tense of regular verbs like "walk" and made-up verbs like "wug" (Both of which should require a rule), and of irregular verbs like "think" (which should require memory lookup). We found that patients with damage to brain structures underlying declarative memory (patients with a stroke in left temporal cortex as well as patients with Alzheimer's disease, who have a degenerative disease primarily afflicting the temporal lobes) were worse at producing or reading past tense forms for irregular verbs than for regular or novel verbs. In contrast, patients with damage to brain structures underlying the procedural system (patients with a stroke in left frontal cortex as well as patients with Parkinson's disease, who have a degenerative disease of the basal ganglia) showed the opposite pattern: They were worse producing forms like "walked" and "wugged" than forms like "thought." Unlike patients with Parkinson's disease, whose basal ganglia damage resulted in suppressed movements (trouble starting and carrying out movements) and suppressed rule use ("Yesterday I walk into town"), the different type of basal ganglia damage in patients with Huntington's disease which leads to unsuppressible movements (irrepressible dance-like movements called chorea) also led unsuppressible rule use ("Yesterday I walkededed into town, and dugged a hole").

The demonstration of an analogous dissociation in another language would strengthen the dual-system hypothesis. Italian is a richly inflected language in which a regular/irregular distinction may be found in

present tense and past participle inflections. Six Italian patients with probable Alzheimer's disease were asked to produce regular and irregular present tenses ("Mi piace *bere* il vino. Allora ogni giorno _____ il vino") and past participles ("A Giovanni piace *chiudere* la porta. Allora ieri Giovanni ha _____ la porta"). All 6 patients had greater difficulty producing irregular than regular present tenses (mean 72% vs. 88% correct, $p < .05$) and past participles (86% vs. 98%, $p < .05$) (Cappa & Ullman, 1998). These results from English and Italian inflectional morphology link the use of irregulars (lexical memory) but not regulars (grammatical rules) to the use of facts, and are consistent with a role for temporal lobe circuits in word and fact use.

PROJECT 2: EVENT RELATED POTENTIAL (ERP) STUDIES OF LANGUAGE

We have been investigating the brain bases of lexicon and grammar using the electrophysiological technique of measuring the Event Related Potentials (ERPs) associated with the presentation of stimuli. Previous evidence had suggested that lexical or semantic violations yield somewhat right lateralized central/posterior negativities ("N400"), whereas grammatical violations can yield left anterior negativities ("LAN"). Unfortunately, the tasks tapping these lexical and grammatical capacities have not been well-matched in factors other than the two capacities. Therefore we have been investigating the electrophysiological basis of lexicon and grammar by probing the use of irregular and regular forms.

Right-handed males viewed sentences that appeared, one word at a time, on a monitor, while ERPs were being recorded. In Experiment 1, all sentences were framed in the past tense. Subjects were shown 64 regular verbs matched on frequency, orthography, and phonology to 64 irregular verbs. Half of each were presented in the correct past tense form (Yesterday I looked at Sue), and half in the stem form (Yesterday I walk after lunch), the latter being a morphological violation. In Experiment 2, these sentences were intermingled with sentences which contained either errors of meaning (e.g., I drank my coffee with *dog*) or of sentence-level grammar ("syntax") (e.g., I drank my *with* coffee sugar).

We found that violations of regular verb inflection and of syntax yielded a left anterior negativity (LAN), while violations of irregulars and of meaning elicited enhanced negativities with a right-lateralized, more central distribution (an N400) (see Figure 1).

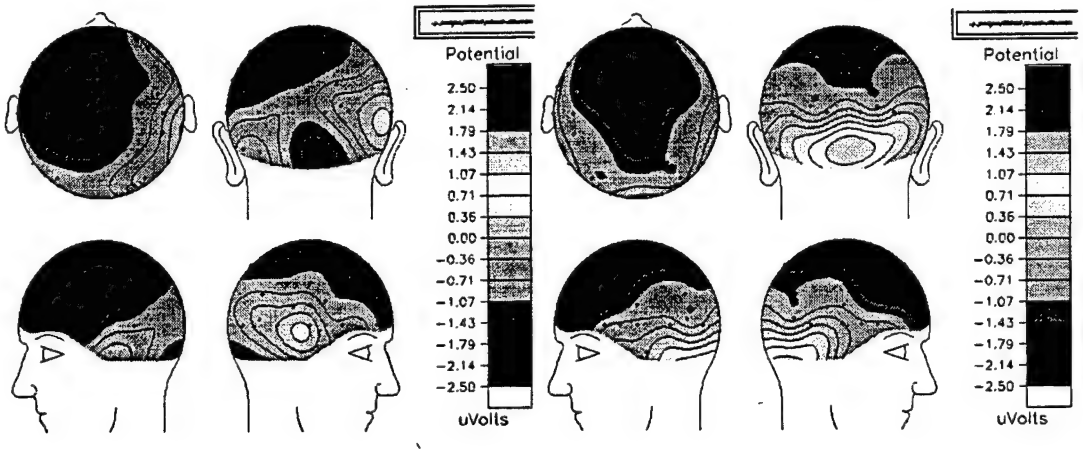

Figure 1: Voltage maps associated with the presentation of incorrect vs. correct regular (left) and irregular (right) past tense forms.

These experimental results indicate that lexicon and grammar are associated with distinct electrophysiological signals and subserved by distinct neural processes. They confirm that grammar is associated with left frontal regions, whereas lexical processes are dependent upon more posterior regions.

PROJECT 3: FUNCTIONAL MAGNETIC RESONANCE IMAGING (FMRI) OF LANGUAGE

We have also been investigating the brain bases of lexicon and grammar with functional brain imaging. In a collaboration with Robert Savoy and Kathleen O'Craven of the Massachusetts General Hospital and Harvard University, we have carried out a functional magnetic resonance imaging (fMRI) study of English irregular and regular past tense production.

Five healthy right-handed men were shown the stems of irregular verbs (*sleep*) and non-rhyming regular verbs (*slip*) on a screen, and were asked to silently produce their past tense forms. Twenty seconds of regulars (10 verbs) were followed by 20 seconds of fixation, 20 seconds of irregulars (10 verbs), and 20 seconds of fixation. This sequence was repeated for 80 irregular and 80 regular verbs. Functional scans were obtained using an Asymmetric Spin Echo pulse sequence with a TR of 2 seconds. We examined 12 axial oblique slices spanning the frontal, temporal, and occipital lobes, and the cerebellum. All functional data were motion-corrected using a modification of the AIR algorithm. Functional data from each subject were then transformed into Talairach space. Signed Kolmogorov-Smirnov statistics were calculated for three comparisons: Regular vs. Fixation, Irregular vs. Fixation, and Irregular vs. Regular. In addition to examining the data from each individual subject, the Talairach transformations allowed us to combine the data from all five subjects.

The 5 subjects showed similar patterns of activation. We found overlapping as well as distinct patterns of brain activation for the irregular and regular conditions. All activation changes were confirmed with time-course analyses (Figure 1). Compared to fixation, both the irregular and regular conditions yielded activation increases in inferior frontal regions (including Broca's area), and in the basal ganglia (in the caudate nucleus). This suggests that these regions may subserve a function common to both past tense types, such as the computation of the grammatical tense feature.

Left temporal and temporo-parietal regions were associated with an activation decrease for irregulars, but not for regulars. In contrast, a left prefrontal region was associated with an activation increase for irregulars, but a decrease for regulars. Interestingly, the activation increase in left prefrontal cortex, and decrease in superior temporal cortex associated with irregulars, but not regulars, was also observed during a verbal fluency task (generating words in a category). While the specific causes of these activation changes remain to be investigated, the double dissociations suggest that irregulars and regulars have distinct neural underpinnings linked to temporal and frontal regions. It is also of interest that the patterns of activation reported for a recent PET study of German regular and irregular past tense processing are similar to those found in this study, and therefore may also in part be explained by activation decreases.

We have tested 4 additional subjects, all women, and are currently examining whether their patterns differ from those of the 5 male subjects. We have also run several subjects on a version of the task in which regular and irregular verbs are presented in a randomized rather than a blocked sequence. We have acquired images after each verb, thus treating each verb as a distinct trial. Such "single-trial fMRI" (also termed "event-related fMRI") is a promising new technique which may allow us to observe the time course for each linguistic event. The technique avoids the problems inherent in presenting blocks of stimuli of the same condition.

PROJECT 4: THE ROLE OF THE CEREBELLUM IN LANGUAGE

The cerebellum has long been thought to have a role in movement. However, recent evidence from studies of patients with cerebellar lesions and from functional brain imaging studies have implicated the cerebellum in cognition. We have been investigating whether the cerebellum has a role in language, and in particular, whether it may play different roles in lexical memory and grammatical processing.

In a collaboration with Jeremy Schahmann of the Massachusetts General Hospital (MGH) and Harvard Medical School and Hilary Bromberg of Harvard University, we tested a 38 year old monolingual man (W.W.), whose brain MR showed diffuse cerebellar atrophy but was otherwise unremarkable, was given 3 tasks: Past tense production ("Every day I *dig* a hole. Yesterday I _____ a hole"), plural production ("Here is one *mouse*. Here are three ____"), and the reading out loud of words with regular (*pool*) or irregular (*wool*) pronunciations.

W.W. was worse at irregulars than regulars: at producing past tenses (5% vs. 22%, $p<.05$) and plurals (33% vs. 89%, $p=.05$), and pronouncing words (67% vs. 92%, $p<.05$).

Cerebellar atrophy can lead to a deficit of lexical memory, while leaving rule processing relatively spared, in the domains of both morphology and reading out loud. These dissociations underscore a role for the cerebellum in the search or retrieval of lexical knowledge, and suggest that it may be less important for rule processing. The results strengthen the link between words and facts, and further dissociate these from rule processing

In a continuing collaboration with Dr. Schahmann, we are testing additional patients with atrophy or lesions of the cerebellum, in the hope of finding one or more patients who show the opposite pattern to that revealed by W.W. — that is, who show greater difficulty with regular than irregular forms, and more generally with grammar and rule use than words and memory use. There is evidence from two Italian patients that such cerebellar patients might exist. If we demonstrated such a double dissociation between W.W. and the rule-impaired cerebellar patient, it would indicate that the different portions of the cerebellum play roles in both memory and rule use, underscoring the importance of the cerebellum in language.

ANIMAL COGNITIVE NEUROSCIENCE: There are four faculty members who are grouped into this area. Dr. Kanwal investigates the processing of communication sounds and modeling of a neural network for multidimensional analysis of speech sounds and pattern recognition. Dr. Pekar utilizes magnetic resonance imaging (MRI) to evaluate brain structure, physiology, and function. Dr. Rauschecker examines the functional organization and plasticity of the cerebral cortex with an emphasis on the auditory cortex and multi-modal processing using single-neuron microelectrode recording, optical recording, and functional MRI. Dr. Wu studies large-scale neuronal events and distributed processes in the CNS.

JAGMEET KANWAL, Ph.D.

The major goal of Dr. Kanwal's research is to elucidate normal auditory processes involved in the coding/decoding and perception of communication sounds. The dogma challenged by his research is that animal studies can teach us little, if anything, about two of the most highly specialized functions of the human CNS, namely, perception of speech and music - two related facets of human cognition that make us unique from all other animals. It appears, however, that to really understand the neural mechanisms and neurophysiological principles underlying speech-sound perception one must study its minimal analogs present in an animal CNS. This has led to significant progress in the last decade, in our understanding of early auditory processing that underlies speech production as well as perception in humans. Similarly, basic phenomena such as perception of the "missing fundamental" that can be equated to certain aspects of music perception have been recently demonstrated at the psychophysical and neurobiological levels in bats and primates, respectively.

Dr. Kanwal's research uses multiple approaches to investigate auditory processing within higher levels of the CNS in auditorily specialized animals, such as bats. These approaches include single cell electrophysiology, evoked potentials and ERPs and functional MRI as well as behavioral techniques. A quantitative methodology incorporating advanced statistical analyses is stressed. One electrophysiology set-up is up and running and a second one is potentially functional. This is presently being used for conducting acoustical and behavioral analysis of communication sounds. Dr. Kanwal together with his colleagues enabled GICCS to set up a core histology/imaging facility that will open up new avenues of research. Results obtained from several ongoing/completed research projects, supported in part by the Institute are categorized under three themes and briefly described below:

PROJECT 1: AUDITORY COMMUNICATION IN BATS: ACOUSTICS, BEHAVIOR AND NEUROPHYSIOLOGY.

Mustached bats depend largely on their auditory systems to survive in their ecological niche just as humans are uniquely equipped for survival by their ability to communicate acoustically. The significance of the single development of "'speech" in humans is especially clear when one considers human evolutionary history. For several reasons, the auditory system of bats is an excellent model to study neural mechanisms that may underlie processing of communication sounds in mammals, including speech sounds in humans. For example, recent studies suggest that the bat's cortex shows hemispheric asymmetry for processing communication sounds. In addition, the presence of combination-sensitive neurons and multidimensional representational schemes for processing complex syllables in the auditory cortex may be applicable to speech sound processing as well. Not surprisingly, the field of communication sound processing is re-emerging as an actively growing field as it attempts to understand

the neural basis of speech perception and its commonalties with the audio-vocal system of mammals at the single neuron level. Bats are useful models also because they employ a complex repertoire of sounds for acoustic communication rivaling that of the most vocal primate species. Even though the auditory system of microchiropteran bats is the best studied among mammals, previous neurophysiological studies on audition in bats have mostly focused on their echolocation behavior.

Project 1A. Call variation in two subspecies of mustached bats, *Pteronotus parnellii:* do bats have dialects? N. Dietz, J. Peng and J.S. Kanwal

The vocal repertoire of any adult animal is constrained by its acoustic environment during development, ontogenetic learning processes and its genetic heritage. Thus, geographically isolated populations of a species, e.g., some song birds, may learn to use different dialects. Among mammals, studies of call variation and ontogenetic vocal learning are limited to only a few primates and one bat species.

To test for significant acoustic variability across different populations of *Pteronotus parnellii*, we compared the acoustic structure of calls obtained from 11 individuals of *Pteronotus portoricensis* that is geographically isolated from *Pteronotus p. parnellii.* The variation in the acoustic structure of social calls in *P.p. parnellii* have been studied in detail and classified into 33 different types of syllables on the basis of sound spectrograms. These may be emitted either independently as "simple syllables" or in combination as "composites" (a sequence of two or more simple syllables without any silent interval). The three main classes of simple syllables include constant frequency (CF), frequency modulated (FM), and noise burst (NB) calls that often contain complex harmonic structures and amplitude-modulations. Audio-video recordings were obtained from groups of 2 to 4 animals of *P.p. portoricensis* in a manner similar to that used for *P.p. parnellii* . Spectrographic analysis showed that *P.p. portoricensis* emitted at least 14 of the 19 simple syllables originally described for *P.p. parnellii*.. Two new FM syllables were observed and two others were categorized as rare variants of those (descending Rippled FM and bent Downward FM) emitted by *P.p. parnellii.* Several composites in the vocal repertoire of the two subspecies were similar. Two new composites observed in *P.p. portoricensis* consisted of combinations of 3 simple syllables emitted within a long "phrase". These data suggest that different subspecies of mustached bats may use different dialects for social communication.

Project 1B: Responses to communication sounds in the A1-posterior region of the primarly auditory cortex. J. P. Peng and J. S. Kanwal

Details of the surgical and chronic recording techniques have been described elsewhere. During the 4 to 8 hour recording session the awake bats were continuously monitored via video for signs of discomfort or distress. Extracellular recordings were obtained from either the left or right side of the A1-p cortical area of mustached bats (n = 5) using custom-made lacquer-coated tungsten microelectrodes (tip diameter: 4-8 μm). Single-units were isolated on the basis of spike height and slope of the waveform with a level and time window discriminator. The calls used as stimuli were digitized, manipulated and played back using an A/D-D/A-converter board (Data Translation, DT2821G; 250 kHz sample rate) and SIGNAL software. Acoustic signals mimicking the bats' echolocation sound ("pulse") and "echo" were generated with conventional analog equipment. The results from this study are summarized below and examples of tuning curves (figure 1) are presented on the following page:

Animal	Sex	# of cells in Right A1P	# of cells in Left A1P	Mean Best Excitatory Frequency (BFE)	Total # of recorded units
Mark	Female	*	10	41.26KHz	10
Mike	Female	11		23.78KHz	11
			10	22.88KHz	10
Dali	Male	6	*	22.54KHz	6
Daisy	Female	10		23.71KHz	10
			6	22.58KHz	6
Lily	Female	3		22.77KHz	3
			2	21.87KHz	2
Total		30	28		58

We conclude that the A1-p "tonotopic" region contains only a diffuse tonal clustering of neurons rather than well defined tonotopy. These neurons are broadly tuned to communication calls as well as to tones. Double or triple-peaked tuning curves have best frequencies that are harmonically related. A specially dense clustering of neurons tuned to 22 kHz and 44 kHz is observed. Although, a somewhat subtle contradiction, this result may have important bearing on what is really important for encoding auditory information. We believe selective, magnified representation and not tonotopy is the primary underlying computational principle for auditory processing.

Project 1C: Computational approaches to call processing: profiling response patterns in the auditory cortex

This project was initiated in collaboration with Dr. Masakiyo Suzuki from Hokkaido University in Sapporo, who visited the laboratory of "Auditory Communication and Cognition" for a two month period. This ongoing project aims to understand what is the most important component (where is the information?) in the response of auditory cortical neurons.

Project 1D: Acoustic communication behavior in mustached bats

This study was begun at Washington University in St. Louis and is being continued at Georgetown University. Significant progress on this project was made by an MD/PhD student, Nicole Dietz, during a second summer rotation in the laboratory.

Different types of calls are associated with different behaviors in bats. These data are promising for planning additional studies to investigate the rate and level of information flow during acoustic communication in mustached bats.

Project 1E: Functional MRI of the auditory cortex in mustached bats

In bats, the auditory system is of critical importance for echolocation and communication. Echolocation involves use of sound pulses for "visualizing" the surroundings and for feeding (insect pursuit), whereas communication is important to carry out the various social activities. Since most insectivorous bats live in the darkness of caves and hunt at night, they cannot use visual cues so that the auditory system is highly developed to compensate for lack of substantial visual information. Studies of neural processing

TCUR-A1P-42# BFE=20.9KHz BAE=-15dB

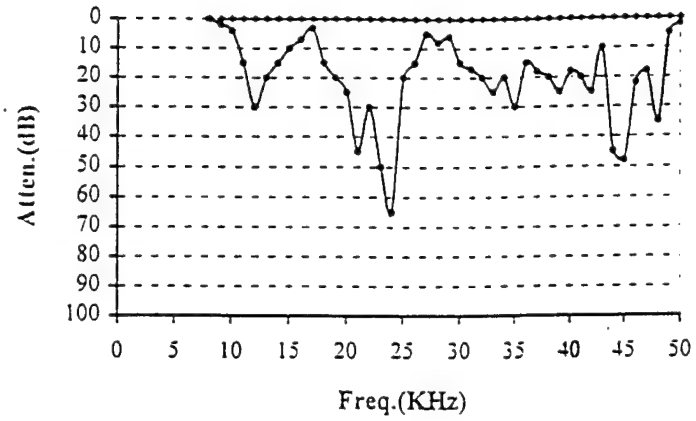

TCUR-A1P-43# BFE=43.2KHz BAE=-10dB

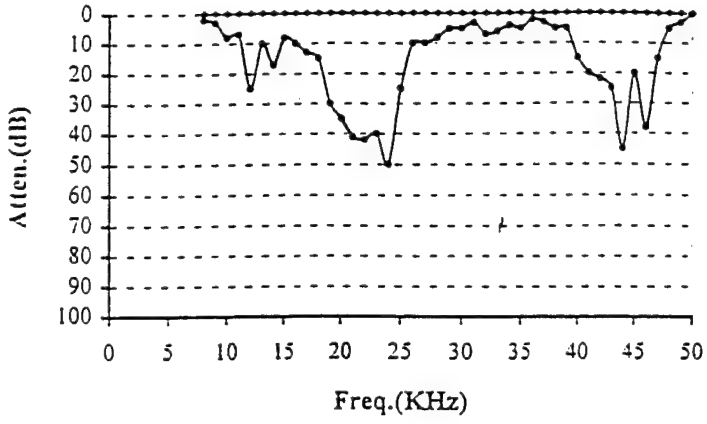

TCUR-A1P-30# BFE=42KHz BAE=-25dB

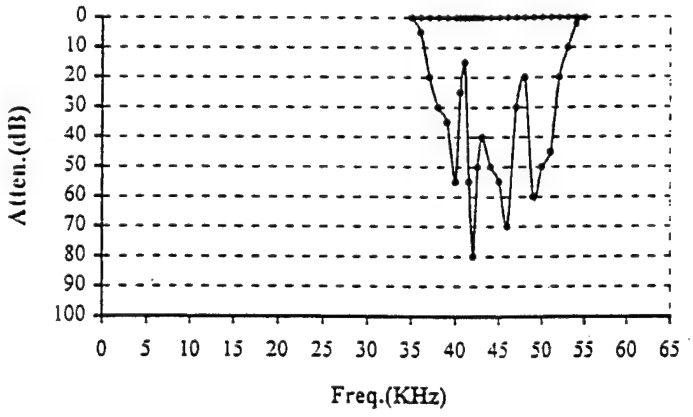

TCUR-A1P-44# BFE=20.5KHz BAE=-15dB

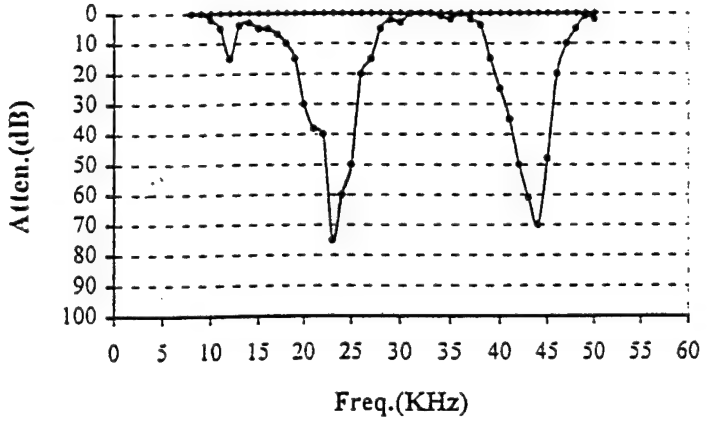

TCUR-A1P-45# BFE=23.2KHz BAE=-20dB

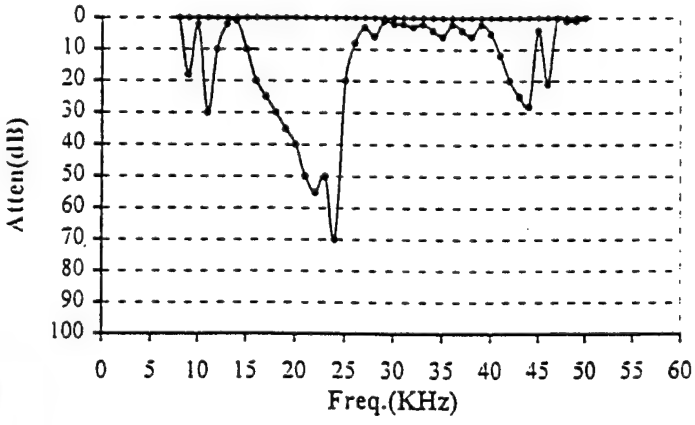

TCUR-A1P-46# BFE=19.2KHz BAE=15dB

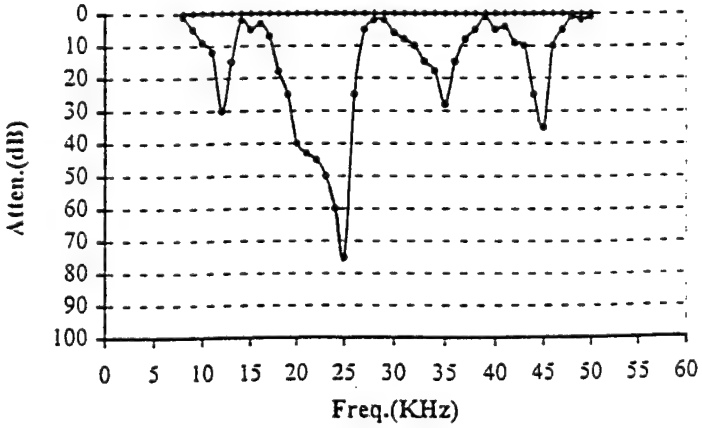

Figure 1

in the auditory cortex have revealed a high degree of mapped organization where different components of the echolocation signal are segregated within the ascending auditory system and analyzed within separate cortical maps. Recent studies of communication sound processing, however, reveal a distributed mode of processing where a complex communication sound is represented synchronously in an unmapped fashion within different areas of the auditory cortex. These different cortical representations for processing echolocation and communication signals do not have a clear anatomical basis, but are reconstructed or "imagined" on the basis of recorded neural activity. This research is aimed at directly imaging these "imagined" cortical representations that appear to be overlaid within the same neural circuitry. A quick way to resolve these distinct representations is to present sounds to the animal and use fMRI technology (in collaboration with Dr. Kamada and Dr. Pekar to visualize the cortical activity).

We have obtained both structural and functional NMR images from unanesthetized animals. This is critical for studies on the neurobiological basis of cognition where cortical activation is necessary. We are now poised to obtain useful new data by presenting various kinds of auditory stimuli. A paper has been submitted to "Brain Research Protocols" for publication.

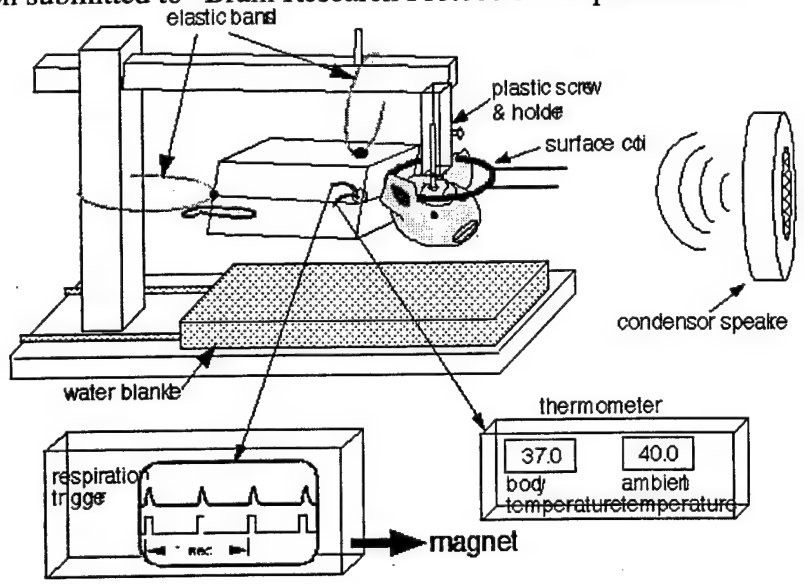

Fig. 2. A. Schematic showing the set-up used to position an awake bat in a surface coil within the bore of the 7 tesla magnet. The nylon post attached on the skull is fixed with a plastic clamp. The auditory stimuli are delivered from a non-magnetic, condenser speaker in front of the immobilized head of the bat. Arrows point to the instruments used to record physiological parameters.

PROJECT 2: MUSIC PERCEPTION IN HUMANS: ACOUSTICS, NEUROPHYSIOLOGY AND IMAGING.

Early psychophysical studies on music perception have yielded interesting data. This independent though related line of research is being pursued in parallel with other studies. Music is the combination of complex and pleasant vocal/instrumental sounds or tones consisting of rhythm, melody and harmony. Music can facilitate all biological drives and motivation and generate states of relaxation and ecstasy which play an important role in creating a sense of well being. The underlying neural basis of these effects, however, is largely unexplored.

Project 2A: Imaging human cortical areas involved in perception of speech, environmental and musical sounds. K. Kamada and J.S. Kanwal.

This research was initiated over an year ago and with adequate postdoctoral support will be continued in collaboration with Dr. Liu (music perception) and Dr. Eden (speech perception). The figures on the following two pages are the results obtained from preliminary studies of auditory processing in the 1.5 T research magnet acquired by GICCS.

Figure 3 shows a single individual showing differences in activation areas based on presentation of one's native language (Chinese), second language (English) and an unknown language (Japanese). Figure 4 shows activation of different cortical areas while actively listening to the first language and music

PROJECT 3: TECHNOLOGICAL INNOVATIONS: SOFTWARE AND HARDWARE ENGINEERING

Project 3A: "Human Auditory Stimulation" software for fMRI studies for Windows 95™

A customized program, "SOAP" (Sound Optimization And Presentation) was developed for use in the MRI environment. A version for the DOS™ platforms is in development. Two devices critical for conducting auditory research on bats were constructed. These are not available commercially and therefore have a marketing potential as well.

Project 3B: Programmable Signal Attenuator

SPECIFICATIONS

Inputs
- signal (analog)
- trigger (digital; TTL and CMOS compatible)
- power supply (12V DC, 1A)

Outputs
- attenuated signal (analog)
- trigger (digital; TTL and CMOS compatible)

Programmable Parameters

signal attenuation	0 - 127 dB
attenuation step size	-99 to 99 dB
total triggers per change in attenuation	1 – 999

Controls
- Three dials: one for each parameter.

Display
- The current attenuation, the attenuation step size, and the trigger countdown are displayed.

Attenuator Specifications:

attenuation range:	0 - 127 dB (resolution = 1 dB)
nominal impedance:	50 ohms
frequency range:	0 - 200 kHz

Chinese

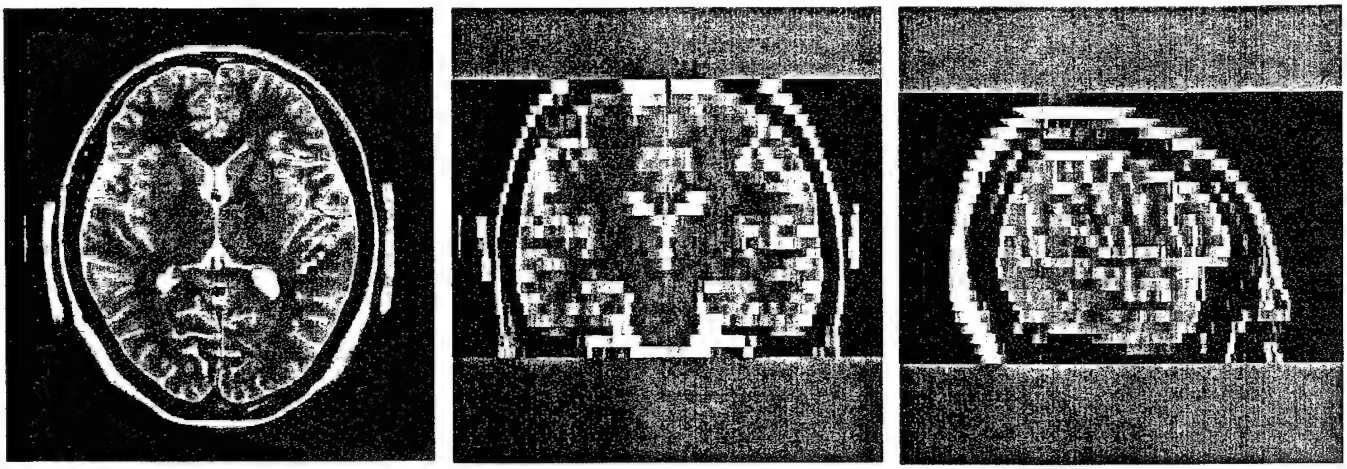

English

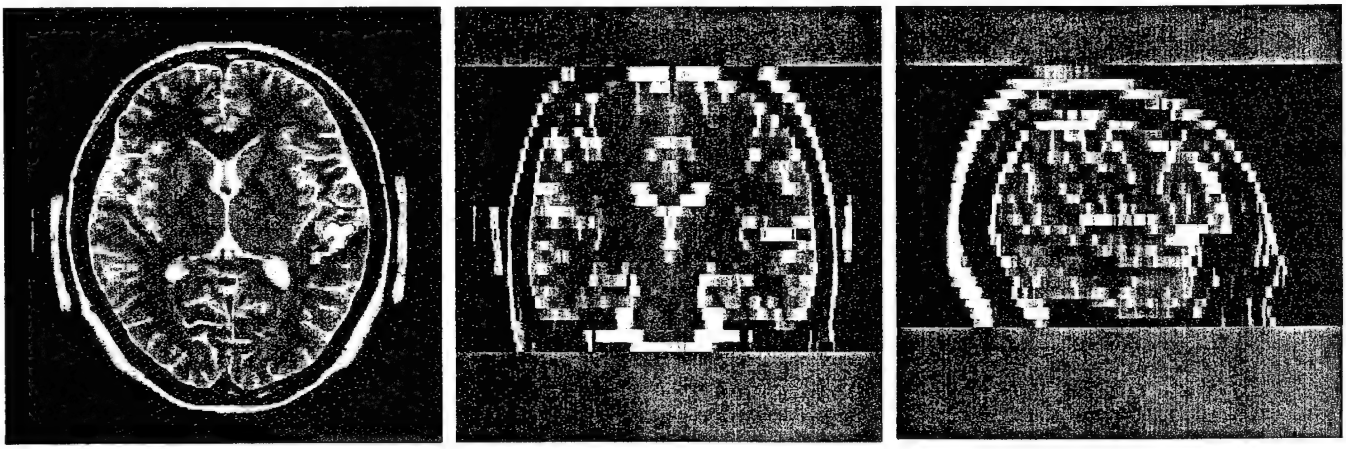

Japanese

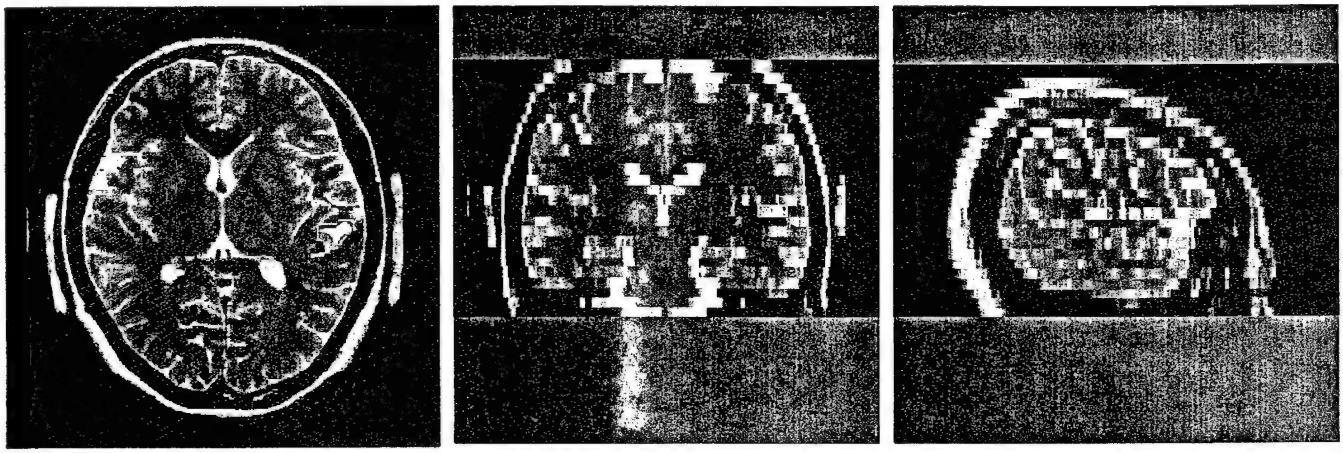

Figure 3

Figure 4

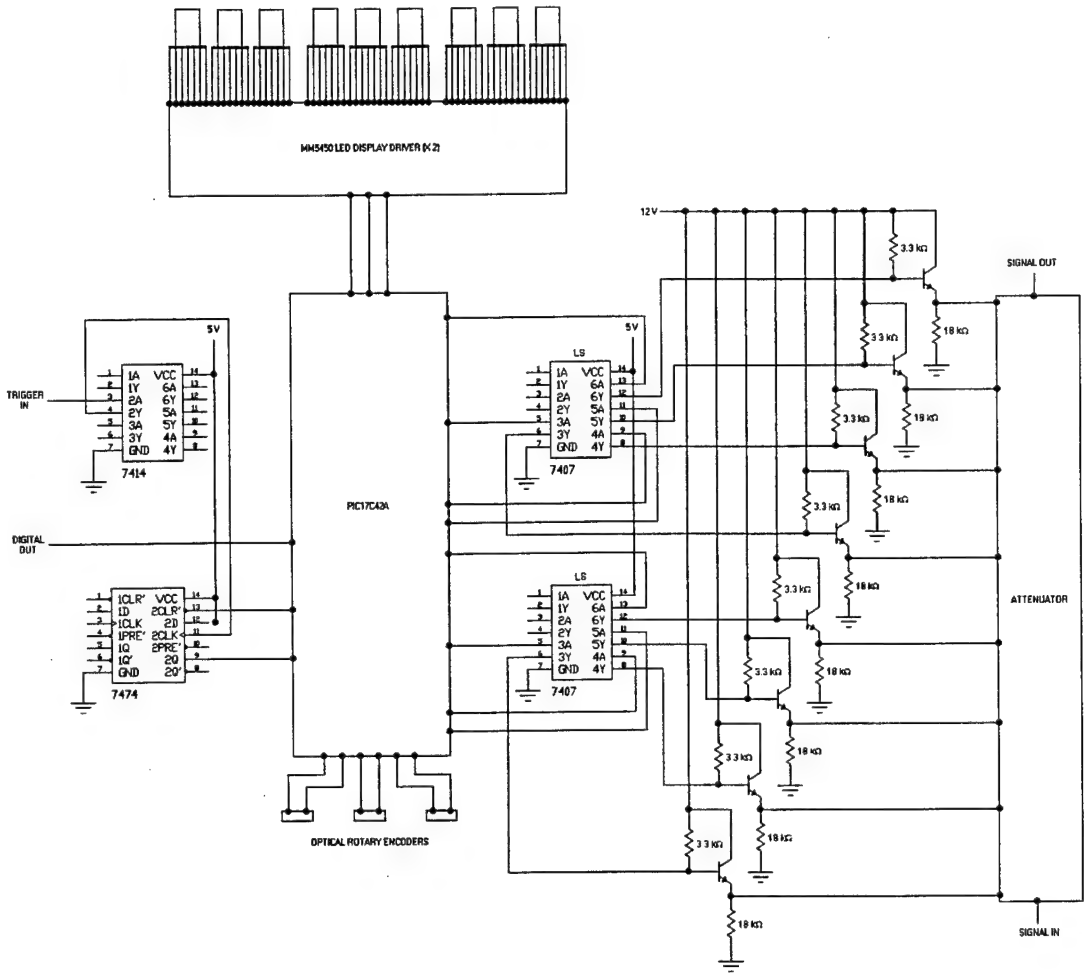

Figure 5: Circuit diagram of the programmable/manual attenuator.

Project 3C: Resting CF_2 Frequency Counter:

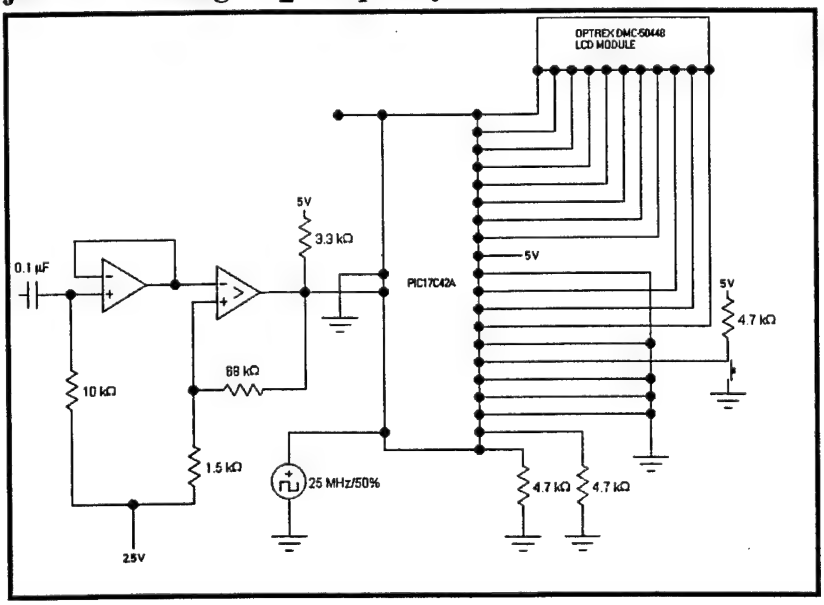

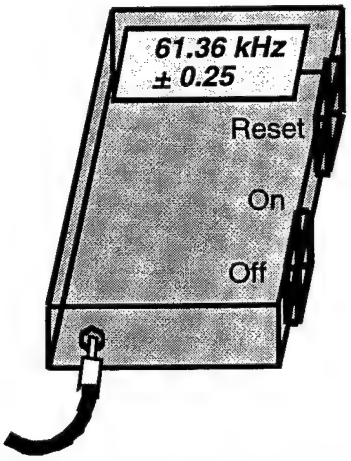

Figure 6: Circuit diagram of the CF_2 counter (left) and the display panel and controls of the device. This device receives input from a commercially available bat detector.

SPECIFICATIONS

Inputs:
signal (analog)
power supply (9 V battery)
Controls:
One reset button.
Display:
Displays average frequency and standard deviation.
Frequency Counter Specifications:
frequency range: 50 - 70 kHz
precision: +/- 10 Hz

This portable device is designed to be connected directly to the high frequency output of a bat detector.

Project 3D: "Bubble tester": for checking integrity of insulation of resin-coated metal electrodes.

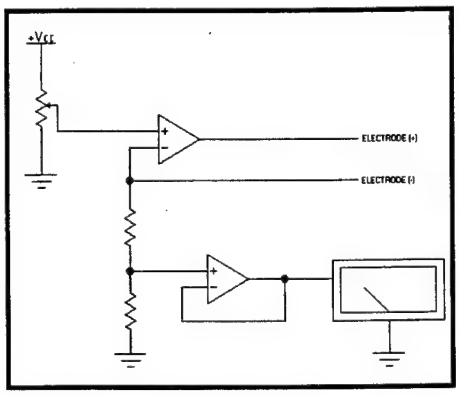

Figure 7. Circuit diagram of the constant current device for testing of electrode insulation.

Data obtained from above described studies on communication sound processing will allow this laboratory to explore novel mechanisms and formulate new principles of auditory processing, especially at the cortical level. New methods to be developed over the next two years include telemetry and multi-site single unit recordings from awake bats and, in collaboration with Dr. Wu, optical imaging of cortical activity. Innovative technological developments expected to take place in this and other laboratories will facilitate this research. The long-term goal is to elucidate both similarities and differences in communicative auditory processing at the cellular and systems levels between animals and humans.

JAMES J. PEKAR, Ph.D.

The Neurobiological Magnetic Resonance Laboratory, dedicated to the application of nuclear magnetic resonance to the study of brain anatomy, physiology, and function, made considerable progress in its third year, both in the development of advanced biomedical engineering technology for brain imaging, and in the application of this technology to questions in neurobiology.

Functional MRI of the brain reveals brain regions subserving a variety of tasks, using deoxyhemoglobin as an endogenous MRI contrast agent reporting on hyperemia concomitant to neural activation. One key to the success of human fMRI is the ability to perform longitudinal studies within the same individual. Such serial studies allow for evaluation of test-retest robustness, as well as investigation of plastic processes including development, learning, and the effects of therapy and therapeutics in cases of pathology. However, while serial studies are of crucial importance to human fMRI, they have not yet been applied to animal models: The application of functional MRI to animal models has generally been performed using acute animal preparations, which rule out studies lasting longer than a single MRI examination. In contrast, we have pioneered the use of non-acute animal preparations for fMRI studies: We are using non-acute animal preparations to pursue functional MRI studies of visual stimulation in cats and auditory stimulation in bats.

The greatest challenge of the last year was that our primary resource, our seven Tesla superconducting magnet, "quenched" (lost it's field) on New Year's Day, 1998. The magnet was re-energized by Bruker Medical Systems, without incident, in early February.

Our goal remains the development of a develop a state-of-the-art facility for magnetic resonance imaging of brain structure, physiology, and function, with outstanding spatial and temporal resolution. Following re-energization of the magnet, our laboratory is fully operational. Recent progress includes enhancement of methods for precise synchronization of MR data acquisition and stimuli provision with the subject's respiration.

Radio-frequency hardware is essential for high-sensitivity imaging. We have recently received two custom-built quadrature head coils sized for mice and rats.

We also are developing a "physiological infrastructure" for MRI in live subjects; this project has three goals: (1) To apply biomedical engineering principles to develop apparatus for the monitoring of physiological parameters (e.g., temperature, respiration, electrocardiogram) during MRI scanning; (2) To develop means of providing multimodal sensory stimulation to animals while they are in the seven Tesla magnet; (3) To synchronize MRI acquisitions and sensory stimuli to the subject's respiration; this last area has shown much progress this year.

Our physiological monitoring setup not only allows us to continuously evaluate the physiological state of the animal, but also enables us to gate the spectrometer to the animal's natural respiratory and cardiac cycles. We see very little motional artifacts in the high resolution images which have been gated to the animal's respiration. Careful choice of delay times enables us to observe substantial structural details. Information on the location of the microvasculature may provide valuable insight into the understanding of functional MRI data.

Because these techniques are minimally invasive, the amount of stress placed on the animal is greatly reduced. This allows repeated scanning of the animal on separate days, enabling the possibility of serial studies to study phenomena such as experience dependent plasticity, or the timecourse of CNS disorders.

Research Area 1: Functional Brain Mapping

This area of our research activities uses magnetic resonance imaging as a non-invasive probe for brain function, by exploiting deoxyhemoglobin as an endogenous contrast agent. We desire to use MRI to study cortical representations of a variety sensory modalities, and to study plasticity of these cortical representations. Our collaborators include Dr. Dae-Shik Kim, a Research Instructor in GICCS; Prof. Josef Rauschecker of GICCS, and Dr. Biao Tian of his laboratory; Prof. Jag Kanwal of GICCS, and Dr. Kyousuke Kamada of his laboratory; Prof. Jian-Young Wu of GICCS; Prof. Guoying Liu of GICCS; Dr. Dov Malonek of the Weitzmann Institute; and Dr. Peter Jezzard of the National Institutes of Health.

PROJECT 1: FUNCTIONAL BRIAN MAPPING: VISUAL CORTEX

Our goals were: (1) To map the hierarchical cortical representations of visual stimuli using functional magnetic resonance imaging in cats; (2) to compare these maps with maps from intrinsic optical imaging; (3) to use the non-invasive functional MRI mapping to study developmental plasticity in the visual cortex. Dr. Dae-Shik Kim plays a leading role in these studies, which are performed in collaboration with the laboratory of Dr. Josef Rauschecker. We have developed fMRI methods especially suited for longitudinal studies in developing animals. As optical imaging studies have shown that the strongest signals in cats result from orientation domains in area 18 of kittens, we performed fMRI studies of the visual cortex of kittens, using stimuli known to drive orientation-specific neurons in area 18.

Figure 1 sketches the he equipment associated with the "cradle" used to position the subject within the magnet for functional MRI of visual-stimulus induced activation in kitten visual cortex. Adolescent cats were anesthetized, intubated, and placed in a water-heated blanket inside a custom-made cylindrical cradle. Mouth-bar and head-holder were used to fix the head position. A 4.5 cm diameter surface coil was placed atop the animal's head. Animals were artificially ventilated (50/50 mixtures of N_20 and O_2; gas anesthetics: 0.8-1.5% isoflurane) throughout the experiment.

Images were acquired (using a seven Tesla horizontal-bore magnet equipped with 20 gauss/cm self-shielded gradients) in a 1.5 mm thick "slice" tangent to primary visual cortex (Figure 2).

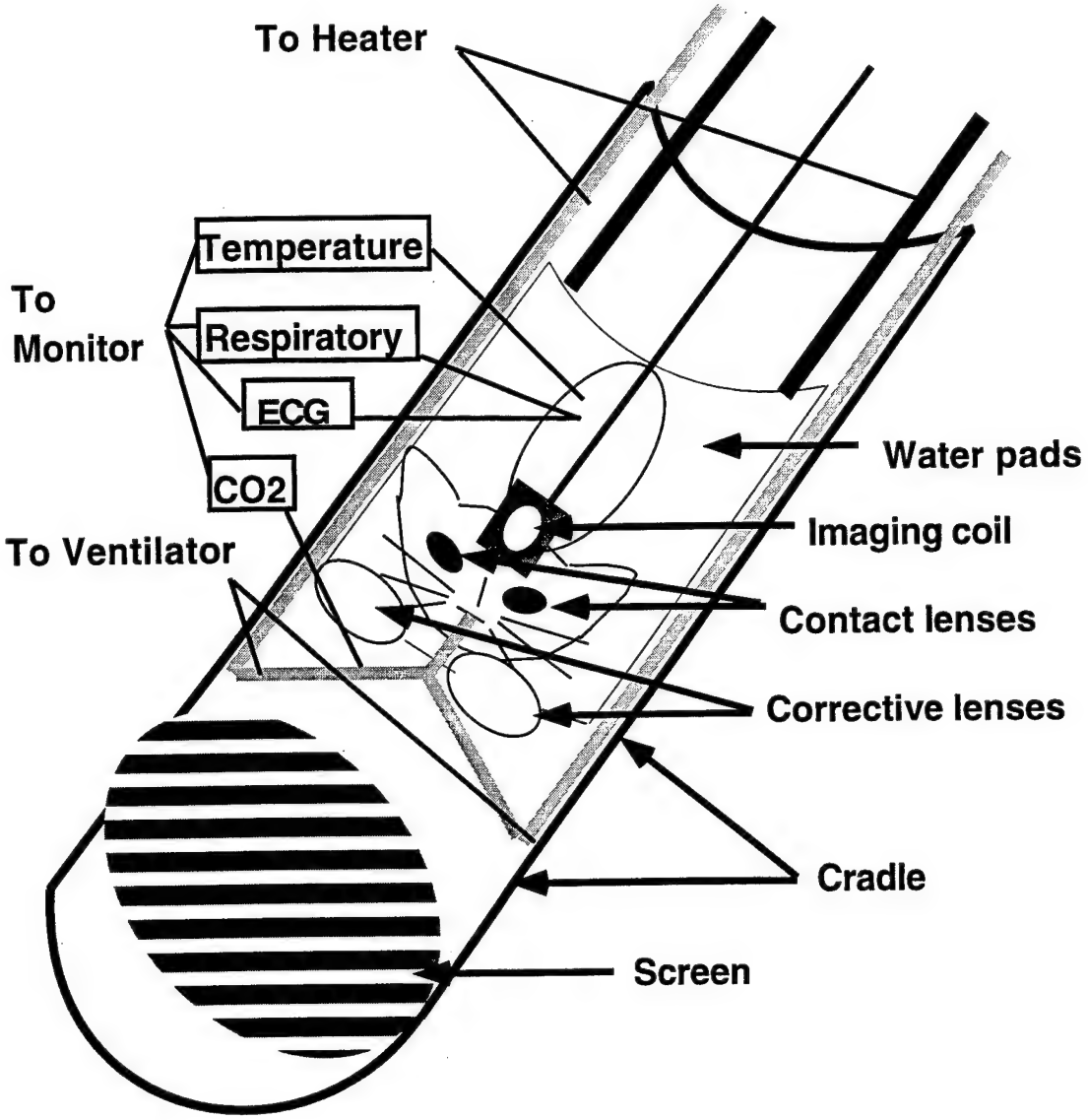

Figure 1. Sketch of animal "cradle," which incorporates equipment for physiological monitoring and stimulus presentation.

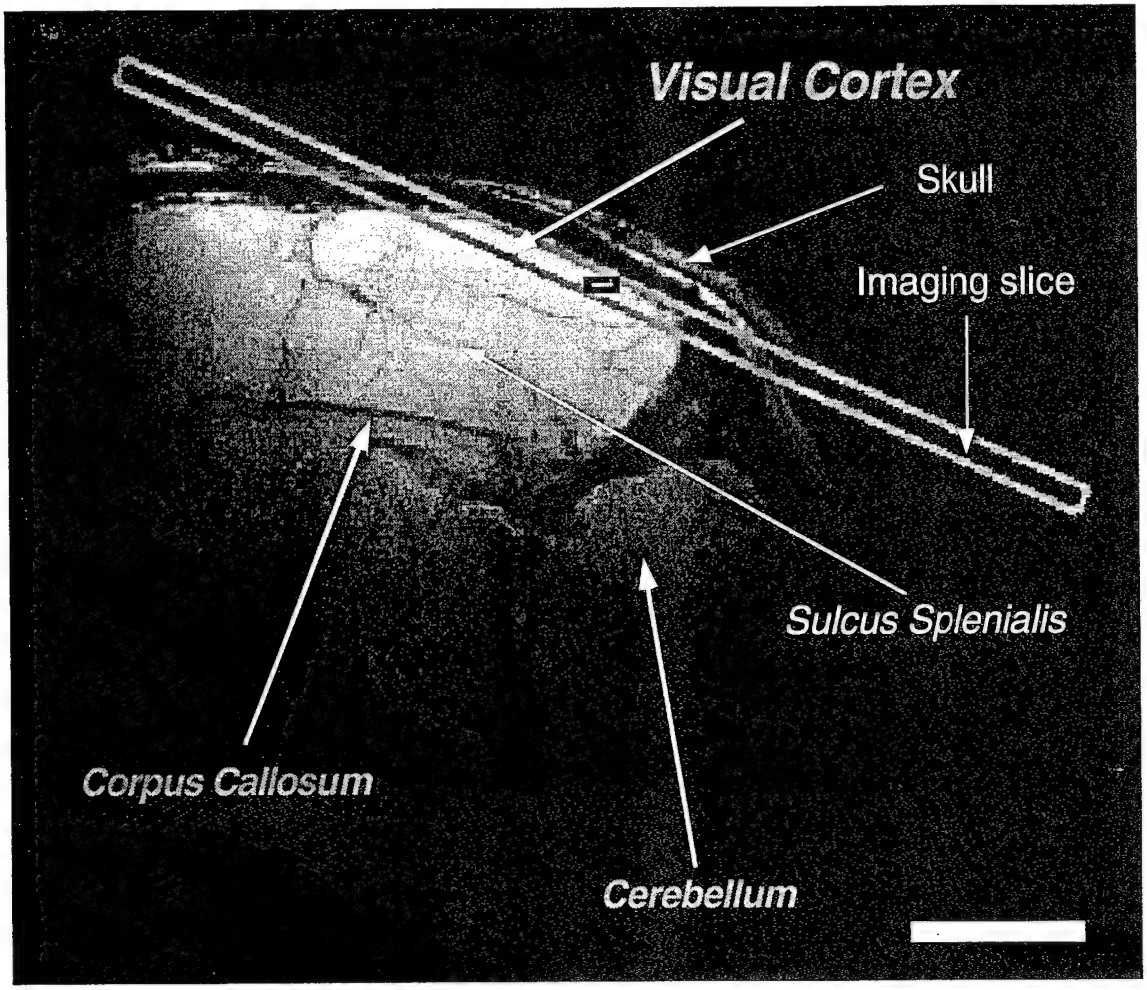

Figure 2. Sagittal image of cat brain, showing location of slice for fMRI experiment. Scale bar = 1 cm.

Visual stimuli consisted of high-contrast square-wave moving gratings (0.15 cyc/deg, 2 cyc/sec) of four different orientations (0°, 45°, 90°, and 135°) which are efficient at driving cortical cells in cat area 18. Consistent with single-unit and optical imaging studies, the stimuli elicited signals in voxels corresponding to area 18 on lateral gyrus (Figure 3). Functional data were processed by calculation of Z-scores (Z-score = activation-induced change in signal divided by the standard deviation of baseline signal) for each pixel. "Activated" pixels showed evoked signals which were synchronized with motion of visual stimulation (Figure 4).

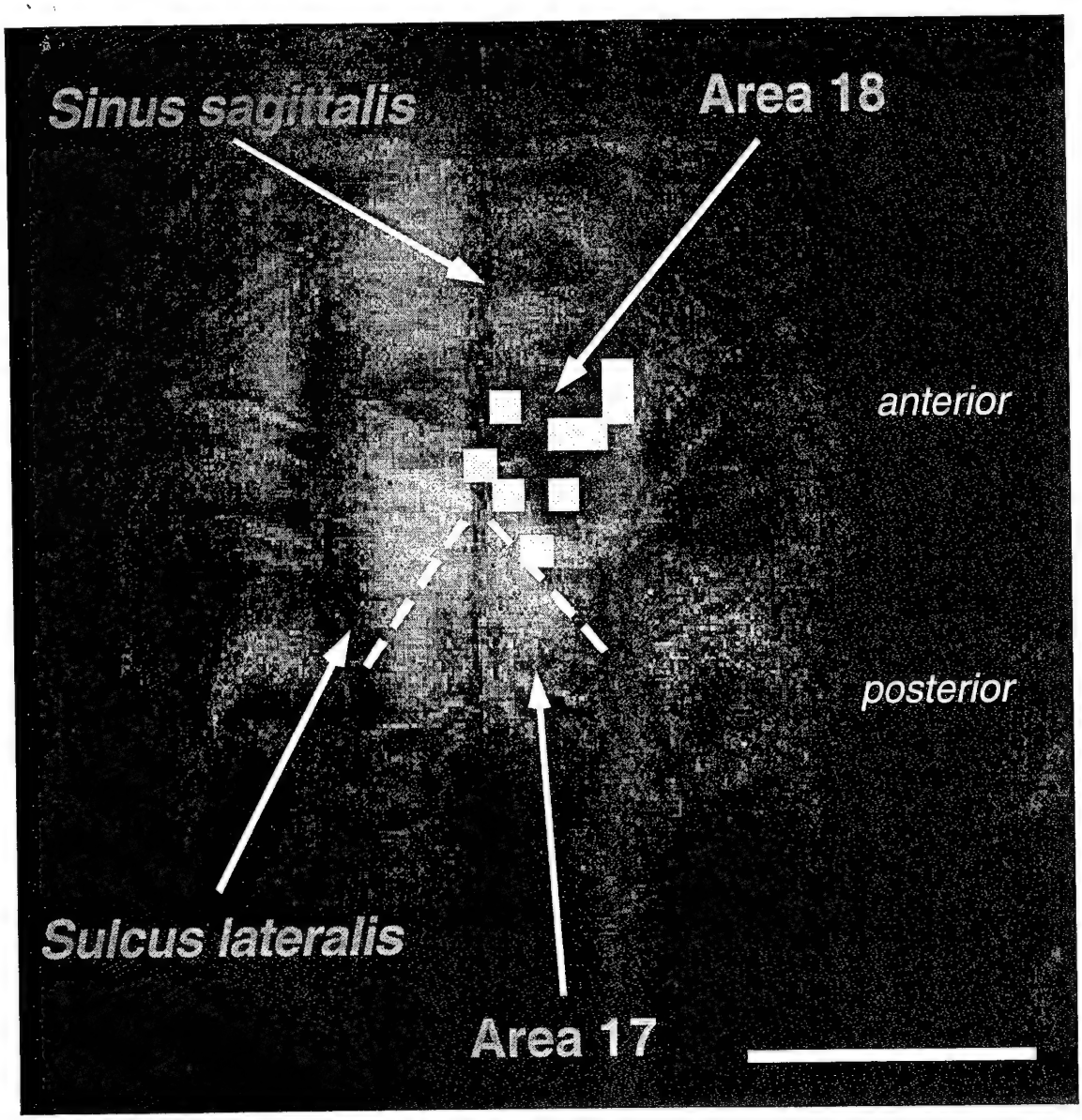

Figure 3. Activation map (spin-echo echo-planar imaging; FOV=60mm, 64x64 matrix; TE/TR=38.9ms / 3 sec; nominal spatial resolution: 1x1x1.5 mm^3/voxel) obtained during stimulation of the animal with a moving grating, oriented at 45 degrees, optimized to drive orientation-specific neurons in area 18. Pixels with stimulus-synchronous time courses are shown in yellow (Z-score > 2). The activation map is overlaid on a high-resolution anatomical image (gradient-echo; 512x512 matrix) of the same slice. Center of the anatomical image: around Horsley-Clarke AP0. The dashed lines on both hemispheres indicate the tentative border between areas 17 and 18. Note that the three pixels closest to the 17/18 border form a diagonal line from anterior-medial to posterior-lateral part of the lateral gyrus. All nine 'activated' pixels in this animal were located in area 18 of the right hemisphere. Scale bar = 1cm.

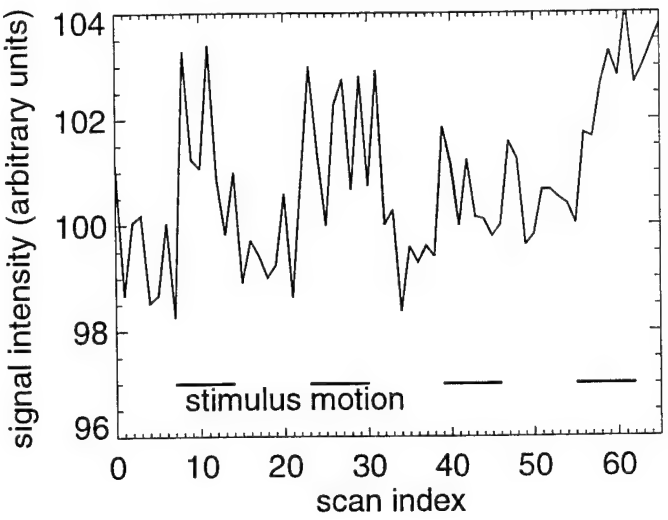

Figure 4. Timecourse for one "activated" pixel from figure 3. Horizontal bars indicate periods of stimulus motion.

Careful analysis of the time courses revealed that the Z-scores varied in a systematic way from voxel to voxel depending on the orientation of the presented stimulus. That is to say, for a given voxel from area 18, the Z-score values varied substantially for different orientations, while no such orientation-dependent differences in Z-score values could be observed from cortical regions outside area 18. Figure 5 shows the tuning curve for a single voxel from area 18 (in this example, the voxel preferentially responds to moving gratings at a 45 degree angle).

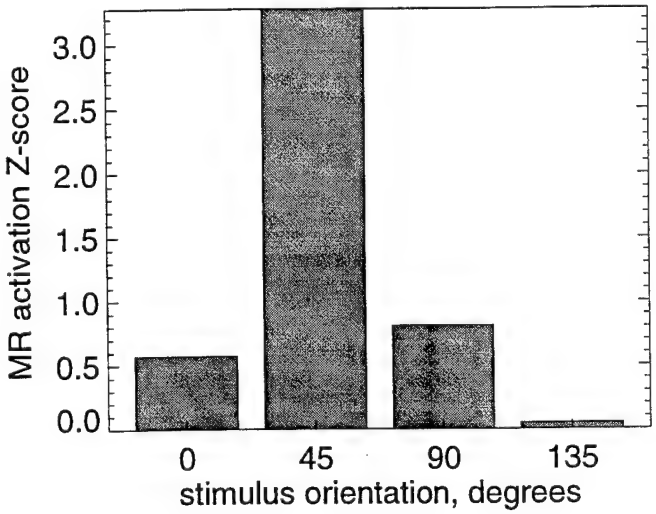

Figure 5. Tuning curve. Z-score for MR activation versus orientation angle of visual stimulus, for single voxel.

Our goals were: (1) To map the auditory cortex of pteronotus parnellii (the "mustached bat") using functional magnetic resonance imaging; (2) to compare these maps with data from single-unit electrophysiological recordings; (3) to use the non-invasive functional MRI mapping to address a

variety of neurobiological questions about auditory processing in the bat. Dr. Kyousuke Kamada plays a leading role in these studies, which are performed in collaboration with the laboratory of Dr. Jag Kanwal.

There are two special characteristics of pteronotus parnellii which make it an exciting candidate for functional brain mapping using magnetic resonance imaging: Firstly, sedation is not necessary in these animals, as they are in general not stressed by immobilization. Hence, functional MRI of awake alert animals is possible. Secondly, as these animal's hearing starts at about seven kilohertz, they are essentially "deaf" to the loud one kilohertz sounds made by the MRI scanner during echo planar imaging. Both of these characteristics are unique.

Figure 6 shows a coronal image of the head of a bat. Functional studies, using computer-generated ultrasonic stimuli, have recently been initiated. We are especially excited by the opportunity to perform functional MRI at seven Tesla in alert awake animals which is provided by the use of pteronotus parnellii.

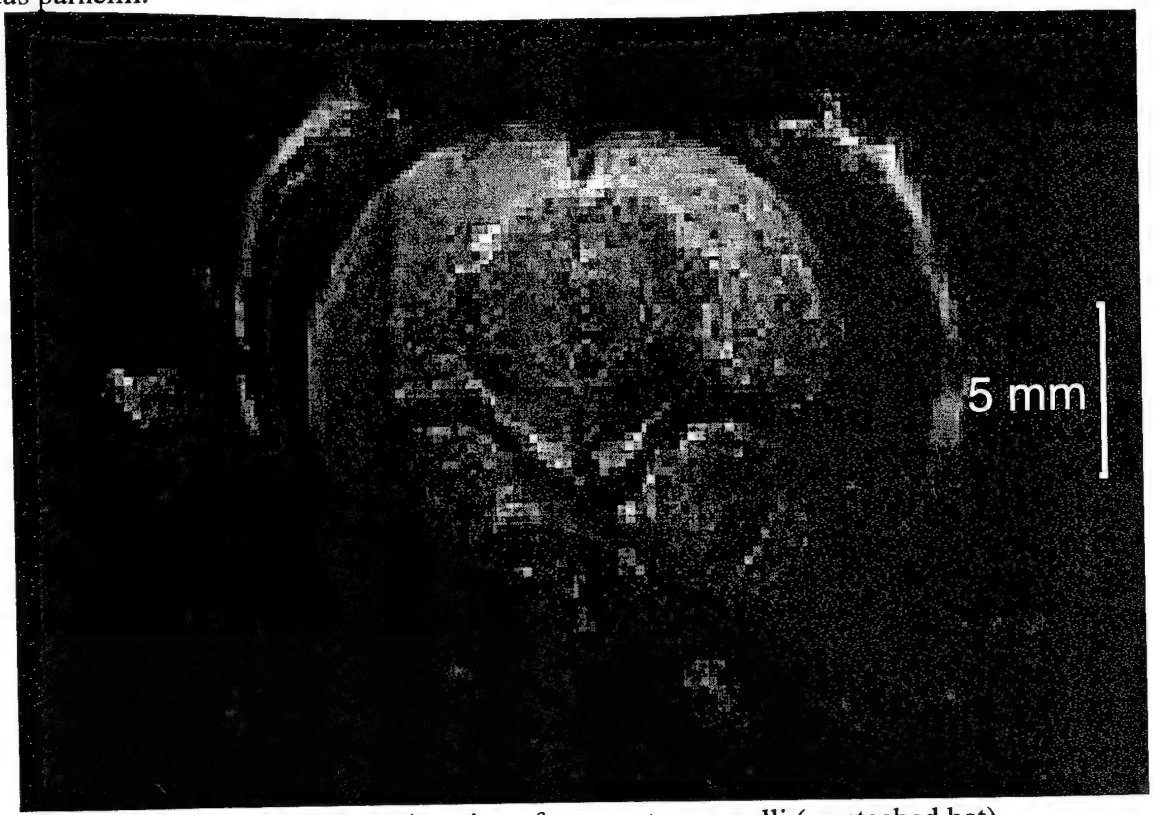

Figure 6. Magnetic resonance imaging of pteronotus parnelli (mustached bat)

PROJECT 2: MAGNETIC RESONANCE OUTCOME MEASURES IN RODENT MODELS OF CENTRAL NERVOUS SYSTEM INJURY

This area of our research activities uses multi-modal magnetic resonance imaging to perform "in vivo histology" by assessing changes in anatomy and physiology following injury. Our collaborators include Prof. Alan Faden and Drs. Gerard Fox and Susan Knoblach of his laboratory. The ability to exploit our minimally-invasive methods to pursue serial studies in order to follow the course of secondary injury over time in individual subjects promises to give great insight into the mechanisms of neuroinjury, and to provide a window into mechanisms of neuroprotection. Two studies were conducted; one using high-resolution magnetic resonance imaging, and the other using phosphorous-31 Nuclear Magnetic Resonance Spectroscopy to report on normal and pathological brain metabolism.

Our goals were: (1) To develop multi-modal magnetic resonance imaging outcome measures for rodent models of CNS injury; (2) to compare these MRI outcome measures with histological and behavioral outcome measures. This year saw the completion of our pilot study combining high-resolution and diffusion-weighted MRI.

In conjunction with Drs. Alan Faden (GICCS) and Robert Vink (James Cook Univ., Australia), we have adapted 31P magnetic resonance spectroscopy (MRS) methods for utilization in studies aimed at deciphering potential relationships between cerebral metabolism, cell death and neurological dysfunction after traumatic brain injury. We are currently examining the effect of novel TRH analogs on cerebral metabolism. Next, we intend to explore the role of specific metabolic substrates in apoptotic cell death. Our focus will be on free magnesium concentration and cytosolic phosphorylation potential, as these are known to correlate with neurologic outcome. Planned studies also include developing methods to perform MRS in relevant transgenic mouse models (i.e. PARP knock-outs), Such studies will be the first of their kind.

JOSEF P. RAUSCHECKER, Ph.D., D.Sc.

Dr. Rauschecker's laboratory continues to focus on the understanding of higher auditory processing in the cerebral cortex, although general aspects of cortical organization and plasticity are always overarching themes. While the ultimate goal for the studies on auditory processing is to reveal the mechanisms of human speech and language, it is important to pursue neurobiological studies in animal models, because studies in humans can, with few exceptions, only be performed noninvasively. The availability of modern imaging techniques has had an enormous impact on the design of such studies, because theses techniques form a direct link between animal and human work. Finally, the enormous capacity of the cerebral cortex to reorganize itself after peripheral injury, deprivation, or during learning merits particular attention. This becomes especially relevant as we consider cortical plasticity in centrally deaf or blind patients, during tinnitus, or in patients with Alzheimer's disease or stroke.

PROJECT 1: CORTICAL MECHANISMS OF AUDITORY PROCESSING IN NONHUMAN PRIMATES

Project 1A: Processing of Complex Sounds in Nonprimary Auditory Cortex

Dr. Rauschecker's group continues to explore the functional organization of nonprimary auditory cortex in macaque monkeys. The analysis of single unit responses to complex auditory stimuli in different cortical fields is the focus of these studies. In particular, monkey vocalizations are used for stimulation, as their spectral and temporal structure resembles human speech sounds in great detail. Using digital signal processing techniques, monkey vocalizations were decomposed into their constituent elements. Temporal and/or spectral combination-sensitivity for these elements was tested, and it was confirmed that non-linear summation in the frequency and time domain is an important mechanism for response selectivity in higher areas, such as the lateral belt. By contrast, neurons in primary auditory cortex A1, if they respond selectively to a particular monkey call, do so simply on the basis of their frequency selectivity, i.e. they show linear summation. Thus, auditory cortical areas are organized into a clear processing hierarchy. It can be inferred that the phonological decoding of speech sounds in humans is based on similar neural mechanisms as those in nonprimary auditory cortex of primates.

As a second finding in the past year, we have established that the nonlinear summation mechanisms mentioned above sometimes lead to suppression of responses to whole calls rather than their facilitation. This may be interpreted as another selection mechanism leading to responses specific for certain types of calls.

Project 1B: Neuroanatomical Connectivity of Auditory Cortex

The processing hierarchies within primate auditory cortex were also further investigated with neuroanatomical tracer studies. During the past year efforts concentrated on the analysis of cortico-cortical connections as well as connections from thalamus to the lateral belt areas in the superior temporal gyrus (STG). Preliminary data were confirmed that MGv provides input to area ML, i.e. a third cortical area in addition to A1 and R. The projections from the STG to parietal and prefrontal cortex were analyzed in detail. It appears that the frontal connections are organized into separate

dorsal and ventral streams, similar to the visual system, which underlie spatial and pattern processing, respectively.

Project 1C: Visual-Auditory Integration in Awake Behaving Monkeys

A new line of investigation, begun in this reporting period, involves the analysis of visual-auditory integration in multimodal areas of the cerebral cortex, most notably in the superior temporal cortex (STG and STS) and in the parietal cortex. Monkeys are being trained to fixate a visual stimulus, while at the same time listening to sounds that are either correlated with the presentation of the visual stimulus or not. Facilitation or suppression of neuronal responses in the cortex will be noted and quantified.

PROJECT 2: NEUROIMAGING OF AUDITORY CORTEX

Project 2A: Optical Imaging of Auditory Cortex in Cats

Whereas previous years had been devoted to the difficult installation and fine-tuning of the optical imaging system (Imager 2001, Optical Imaging Inc.), we are now beginning to reap the benefits of this powerful technique. Intrinsic optical signal changes related to blood oxygenation are measured that reveal neuronal ensemble activity in the cortex at a scale of about 500 μm. This gives insight into the organization of functional columns in the cerbral cortex. Studies of cat visual cortex in the past had revealed the organization of orientation columns. By analogy, the organization of FM direction columns in auditory cortex is now the focus of our investigations. Comparison with electrophysiological work demonstrates that the activation seen in the optical recording experiments is indeed closely correlated with neural activity specific for the direction and rate of FM stimuli.

Project 2B: Functional MRI of Visual Cortex in Cats

In an intense collaboration with Dr. Pekar's laboratory in GICCS, we are exploring the functional organization of orientation columns in the visual cortex of young kittens using Dr. Pekar's high-field (7-Tesla) Bruker magnet. The use of kittens for these studies is mandated by two factors: First, a wealth of established knowledge exists about visual cortex of cats and monkeys, which is necessary and important as a baseline for this completely new approach of studying visual cortex with fMRI. Second, adult cats or monkeys cannot be used due to the limitations of the bore size of the magnet. Robust activation of visual cortex by drifting square-wave gratings is found in all of our studies. Initial results indicate that there is indeed domain-specific activation of visual cortex by gratings with different orientations.

Project 2C: Functional MRI of Auditory Cortex in Humans

Over the last year, we have vastly expanded our program of studies using fMRI of human auditory cortex on the new 1.5T Siemens Vision scanner at Georgetown. Similar types of auditory stimuli, such as bandpass noise (BPN) pulses and frequency modulated (FM) glides, as in the animal studies on cats and monkeys, are used in human studies with functional magnetic resonance imaging (fMRI). In addition, we now use human speech sounds ("phonemes" or "consonant-vowel [CV] combinations"), which are composed of similar types of information-bearing elements as the subcomponents of monkey calls, i.e. bandpassed noise and FM sweeps. Use of phonemes or CVs results in even larger activation than BPN and FM stimuli, and in some subjects this activation is mainly restricted to the left hemisphere. The transition between non-speech and speech sounds is

being addressed specifically by two studies ongoing in our laboratory: One study looks at the activation of different auditory cortical areas by vowels; another study looks at the representation of nasal consonants. Both types of speech sounds were selected because they can be extended over periods of 500 msec or more, which should permit reliable activation. By contrast, stop consonants last only for less than 100 msec, which may not be long enough.

Project 2D: Functional MRI of Visual-Auditory Integration in Humans

There is evidence from a number of previous studies that what we see influences what we hear. Most recently, an fMRI study has demonstrated that silent lip-reading leads to activation auditory cortex. Even better known is the phenomenon of the McGurk effect: a lack in congruence of lip movements and sound originating from a "speaking face" (which can be generated experimentally by swapping the audio and video portion of different speech samples) leads to the perception of a different speech sound. Both findings demonstrate that visual and auditory portions of the speech signal are processed together and are integrated into a common percept. Especially under noisy conditions the visual signal helps to perceive the auditory speech signal, and there is also a role of this integration during speech development in infants. We have now preliminary results of activation by the McGurk effect in auditory and frontal regions of the brain.

PROJECT 3: COMPENSATORY PLASTICITY OF THE CEREBRAL CORTEX

Dr. Rauschecker's group is one of the protagonists of the view that early deprivation in one sensory modality leads to compensation in another. While some of our early evidence came from studies in visually deprived cats, we have recently concentrated on studying sensory deprivation in humans with the use of neuroimaging techniques. In the past year, we have completed one collaboration on compensatory plasticity in the congenitally deaf and continued another on early blind humans.

In our continuing collaboration with the group of Dr. Mark Hallett at the National Institute of Neurological Disorders and Stroke (NINDS), positron emission tomography (PET) is used to investigate the organization of higher auditory processing in the human brain and its plasticity. Sound localization of "virtual auditory space" stimuli activated two centers in the posterior parietal lobe, one of them modality-specific for auditory spatial processing, the other activated by both visual and auditory spatial tasks. The plasticity of this system had previously been demonstrated by the fact that the area of activation in the parital areas is significantly enlarged in congenitally blind people and extends far into normally visual areas (18 and 19) in the occipital lobe.

The plasticity of auditory cortex is expected to prove a valuable tool for the study of other forms of neural plasticity important for functional recovery in patients with central deafness and blindness. Furthermore, it may lead to a more complete understanding and treatment of tinnitus. Finally, understanding of cortical plasticity is necessary for development of treatment of patients with stroke or Alzheimer's disease.

JIAN-YOUNG WU, Ph.D.

My laboratory, the GICCS Optical Imaging Laboratory (OIL), studies the neuronal activity in neocortex. Neocortex is one of the last frontiers in neuroscience. There are about one trillion neurons in neocortex. These neurons are simple devices and each can represent only a small portion of the outside world. However, human consciousness is generated by the collective activity of these neurons. Thus, one ultimate goal for system neurobiologists is to understand how complete and complex cognition develops from a simple and partial representation of individual neurons.

My research fits into an intermediate step between neurons and brainóthe role of dynamic neural assemblies which are subconscious functional units with complex internal representations. My laboratory uses optical imaging to analyze the population neural events in neocortex. About sixty years ago, Sir Charles Sherrington, a neuroscientist (and Noble laureate) had imagined a fascinating way of viewing the brain activity:

"Imagine activity in (the brain) shown by little points of light. Of these some stationary, flash rhythmically, faster or slower. Others are traveling points, streaming in serial trains at various speeds. The rhythmic stationary lights lie at the nodes. The nodes are both goals whither converge, and junctions whence diverge, the lines of traveling lights.

At that time brain imaging was only a dream. After years of continuous effort from a number of laboratories, optical imaging has become a powerful technique. Imaging population activity rather than recording from individual neurons (a metaphor would be viewing a whole TV screen versus analyzing the intensity of individual pixels) now has a unique position in system neuroscience.

Voltage sensitive dye imaging (Figure 1), the major approach of my laboratory, directly reports the electrical activity of the neurons and can have a temporal resolution of 0.5 ms, enough to follow dynamic neural events. Currently we have two major projects in my laboratory. One is aimed at understanding the localized dynamic neural assemblies, and the other is aimed at understanding the initiation site (as a pathological neural assembly) of epileptiform activity. From the images included in this report you can see that we are able to image the activity of small groups of neurons and study their roles in cortical processing and epileptogenesis.

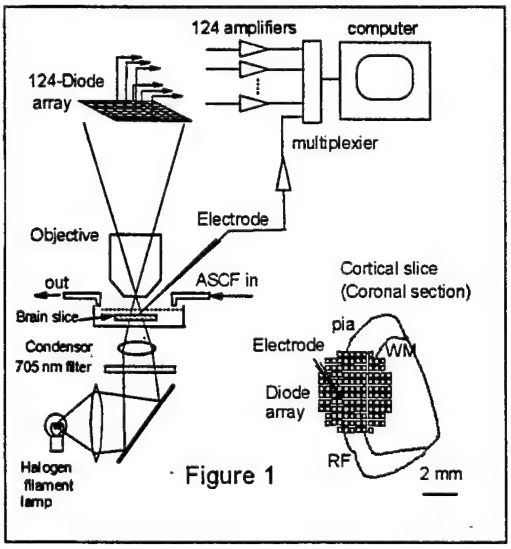

Figure 1

PROJECT 1. DYNAMIC CORTICAL NEURAL ASSEMBLY

The long term goal of this project is to understand the basic building blocks of population activities in neocortex. We are studying a propagating event in cortical slices. These local population events occur during 7 to 10 Hz oscillations. They can also be evoked in cortical tissue when a small number of neurons are activated by electrical stimulation. Throughout the proposal we use the words, "dynamic ensemble" as the name for this phenomenon. Our goal in 1998 is to distinguish it from known population events such as epileptiform activity and evoked population response. Most of the experiments have been reliably repeated and published in abstract forms. Some data is accepted for publication in full papers.

The oscillations appear in cortical slices from the somatosensory areas as spontaneous epochs when the preparation is bathed in low [Mg] ACSF. Each epoch started with an epileptiform spike, and oscillations emerged afterwards. In each epoch there were various numbers (usually 5 to 100) of oscillation cycles. In LFP recordings the low amplitude peaks of oscillations emerged from low amplitude, asynchronized activities. With more and more cycles, the oscillation frequency gradually decreased while the amplitude increased. At 26°C, the frequency was about 5 to 8 Hz.

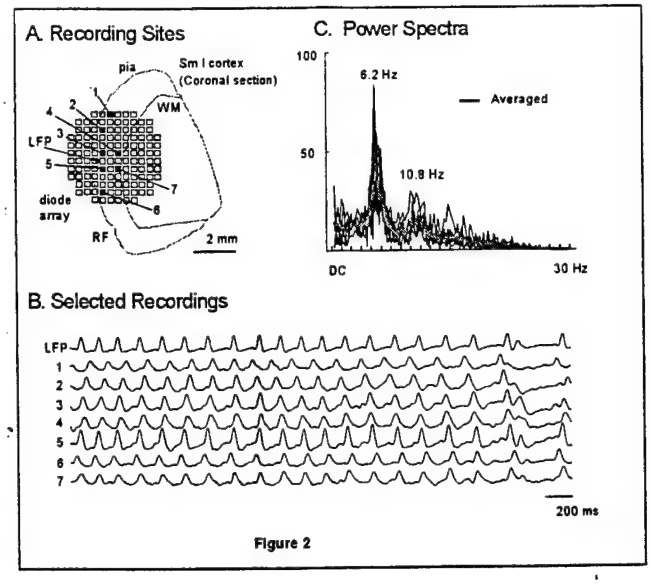

Figure 2

In a 4 mm wide cortical slice, we optically recorded from 30 to 40 locations simultaneously. In most of the preparations examined (n > 20), all locations oscillated at the same overall frequency (Figure 2, C). To our surprise, the correlations between two locations did not decrease significantly with distance, although there were large phase shifts at a large distance (Figure 3, A). The correlation was better between two points within one vertical "beam" than two points separated by the same distance but in different columns (Figure 3, B). Auto-correlations of all the traces (Figure 3, B) suggested that the entire preparation was dominated by one frequency. The auto-correlation peaks became scattered after two cycles, suggesting that there were slow variations in frequency at different locations (Figure 3, B).

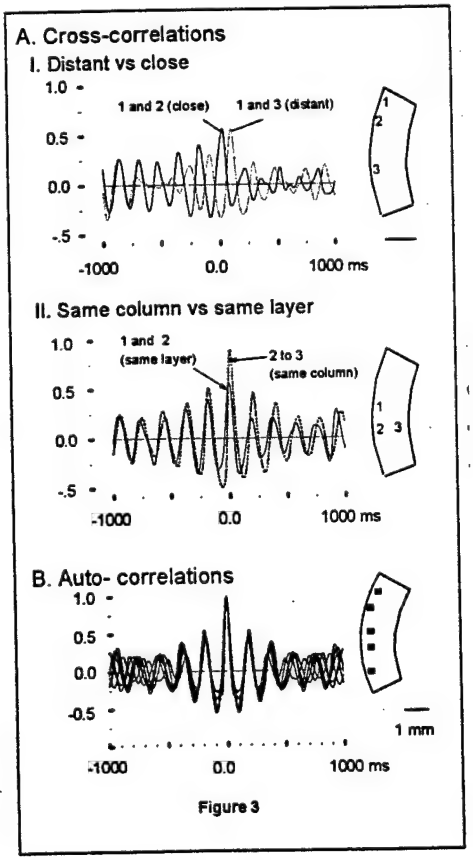

Figure 3

The images derived from all the optical detectors revealed that the neurons activated during oscillations were not uniformly distributed over the slice. Instead, each oscillation peak appeared as a localized hot spot propagating across the cortex. In Figure 4 we made pseudocolor images according to the amplitude of the voltage-sensitive dye signals, from three sections (I to III) within one epoch. Comparing LFP recordings in panel B and images in panel C of Figure 4, it is obvious that each oscillation peak correlated to a propagating hot spot. In each oscillation cycle, when a hot spot passed through a LFP electrode (or an optical detector), a depolarization peak was detected. When hot spots repeatedly passed a detector, a periodic depolarization was recorded which appeared as oscillations (Figure 4, B). Thus at each individual recording point, the activity could be defined as an oscillation by its periodicity in FFT and autocorrelations (Figure 2, B). However, the images of the same data set revealed propagating hot spots, suggesting that the periodicity is in part determined by the propagation velocity (Figure 4, C).

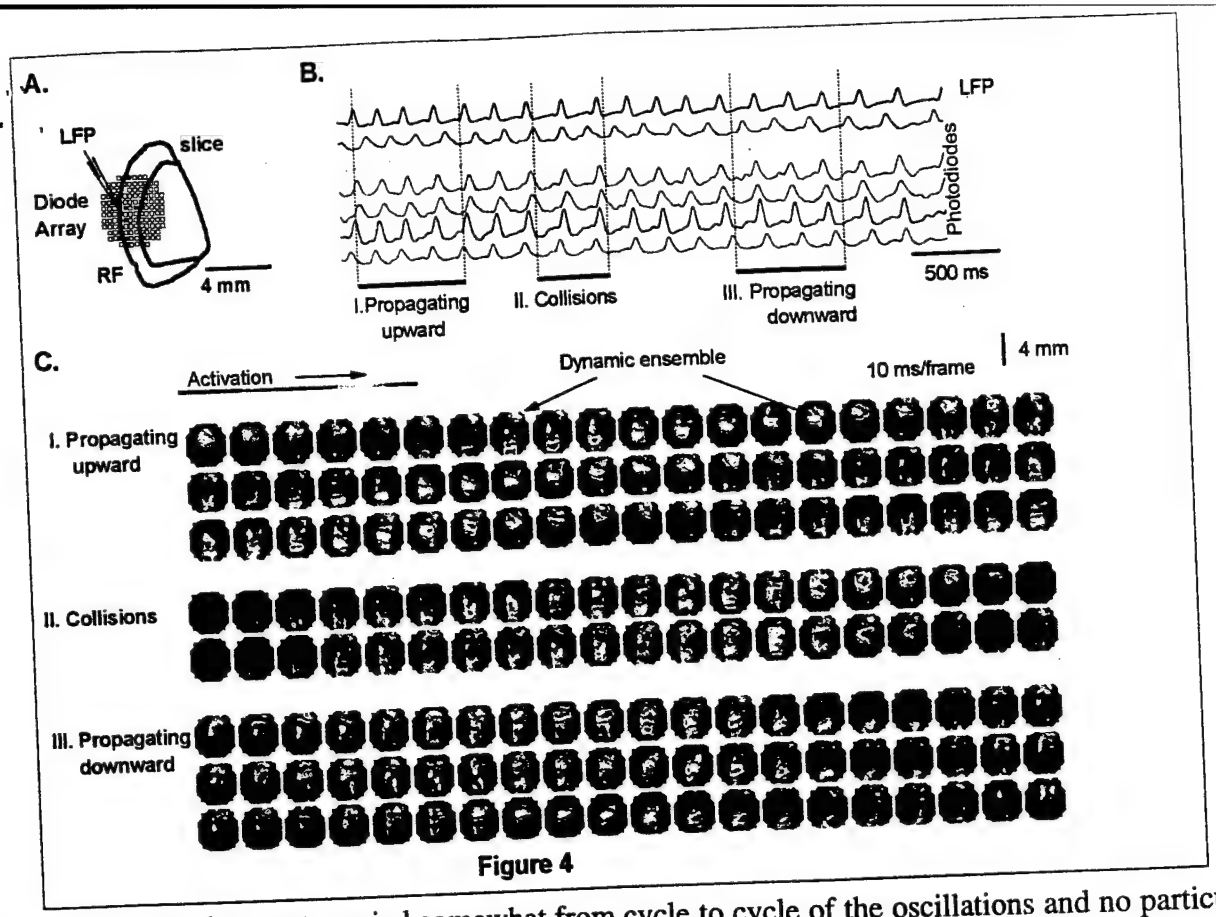

Figure 4

The shape of the hot spots varied somewhat from cycle to cycle of the oscillations and no particular pattern was correlated to each preparation. From the amplitude pseudocolor image it is difficult to determine the physical size of a hot spot. However, using the iso-potential lines of the contour map we can tell that the spots were relatively similar in size but somewhat irregular in shape. The active area encompassed all cortical layers. The cycle-to-cycle variability of the shape and size suggested that these propagating hot spots were most likely dynamically organized. They were seen in most of the slices ($n > 20$) with different slicing angles from the barrel cortex. The iso-potential contour did not appear to be correlated to the barrel patterns suggesting that the activity is likely to be organized by distributed intracortical connections. Since the hot spots are likely to be dynamically organized and they are not a classical stationary oscillation, we give them the name, "dynamic ensembles", to describe this propagating activation and to distinguish it from other kinds of population activity.

For each cycle of an oscillation, one and occasionally two dynamic ensembles emerged and propagated away. The overall propagation velocity was 30 + 10 mm/sec (mean + SD, N=15, at 26°C) and the distance traveled was usually larger than the field that was imaged (>5 mm). In a brain slice only two propagation directions are possible. A consecutive series of dynamic ensembles usually propagated in the same direction and most of them (97%, n= 200) kept the same direction as their predecessor. However, the propagating direction was not fixed. The direction could reverse in the middle of an oscillation epoch (Fig. 4, C). When two dynamic ensembles emerged simultaneously at different locations, they sometimes propagated toward each other, resulting in collision and annihilation of the activity (Fig. 4, C). These collisions and changes in propagation direction explain why the oscillation frequencies varied drastically in the middle of some epochs.

Dynamic ensembles could be distinguished from epileptiform activity in several ways. Although in local field-potential recordings the two events were similar in amplitude and time course, they were very different in the voltage-sensitive dye recordings. First, the activation area of a dynamic ensemble was cohesive, i.e., its physical size remained relatively constant during propagation

(Figure 4, C; 6, B, bottom row). In contrast, epileptiform events appeared in the imaging as a spreading of an excitation wave, starting from a small initiation site and expanding to the entire preparation (Figure 6, B). Second, the amplitude of the dye signal of epileptiform events was 5 to 20 times larger than that of dynamic ensembles (Figure 6, A). Third, epileptiform events generated a large peak in the intrinsic optical signal that was slow and wavelength independent (Figure 6, A, right panel). This intrinsic signal was not found with dynamic ensembles. Fourth, when spikes of cortical neurons were measured with an extracellular electrode, epileptiform events had many more spikes than dynamic ensembles (data not shown). Finally, epileptiform events and dynamic ensembles had different refractory periods. The former usually occurred not more than 4 episodes per minute and the latter occurred at 7 to 10 Hz.

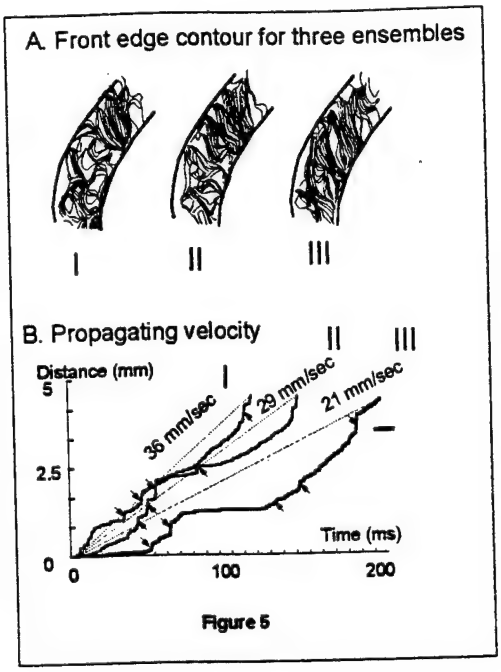

Figure 5

In this report we have characterized propagating activation during 7 to 12 Hz oscillations, and call this confined, propagating activation "dynamic ensembles". We have also distinguished this kind of population activation from epileptiform events and tried to evoke dynamic ensembles in normal excitability conditions (slice in normal ACSF).

Our data shows that some population oscillations in cortical tissue appeared as self-sustained, spatially cohesive and propagating events, which we name dynamic ensembles. In the 7 to 10 Hz oscillations, during each cycle one (occasionally two) dynamic ensemble(s) emerged and propagated through the cortical tissue. These population events can be described as oscillations by an individual detector (optical or LFP electrode), or as propagating dynamic ensembles by imaging (Figure 4; Figure 6, B). The images offer a simple explanation for the complicated frequency variations in the preparation.

In ferret thalamus slices, the 4 to 7 Hz spindle oscillations also appear as propagating activations. In cortical slices the dynamic ensembles propagate ten times faster than the thalamus spindle waves although they have similar frequencies. Propagation velocity determines the wavelength, or distance between dynamic ensembles. Thus, in the same spatial distance there would be ten thalamic spindle waves but only one dynamic ensemble.

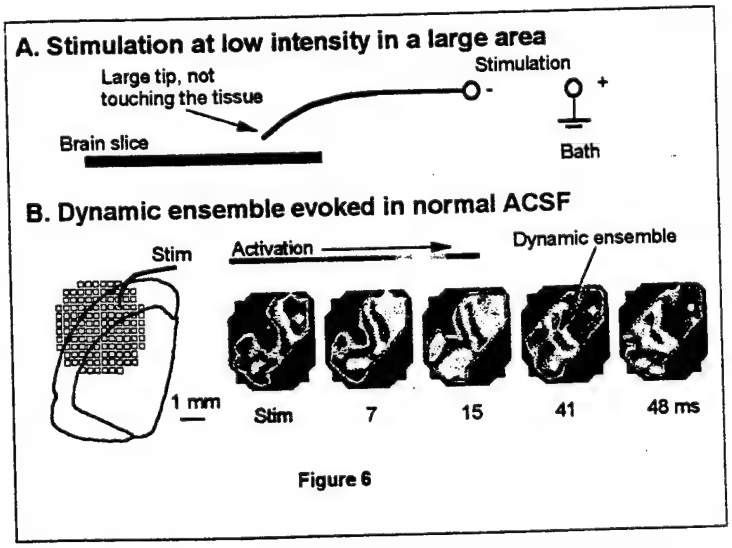

Figure 6

Slice preparations from different parts of the brain have been developed which have a similar oscillation frequency as that found in situ. These oscillations include 7-10 Hz in somatosensory cortex, 6-10 Hz spindles in thalamus, 20-80 Hz in auditory cortex, 40 Hz in hippocampus and 10-50 Hz in neocortex. In the auditory cortex preparation, multi-electrode recordings revealed that afferent input evoked a propagating activation. This evoked activation lasted 50 to 200 ms and propagated at

30 mm/sec; within each such propagating activation, there were 40 Hz fluctuations in local field potentials. It would be interesting to compare the images of these oscillations with different frequencies in different slices. This would allow us to examine whether "dynamic ensembles" are of more general occurrence in the cortical neuronal network.

Although the spatial pattern of in vivo oscillations has only been examined in invertebrates and reptiles, the images of most of these in vivo oscillations appeared as traveling excitation waves which are strikingly similar to what we have seen in vitro. The rostral oscillation in turtle olfactory bulb appeared as a simple propagating activation. At each cycle of oscillation a "blob" of activation emerged from one location and propagated with a certain velocity and direction in the bulb. The physical size, active neuron density, and propagating velocity of the "blob" were very similar to the dynamic ensembles that we observed in vitro. Visually induced oscillations in turtle cortex have more complex patterns with several frequency domains but the spatial pattern still appeared as propagating activation, with several "blobs" representing each frequency domain traveling along different paths with different velocities.

Oscillation in the somatosensory cortex of behaving rats is also in the 7 to 10 Hz range and also organized in epochs during "whisking". Electrical recordings from these oscillations suggested that they appeared as traveling waves. Unfortunately, the spatial patterns of in vivo oscillation in somatosensory cortex are not available for comparison with our results in brain slices.

In some systems such as salamander olfactory bulb, evoked population activity does not have rhythmic oscillations but the activation still appears as propagating waves.

Oscillations are common population events and it has been proposed that they may serve as synchrony timing signals, as reference carrying waves for temporal coding, or for arousal or attention. Although it is still debatable whether oscillations really serve any function or are just a by-product of the population activity, their ubiquitous existence suggests that the spatio-temporal pattern of an oscillation is shared by many kinds of population events in the central nervous system.

Neocortex is a relatively homogeneous neuronal network with similar basic neuronal organization in different areas. The similarity in the intrinsic cortical circuitry suggests a universal role for local population activation in different cortises. As a continuation of this work, it would be interesting to compare oscillations and evoked population events in different cortical areas, to test whether dynamic ensembles can be evoked in all cortical tissues.

We estimate that a dynamic ensemble has only about 5 to 7 percent of the maximum activation of the cortical network. The voltage sensitive dye signals come from a combination of spikes and synaptic potentials. Assuming that our signals were a linear summation of spikes and synaptic potentials in the population, then one spike (100 mV) of one neuron would contribute equally to 10 neurons with 10 mV depolarization. At one extreme on could assume that all signals were contributed by spikes so that 5 to 7 percent of the total population was firing simultaneously in each sampling period. Thus during the 200 ms duration of a dynamic ensemble each activated neuron would fire about ten times. However, extracellular unitary recordings revealed that each neuron only fired one to two spikes. Thus it seems likely that subthreshold depolarizations of many cells are an important contributor to the dynamic ensemble signals. Thus a dynamic ensemble would be organized with a large portion of moderately depolarized neurons. We thus speculate that a dynamic ensemble is a domain of population depolarization in which some neurons will increase their firing probability to reach one spike per period of two hundred milliseconds. This kind of organization is similar to the spontaneous population co-activation observed in developing cortex and retina.

The activation of dynamic ensembles lasted much longer than an "ordinary" evoked response. We considered this activation to be "self-sustaining", sustaining a certain level of activity in cortex without afferent input. We hypothesize that self-sustainability is a population property of a reciprocally activating neuron network. The development of a dynamic ensemble might follow certain "population rules", e.g., depend on the size of the activation, density of active neurons in the area and the temporal pattern of the input. Self-sustained evoked responses have also been observed in thalamocortical slices. By stimulating thalamic afferent fibers, the evoked response lasted 100 to 200 ms, and also propagated a few mm away. In contrast, a stimulus to the white matter of the same preparation only evokes an ordinary short lasting response. In this report we evoked dynamic ensembles when activating a low density of neurons in a large area involving all cortical layers. In contrast, evoking a high density of active neurons in a small area in the deep layers would induce strong synchronized evoked potential and the activity would fail to become self-sustaining.

Dynamic ensembles are relatively unitary in size, suggesting that cortical neurons are activated in population modules. Dynamic ensembles may provide an uneven local excitability, where the same input may elicit a higher population firing rate within an ensemble than in the regions outside of it. In intact brain, dynamic ensembles may be evoked by sensory input, or emerge during evoked oscillations. This would allow spatial interactions between different ensembles, and temporal interactions between concurrent input and dynamic ensembles evoked by previous input. The existence of this kind of population module has been postulated as a "cell assembly" which reverberates with afferent input and may plays a role in sensory discrimination, temporary information storage, and transition from short to long term plasticity.

PROJECT 2. INITIATION AND SPREADING OF SEIZURE-LIKE ACTIVITY IN CORTICAL SLICE PREPARATION

The long term objective of this research is to understand the development of organized epileptiform events from the interactions of local neuronal groups in neocortex.

Epileptiform activity (EA) can be initiated from cortical structures in a number of epilepsy models, indicating that the initiation of EA can be intrinsic within the cortex. Pyramidal neurons in layers V have been thought to be responsible for the initiation, because pyramidal neurons have the highest excitability in the neocortex, they have little detectable inhibition, and layer V containing pyramidal neurons alone is sufficient for generating EA in a zero Mg^{2+} epilepsy model. However, it has been reported that isolated superficial layers can also initiate EA and may even dominate the initiation process in the intact cortex perfused with 10-20 mM bicuculline methiodide. Current source density analysis on field potential recordings indicated that EA started in layer II/III of the cortex. Intrinsic firing properties of cortical neurons may be the mechanism underlying EA initiation, and neurons with repetitive firing properties are capable of initiating EA. According to this criterion, various neurons from different layers may potentially become EA initiation cells when they possess repetitive and rhythmic firing properties. In fact, cortical neurons in both superficial and deep layers can be induced to fire rhythmically, and therefore these neurons may potentially be able to initiate EA.

Examination of the spatial and temporal characteristics of EA using conventional electrophysiological techniques requires a cumbersome array of electrodes and careful current source analysis. The number of such an electrode array has been limited to a few ones because of the

difficulty in practice. Current source analysis has been attempted in study on EA origin but the location of epileptic focus could not be determined by such analysis. The timing of EA onset from the different regions can only be compared and EA initiation site thus be determined when all the cortical layers and the adjacent regions are simultaneously measured. This is best achieved by means of imaging techniques with high temporal resolution as the transient signal tends to be in the millisecond domain. We applied high speed (1 frame per msec) optical recordings using voltage-sensitive dyes to measure EA over a region of the cortex about 4.5x1.5 mm^2 and so the initiation site can be imaged with few location adjustments. We have demonstrated that a single dominant focus for originating EA emerges when the preparation is perfused with zero Mg^{2+} artificial cerebral spinal fluid (ACSF) or normal ACSF containing bicuculline (20-50 μM). Therefore, the stationary focus can easily be located by imaging techniques. Here we present the imaging data showing the direct evidence where EA is spontaneously initiated in the cortical slice and how the epileptic foci are organized; we also apply electrical stimulation via a microelectrode in one of six cortical layers to visualize the initiation process where EA is triggered by single pulse stimulation.

Spontaneous paroxysmal activity emerged 20-40 min after the preparation was perfused with a modified ACSF. The PDS was a spontaneously occurring all-or-none population spike in the field potential recordings and in optical recordings. The optical signal had a similar waveform and time course as the recordings from electrodes in adjacent areas. To identify the initiation site of the paroxysmal events, the PDS spike from each detector was normalized to its maximum amplitude and pseudocolor images were made from the contour display. Images from 10 animals showed that the paroxysmal events always started as a confined spot smaller than one photodetector (375 x 375μm) and propagated over the entire preparation. Since the voltage sensitive dye image is a direct measurement of transmembrane potential, the site of origin is accurately localized, and not subject to the concerns about the volume spread of extracellular currents. However, the resolution of our imaging device only allows us to set an upper limit on the actual size of the initiating region. Repeated optical recording trials suggested that the spontaneous paroxysmal events started from the same initiation focus. Since prolonged optical recording is limited by dye bleaching and photo-toxicity, we used two electrodes placed between the possible initiation foci to determine the locations of the initiation sites. Since the initiation foci were much smaller than the distance between measuring electrodes, the location of the foci can be determined by the time difference for the PDS spike to propagate from its initiation focus to the two electrodes if the propagation velocities of spontaneous PDS in vertical and horizontal directions are known. These were measured directly from the optical images, and were 36.1±9.9 mm/sec (n=14) and 31.0±13.2 mm/sec (n=14), respectively.

Over a two hour recording period usually 300 to 400 spontaneous PDS events can be recorded (n= 7). In zero [Mg] ACSF, the latencies were clustered around a few values, consistent with the idea that the PDS events were initiated from only a few sites. An initiation focus which initiates one paroxysmal event is more likely to be the initiation site for successive events. Among co-existing initiation foci, one often became dominant for a period and initiated the majority of the spontaneous PDS events. Dominant foci were also observed. During different recording periods the dominant focus could be different. The old dominant center became non-dominant with time and another initiation focus became dominant. Occasionally, however, there were three or four initiation foci with no obvious dominant one.

Dominant initiation sites also occurred in ACSF containing bicuculine and high extracellular potassium data not shown), suggesting that in these epilepsy models the initiation of spontaneous epileptiform events follows the same pattern as in the low magnesium model.

The main findings of this report are: 1) In the deafferented and hyperexcitable neocortical slice, spontaneous epileptiform events start from confined foci rather than large diffuse areas. 2) There were only a few initiation foci in each preparation. 3) Among co-existing foci, one often became dominant for a period of many minutes. The domination was not permanent; an old dominant focus was often replaced by a new one.

Initiation foci are confined to a small size and have a relatively fixed location, suggesting that even in the hyperexcitable tissue, PDS events do not start everywhere. A specialized local process may be needed for this all-or-none population event. The phenomenon of dominant foci indicates that only a few loci in the tissue execute this specialized process. We observed that the PDS events always became visible in the image from a spot, smaller than one detector, suggesting that the initiation process is relatively localized. Coherent activation of a local group of neurons may be needed to initiate an all-or-none cortical event. The traditional view about cortical connectivity is sparse and divergent, and not in favor of a highly localized process. However, a recent study showed that local neurons can be highly interconnected. In our experiments, the volume of cortical tissue under each photo-detector contains about 4,000 cortical neurons, which is similar to the cortical domains of co-activation demonstrated in the developing neocortex. An initiation focus may also be a single pacemaker neuron or a small cluster of interactive neurons. Although it is possible to drive one neuron intracellularly to start a PDS in hippocampus, similar attempts in neocortex were not successful. In contrast, a weak stimulus applied extracellularly to simultaneously activate a group of neurons in cortex is capable of evoking a PDS event, suggesting that in cortex the initiation site might be a small group of simultaneously activated neurons.

Analysis of the frequency of spontaneous PDS events suggests complex non-linear dynamics . Our data suggest that the global frequency of the whole preparation may be determined by two levels of interactions: a local process to determine the frequency of each initiation focus and the global frequency determined by the dominant focus or a competition among non-dominant foci.

We propose that asynchronized local interactions among hyperexcitable neurons may undergo activity-dependent potentiations to become a local cluster with coherent activity. If this activity passes a certain threshold, it becomes an all-or-none PDS event. The activity of the PDS event itself, in contrast, may have an opposite effect of disrupting the formation of other potential initiation foci. This allows an initiation focus to become dominant over the whole slice. Activity dependent facilitation and LTP might be candidates for the dynamically potentiating connections within a local cluster of neurons.

In conclusion, spontaneous epileptiform activity may start from a small group of cortical neurons. Potentiation among the neurons in the group may play an important role so that local interactions which start one paroxysmal event become more likely to start successive paroxysmal events.

We have demonstrated that spontaneous paroxysmal events can be initiated in various cortical layers and so it seems that cortical neurons in various layers are capable of initiating EA. There might be a possibility that the initiation site in middle or superficial layers is controlled by layer V pyramidal neurons which start paroxysmal events before the activation in upper layers is detected. Optical recordings may be not able to detect such starting discharges from layer V pyramidal neurons if the signal is too small. This implies that even though we have seen the activity starting from the superficial or middle layers, it might actually be triggered by undetectable activities in the deep layers. To verify this possibility, a glass microelectrode was applied to measure the ability of stimuli

to initiate paroxysmal events in different layers. A single electrical pulse (10V 0.1 msec) was delivered at the electrode's tip which was less than 1 mm (usually about 0.1 μm) in diameter and placed in one of the six layers. The total current of stimulation was about 2-5 μA at the electrode's tip and the current density was 2500 times smaller at the distance of 50 μm from the tip according to sphere area role. Therefore, only a few neurons around the tip were affected by the stimulation. We found that paroxysmal events were reliably evoked in all cortical layers by the stimulation. The evoked paroxysmal events had the same characteristics as spontaneous paroxysmal events, and propagated vertically and horizontally. The initiation site depended only on the position of the stimulation electrode's tip . The images show clearly that activation first appeared at the stimulus electrode's tip with no delay and then spread smoothly to the neighboring areas. No saltatory activation from the stimulus electrode's tip to deep layers or other cortical areas was observed in any of the experiments (n=8). Various areas of the cortex including frontal occipital, parietal, temporal, perirhinal, and hippocampal cortices were tested; all the cortical structures were found to be capable of generating evoked paroxysmal events. Since the evoked paroxysmal events start regardless of layer V pyramidal neuron discharges, it is possible that EA initiation in various layers is independent of the control from layer V pyramidal neurons.

Pyramidal neurons in layer V tend to have oscillations which may trigger spikes and initiate EA when bathed in zero Mg^{2+} ACSF. These neurons are more easily studied by conventional intracellular recordings as they are bigger than others. On the other hand, neurons in the superficial layers tend to be smaller and more difficult to access for conventional electrical recordings. As optical recordings reflect the transmembrane potential change in all neurons stained with voltage-sensitive dyes and all these neurons contribute to the optical signal regardless their physical size, this difficulty can be overcome by using optical recording techniques. In our experiments, imaging data from optical recording using voltage-sensitive dyes revealed that paroxysmal events could spontaneously be initiated in various cortical layers. Paroxysmal events could be evoked by electrical stimulation in any layer of the neocortex regardless of discharges from layer V pyramidal neurons. Therefore, it is possible that neurons in various layers may become initiation cells and trigger EA in zero Mg^{2+} epilepsy model, although layer V pyramidal neurons may provide background excitability for the neurons in other layers as suggested by the evidence that elimination of layer V abolishes the activity in superficial layers. In fact, neurons in both superficial and deep layers can have repetitive discharge properties, and neurons with repetitive discharge properties are capable of initiating EA. It is likely that cortical neurons may initiate EA when they burst autonomously at a higher firing rate than other neurons, particularly when a number of neurons burst simultaneously. This implies that various cortical neurons in all layers are capable of initiating paroxysmal events once they are active, and such initiation processes do not rely on a specific type of neurons.

The epileptic focus revealed by imaging data was composed of a small confined area less than 0.04 mm^3, indicating that relatively few cortical neurons were activated when paroxysmal events started. As this is the smallest area a photodiode can detect in our experiments, a real epileptic focus could be much smaller. Further investigation of the organization in the focus can be made by multineuronal recording on those neurons within the focus at higher spatial resolution. However, it is difficult to distinguish individual neurons with massive staining method used in this study, and other staining methods are needed to individually label the cortical neurons with voltage-sensitive dyes, such as using retrograde staining method. We hypothesize that a neuron (pool) with repetitive discharge properties in the epileptic focus may synchronously activate its adjacent neurons and thus initiate EA. This is simulated by the electrical stimulation which generates synchronized activation of cortical neurons around the microelectrode tip. The activation area was estimated to be small,

probably within the distance less than 50 mm, and was calculated less than 5 x 10-4 mm3. Such synchronized activation by stimulation was found to be able to further activate more adjacent areas and result in paroxysmal event propagation in all our experiments. The majority of active neurons were excitatory or only had excitatory effect on adjacent cells even when inhibitory neurons could also be activated. This was not caused by dormancy of GABAergic neurons, since addition of inhibitory transmitter GABA (200 mM) in zero Mg^{2+} ACSF did not abolish the capacity of paroxysmal event initiation (unpublished results), suggesting that the inhibitory function in the cortex may not be effective during zero Mg^{2+} induced EA. Furthermore, GABAergic neurons may function as reciprocal excitatory neurons during EA via activation by glutamate and direct excitatory effect on target neurons, as all neurons are highly excited via sensitized NMDA receptors in zero Mg^{2+} ACSF . In conclusion, our optical imaging study on EA initiation have shown that spontaneous EA can start in various cortical layers, suggesting that the mechanism for forming the epileptic focus may exist in all cortical layers. Different types of neuron in all cortical layers are activated during EA and so may participate in EA initiation and propagation.

COMPUTATIONAL NEUROSCIENCE: Two faculty Members work in this area. Dr. Goodhill models neuronal development, including the structure of cortical mappings and axonal guidance. Dr. Pouget uses mathematical analysis and computer simulations to study mechanism of information processing in selected cortical regions.

GEOFFREY GOODHILL, PH.D.

Dr. Goodhill has two main research goals, both broadly relating to neural development. The first goal is to understand the theoretical principles governing the development and structure of cortical mappings. The second research goal is to understand quantitatively how gradients of chemotropic factors guide axons to appropriate targets in the developing brain.

PROJECT 1: DEVELOPMENT OF CORTICAL MAPS

Two key questions for understanding sensory processing are, how is information about the world represented in the cortex, and how are these representations formed during development. The best studied cortical areas in this regard are V1 and V2, where features of the visual scene such as position, orientation, direction and spatial frequency are represented in maps. Understanding how these maps and the relationships between them come about is an important step in answering the questions posed above. The relative importance of genetic versus epigenetic (particularly activity-dependent) mechanisms in determining cortical structure is still a subject of intense debate. This debate impacts directly on the design of effective therapies for treating the effects of early sensory visual experience.

Dr. Goodhill has been testing the hypothesis that cortical map structure arises from activity-dependent learning rules that attempt to represent highly correlated input features close together, acting in conjunction with genetically determined constraints such as the shape of the target area. To do this he has been using the elastic net algorithm, a theoretical model of cortical development that is well suited to exploring questions of large-scale map structure. Figure 1(a) shows results of the algorithm applied to a four dimensional feature space representing spatial position and orientation preference((coded as two cartesian dimensions ($\cos\theta$, $\sin\theta$). The model reproduces the characteristic pattern of "pinwheels", points around which all orientations are represented. Figure 1(b) shows the movement of receptive field profiles across visual space for an imaginary "electrode track" across the cortex, and figure 1(c) shows the pattern produced by a more generous annealing schedule. The results are now being quantitatively compared with recent experimental data (e.g. Das & Gilbert, Nature, 387:594) in order to understand the relative significance for map structure of each of the biological mechanisms reflected in the model. This work is now partly supported by an NSF grant (IBN-9808364) awarded to Dr. Goodhill entitled "The Development and Structure of Visual Cortical Maps".

PROJECT 2: AXON GUIDANCE BY GRADIENTS

Axon guidance by gradients plays an important role in wiring up the developing nervous system. Growth cones sense a concentration difference between their two ends, and convert this into a signal to move up or down a gradient. Previously, Dr. Goodhill formulated a very simple mathematical framework to understand when and where gradient detection can occur as a function of gradient

shape. This framework was applied to two examples: the guidance of axons by target-derived diffusible factors in vivo and in collagen gels, and to guidance by substrate-bound gradients of optimal shape, as might be relevant in the retinotectal system. More recently, in collaboration with Dr.Jeffrey Urbach (Physics Dept.), Dr. Goodhill has been investigating a much more sophisticated model of gradient sensing (originally developed by Berg & Purcell (1977)) and derived its predictions for growth cones. The model predicts that the minimum detectable gradient steepness for a diffusible ligand in three dimensions is about 1%, in good agreement with the (extremely crude) experimental data that currently exists. However, the model also predicts that this value should be much higher, about 10%, for detection of a substrate bound factor (due to the lower ligand diffusion rate). This predicted difference remains to be investigated experimentally.

A

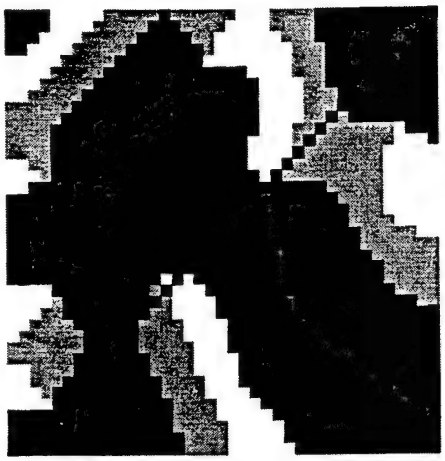

B

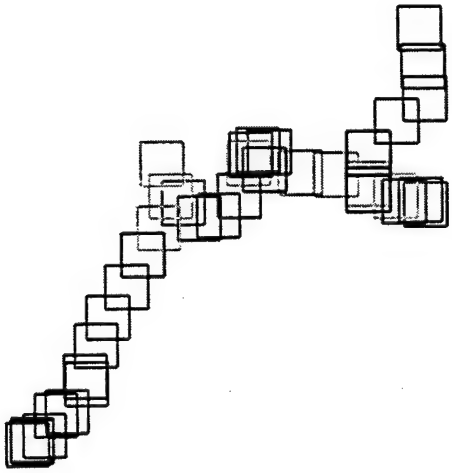

C

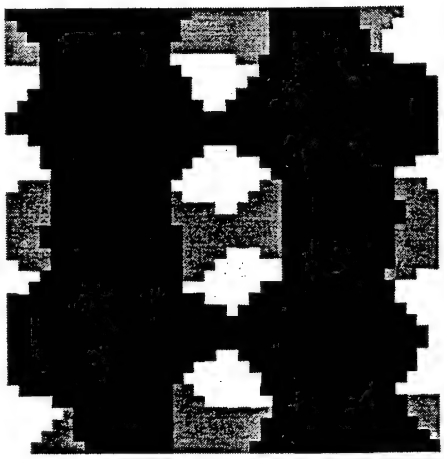

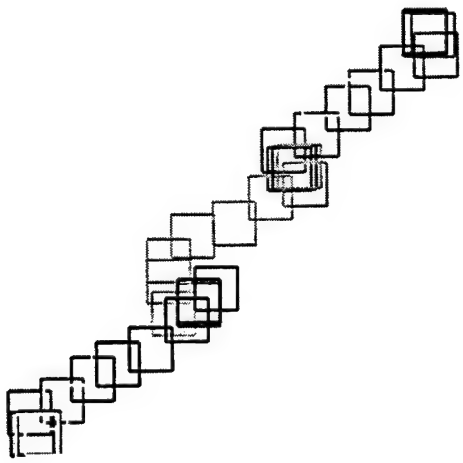

Figure 1: **A** Orientation map produced by the elastic net algorithm. Each color represents a particular orientation in a regular progression between 0 and 180 degrees. Note the presence of "pinwheels", where all orientations are represented around a point. The black squares show an imaginary "electrode track" across the cortex. **B** Receptive field (RF) position in the visual field for the cortical cells marked in A. RF position advances most rapidly in regions where orientation preference remains constant. **C** Orientation map produced by the elastic net using the same parameters as in A, except with a much slower annealing schedule. This means that the algorithm can find a better solution of the abstract optimization problem that this representation of the problem implies. As expected, this more optimal solution is highly symmetric. The fact that it resembles real maps less than in case A suggests that either this formulation of the problem is wrong, or that biology operates in a regime of less than perfect optimization. **D** RF progression for map C (same electrode trajectory as in A). Note that the progression is more regular than in B.

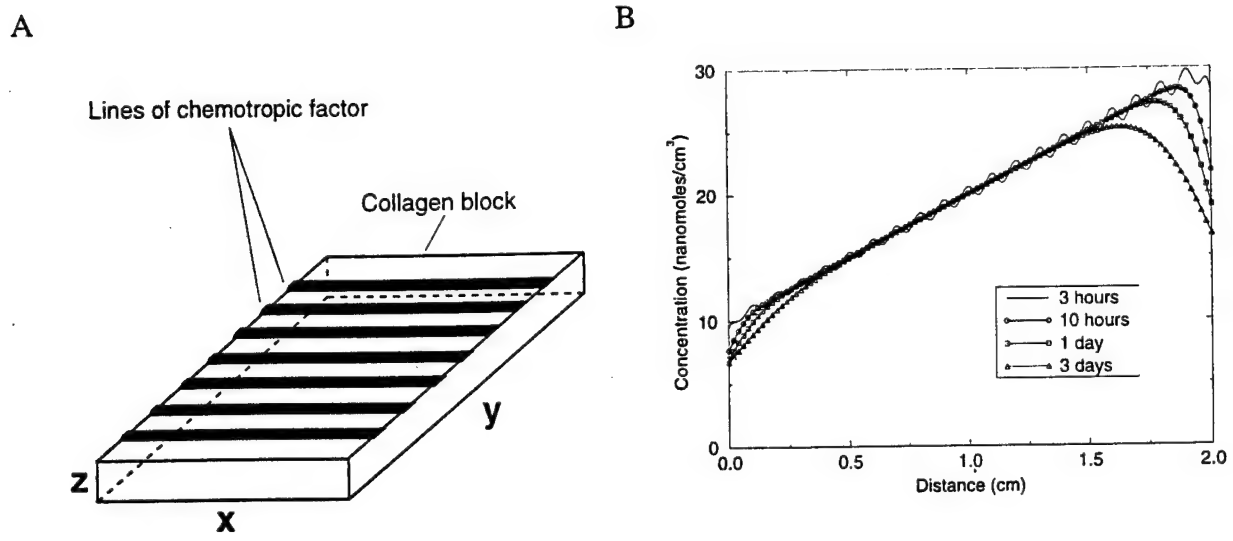

Figure 2: **A.** Formation of a smooth gradient from a non-uniform pattern. A block of gel is used that is much thinner (*z* dimension) than it is long (*y* dimension). Uniformly spaced lines of a chemotropic factor are painted onto the surface of the block. concentration is uniform along the *x* dimension of each stripe, but the concentration of factor applied gradually increases between successive stripes moving from one end of the block to the other. A uniform concentration is then formed rapidly in the *z* direction but extremely slowly along the *y* direction. **B.** The concentration as a function of position resulting from 21 equally spaced narrow lines of growth factor in a wide, thin block (modeled as one-dimensional, with no variation across the *x* axis) for times of 3 hrs, 10 hrs, 1 day, and 3 days. The quantity of factor in the initial lines varies linearly from one end of the block to the other. After 3 hrs these lines have decayed to a faint oscillation superimposed on an overall gradient. By 10 hrs these oscillations have disappeared, and only the smooth gradient remains. This persists for several days, which is sufficiently long for significant axon growth. For this calculation, $D = 10^{-7}$ cm^2/sec and the strengths of the initial lines ranged from 1 millimole/cm at 0 cm to 3 millimole/cm at 2 cm.

In addition to this purely theoretical work, Dr. Goodhill (again in collaboration with Dr. Urbach) is also developing a novel experimental system for testing hypotheses about the mechanisms of axonal gradient detection. Using cutting-edge nanotechnology, they are building a device to "paint" a pattern of varying concentration of a guidance molecule (initially NGF) onto the surface of a long, thin block of collagen gel. The molecules then diffuse into the collagen, creating a gradient. Numerical calculations show that the concentration will quickly become uniform across the (small) thickness of the block, but that a stable gradient, reflecting the original pattern on the surface, will exist along the length of the block for several days (see figure 2). Axons, initially from dorsal root ganglion explants, will then be grown in gradients of different shapes, and their behavior analyzed as a function of parameters such as gradient steepness. This will yield precise, quantitative data to constrain models of the mechanisms of gradient sensing by growth cones. This work is now partly supported by an NIH Shannon Award granted to Dr. Goodhill entitled "Precisely Controlled Gradients for Axon Guidance".

We have been pursuing two lines of research over the past year. The first project is concerned with the issue of neural coding and involves computer simulations and mathematical analysis. The goal is to understand how large populations of neurons encode sensory, or motor, variables through their firing rate and how this code is used in simple behavioral tasks. We have been able to show, in particular, that every cortical layer can read out the code from the preceding layer in a statistically optimal way.

The second line of research is concerned with the issue of spatial perception. We address this issue from both a theoretical and experimental perspective. Most of our theoretical work has been devoted to extending our model of hemineglect--- a neuropsychological syndrome in which patients ignore half of space--- to what is known as object-centered neglect. Object-centered neglect refers to the fact that most neglect patients tend to ignore the left side of objects regardless of the location of the objects in space. Our model shows how this behavior can be linked to the response properties of single neurons involved in object-centered representations. We are also currently developing several experimental protocols on normal subjects and hemineglect patients. These studies aim at testing some of the predictions that have emerged from out modelling work as well as investigating multisensory integration. They are conducted in collaboration with the laboratory of Jon Driver at the University College of London, UK, and the National Rehabilitation Hospital in Washington DC.

PROJECT 1: NEURAL THEORY OF IDEAL OBSERVERS

Information processing in the cortex is often formalized as a sequence of a linear stages followed by a nonlinearity. In the visual cortex, the nonlinearity is best described by a rectification and squaring combined with a divisive pooling of local activities. The divisive part of the nonlinearity, referred to here as Heeger's normalization, has been extensively studied by Heeger and colleagues. Several authors have explored the role of Heeger's normalization in the computation of high order visual features such as orientation of edges or first and second order motion. We show in this paper that Heeger's normalization can also play a role in noise filtering. More specifically, we demonstrate through network simulations that this normalization can be used to perform maximum likelihood estimation of visual features encoded in a population code.

Maximum likelihood estimation is a framework commonly used in the theory of ideal observers. A recent example comes from the work of Itti et al., 1998, who have shown that it is possible to account for the behavior of human subjects in simple discrimination tasks. Their model comprised two *distinct* stages: 1) a network, which models the noisy response of neurons with tuning curves to orientation and spatial frequency combined with Heeger's normalization, and 2) an ideal observer (a maximum likelihood estimator) to read out the population activity of the network.

Our work suggests that there is no need to distinguish between these two stages, since, as we will show, Heeger's normalization comes close to providing a maximum likelihood estimation. More generally, we propose that there may not be any part of the cortex that acts as an ideal observer for patterns of activity in sensory areas but, instead, that each cortical layer acts as an ideal observer of the activity in the preceding layer.

Project 1.1 The network

Our network is a simplified model of a cortical hypercolumn for spatial frequency and orientation. It consists of a two dimensional array of units in which each unit is indexed by its preferred orientation, θ_i and spatial frequency, λ_j. Activities in the cortical layer are updated over time according to:

$$u_{ij}(t+1) = \sum_{kl} w_{ij,kl} o_{kl}(t), \quad o_{ij}(t+1) = \frac{u_{ij}(t+1)^2}{S + \mu \sum_{kl} u_{kl}(t+1)^2}, \qquad (1)$$

where $\{w_{ij,kl}\}$ are the *filtering* weights, $o_{ij}(t)$ is the activity of unit *ij* at time t, S is a constant, and μ is what we call the *divisive inhibition* weight. The filtering weights implement a two dimensional Gaussian filter:

$$w_{ij,kl} = w_{i-k,j-l} = K_w \exp\left(\frac{\cos[2\pi(i-k)/P] - 1}{\sigma_{w\theta}^2} + \frac{\cos[2\pi(j-l)/P] - 1}{\sigma_{w\lambda}^2}\right) \qquad (2)$$

Where K_w is a constant, $\sigma_{\omega\theta}$ and $\sigma_{\omega\lambda}$ control the width of the filtering weights, and there are P^2 units.

At each iteration, the activity is filtered by the $w_{ij,kl}$, squared, and normalized by the total local activity. Heeger's normalization *per se* only involves the squaring and division by local activity. We have added the filtering weights to obtain a local pooling of activity between cells with similar preferred orientations and spatial frequencies. This pooling can easily be implemented with cortical lateral connections and it is reasonable to think that such a pooling takes place in the cortex.

Our simulations consist of iterating the dynamical equation of the network with initial conditions determined by the presentation orientation and spatial frequency. The initial conditions are chosen as follows: For a given presentation angle, θ_0 and spatial frequency, λ_0, determine the mean cortical activity $f_{ij}(\theta_0\lambda_0)$. Then generate the actual cortical activity, $\{a_{ij}\}$, by sampling from the distribution of the noise (which we assumed to be Poisson). This serves as our set of initial conditions: $o_ij(t=0) = a_{ij}$.

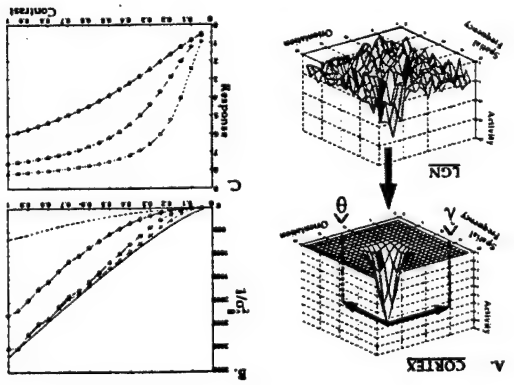

Figure 1. A- LGN input (bottom) and stable hill in the cortical network after relaxation (top). The position of the stable hill can be used to estimate orientation (θ) and spatial frequency (λ) B- Inverse of the variance of the network estimate for orientation using Gaussian noise with variance equal to the mean as a function of contrast and number of iterations (0, dashed, 1, diamond, 2, circle, and 3, square). The continuous curve corresponds to the theoretical upper bound on the inverse of the variance (i.e. an ideal observer). C- Gain curve for contrast for the cortical units after 1, 2 and 3 iterations.

Iterating equation 1 with the above initial conditions, we found that for very low contrast the activity of all cortical units decayed to zero. Above some contrast threshold, however, the activities converge to a smooth stable hill (see figure 1-A for an example with parameters $\sigma_{\omega\theta} = \sigma_{\omega\lambda} = \sigma_{\theta} = \sigma_{\lambda} = 1/\sqrt{8}$, K = 74, C = 1, μ = 0.01). The width of the hill is controlled by the width of the filtering weights. Its peak, on the other hand, depends on the orientation and spatial frequency of the LGN input, θ_0 and λ_0. The peak can thus be used to estimate these quantities (See figure 1-A). To compute the position of the final hill, we used a population vector estimator although any unbiased estimator would work as well. In all cases we looked at, the network produced an unbiased estimate of θ_0 and λ_0.

In the first set of simulations, we adjusted $\sigma_{\omega\theta}$ and $\sigma_{\omega\lambda}$ such that the stable hill has the same profile as the mean LGN input. As a result, the tuning curves of the cortical units match the tuning curves specified by the pooled LGN input. For this case, we found that the estimate obtained from the network has a variance close to the theoretical minimum, known as the Cramer-Rao bound. For Gaussian noise of fixed variance, the variance of the estimate was 16.6% above this bound, compared to 3833% for the population vector applied directly to the LGN input. In a 1D network (orientation alone), these numbers go to 12.9% for the network versus 613% for population vector. For Gaussian noise with variance proportional to the mean, the network was 8.8% above the bound, compared to 722% for the population vector applied directly to the input. These numbers are respectively 9% and 108% for the 1-D network. The network is therefore a close approximation to a maximum likelihood estimator, i.e., it is close to being an ideal observer of the LGN activity with respect to orientation and spatial frequency.

As long as the LGN and cortical tuning curves had the same width, large variations in the width of the filtering weights did not affect our results (except for extreme settings such as infinite or zero width). Likewise, as long as the contrast was superthreshold, large variations in contrast, C, did not effect our results (figure 1-B). A match between the width of the LGN hill of activity and the width of the output stable hill, however, was important: mismatches of 10% or more--- obtained by adjusting $\sigma_{\omega\theta}$ and $\sigma_{\omega\lambda}$ --- led to a rapid degradation in performance (not shown).

Using a perturbative approach, we confirmed analytically that Heeger's normalization is indeed a close approximation to a maximum likelihood estimator. Our derivation of this result is general and applies to a large class of nonlinear networks with M-dimensional attractors, of which Heeger's normalization in only a subcase. By M-dimensional attractors we mean an M-dimensional manifold in activity space that is stable with respect to the action of the network; e.g., with respect to the dynamical equations of the network. For the network described above, the stable state forms a 2-dimensional manifold, because we encode two visual features, orientation and spatial frequency, simultaneously. Each point on the manifold corresponds to a stable hill peaking at a different location.

Our analysis shows that the variance of the estimates is well approximated by:

$$\langle(\hat{\theta} - \theta)^2\rangle \approx \frac{\sigma^2}{|\mathbf{f}'|^2 \cos^2 \delta} \qquad (3)$$

where **f**, which is the mean input to the network, is a vector with components f_{ij} (θ,λ) prime denotes derivative with respect to θ, $|f^2| \equiv \Sigma_{ij} (\partial_\theta f_{ij})^2$ (this definition of absolute value applies to any of the two-index vectors we consider here), and δ is the angle between $v^\dagger$ the adjoint eigenvector of the network Jacobian with eigenvalue one, and **f'**. This last quantity is given by $\cos \delta = \Sigma_{ij} f'_{ij} v^\dagger_{ij} / |\mathbf{f}'| |v^\dagger|$.

The Cramer-Rao bound for this case, i.e., the theoretical minimum, is equation 3 without the term $\cos^2 \delta$. For the implementation of Heeger's normalization described above, $\cos^2 \delta$ was equal to 0.94. (See methods for the parameters used in this set of simulations.) This predicts a standard deviation 6% above the Cramer-Rao bound for independent Gaussian noise with fixed variance, consistent with the 8.7% we obtained in the simulations.

In general, any network for which δ is small will be a close approximation to a maximum likelihood estimator. Thus, as long as δ is small our conclusions apply to future theoretical formulations of cortical nonlinearities, not just Heeger's normalization.

We have recently shown that a subclass of line attractor networks can be used as a maximum likelihood estimators . This paper extend this conclusion to a much wider class of networks, namely, any network with a weak nonlinear activation function and a line attractor. This is true in particular for networks using Heeger's normalization, a normalization which is thought to match quite closely the nonlinearity found in the primary visual cortex and MT.

To conclude, we propose that each cortical layer may read out the activity in the preceding layer in an optimal way thanks to the non linear pooling properties of Heeger's normalization, and, as a result, may behave like an ideal observer. It is therefore possible that the ability to read out neuronal codes in the sensory cortices in an optimal way may not be confined to a few areas like the parietal or frontal cortex, but may instead be a general property of every cortical layer.

PROJECT 2: OBJECT-CENTERED NEGLECT

One of the first evidence for object-centered neglect came from the work of Caramazza and Hillis who reported a patient with a right *word-centered* neglect. This patient made spelling mistakes, primarily on the right side of words, whether the words were presented horizontally, vertically or mirror reversed (in the latter case, the right side of the word appeared in the left hemispace). Since then, several studies claim to have observed similar behaviors not just for words but for object as well.

We argue that in most cases, their results can be explained with what we called *relative* neglect, a form of neglect that does not involve a lesion of an object-centered representation. There are however a few studies that cannot be explained by relative neglect. We address these cases in the second part of this section. We show that recent single cell data suggest a natural extension of the basis function framework to object-centered representations and we explain how this extension of the basis function hypothesis can account for Driver et al results.

Project 2.1 Object-centered neglect or relative neglect?

A paper by Arguin and Bub provide a good illustration of the kind of data typically used in support of object-centered neglect. As shown in figure 2A, they found that reaction times were faster when a target (the "**x**"}" in figure 2B) appeared on the right of a set of distractors (C2) instead of on the left side (C1), even though the target is at the same retinotopic location in both conditions.

Although this result is certainly consistent with object-centered neglect, it is just as consistent with the idea that patients tend to neglect the parts of the object the furthest to the left, where left is defined with respect to the viewer, not the object. In other words, what matters may be the relative position of stimuli, or subparts of an object, along the left-right defined with respect to the viewer. This is what we call *relative* neglect. The result of several other studies can be accounted with relative rather than object centered neglect. The only way to distinguish between these alternatives is to rotate the object such that the left-right axis of the object if no longer lined up with the left-right axis of the object.

This comment applies as well to standard clinical tests such as line cancellation and line bisection. Lime bissection is a test in which patient are asked to judge the midpoint of a line. Left neglect patients typically estimate the midpoint to far to the right. One might be tempted to conclude this right overshoot is due to neglect of the left side of the line--- an line-centered interpretation. If this was the case then rotating the line by 45 degree with respect to the viewer should have no effect on subject performance. The left side of the line should still be neglected by the same amount. On the other hand, if this is an example of relative neglect, then the overshoot is due to the fact that subject ignore the part of the line the furthest to the left with respect to the viewer. This would predict that when the line is vertical, the overshoot should disappear since no part of the line if further to the left than any other part. Experimental evidence support the latter hypothesis. The amount of overshoot is proportional to the cosine of the angle between the line and the viewer with a minimum when the line is near vertical.

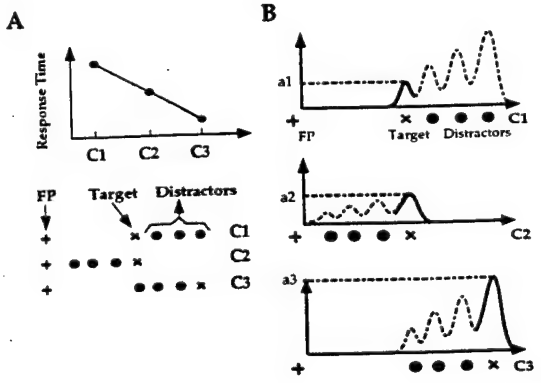

Figure 2: A. Response times for Arguin and Bub (1993) experiment for the three experimental conditions illustrated below the graph (**FP**, fixation point). See text for details. **B**. Reaction time between conditions 1 and 2 decreased due to the change in the relative saliency of the target with respect to the distractors, even though the absolute saliency of the target was the same in these two conditions (**a1** = **a2**). **FP**, Fixation point; **C3**, condition 3.

Interestingly, relative neglect emerges naturally in our basis function model of neglect. The network reaction times in simulations of the Arguin and Bub experiments followed the same trends reported in human patients (figure 2A). This result can be easily understood if one examine the pattern of activity in the retinotopic output layer of the network for the three conditions in those experiments. Although the absolute levels of activity associated with the target (solid lines) in conditions 1 and 2 were the same, the activity of the distractors (dotted lines) differed in the two conditions. In condition 1, they had relatively higher activity and thereby strongly delayed the detection of the target by the selection mechanism. In condition 2, the distractors were less active than the target and did not delay target processing as much as they did in condition 1. The network also reproduced the behavior of patients on a line bisection task. In particular, the overshoot goes away for vertical lines.

The network also reproduces the further decrease in reaction time when the whole display, target and distractors, are moved further right on the retina (condition 3). This indicates that both the relative and absolute retinal position play a role in neglect. This is another example of multiple frames of reference being affected concomitantly in the same patient (and model).

To really establish object-centered neglect, one needs to test patients with rotated objects. Object-centered neglect predicts that the neglected part will be the left side of the object whereas relative neglect predicts that it will be the part of the object the furthest on the left with respect to the viewers.

Farah et al. have run such an experiment and reported results consistent with relative neglect. Behrmann obtained similar result expect for asymmetric letters for which the results seem to indicate object-centered neglect. However, Drain and Reuter-Lorenz have obtained similar results on asymmetric letters in normals, casting doubt on the object-centered neglect interpretation.

Tipper and Berhmann have also reported data consistent with object-centered neglect. They used stimuli made of two circles, one on the left and one on the right. The circles could be linked by a bar, forming a barbell-like object, or not. They explored whether priming can be defined in object—centered coordinates and found that when the right circle was primed, followed by a $180° rotation which brought the right circle to the location of the left circle and vice-versa, the priming stayed with the right circle (now on the left), but *only* If the two circles were linked by the bar.

This result is certainly consistent with the idea that attention can be allocated in object-centered coordinates. A simpler interpretation however is that attention is allocated in retinal coordinates and that the attentional spotlight can move with an object. Moreover, the fact that attention followed the left circle only when linked to the other circle would imply that that the dynamic of the attentional spotlight is influenced by segmentation factors. Our network model does not include this mechanism and, consequently, cannot account for this experimental result on priming. However, simulations by Mozer shows that Tipper and Behrmann's result can indeed be explained by using an attentional spotlight that works in retinal coordinates (see Mozer's chapter in this book). What make this demonstration particularly interesting is the fact the Mozer's model was originally designed to perform word recognition. It is therefore possible that Tipper and Behrmann's result are not related to the existence of explicit object-centered representations (a term we defined more precisely in the next section) but could be a byproduct of the way the visual system segments and recognizes words and objects.

Ultimately, there appears to be only one result that could not be explained without invoking object-centered representation, namely, the experiment by Driver et al. in which patients were asked to

detect a gap in the upper part of a triangle embedded within a larger object. They reported that patients detected the gap more reliably when it is associated with the right side of the object than when it belonged to the left side even when this gap appeared at the same retinal location across conditions.

Project 2.2: Basis function applied to object-centered representations

The existence of object-centered representations at the neuronal level appears to be supported by the recent work of Olson and Gettner. They trained monkeys to perform saccades to a particular side of an object (right or left, depending on a visual cue) regardless of its position in space. Ideally, it would have been important to test the monkey for multiple orientations of the object but these conditions were omitted in the first study. Once the monkey had acquired the task, they recorded the activity of cells if the supplementary eye field during the execution of the task.

They found that some cells respond selectively prior to eye movements directed to a particular side of an object. For example, a cell might give a strong response before an upward saccade directed to the left side of the object but no response at all to the *same* upward saccade but directed to the right side of the object. This behavior suggests that some cells have motor fields defined in object-centered coordinate which would constitute what we call an explicit object-centered representation. However, *all* the cells recorded by Olson and Gettner can be interpreted as having an oculocentric motor field --- a bell-shaped tuning to the direction of the next saccadic eye movement, where direction is defined with respect to the fixation point --- which is *gain modulated* by the side of the object .

More experimental data are needed to determine which ones of these interpretations are right. The gain modulation assumption however possesses obvious computational advantages. Performing saccades to the side of an object specified by an instruction can be formalized as a non linear mapping between the inputs, the image of a bar and an instruction, and the output, the motor command for the saccade. An efficient way to proceed is to use basis functions of the input variables in the intermediate stage of processing. These basis functions could be retinotopic receptive fields gain modulated by the command, which would be consistent with Olson and Gettner's results. Figure 3A shows a basis function neural network that can generate saccades to a particular side of an object according to an instruction and independently of the position and orientation of the object. This is a slightly more general situation than the one considered by Olson and Gettner since the model can handle arbitrary orientation.

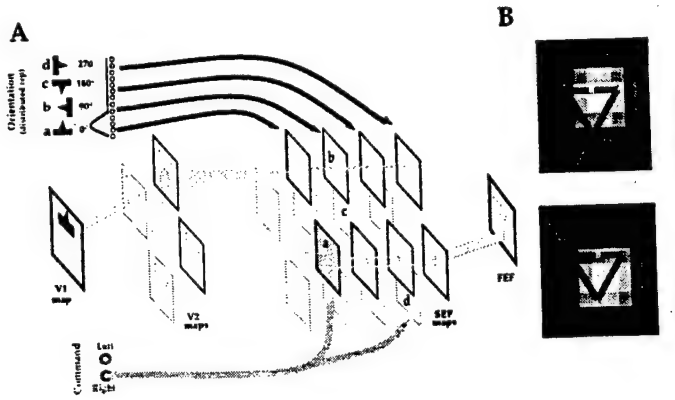

Figure 3: *A*, Neural network model for performing saccades to a particular side of an object in response to the image of the object and in instruction. The input contains a V1-like representation of

the image of the object, a set of cells tuned to the orientation of the object and a set of cells encoding the current command. The SEF layer contains gain modulated cells like the one found by Olson and Gettner, which compute basis function of the inputs. *B* summed activity generated in the SEF in response to the display used by Driver et al. in a lesioned network. The dotted line indicated the general orientation of the object. The activity associated with the upper edge of the triangle is the weakest when the object is tilted clockwise (bottom). This is consistent with Driver's finding that left neglect patients perform worse in this condition.

Deneve et al. have explored the effect of a unilateral lesion in this basis function model. They assumed that the left hemisphere over represents right retinal location and counterclockwise object rotation (and vice-versa for the right hemisphere). The retinal gradient is identical to the one used by Pouget and Sejnowski (see the preceding sections). The preference for counterclockwise object rotation is consistent with the general principle used for setting the gradients, namely, the left hemisphere favors any posture toward the right, such as moving the eye to the right, rotating the head to the right, or tilting the head to the right. Indeed, when the head is tilted to the right, the retinal image rotates *counterclockwise*. The hemisphere preferring head tilt to the right should therefore also favor counterclockwise image rotation.

Figure 3B shows the amount of activity in the basis function layer of a lesioned network, in response to the presentation of the triangle display of Driver et al. The important part to focus on is the upper edge of the central triangle, the edge for which the patients are asked to detect the presence of a gap. As one might expect given the hemispheric gradient, the highest activity is obtained when the object is tilted counterclockwise. This is the case for which subjects perceive the edge to be on the right of the main axis.

This network was not designed to detect the presence of a gap but a simple signal-to-noise argument would predict that the presence of the gap should be more readily detected for counterclockwise than clockwise rotation, which is what Driver et al. reported in patients.

The interesting point here is that object-centered neglect is obtained here even though the network does not contain an explicit object-centered representation, i.e., it does not use cells with motor, or receptive, fields in object coordinates. Instead, the representation use a more implicit format, involving basis functions of the inputs, which is computationally more efficient and consistent with single cell data.

DRUG DISCOVERY AND DESIGN: There are currently two faculty members in this area. Dr. Kozikowski's work relates to the design and synthesis of new pharmacological research tools for understanding brain mechanisms, including cognitive drug development. Dr. Wang utilizes molecular modeling techniques as part of drug development.

ALAN P. KOZIKOWSKI, Ph.D.

The drug discovery efforts at GU have been very productive, and led to the filing of 10 full or provisional patents. In particular, the DOD funds have been used to support research relating to the creation of novel TRH analogs for the treatment of neurodegenerative diseases, and to initiate a program directed to the discovery of small molecule inhibitors of one of the key enzymes involved in the cell death cascade, CPP32. Also, some effort has been directed to the design of novel analogues of the Alzheimer's drug huperzine A. Moneys are requested to continue these already very productive lines of research. Optimization of the TRH analogues will be undertaken. Further iterative synthesis, design, and testing of inhibitors of CPP32 will be conducted with the goal to find cell permeable, nanomolar inhibitors of this enzyme. Also, moneys are requested to pursue the idea of using huperzine A as a lead compound in the creation of an Alzheimer's diagnostic for PET imaging.

To date we have prepared a number of analogues of thyrotropin-releasing hormone (TRH) that may find use in traumatic brain injury, stroke, Alzheimer's disease, and other neurodegerative conditions. Recent work that involves extensive collaborations between the research groups of Dr. Kozikowski and Dr. Faden has shown that two classes of compounds which may be viewed as distant analogs of TRH show superb neuroprotective properties. Two prototype molecules, which are the subject of two recently filed GU patents, are exemplified by the tripeptide disulfide **I** and the cyclohexyl bearing diketopiperazine **II** (Figure 1). Neither of these molecules show much affinity for the TRH receptors per se, and thus their mechanism of action is unlikely to involve direct interaction with these receptors. Interestingly, compound **I** contains the chemically reactive disulfide linkage, which is likely to be converted in vivo to its monomeric mercaptan. Therefore, in analogy to the mechanism of action of glutathione,[1] we believe that the neuroprotective properties of **I** may be associated with its free radical scavenging properties. As such, we believe that it is likely that additional novel structures can be created by combining the remote TRH-like mimicry of these compounds with another pharmacological action known to be linked to neuroprotection. Therefore, with the aid of continued funding from the DOD moneys, it is our plan to synthesize other structures that are likely to disrupt radical damage inducing cascades, those involving both reactive oxygen intermediates and nitric oxide. As such our design rationale involves building additional novel diketopiperazine and tripeptide structures in which nitric oxide synthase inhibitors and oxygen radical traps are embedded. Tables 1 and 2 provide structures for the new compounds to be created.

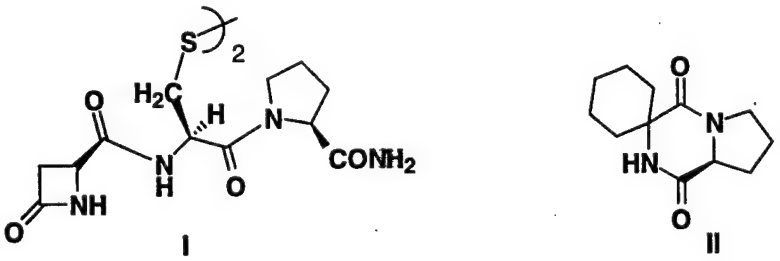

Figure 1. Structures of Neuroprotective Tripeptide **I** and Diketopiperazine **II**.

Reactive oxygen intermediates include the superoxide radical anion, hydrogen peroxide, and the very aggressive hydroxyl radical. The free radical mediated oxidation of cellular macromolecules (lipids, proteins, DNA, etc.) has been implicated in a number of disease states, including stroke and head trauma.[2] These radicals, acting mainly through the initiation of chain reactions, can cause extensive damage to unsaturated lipids found in neuronal membranes, thereby resulting in neuronal cell death and consequent neurological impairment. Thus, one novel approach to the development of neuroprotective agents has been based upon the discovery of molecules that act as free radical traps that are capable of intercepting chain initiators and/or chain carriers. Small molecular weight antioxidants already present in the body which are able to act in this manner include glutathione, thioredoxin, and vitamins C, and E.[1]

Therefore, within the context of further exploring TRH-like structures possessing an antioxidant action, we will incorporate moieties into our tripeptide and dipeptide structures that are known to function as free radical traps. Chemical entities will be synthesized that incorporate di-*t*-butyl catechol (**1a**, **2a**),[1] tocopherol analogs (**1b**, **2b**),[3] and nitrone groups (**1c**, **2c**)[4] into our dipepetide and tripeptide templates (Tables 1 and 2). Also, in view of the substantial activity already found for the disulfide, it will be appropriate to examine the activity of both its reduced form, i.e., the free SH form **1g/2g**, as well as the *t*-butylthio derivative **1h/2h**, as preliminary studies already reveal substantial activity for the diketopiperazine derivative incorporating the *t*-butylthio group. The synthesis of these materials will follow steps already worked out in our laboratories, with appropriate changes in protection/deprotection steps being made as necessary.

The nitric oxide produced by the neuronal enzyme nitric oxide synthase (NOS) is believed to play a role as a neurotransmitter under normal conditions of brain activity. However, since the inducible form of NOS plays a role in host defense mechanisms, it is also likely that excess production of this free radical can destroy functional tissue in cases of chronic inflammation.[5]

Thus, considerable attention has been given to the discovery of inhibitors of both the constitutive (brain and vascular endothelium) and inducible (macrophages) forms of NOS. The majority of these sturctures are analogs of L-arginine.[6] Based upon this relatively rich body of SAR information concerning NOS inhibitors, we will incorporate the L-arginine analogs **1d-1f** and **2d-2f** into our dipeptide and tripeptide structures. The methods of synthesis will again follow the general schemes that have already been used to prepare related compounds in our laboratories, and which are summarized in the following sections.

Table 1. New tripeptide analogs to be synthesized containing a variety of amino acid residues possessing radical scavenging activity.

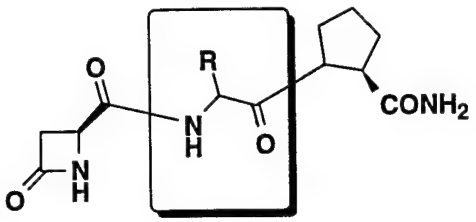

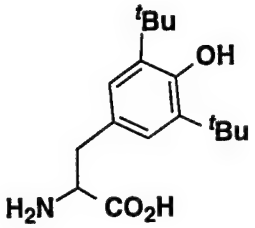

1a

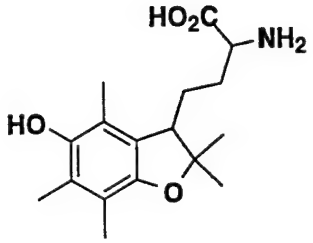

1b

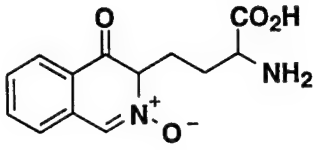

1c

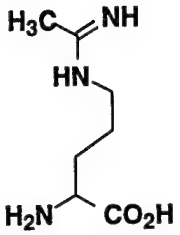

1d

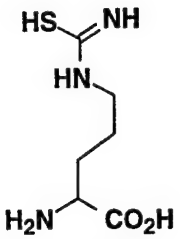

1e

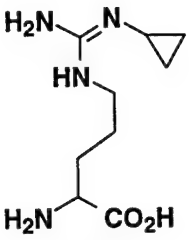

1f

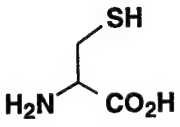

1g

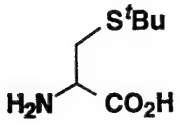

1h

Table 2. New diketopiperazine derivatives to be synthesized that contain radical trapping groups.

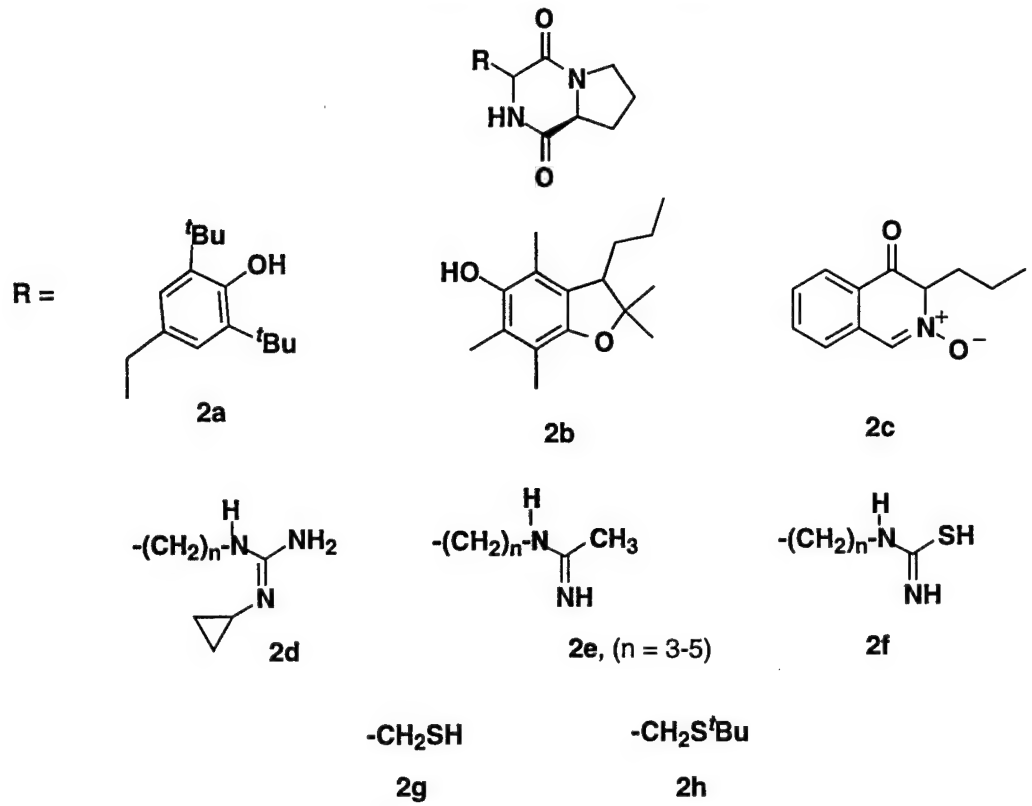

Apoptosis derives from a Greek word that means to fall off, as leaves from a tree. It is a process in which the cell shrinks, and eventually the apoptotic cell bodies that are produced are phagocytosed. Apoptosis is characterized by preservation of membrane integrity, cytoplasmic and nuclear condensation, reduction in cellular volume, plasma membrane bleb formation, and nuclear fragmentation. During apoptosis the morphological changes are often accompanied by internucleosomal cleavage of genomic DNA; the breakdown of the DNA occurs in discrete fragments of 180-200 base pairs, which appear as a DNA ladder in agarose gel electrophoresis. Apoptosis differs from necrosis in that the latter involves cell death that is accompanied by inflammatory processes. Thus in apoptosis cells can die one at a time, among a group of healthy cells, whereas in necrosis a whole group of cells may die at the same time. Death by necrosis is generally associated with a traumatic injury, ischemia, chemical exposure, and the like. Apoptosis is often confused or mixed up with programmed cell death (PCD). The latter term originated to describe cell death occurring at normal stages of the developmental program and that is initiated by some physiological trigger. In some cases PCD of cells shares morphological changes that are similar to those of apoptosis, but this is not always so.

While a complete pathway for cell death has not been defined, it is very clear from a number of studies that the CED-3/ICE family of proteases plays an essential role in apoptosis. The CED-3 homolog, CPP32, also known as apopain, plays a definitive role in cell death, for it is involved in the destruction of certain key homeostatic and repair enzymes at the onset of apoptosis. CPP32 degrades

proteins by effecting cleavage of functional domains comprised of the (P_4)Asp-X-X-Asp(P_1) motifs. Targets for destruction by CPP32 include poly(ADP-ribose) polymerase (PARP, which is an enzyme involved in DNA repair), the 460,000 M_r catalytic subunit of the DNA-dependent kinase essential for double-strand break repair, the 70000 M_r small nuclear ribonucleoprotein necessary for mRNA splicing, and other enzymes including protein kinase C delta. Studies have revealed that levels of CPP32 are elevated during apoptosis, and that its removal from apoptotic cellular extracts can lead to a reduction in apoptosis in an *in vitro* type of assay.

Of particular interest to our own research is the structural work that has been done on apopain. Researchers at the Merck Research Laboratories have recently been able to determine the three-dimensional structure of apopain in complex with the tetrapeptide aldehyde inhibitor, Ac-DEVD-CHO. This inhibitor has been shown to have a 49-fold preference for CPP32 versus ICE (interleukin-1β converting enzyme, which belongs to a second phylogenic subfamily of proteases, and whose role in apoptosis is less secure). In contrast, the tetrapeptide aldehyde Ac-YVAD-CHO is far more selective for ICE (K_i = 0.76 nM) than for CPP32 (K_i = 10,000 nM).

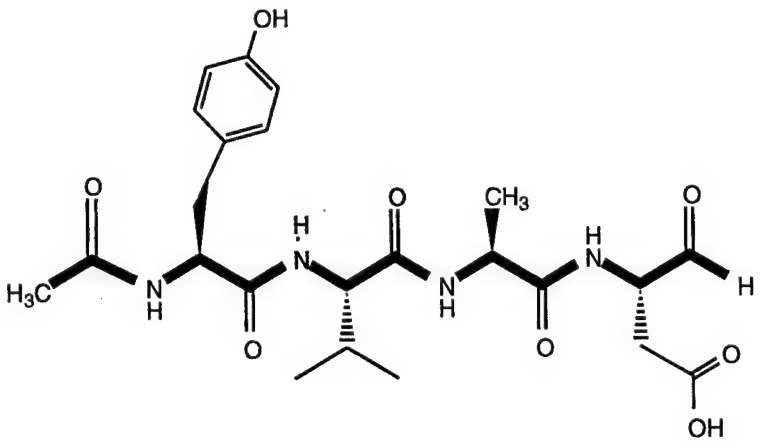

Figure 1. Ac-YVAD-CHO, selective inhibitor of ICE

The x-ray work reveals that the tertiary and quaternary structure of these cysteine proteases are similar. In both proteases two heterodimers associate to form a tetramer, a four-chain assembly with two-fold rotational symmetry. A diagram of the tetrapeptide aldehyde inhibitor bound to CPP32 is provided below. As is clear from this diagram, Cys 285 engages in thiohemiacetal formation with the aldehyde group, thus mimicking the transition state for amide bond hydrolysis. The binding pockets of ICE and apopain are similar, with the exception particularly of the S_4 subsite which appears to be responsible for the differences in substrate specificities. As expected from the preference for a P_4 Tyr in the ICE inhibitors, the corresponding subsite in the ICE enzyme corresponds to a large, shallow hydrophobic depression, while the P_4 site in apopain is narrow and intimately engulfs the P_4 aspartate residue side chain. Time dependent irreversible inhibitors of ICE have been designed that are acyloxymethylketones, and which react by displacement of the carboxylate group by the active site cysteine 285.

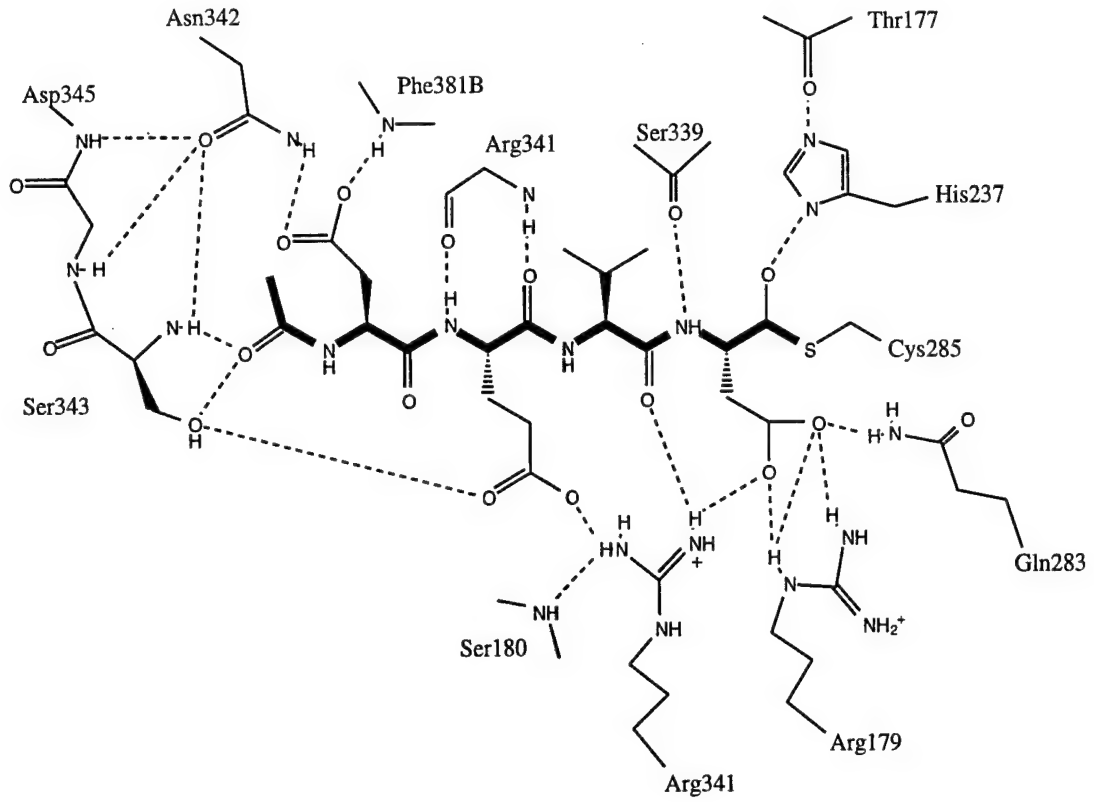

Figure 2. Hydrogen bonds and other polar interactions between the bound tetrapeptide aldehyde inhibitor and CPP32/apopain.

In order to discover compounds that may serve as cell permeable and selective inhibitors of these cysteine proteases, and in particular CPP32, we have chosen to investigate approaches based upon database screening methods in which a pharmacophore query is set up employing various elements of the x-ray structural information of the tetrapeptide inhibitor Ac-DEVD-CHO in complex with CPP32. Using this information, several very weak lead compounds were identified by Dr. Wang, and this information has being used in conjunction with rational drug design concepts to devise new inhibitors of CPP32. To date, Dr. Nan working in the laboratory of Dr. Kozikowski has synthesized approximately 10 molecules that have been tested for their inhibitory activity in the laboratory of Dr. Faden. One of these molecules was able to inhibit the enzyme with a K_i of approximately 7 μM. The activity of this compound is rather remarkable, in that it mimics only the VD-CHO part of the known tetrapeptide aldehyde inhibitor. Needless to say, this important result is being pursued vigorously in the laboratory, and other analogues designed with the aid of moleucular modeling are being assembled. It is our aim to achieve the design of selective inhibitors of CPP32 that: 1) contain no hydrolyzable peptide bonds, 2) are cell membrane permeable, and 3) are capable of functioning without the need for a "reactive" aldehyde group. This project represents a significant new area of our research program, and one which we believe holds tremendous promise in the search for new therapeutics in the treatment of major brain disorders including stroke and Alzheimer's disease.

We have conducted extensive modeling studies on huperzine A, a naturally occurring alkaloid that has shown promise in the treatment of Alzheimer's disease. Through the modeling studies we have now identified compounds that may have an increased potency for inhibiting acetylcholinesterase. The modeling studies make use of a co-crystal x-ray structure of HA in complex with AChE. By placing analogues into the same site as that occupied by HA in the crystal, and performing dynamics

simulations, we are able to estimate whether the new analogues are likely to serve as improved inhibitors of the enzyme. For example, using the modeling techniques, we have been able to explain why the location of a methyl group at HA's C-10 position leads to a compound exhibiting 8-fold improved potency, whereas introduction of a C-10 equatorial methyl leads to a compound possessing a higher K_I. In the former case the methyl group points into a hydrophobic region, whereas in the latter, the methyl group points into a more polar pocket. As the size of the C-10 substituent is increased from methyl to ethyl and propyl, activity drops off dramatically, possibly indicating a serious steric interaction of this substituent with the "walls" of the active site gorge. Clearly, while some additional steric volume is available in the region of the AChE binding site occupied by the C-10 axial substituent of HA, the available space is small, with the methyl analogue serving as the optimal structure.

Using such modeling studies, we have now selected additional compounds for synthesis that are likely to show improved activity. By identifying compounds that show altered AChE inhibitory potency, lipophilicity, improved duration of action, etc. it is likely we will be able to identify superior AChE inhibitors for the treatment of Alzheimer's disease. In this direction, we have recently completed the synthesis of the C-10 cyclopropyl analogue of huperzine A (see accompanying scheme). Since the 10,10-dimethyl analogue is slightly more potent than huperzine A, we anticipate that by tying the two methyl groups together, as in the cyclopropyl analogue, we should obtain an even more potent compound that may exhibit a slower off-rate from the enzyme. This change in enzyme off-rate may in turn confer an enhanced therapeutic advantage to the compound, since a smaller amount of drug would be needed to inhibit the enzyme. Additionally, this more lipophilic compound may more readily penetrate the blood brain barrier. The synthesis of the new analogue is detailed in Scheme 1, and the compound is presently in testing by Doctor Doctor's group at Walter Reed Army Institute of Research for it AChE inhibitory activity.

Using chemistry methods similar to those shown in the accompanying scheme, it is our intention to explore the chemistry and biology of C-10 functionalized huperzine analogues bearing ^{18}F or a $^{11}CH_3$ group at this position. In particular, as it has been shown that levels of AChE are decreased in the Alzheimer's brain, it would be our intention to examine the possibility of using this labeled form of huperzine as a diagnostic agent. As there currently exist no such PET imagining agents for AD, we believe that this effort is an extremely timely one to pursue given the aging of the world's population and the increased incidence of AD. Some effort would also be given to the notion of developing other imaging agents that are targeted to other enzymes known to exhibit altered levels of expression in the AD brain (e.g., 5-lipoxygenase).

Using chemistry methods similar to those shown in the accompanying scheme, it is our intention to explore the chemistry and biology of C-10 functionalized huperzine analogues bearing ^{18}F or a $^{11}CH_3$ group at this position. In particular, as it has been shown that levels of AChE are decreased in the Alzheimer's brain, it would be our intention to examine the possibility of using this labeled form of huperzine as a diagnostic agent. As there currently exist no such PET imagining agents for AD, we believe that this effort is an extremely timely one to pursue given the aging of the world's population and the increased incidence of AD. Some effort would also be given to the notion of developing other imaging agents that are targeted to other enzymes known to exhibit altered levels of expression in the AD brain (e.g., 5-lipoxygenase)

Scheme 1. Synthesis of the 10-Cyclopropyl Derivative of Huperzine A.

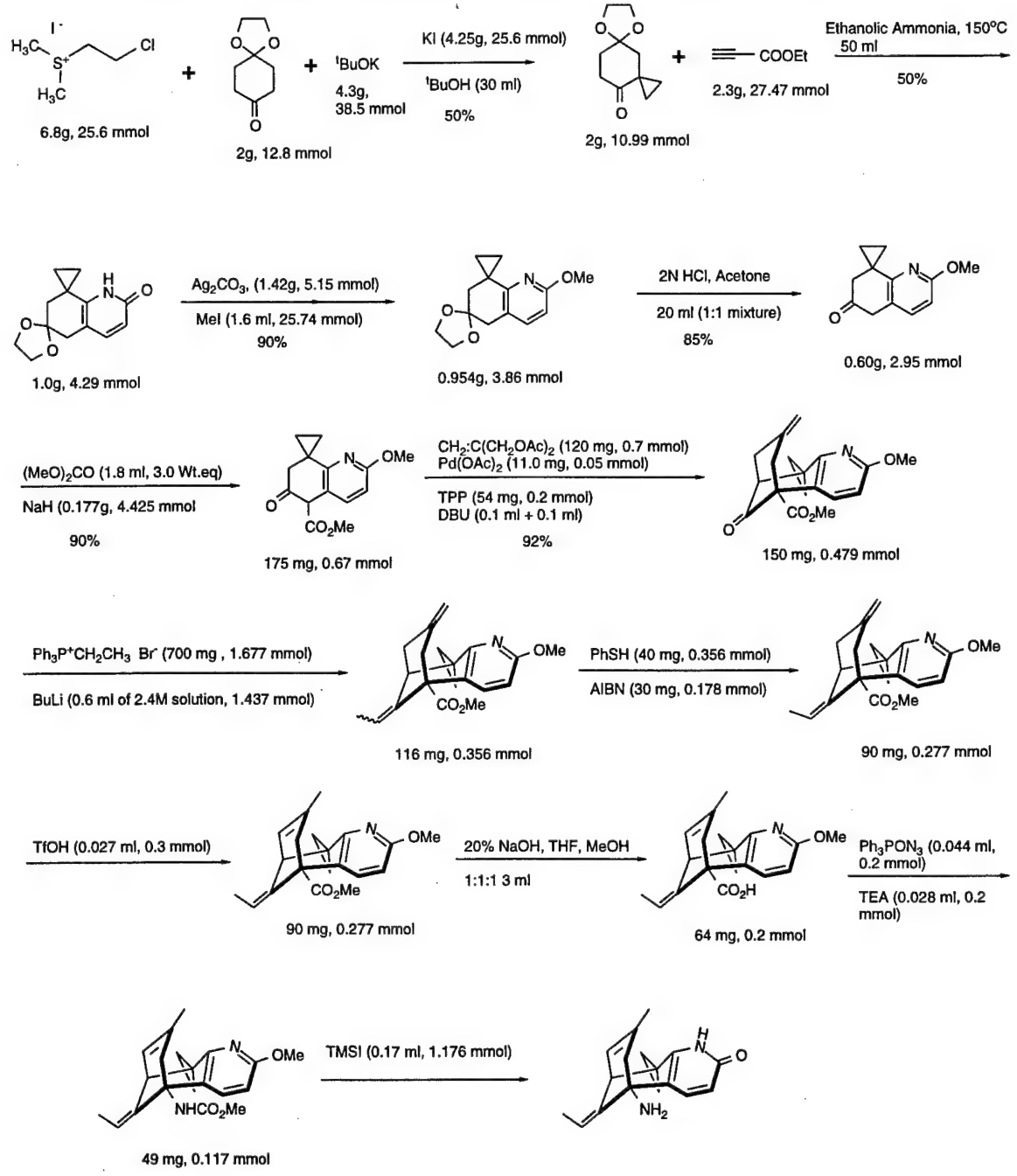

SHAOMENG WANG, Ph.D.

Dr. Wang is interested in computational structural biology (protein folding, drug and receptor interactions), design and discovery of novel therapeutic agents. He joined the GICCS in July 1996.

PROJECT 1: PROTEIN FOLDING

Three-dimensional structures of enzymes ultimately determine their biological properties. As genome science rapidly evolves and develops, it is increasingly important to have the ability to predict the three-dimensional structures of enzymes of interest since experimental determination of the 3D-structures of enzymes of interest using either X-ray diffraction or multi-dimensional NMR techniques is painstaking and slow. Toward this end, we have developed a novel and powerful computational method termed "self-guided molecular dynamics simulation method" and applied this method to the protein-folding problem for the studies of the dynamics, thermodynamics and kinetic properties of protein folding and the prediction of protein structure.

Among many prediction and search approaches, molecular simulation method displays a number of promising prospects. It takes atomic interaction details into account and directly incorporates both enthalpy and entropy effects. However, molecular simulation of a large system such as enzymes with thousand atoms is very time consuming and the time scale it can access is very limited (often limited to nano-seconds). Many important biological processes such as protein folding and drug-receptor binding takes place in a time scale of from micro- to milliseconds and there are beyond the reach of current computer power with conventional simulation techniques. Therefore, in order to study these biological processes using simulation methods, we have to either simplify the systems of interest or to improve the simulation efficiency dramatically.

We have developed a new algorithm called "self-guided molecular dynamics simulation approach", which has been shown to improve the conformational searching efficiency by 100- to 1000-folds. This algorithm was presented in the Gordon Research Conference in Computational Chemistry in June 1998 and was cited by many researchers as the most exciting paper in the Gordon Conference. A paper described this algorithm has been published in Journal of Physical Chemistry, B. (1998, 102, 7238-7250). This new method provides us with the opportunity to investigate one of the most challenging and difficult problems in modern biological science, i.e. the protein-folding problem. Since October 1, 1997, we have applied this method to the folding of peptides and proteins with defined secondary and tertiary structures. First, we have studied the folding of protein secondary structure because Protein structures are composed of elementary secondary structures, including turns, a-helices and b-sheets. The formation of these secondary structures is believed to play an important role in protein folding, which remains to be one of the major unsolved and most challenging problems in modern biological science. An in-depth understanding of folding of these basic secondary structures is an important step toward solving the protein-folding problem. Short peptides (<20 residues), which adopt significant populations of secondary structures in solution are excellent model systems with which to study folding of protein secondary structures. Up to date, we have successfully simulated the folding of peptides with turns, helices or b-sheets. Our studies have begun to provide important insight into the folding of protein secondary structures in a number of important aspects including the folding mechanism, factor that govern the folded structure and folding dynamics. One manuscript on the folding of a type II turn structure has been submitted for publication in the Journal of the American Chemical Society and two other manuscripts concerning the folding of a-helix and b-hairpin are being prepared. After we have made significant progress in

the folding of peptides with defined secondary structures, we have started to investigate the folding of peptides and proteins with defined tertiary structures. To date, we have successfully simulated the folding of a 23-residue small protein designed to mimic the zinc finger binding protein. In addition, we have successfully simulated a 33-residue protein with 3-helices and a 56-residue protein with 4-helices. Two manuscripts on the folding of these two proteins are being prepared. Collectively, these studies will provide important clues to the protein-folding problem.

Since this new algorithm improve the simulation efficiency in an order of 100- to 1000-fold in comparison with convention simulation methods, we will be able to apply this efficient and novel new algorithm to fold peptides with up to 50 amino acids to investigate the detailed protein folding mechanism such as b-amyloid, which has important implication in Alzheimer's disease. We will also be interested to utilize our new method in protein structure prediction. In addition, we will investigate the detailed kinetic process of a drug molecule binding to its enzyme using this efficient computer simulation technique.

PROJECT 2. DESIGN AND DISCOVERY OF CASPASE-3 SPECIFIC INHIBITORS

Apoptosis, or programmed cell death (PCD), is triggered by a number PCD factors. Inappropriate apoptosis is now believed to contribute to the pathology of several human diseases, including neurological diseases such as Alzheimer's disease and Parkinson's disease, and solid tumors. A number of genes have been identified to play key roles in apoptosis. In C. elegans, these genes include CED-9, CED-4, CED-3. In addition, two additional factors, cytochrome C (also designated as Apaf-2, apoptotic protease activation factor 2) and dATP play crucial roles in the activation of CED-3. It has been shown that CED-9, which functions upstream of CED-3 and CED-4, negatively regulates the apoptotic program by preventing the activation of CED-3 and CED-4, probably through blocking the release of cytochrome C, a key activation factor for CED-3, from mitochondria. CED-4 is required for the activation of CED-3, in addition to cytochrome C.

The apoptotic program delineated in C. elegans is conserved in mammalian cells. The corresponding homologs to CED-9, CED-4 and CED-3 are Bcl-2, Apaf-1, and caspase-3. Bcl-2 can block the release of cytochrome C from mitochondria, which prevents the activation of caspase -3 (caspase was derived from cysteine aspase for these cysteine proteases always a site with aspartate residue on the C-terminal). In the presence of cytochrome C and dATP, Apaf-4 binds to cytochrome C and activates caspase-3, although the precise mechanism of this activation is not known. The activated caspase-3 is capable of autocatalysis as well as cleaving and activating other members of the caspase family, leading to rapid and irreversible apoptosis. Activated caspase-3 will cleave and activate the DNA fragmentation factor, DFF, which in turn leads to the degradation of DNA into nucleosomal fragments, a hallmark of apoptosis. Deletion of caspase-3 from the mouse genome through homologous recombination results in excessive accumulation of neuronal cells, owing to a lack of apoptosis in the brain. Addition of active caspase-3 to normal cytosol activates the apoptotic program. A specific, high affinity (K_i<1 nM) caspase-3-specific tetrapeptide inhibitor, Ac-DEVD-CHO, can abolish the ability of cytosol from apoptotic cells to induce apoptosis in normal nuclei and block the initiation of the cellular apoptotic program in response to apoptotic stimuli. These data clearly suggest that caspase-3 is both necessary and sufficient to trigger apoptosis. Although a tetra-peptide inhibitor, Ac-DEVD-CHO, is of high specificity and of high affinity and has served a useful role in defining the enzymology and function of some members of caspase-3 protease family, it is of limited utility for advanced drug development. Clearly, a high affinity, non-peptide, specific caspase-3 inhibitor is of great value to study the functions of caspase-3 in vivo systems. Unfortunately, non-peptide caspase-3 inhibitors have not been reported.

We are well poised for the structure-based discovery and design of non-peptide caspase-3 inhibitors since the X-ray structure of the tetra-peptide inhibitor Ac-DEVD-CHO in complex with caspase-3 has been determined. Based upon the X-ray structure, the cysteine 285 sulfur reacts with the aldehyde group on the tetra-peptide inhibitor and forms a thiohemiacetal, which is stabilized by His 237 through a hydrogen bond formed between the hydroxyl of the thiohemiacetal group and the nitrogen at the d1 position on the His 237 ring. The carboxylic group of the aspartic residue at P1 position plays an important role by forming a number of hydrogen bonds with Arg 179, Gln 283 and Arg 341. The hydrophobic side chain of valine residue at P2 position in the inhibitor interacts with a number of hydrophobic residues, including Tyr 338, Trp 340, and Phe 381. The glutamate residue at P3 position forms a number of hydrogen bonds with the side chain of Arg 341 and Ser 343. The aspartic acid at P4 position forms two hydrogen bonds between its carboxylic group and the side chain of Asn 342, and with the backbone NH group of Phe 381. The carbonyl group of the acetyl group forms a strong hydrogen bond with the backbone NH group of Ser 343.

Based upon the X-ray structure of caspase-3 in complex with the tetra-peptide Ac-DEVD-CHO, the aldehyde group is essential for the inhibitor to react with the sulfur group of Cys 285. In addition, the carboxylic group of the aspartate residue at the P1 position on the inhibitor plays a crucial role through interacting with a highly charged positive pocket in the receptor binding site. The isopropyl side chain of the valine residue at the P2 position on the inhibitor appears to be of importance since it interacts with a number of hydrophobic residues in the receptor. As mentioned above, the glutamate residue at the P3 position and the aspartate residue at the P4 position may be important for both binding affinity and specificity. Attempts to identify compounds that will mimic all these important interactions were not successful. Thus, we turned our efforts to identify compounds that will mimic the crucial interactions at the P1 and P2 positions. We have therefore constructed a pharmacophore model that consists of the aldehyde group and the carboxylic group on aspartate residue. The geometric parameters between these two groups, as revealed by the X-ray structure, were incorporated into the pharmacophore model since these parameters are probably important for the effective interactions between the inhibitor and the receptor. A 3D-database search of the National Cancer Institute 3D-database of 216,000 compounds retrieved a number of compounds that meet the requirements of the pharmacophore model. The samples of these compounds were obtained and these compounds were then evaluated for their ability to block the caspase-3-like activity in cellular extract in collaboration with Dr. Alan Faden. One compound with molecular weight less than 300, displays significant activity (we estimated that it's activity is about 500-fold less potent than the extremely potent tetra-peptide inhibitor, Ac-DEVD-CHO). Based upon this compound, we have designed new compounds that can mimic all the essential moieties in the tetra-peptide inhibitor. A number of these newly designed compounds have been made, in collaboration with Dr. Alan Kozikowski, also a member of GICCS. We have undertaken an interactive process consisting of modeling and design, chemical synthesis and biological evaluation. From Oct. 1, 1997, by working closely with Drs. Alan Faden and Alan Kozikowski, we have advanced the original lead compound significantly further in improving its inhibitory activity.

New inhibitors will be designed based upon the molecular modeling studies of the interaction between inhibitors and the CPP32 enzyme and these newly designed compounds will be synthesized by Dr. Alan Kozikowski's laboratory and tested by Dr. Faden's laboratory. Our present results indicate that it is possible to design compounds with greater binding affinity.

PROJECT 3: THE DEVELOPMENT OF A DOCKING METHOD FOR STRUCTURE-BASED DRUG DESIGN

There are now more than 7000 three-dimensional (3D) coordinates of proteins or nucleic acids determined by X-ray crystallography or nuclear magnetic resonance (NMR) spectroscopy available from the Protein Data Bank (PDB, 1998) and the total number of the 3D structures is increasing with even greater speed every year. Many of these macromolecules serve as potential therapeutic targets and the availability of 3D structures of these macromolecules offers us unprecedented opportunities for structure-based drug design and discovery. To effectively carry out structure-based drug design, two fundamental questions need to be addressed. The first question is how a drug (or ligand) fits into the receptor binding site (the docking problem) and the second question is how well it binds to its receptor (the binding affinity prediction problem). We have developed a new docking method, Monte Carlo Docking (MCDOCK) to address the docking problem.

In the MCDOCK, receptor and ligand 3D structures are used as the input data. Often the 3D-structure of the receptor (enzyme) is obtained through X-ray diffraction or NMR techniques, or computer predictions. The structure of the ligand can be generated from computer programs such as CORINA. Then, ligand is placed into the binding pocket of receptor by comparing the relative orientation of them. This step is called geometry-based docking, which serves as a pre-docking. This step is quick but not very accurate. Although in some cases, it can predict the binding-mode of a ligand quite well. After the pre-docking step, energy-based MCDOCK is performed to search potential energy minimums by combining different Markov chains and different sampling techniques. There are two kinds of Markov Chains employed in the energy based docking, single main chain and multiple side chains. Each point along these chains represents a random sampled configuration. We split the searching task into non-localized and localized searching, which are performed in the main chain and side chains respectively. The main chain searching is assigned with a higher temperature in the canonical sampling. This is a non-localized searching and the probability to overcome certain energy barrier is increased with increasing temperature. Larger step lengths are employed in the main chain searching. Consequently, it is less precise to locate the accurate local minimum in the potential surface. This main chain is divided into several segments and the configuration with the lowest energy within each segment is recorded. Those side chains are propagated from these recorded configurations in main chain by a simulated annealing method, which is to gradually reduce the temperature in the MC simulation and more precisely locate local minimum. The step lengths in the side chain simulations are normally set to be about 10 to 50% of that in the main chain simulations. The side chain searching is a localized searching. The main purpose of the side chain simulations is to more precisely locate the local minimum. The lowest energy configuration from these side chains is then further refined by increasing interaction cut-off value. We also implemented different sampling schemes to optimize the probability to overcome different energy barrier, such as global sampling of three overall Euler's angles and all torsion angles of ligand as well as Markov chain sampling of all variables. To enhance the searching efficiency, there is one importance sampling distribution developed in our Monte Carlo searching using an effective temperature.

We have tested 29 complexes which their binding modes are known from X-ray diffraction. For the rigid body docking, an average RMS (root of mean square) value of 0.5 D was obtained for all-non hydrogen atoms for the ligand between the predicted and the X-ray determined binding modes. For flexible ligand docking, RMS of 1 D was obtained. In addition, our method is very fast. On average, it takes about 60 seconds for rigid body docking and less than 900 seconds for flexible ligand docking. Therefore, this new method will be a powerful tool for the studies of drug-receptor

interactions and for structure-based drug design and discovery. A manuscript described this method and the results obtained using this method has been submitted to Journal of Computer-Aided Molecular Design.

We plan to take the flexibility of the receptor into account in our MCDOCK program. We will investigate the role of X-ray crystallographic water molecules in drug-receptor interactions. This method is now being used as a powerful tool in a number of drug design and discovery projects.

MOLECULAR NEUROBIOLOGY AND PLASTICITY: There are three faculty in this research area. Dr. Etcheberrigaray evaluates molecular mechanisms of Alzheimer's disease with particular reference to a novel potassium channel and a novel G- protein. Dr. Faden's group evaluates the molecular and cellular correlates of secondary neuronal injury following trauma, including apoptosis. Dr. Swope's research relates to the actions of novel receptor protein kinases.

RENE ETCHEBERRIGARY, M.D.

The principal aim of my research program is to study cellular molecular alterations in Alzheimer's disease. The research focuses on ion channels , second messengers, and phosphorylating enzymes such as protein kinase C. These molecules have been implicated in mechanisms of memory storage and also in cell toxicity events. Additional projects include the possible link between the β-amyloid fragment C100 on IP_3 mediated calcium release and regulation of soluble APP secretion by various novel PKC activators.

PROJECT 1. – RESTORATION OF K^+ FUNCTION IN AD FIBROBLASTS BY NOVEL ACTIVATORS OF PKC.

Alterations of potassium channel function have been identified in fibroblasts and in blood cells obtained from AD patients. An earlier observation of hippocampal alterations of apamin-sensitive K^+ channels in AD brains provides additional support for the suggestion that K^+ channels may be pathophysiologically relevant in AD. Protein kinase C (PKC) also exhibits parallel changes in peripheral and brain tissues of AD patients. Studies have revealed that of the various PKC isozymes, primarily the α isoform was significantly reduced in fibroblasts while both α and β isoforms are reduced in brains of AD patients. Thus, both PKC and K^+ channel alterations appear to co-exist in AD, with peripheral and brain expression in AD.

Because PKC is known to regulate ion channels including K^+ channels, we hypothesize that a defective PKC may lead to defective K^+ channels. To test this hypothesis we used AD fibroblasts where both K^+ channels and PKC defects have been independently demonstrated. Fibroblasts with known dysfunctional K^+ channels were treated with PKC activators and restoration of channel activity was monitored as presence/absence of TEA-induced calcium elevations. Here we show that the use of a potent novel PKC activator, benzolactam (BL), restores the responsiveness of AD fibroblasts cell lines to the TEA challenge. We also present immunobloot evidence that this restoration might be related to a preferential participation of the α isoform since BL shows improved selectivity for this isozyme that is defective in AD fibroblasts.

Fibroblasts were obtained from the Coriell Cell Repositories. The culture medium in which cells were grown was Dulbecco's modified Eagle's medium supplement with 10% fetal calf serum. Seven age-matched controls (AC), and three sporadic AD (SAD) cases and four familial AD (FAD) cases were tested in the calcium-imaging experiments. Mutations in the PSI gene are expressed in familial cases used here. For immunoblotting experiments, the same set of seven AC and AD cell lines tested in the imaging experiments were used.

The compounds used in this study (2S, 5S)-8-(1-Decynyl) benzolactam (benzolactam), a derivative of the natural product indolactam V. For comparison purposes, we also used the non-selective well-known PKC activator, phorbol-12, 13-dibutyrate.

Cells were seeded in 25mm glass cover-slips placed inside 35 mm Nunc petri dishes and used 3 to 5 days post seeding. Culture medium was removed and cells were washed at least three times with

basal salt solution (BSS in mM: NaCl 140, KCl 5, CaC12 2.5, MgC12 1.5, HEPES 10, Glucose 5, pH=7.4). After 1 h incubation with 1 μM fura 2-AM, cells were washed thorougly with BSS and 1 ml of fresh BSS was added for $[Ca^{2+}]_I$ baseline measurements. Fluorescent images with a Zeiss-Attofluor Ratio Arc Imaging System (Zeiss). A 40x Zeiss Fluor (oil immersion) objective lens was used.

Cells from all treatment groups were tested with 100mM of tetraethylammonium chloride (TEA; SIGMA) by applying 3ml of TEA-modified BSS (in mM : TEA 133.3, nACl 6.7, KCl 5, CaCl2 2.5, MgCl2 1.5l, HEPES 10, Glucose 5, pH=7/4) to the dish. A group of cells were treated with the PKC activator benzolactam prior to the TEA challenge (50nM). A second group of cells was incubated with phorbol 12-13 dibutyrate (PDBu, 50nM for 45 min). The control group of cells included cells which received no treatment prior to TEA challenge (untreated), cells pre-treated with 50 nM of DMSO for 1 minute and cells incubated with 50 nM of 4αphorbol (4αPHR, Calbiochem), an inactive form of phorbol ester (negative control) for 45 minutes.

Patch clamp experiments were performed at room temperature (21-23°C) following standard procedures on thirteen separate replicate representative experiments in a well-characterized AD cell line (AG06848) which is normally silent for the 113pS TEA-senstive K^+ channel. The culture medium was replaced with (mM) : NaCl 150, KCl 5, CaCl2 2, MgCl2 1, HEPES (NaOH) 10, pH=7.4, prior to recording. Benzolactam was added to a dish after ensuring that the patch is silent for the 113ps K^+ channel. The electrodes, filled with a high K^+ solution (mM) : KCl 140, CaCl2 2, MgC12 1, HEPES (NaOH) 10, pH=7..4, were made from Blu Tip capillary tubes by using a BB-CH-PC Mecanex puller. An Axopatch-1C amplifier was used to obtain records and a JVC Vetter PCM video recorder was used to store the data on tape. The data was acquired and analysed on a personal computer with apClamp suite of programs (Axon Instruments).

Cells were grown to confluency (~90%) in T-75 flasks. Levels of α isozyme in response to treatment with 50nM of BL for 1 and 15 minutes or 50nM of PDBu for 1 and 45 minutes were quantified using procedures slightly modified from that established by Racchi *et al.*, 1994. After protein determination, 20 μg of protein was diluted in 2x electrophoresis sample buffer (NOVEX), boiled for 5 min, run on 12% SDS-PAGE and transferred electrophoretically to nitrocellulose membrane. The membrane was saturated with BLOTTO blocker (PIERCE) by incubating it at RT for an hour. The primary antibody for PKC α-isoform (Transduction Laboratories) was diluted (1:1000) in blocking solution and incubated with the membrane of 1h at RT. After incubation with the secondary antibody, alkaline phosphatase anti-mouse IgG (Vector Laboratories), the membrane was developed using an alkaline phosphatase kit (Vector Laboratories) as per manufacturer's instructions.

Treatment of AD cell lines with 50 nM BL for 1 min (black bar) significantly increased the percentage of cells responding to TEA compared to the untreated (open bar; t=2.99, p=0.017) and DMSO-treated (light grey bar; t=3.60, p=0.0113) controls. AD cells incubated with 50 nM PDBu for 45 min did not differ in their TEA response (hatched bar) from the 4-αPHR treated cells (dark grey bar). In controls, % of PDBu-treated cells did not differ from untreated or DMSO-treated AC cells. Likewise, the % of PDBu-treated cells responding to TEA was not different from the 4αPHR treated AC cells. The significantly higher percentage of 'responsive' untreated AC (39.19+6.27) versus the untreated AD (6.31+1.75) cells (open bars in main graph and inset; t=4.97, p=0.0025) is consistent with previous findings.

Patch-clamp analyses revealed that none of the thirteen recordings showed K^+ channel activity before application of BL to the medium. However, after 1 min BL treatment, seven of the same thirteen cells showed unambiguous 113pS K^+ channel activity.

Treatment of AD cell lines with 50nM BL for 1 min (Fig. 3, black bar) revealed a pronounced redistribution of the α-isoform of the enzyme from cytosol to membrane ($t=3.67$; $p<0.05$). A longer incubation time (15 min; data not shown) with BL further increased the particulate/soluble ratios. Although 1 min treatment with 50nM PDBu (Fig. 3B, grey bar) yielded a significant change from the basal ratio level ($t=3.67$; $p<0.005$) in AD cells it was not as effective as the 1 min treatment with 50 nM BL (black vs grey bar: $t=2.27$, $p<0.05$). Longer incubation (45 min) with PDBu (Fig. 3B, hatched bar) resulted in levels of PKC translocation comparable to that observed with 1 min Bl treatment in AD cells ($t=10.52$; $p<0.001$).

In AC cells, effect of BL on enzyme translocation was significant only after 15 min treatment with the PKC activator (data not shown; ratio=1.72; $t=10.37p$; $p<0.01$) but not after 1 min treatment (Fig. 3, inset; black bar, $t=0.56$, ns) compared to basal levels (open bar). Likewise, long term incubation (45 min) with PDBu had an effect on redistribution of the enzyme from cytosol to membrane (hatched bar; $t=6.78$, $p<0.001$). There was no effect of 1 minute incubation with PDBU (grey bar; $t=2.16$, ns) on PKC translocation in AC cells.

Restoration of the TEA-induced $[Ca^{2+}]$ I responses in BL-treated AD cells indirectly implies restoration of their K^+ channel function. Patch-clamp data strongly support the conclusions from imaging studies even within a representative sample obtained from a well-characterized AD cell-line. The immunoblot assay, under conditions approximating the imaging studies as closely as possible, provided an independent method of assessing that PKC is, indeed, involved in the restoration of the normal K^+ channel phenotype. At equimolar concentrations, the effect of BL treatment was clearly stronger at 1 min compared to the effect of PDBu at 1 min for both imaging and immunoblot studies. However, PDBu was able to induce a noticeable change in PKC translocation but not in TEA-induced Ca^{2+} elevation at a longer (45 min) time interval. Perhaps, this singular disparity between imaging and immunoblot results is due to the different dynamics between activation of PKC and TEA-induced Ca^{2+} elevations.

In summary, our data suggest that the strategy to upregulate PKC function targeting specific isozymes restores normal K^+ channel function. These studies and such a fibroblast model could be expanded and used as tools to monitor the effect of compounds (BL, for example) that alter potential underlying pathological processes.

PROJECT 2. - C100 FRAGMENT AND CALCIUM HOMEOSTASIS IN PC12 CELLS.

Numerous studies have implicated the amyloid precursor protein (APP) and its cleavage products as major players in Alzheimer's disease (AD) pathophysiology. The 40-42 amino-acid product of APP termed β-amyloid (Aβ), has been shown to have a number of deleterious effects in cultured cells. These include direct cellular toxicity, disruption of intracellular calcium regulation, formation and/or modulation of ion channels, and other miscellaneous effects. It has also been demonstrated that familial AD (FAD) APP mutations flanking the Aβ segment lead to increased production of amyloidogenic fragments in both cellular models and in circulating fluids of (symptomatic and asymptomatic) individuals carrying the mutations. Mutations in the presenilins (PS1 and PS2) have also been shown to cause an increased Aβ 1-42/Aβ 1-40 ratio.

An amyloidogenic fragment comprising 100 amino acids in the C terminus of APP termed C100, which contains the entire Aβ42 amino-acid sequence and which is a product of enodosomal/lysosomal processing presumably involving the β-secretase, has also been linked to the pathophysiological process. It was initially reported that PC12 cells transfected with this fragment gradually degenerated when induced to differentiate. C100 has been reported to be toxic to neuronal cells in culture and is itself amyloidogenic. Moreover, this fragment has been shown to induce AD-like pathology in vivo. Rat brains transplanted with cells expressing this fragment showed cortical atrophy; some animals had Alz-50 immunoreactivity and axonal disorganization in parts of the hippocampus ipsilateral to the transplant. Transgenic mice expressing the C100 fragment exhibited age-dependent neuronal degeneration, abnormal intracellular Aβ immunoreactivity, and deficits in spatial learning. The C100 fragment has also been reported to induce non-specific ionic currents in Xenopus oocytes and to form cationic channels in lipid bilayers. A recent study showed that expression of FAD mutants of APP in neurons caused increased intracellular accumulation of the C100 fragment and increased secretion of the Aβ 1-40 and Aβ 1-42 fragments, suggesting a direct link between C100 and FAD. Perturbations of intracellular calcium handling have been long implicated as relevant in AD, with supporting evidence from both non-neuronal and neuronal cell models. To determine whether C100 alters calcium handling in neuronal cells, we studied IP3-mediated calcium release in PC12 cells expressing the C100 fragment. We report here that the transfected cells have, as shown previously in AD fibroblasts, an enhanced calcium response to bradykinin, a peptide that causes IP3 generation.

Two independently-isolated pheochromocytoma PC12 cells expressing C100 from the retroviral Doj vector were used. They will be referred to as PC12-C100#1 (formerly B17) and PC12-C100#2 (formerly B11). The parental cell line served as the control. All cell lines were maintained in polylysine coated T75 plastic flasks or in negatively charged flasks in DMEM supplemented with 10% horse serum, 5% calf serum, and 1% of a mixture of penicillin (5,000 units/ml in G sodium) and streptomycin (5,000 μg/m). For calcium imaging experiments, cells were seeded (750,000 cells/mm^3) onto polylysine-coated 25 mm cover slips. C100-transfected and control cell lines were treated with nerve growth factor (NGF, Boehringer) in some experiments. To study the effect of acute expression of C100, control cell lines were infected with HSV-1 vectors expressing C100 and flagC100 and E. Coli β-galactosidase. Thapsigargin (Tg 1 and 10 μM), an inhibitor of calcium ATPase, and the calcium ionophore Ionomycin (10μM) were also used.

We prepared replication defective HSV vectors expressing C100 (HSV/C100) and a flag-tagged version of C100 (HSV/flag C100) β-galactosidase (HSV/Lac; negative control) in the expression vector pHSPrpUC as described. The titer of the helper virus component of each stock was $1\text{-}1.2x10^6$ plaque forming units (pfu)/ml on 2-2 cells. The titer of the recombinant virus component of each stock, as assayed by expression of the exogenous gene in PC12 cells, was consistently $3x10^7$ infectious units (iu)/ml.

The BK challenge caused measurable responses in control and C100-transfected cells. However, significantly higher percentage of PC12-C100#1 cells than controls responded to BK with calcium elevations of at least double the base line level. The same protocol was repeated in cells treated with NGF, since it has been shown that some of the deleterious effects of the C100 fragment in PC12 cells were linked to the cellular differentiation process. The proportion of cells that were "LARGE" responders (Fig. 3A) was significantly higher in PC12-C100#1 cells compared to controls at both DPP 3 ($t+2.91$, $p<0.01$) and DPP 7 ($t=4.98$, $p<0.001$). The PC12-C100#1 cells had a significantly higher proportion of "ALL" responders (Fig. 3B) compared to the control (DPP 3:$t=14.81$, $p<0.001$; DPP 7: $t=16.27$, $p<0.001$). Since days post plating did not influence the effect

of C-100 expression on BK response with or without NGF treatment, additional experiments were carried out on DPP3 only.

The calcium responses as well as the differences between PC12-C100#1 and control cells treated with 1μM BK at DIC 3 without NGF-treatment were preserved in calcium-free (0-CA^{2+} BSS) medium (data not shown). There was a significant effect of C100 expression on proportion of "ALL" responders in calcium-free medium (PC12-C100#1:69.17+6.69; t=8.14; p<0.001) similar to that observed for regular medium even though the proportion of "LARGE" responders were not significantly different for the two groups (PC12-C100#1:8.07+3.39; t=0.55, p=0.30).

To confirm the effect of C100 expression on 1μM BK-induced calcium elevations, we repeated the experiment with control, PC12-C100#1 and an independent PC12 transfected cell line (PC12-C100#2) on DPP 3. PC12-C100#2 cells have a significantly higher proportion of "LARGE" responders compared to the control and PC12-C100#1 cells (F=39.80, p<0.001; all post-test comparisons: p<0.001). Among the "ALL" responders, there was a significant effect of C-100 expression with the two-independently (F=622.9, p<0.001; control vs PC12-C100#1 or PC12-C100#2 : [<0.001; PC12-C100#1 and PC12-C100#2 : NS).

The experiments described to this point were carried out on stably transfected PC12 cells expressing C100 from retroviral vectors. It was important to show that a completely different expression system would yield the same or similar phenotype in response to overexpression of C100. We therefore generated HSV-1vectors expressing C100, a flag-tagged version of C100, and E. Coli β-galactosidase as a control. PC12 cells were plated at [750,000 cells/mm3] and 3 days later was infected with the appropriate recombinant virus. Five or 14 hrs post-infection, the cells were challenged with BK and calcium responses were measured. The proportion of "LARGE" responders (Fig. 3C) after BK challenge were significantly higher in control cells incubated for 5 hrs with either HSV/C100 (t=2.48, p<0.01) or HSV/flag C100 (t=2.35, p<0.05) compared to cells treated with HSV/Lac. The significant difference in calcium responses between HSV/Lac controls versus HSV/C100 or HSV/flag C100-transfected cells was conserved among the "ALL" responders (Fig. 3D; HSV/C100: t=2/54, p<0.01; HSV/flag C100: t=3.93, p<0.01). Similarly, after overnight incubation with the viruses, HSV/Lac-treated cells had significantly lower BK-induced calcium elevations (Fig. 3A, B) compared to cells treated with HSV/C100 ("LARGE" t=3.66, p<0.01; "ALL" t=5.90, p<0.001).

Thapsigargin (Tg), an inhibitor of the calcium ATPase, and the calcium ionophore, Ionomycin were used to determine whether IP-3 independent calcium pools and buffering systems, respectively were affected by C100 expression. Since the criteria for a "LARGE" response was established for BK only, all discernible calcium elevations in response to Tg or Ionomycin challenge were considered for analyses. Tg induced in control cells, calcium responses of different magnitude, shape and duration from those elicited by BK. The pattern of response of control vs. PC12-C100#1-transfected cells to Tg was opposite to that observed with the BK challenge. The overall proportion of control cells responding to both concentrations of Tg tested was significantly higher compared to PC12-C100#1 cells (1μM: t=9.03, p<0.001; 10μM: t=3.28, p<0.01). C100 expression did not have an effect on Ionomycin-induced responses (data not shown). Almost every one of the cells tested from both groups had discernible calcium elevations upon Ionomycin stimulation (control: 99.76+0.24; PC12-C100#1:100.0+0.00).

This exaggerated response to BK caused by C-100 BK has been shown in fibroblasts from AD patients. In addition, enhanced IP_3 mediated release was recently reported in human neuroblastoma cells transformed with mitochondrial DNA from AD patients. Thus, alterations in IP_3-mediated

calcium release seem to be a prevalent cellular alteration in AD. This enhanced calcium response could itself be a direct mechanism of toxicity, or it could contribute to processes that ultimately cause cell death.

Thapsigargin induced larger responses in control cells than in C100-transfected cells, so that its effects were opposite to those of BK. These results indicate that the calcium pools (presumably overlapping with the IP_3-sensitive stores) may be smaller in transfected cells than in control PC12 cells. Thus, the enhancement of the IP_3 pathway is capable of rendering larger responses in C100-transfected cells than in controls despite smaller calcium pools in the former. These data suggest that differences are most likely to be primarily due to alterations at some level of the IP_3-mediated calcium release cascade. Since the calcium elevations in response to the ionophore in both cell lines recovered at a similar rate, we can conclude that there are no major differences in calcium buffering systems between the two lines. The demonstration that C100 induces significant alterations of calcium homeostasis in neuronal cells suggests that this peptide is relevant to the pathophysiology of AD.

The data collected from the projects have been published or submitted for publication. We have also presented these findings at national and international meetings. The results strongly suggest that PKC might play a major role in the pathophysiology of AD. The results also begin to present causal connections between amyloid metabolism, calcium regulation, ion channel function and PKC. Future efforts will continue to expand the previously mentioned studies, including the study of similar or comparable phenomena in brains of AD patients

FIGURE LEGENDS:

Figure 1: Calcium elevations in response to TEA expressed as percentage of responding cells. Data was pooled across the 7 AD cell lines for each treatment. Benzolactam pre-treatment significantly increased the TEA responsiveness compared to untreated or DMSO–treated controls (*$p<0.05$ in either case). In contrast, there was no difference between PDBu and 4αPHR pre-treated AD cells. **Inset:** Normal response to TEA in AC cells irrespective of treatment. Percentage of cells responding to TEA is significantly higher in untreated AC versus untreated AD cells (p0.005).

Figure 2: Translocation of PKCα induced by benzolactam. PKC redistribution from cytosol (soluble fraction) to membrane (particulate fraction) expressed as ratio of particulate to soluble fraction immunoreactivity measured by densitometric analyses in 7 AD cell lines. Benzolactam treatment of AD cells significantly increased the level of immunoreactivity from basal levels (*$p<0.05$). Incubstion with PDBu for 1 or 45 min also enhanced the level of enzyme activity from basal level (*$p<0.05$). Inset: PKC immunoreactivity in AC cells. Benzolactam or PDBu-treatment for 1 min did not have an effect on immunoreactivity of the enzyme in AC cells. However, incubation with PDBu for 45 min significantly increased the level of enzyme activity as compared to the basal level (*$p<0.05$; two-tailed *t*-test).

Figure 3: Bradykinin-induced calcium responses in control (hatched bars) and transfected (solid bars) PC12-C100#1 cells after 3 or 7 days post plating. **A.** Percentage of "LARGE" responders (i.e., double the baseline calcium level) following 1μMBK stimulation. **B.** Percentage of all responders (i.e., all discernible responses) within the same group of cells. Vertical bars represent standard errors of the mean. One-tailed unpaired *t* – test was performed on the data.***$p<0.001$. Calcium responses to BK challenge in control cells infected for 5 hours with HSV/lac (hatched bars), HSV/C100 (grey bars) or HSV/flagC100 (black bars) expressed as mean (+ standard error)

percentage of responders. **C**. "LARGE" responders. **D**. "ALL" responders. One-tailed unpaired *t* –test was performed to compare responses between HSV/lac-treated cells and the HSV/C100 or HSV/flagC100-treated cells. *$p<0.05$; **$p<0.01$.

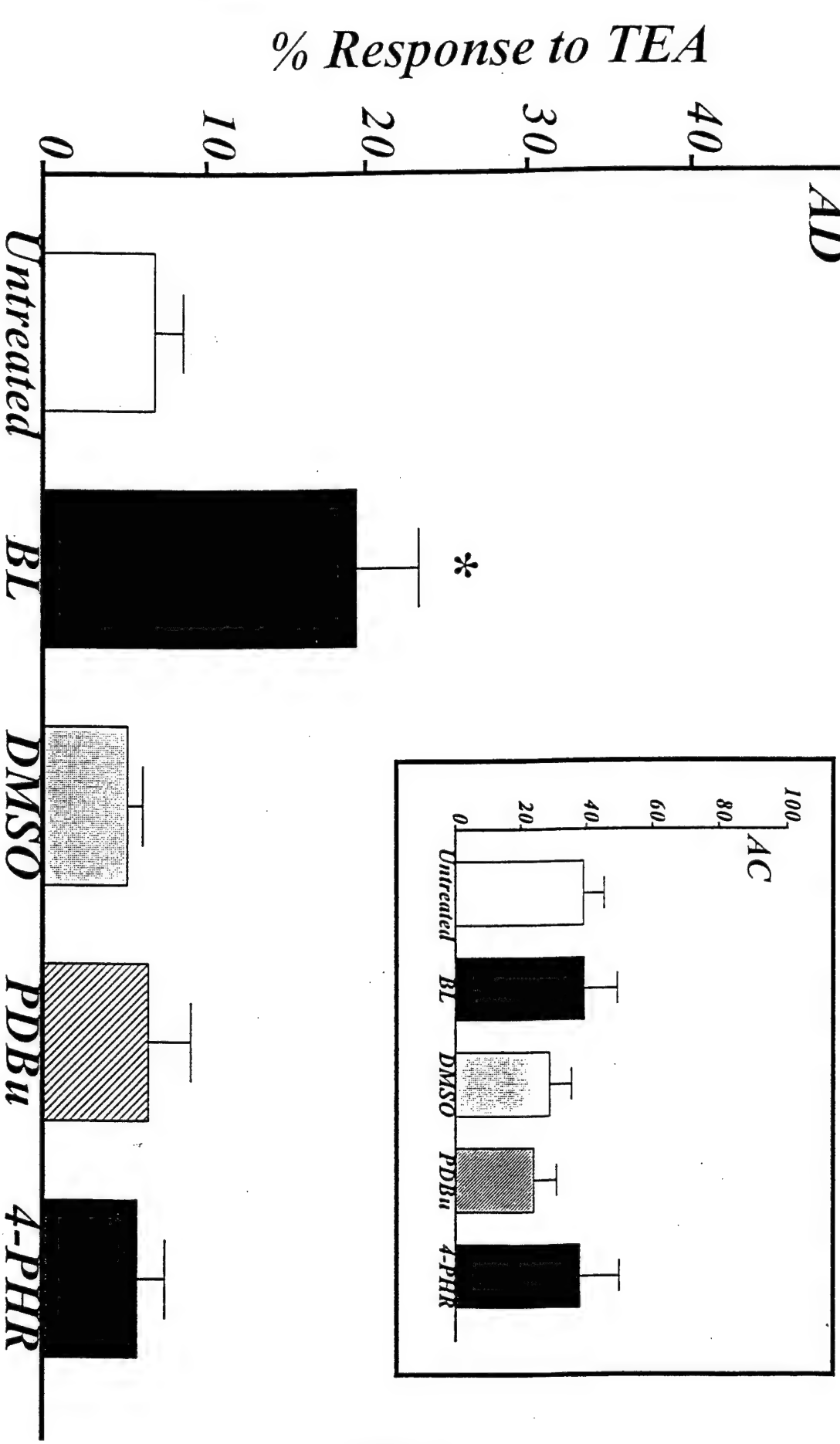
% Response to TEA
0
10
20
30
40
50
AD
Untreated
BL
DMSO
PDBu
4-PHR
*
100
80
60
40
20
0
AC
Untreated
BL
DMSO
PDBu
4-PHR

Figure 1

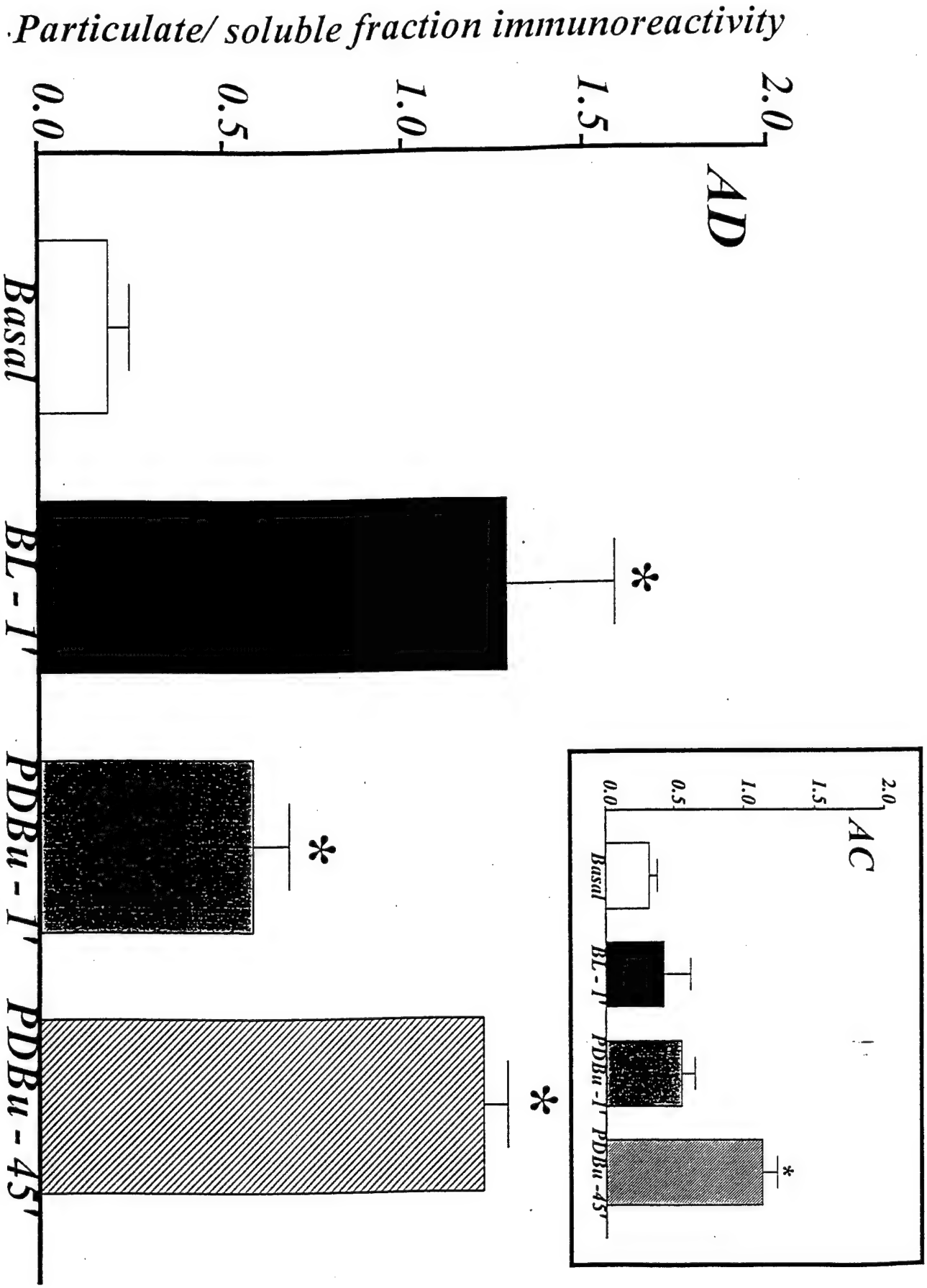
Particulate/ soluble fraction immunoreactivity
0.0
0.5
1.0
1.5
2.0
AD
Basal
BL - 1'
PDBu - 1'
PDBu - 45'
*
*
*
AC
0.0
0.5
1.0
1.5
2.0
Basal
BL -1'
PDBu -1'
PDBu -45'
*

Figure 2

Figure 3

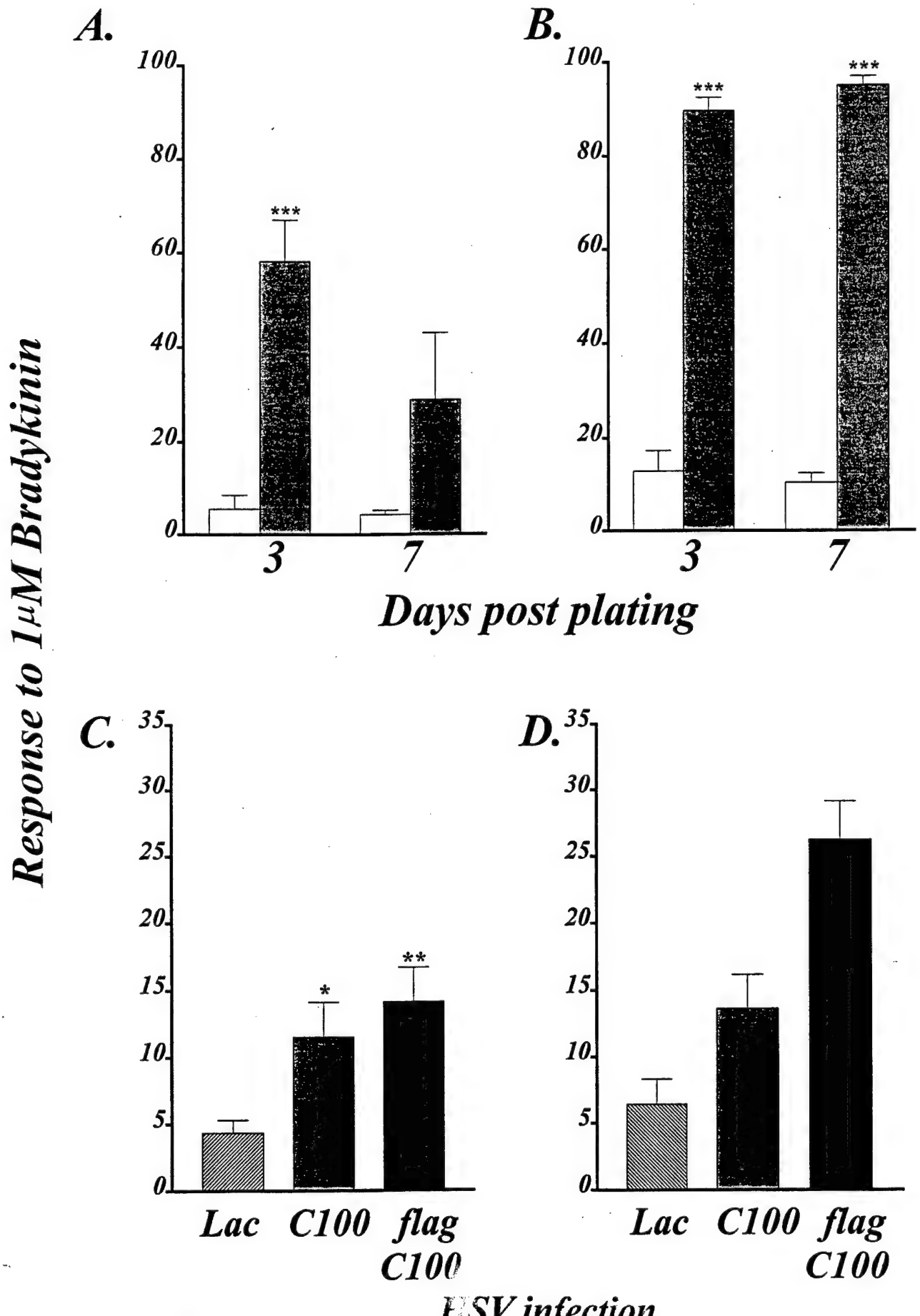
A.
B.
100
80
60
40
20
0
***
3
7
Days post plating
Response to 1μM Bradykinin
C.
D.
35
30
25
20
15
10
5
0
*
**
Lac
C100
flag C100
HSV infection

Our laboratory studies the pathobiology of neuronal cell death associated with central nervous system injury and examines both mechanisms of neuronal cell death as well as the development of novel pharmacological treatment strategies. The central underlying hypothesis being evaluated is that the initial insult (trauma or ischemia) initiates an endogenous autodestructive response, leading to delayed cell death through both necrosis and apoptosis. Elucidating the specific factors involved and their temporal profile can permit the development of drug approaches that serve to limit secondary injury, thereby improving outcome.

There are four major projects within the laboratory: Project 1 involves experimental modeling of neurotrauma, both *in* vivo and *in* vitro, as well as developing new behavioral and cognitive assessment strategies. Project 2 explores the role of metabotropic glutamate receptors (mGluR) in models of neurotrauma both *in vivo* and *in vitro*. Emphasis is on understanding the relationships among Group I, Group II, and Group III receptors with particular reference to signal transduction pathways, and the modulation of those pathways. Project 3 examines the role of selected cysteine proteases (caspases) in neuronal apoptosis and traumatic neuronal injury. Project 4 is in collaboration with two other institute faculty members – Drs. Kozikowski and Wang – and incorporates molecular modeling, synthetic chemistry and biological modeling to develop and evaluate novel neuroprotective agents for CNS injury.

Project 1: Experimental Modeling

A variety of *in vivo* and *in vitro* models have been developed to provide better experimental systems for elucidating molecular and cellular mechanisms of secondary injury, and additional methods have been introduced for behavioral analysis and cognitive assessment. *In vitro* models include: (1) cerebellar granule cells (CGC) subjected to withdrawal of trophic support as a model of neuronal apoptosis; (2) neuronal-glial cultures subjected to mechanical injury as a model of excitotoxic induced neuronal necrosis; (3) cellular ischemia in which neuronal glial cultures are subjected to deprivation of oxygen and glucose; (4) a combined model of trauma and "chemical ischemia" using neuronal-glial cultures; (5) β-amyloid toxicity in CGC and cortical neurons; and (6) staurosporine or etoposide induced apoptosis in a variety of cell lines. Collectively, these models allow us to address the pathobiological role of a proposed injury factor across different injury systems, which permits determination of whether an injury factor is model specific or generic, as well as helping to define probable mechanisms involved (Figures 1 and 2). These new models have been successfully applied to assess the pathophysiologic roles of metabotropic glutamate receptors and caspases respectively (see below).

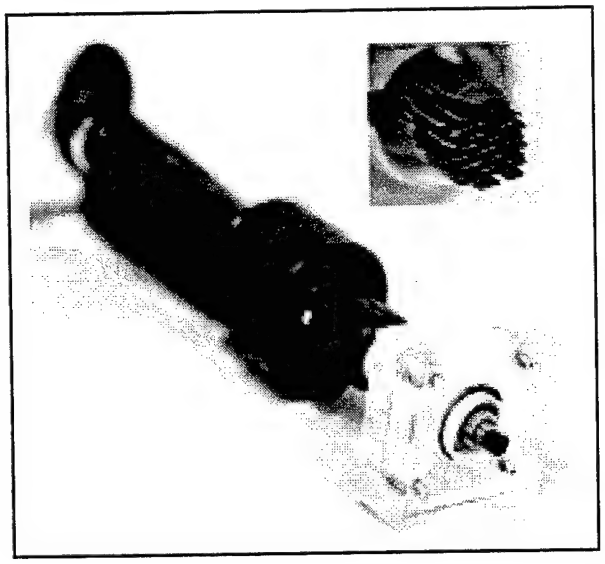

Figure 1. Mechanical punch device. Our punch device consists of 28 parallel blades banded together. These blades are connected to a steel piston is housed within a plastic handle. A piece of plexiglass is located above and perpendicular to the blades, and is used to align the device so that each blade is equidistant from the bottom of the well. A plunger located at the top of the device is connected to the steel piston. When depressed, the blades contact the well surface. A consistent level of downward force is applied to the blades by activation of an electromagnet. Increased magnification of the blades is illustrated in the inset.

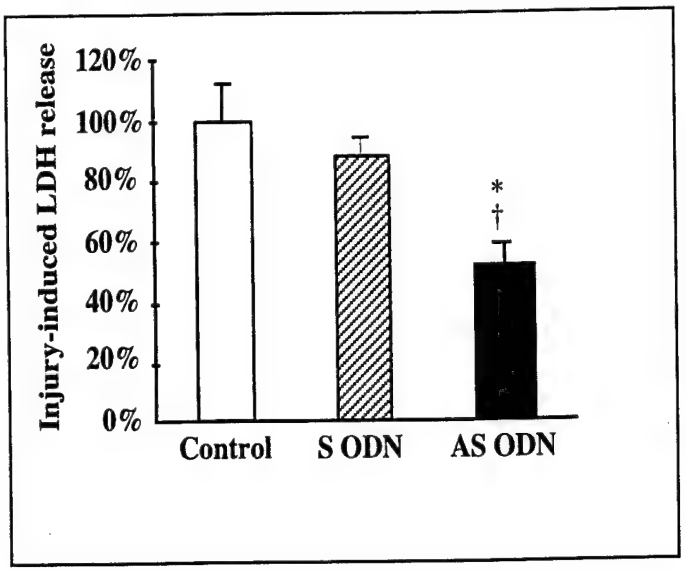

Figure 2. Neuroprotective effects of AS ODN versus NMDAR1 subunit. Antisense oligodeoxynucleotides (AS ODN) or sense ODN (S ODN) was administered for 3 d prior to injury. Neuronal/glial cultures were injured and washed 30 min later. LDH release was assessed 16-18 h after trauma. Administration of S ODN had no effect on injury-induced LDH release as compared to control values. Injury-induced LDH release measured after AS ODN pretreatment was significantly reduced as compared to S ODN or control. AS ODN treatment provided similar levels of protection to optimal levels of MK-801. Data are expressed as a percentage of injury-induced LDH release in control injured cultures. Values represent mean $\pm$ SEM, n = 11-16 cultures per condition. *$p < 0.05$ vs. control, †$p < 0.05$ vs. S ODN, ANOVA followed by Student-Newman-Keuls test.

A new head injury model has been developed in the mouse. The controlled cortical impact system (CCI) was designed "in-house" and has the advantage of being able to independently control the velocity of trauma and the degree of tissue deformation. This model has now been fully characterized with regard to histology, motor and cognitive deficits, and pharmacological profiles (Fig.3). An important feature of this CCI model is that it shows both neuronal necrosis and apoptosis, produces sustained cognitive and motor deficits that can be modified pharmacologically, and permits assessment of gene manipulations or gene-targeting strategies. Using the cognitive assessments developed were the standard Morris water maze, a varient that permits assessment of working memory, and the Barnes circular maze.

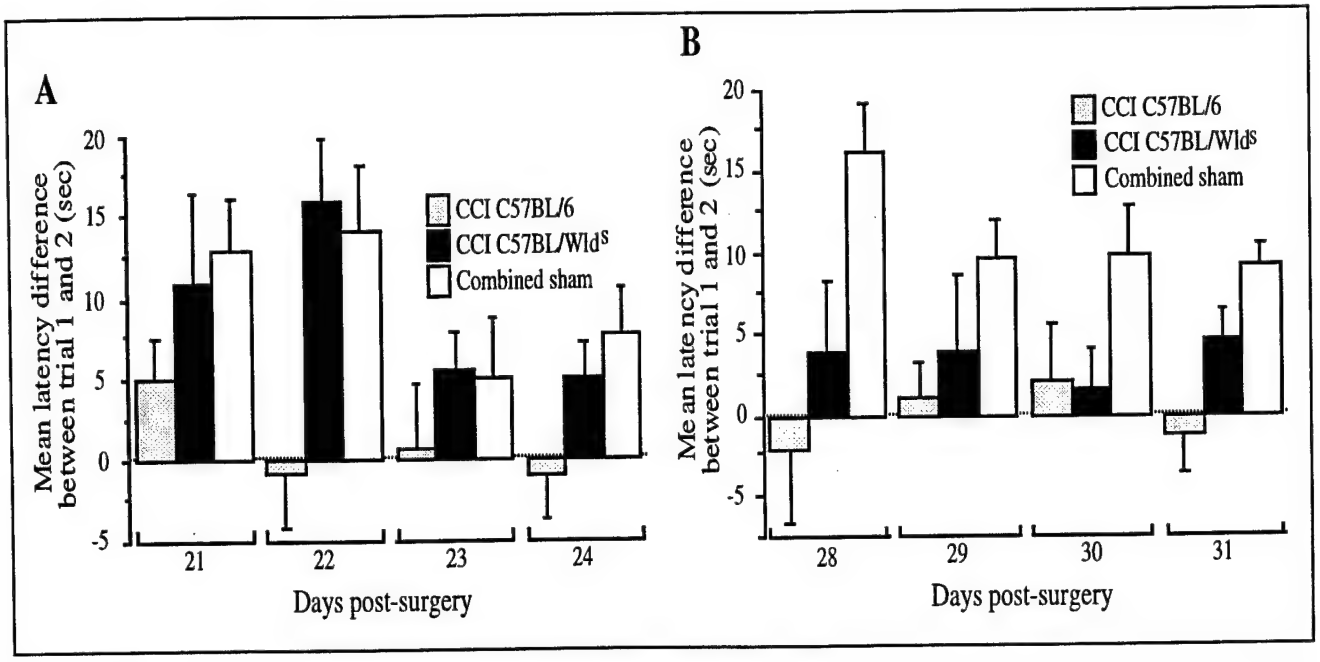

Figure 3. Comparison of effects of CCI on cognitive function in normal C57BL/6 mice and a strain with a genetic modification that causes delayed Wallerian degeneration. Mean difference in latency (+ SEM) to locate the hidden platform between the first and second of the trial pairs in a working memory version of the Morris water maze, conducted 21-24 (A) and 28-31 (B) days after surgery. A large difference indicates a shorter latency on the second of the trial pairs, and hence good working memory function. Sham-operated mice perform well in this task through both time periods as compared with CCI-injured C57BL/6 mice, reaching significance on days 22, 24, 28, and 31 ($p < 0.05$). CCI-injured C57BL/Wld^s mutant mice also performed well during the earliest times tested (A), reaching significance on day 22 post-injury as compared with CCI-injured C57BL/6 animals ($p < 0.05$), although this effect was lost at all subsequent testing times (B).

Project 2: Role of Metabotropic Glutamate Receptors in Traumatic Neuronal Injury

We have extensively examined the roles of Group I, Group II and Group III metabotropic glutamate receptors in secondary cell death in a variety of model systems: a well-characterized, mechanical trauma model in rat; mixed neuronal-glial cultures; neuronal-glial cultures subjected mechanical trauma with metabolic impairment; β-amyloid induced neurotoxicity in cultured cerebellar granule cells and cortical neurons; and staurosporine or etoposide induced apoptosis (Fig. 4-6). Using both pharmacological methods and molecular techniques (e.g. antisense oligonucleotides), we have demonstrated that Group I receptors are activated following trauma and contribute to neuronal cell death in part by positive modulation of NMDA receptors. The signal transduction pathway involved includes phospholipase C, phosphoinositide hydrolysis and protein kinase C. However, other mechanisms appear to play a role in the effects of group I mGluR, including the release of aracidonic acid and the activation of cyclic AMP. The pathological actions of Group I mGluR appear to be mediated predominantly by mGluR1 and not mGluR5.

In contrast to the actions of Group I receptors, Group II and Group III receptors are believed to be negatively coupled to adenylate cyclase activity. We have demonstrated that both Group II and Group III agonists are neuroprotective following *in vitro* trauma. The protective mechanisms appear to involve both adenylate cyclase modulation and pre-synaptic inhibition of glutamate release.

Interestingly, Group III receptors are activated by trauma and serve as an endogenous neuroprotective mechanism, whereas Group II receptors do not. Using a well-established model of percussion-induced traumatic brain injury in rats, we showed that Group I antagonists also improve neurological recovery after trauma *in vivo,* as does a Group II agonist.

Lastly, and importantly, modulation of Group I, Group II and Group III receptors appear to be additive in their neuroprotective effects, as well as additive to the neuroprotective actions of NMDA receptor antagonists.

A similar profile of effects for Group I, Group II and Group III mGluR was found in a newly developed model combining mechanical trauma and metabolic impairment (hypoglycemia and administration of the succinate dehydrogenase inhibitor 3-nitropropionic acid). However, in this model, which better simulates *in vivo* trauma models by causing both necrosis and apoptosis, Group I activation may reduce apoptosis while exacerbating necrosis. Such an observation, if confirmed and extended, could have important implications for treatment.

Collectively, these observations suggest that modulation of metabotropic glutamate receptors may provide a novel and effective approach to the treatment of clinical neurotrauma and other related conditions.

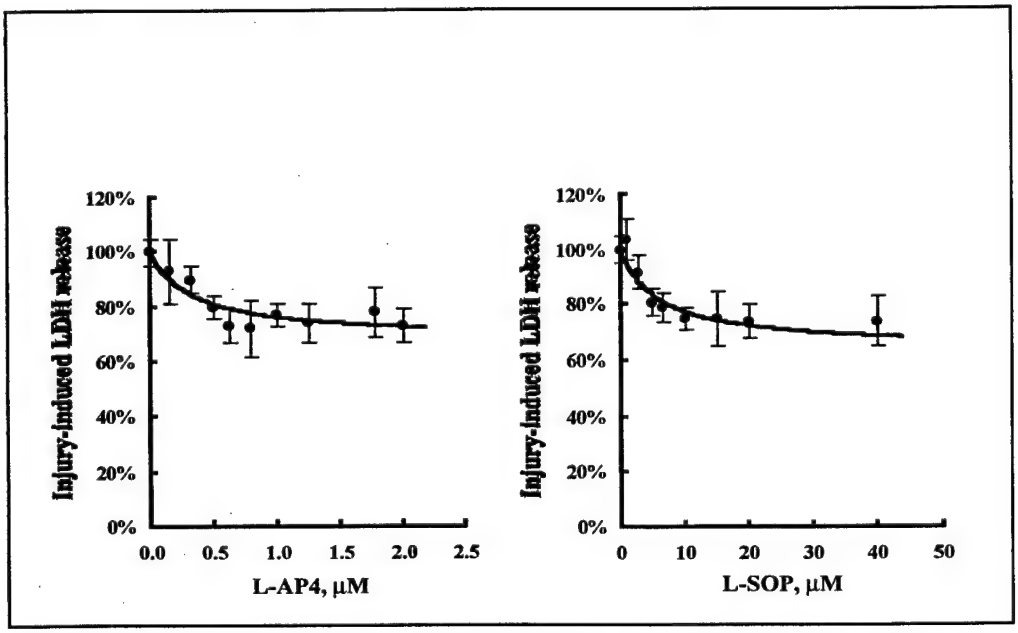

Figure 4. Dose-dependent neuroprotective effects of group III mGluR agonists (A) L-AP4 and (B) L-SOP on injury-induced LDH release. Cultures were incubated in presence of L-AP4 (0.125 - 2.0 μM) or L-SOP (2 - 40 μM) 30 min before and 16-18 hr after injury. LDH activity was measured 16-18 hr after injury. Data expressed as a percentage of injury-induced LDH release in the absence of agonists. Values represent mean ± s.e.m., n = 32 - 64 per each concentration. Significant concentration dependent protection is observed using Spearman's Rank correlation test for L-AP4 ($p < 0.025$) and L-SOP ($p < 0.001$).

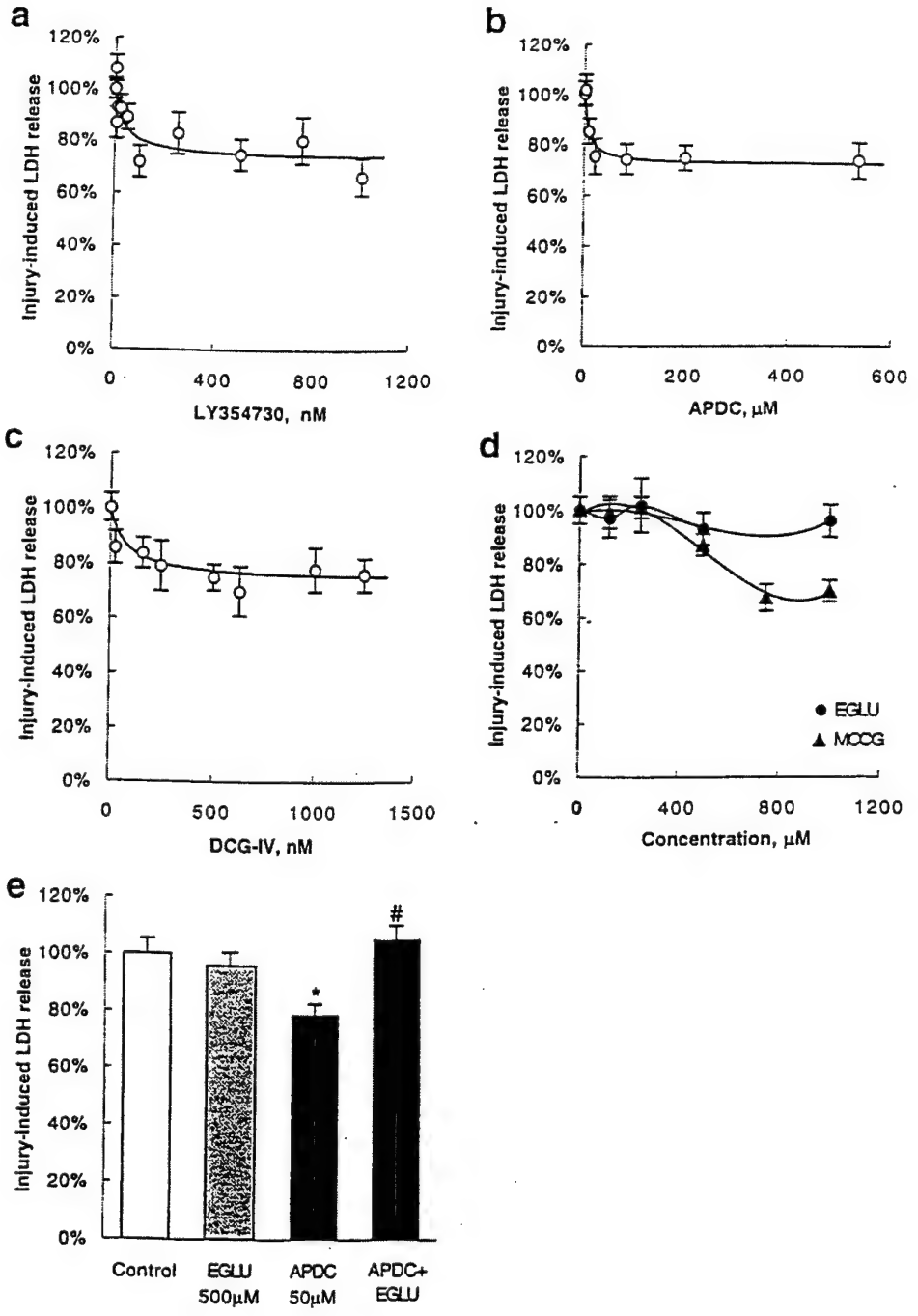

Figure 5. Treatment with group II mGluR agonists attenuated injury-induced LDH release in neuronal-glial cultures (18-20 DIV). Activation of group II mGluR by (**a**) LY354740 (0.5 – 1000nM), (**b**) APDC (2.5 – 550 uM), (**c**) DCG-IV (10 – 1250 nM) exhibited dose-dependent protection. (**d**) Inhibition of group II mGluR by EGLU (200 – 1000 uM) or MCCG (200 – 1000 uM) did not exacerbate injury-induced LDH release. (**e**) Co-administration of EGLU (500 uM) with APDC (50 uM) completely reversed the neuroprotective effect of APDC. All treatments were applied 30 min. prior to injury and for 16 – 18 h post-injury. Data are expresses as a percentage of injury-induced LDH release in the absence of treatment. Values represent mean ± SEM, n = 32 – 64 cultures per condition. *$p < 0.05$ versus control; #$p < 0.05$ versus APDC; ANOVA followed by Student-Newman-Keuls test.

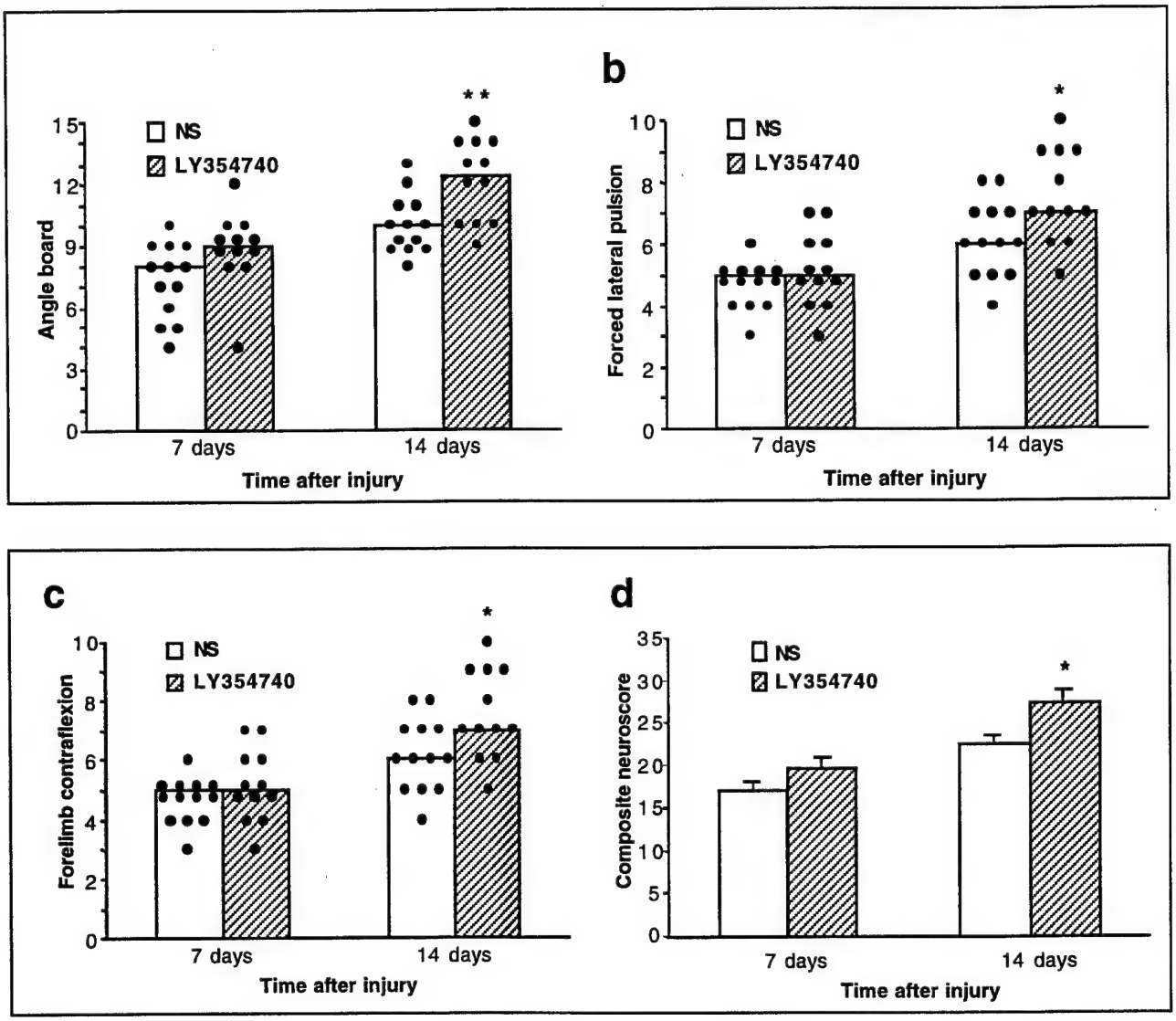

Figure 6. Treatment with intravenous LY354740 (5 mg/kg) 30 min. after fluid percussion traumatic brain injury (TBI) in rats improved neurologic outcome 2 wk post-injury. Significantly better functional scores were obtained at 14 d in animals treated with LY354740 (hatched bars) as compared with animals that received normal saline vehicle (NS, open bars) in (a) angle board, (b) lateral pulsion, and (c) forelimb contraflexion tests, as well as in the (d) composite neuroscore. Histograms (a – c) represent median neuroscores at 7 or 14 d after TBI. Individual animal scores are represented as dots. Histograms (d) represent ± SEM, n = 12 (NS) or 13 (LY354740) animals. *$p < 0.05$ vs NS; **$p<0.01$ versus NS, Kruskal-Wallis nonparametric ANOVA followed by Mann-Whitney U test.

PROJECT 3: ROLE OF CASPASES IN TRAUMATIC NEURONAL INJURY AND NEURONAL APOPTOSIS

We have used both pharmacological methods and molecular techniques to establish that caspases, in particular the caspase-3 family, are activated following neurotrauma and contribute to the subsequent neuronal cell death. Withdrawal of potassium and serum to cerebellar granule cells (CGC) in culture is a classical model for demonstrating neuronal apoptosis. Using this model, we found that neuronal apoptosis was associated with activation of caspase-3 but not caspase-1 mRNA

and activity. Moreover, selective inhibitors of caspase-3, but not caspase-1, could significantly attenuated neuronal apoptosis produced in the model. Subsequent studies used transfected CGC to examine the effects of caspase-3 modulation. Transfections included ribozymes directed against caspase-3, an inhibitor of apoptosis protein (IAP), as well as the anti-apoptotic factor Bcl-2. Both the ribozymes, which are highly selective for caspase-3, as well as the IAP, which is selective for caspase-3 and caspase-7, showed significant neuroprotective effects against apoptosis produced CGC following withdrawal of serum and potassium (Fig.7). Even more striking were the neuroprotective effects provided by Bcl-2, which nearly eliminated subsequent apoptosis. Collectively, these findings demonstrate a clear role for caspase-3 in this apoptosis model.

Using our combined model of mechanical injury with metabolic impairment, we found that injury induced both necrosis and apoptosis. The apoptosis in this model was clearly caspase-3 dependent, as reflected by the activation of caspase-3 using fluorometric methods and the inhibition of apoptosis by selective caspase inhibitors. We also demonstrated, using the lateral fluid-percussion traumatic brain injury model in rats, that trauma caused neuronal apoptosis associated with the activation of caspase-3, which could be inhibited by a caspase-3 inhibitor administered I.C.V. Most importantly, inhibition of caspase -3 in this trauma model led to significant neurological recovery, indicating that caspase-3-mediated neuronal apoptosis plays an important role in the functional disabilities following trauma.

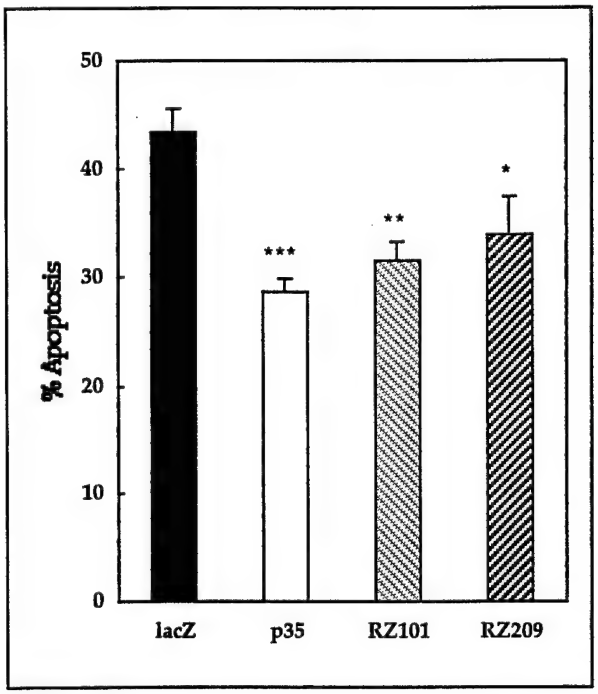

Figure 7. Apoptosis after 24 h of serum/K^+ deprivation in CGCs expressing B-galactosidase, p35, or ribozymes against caspase-3. Apoptosis was 44 ± 2% in negative control cells, 29 ± 1% with p35, 32 ± 2% with RZ101, and 34 ± 4% with RZ209. ***$p<0.001$, **$p<0.01$, *$p<0.05$ compared to negative control by ANOVA and one-tailed Dunnett's post-hoc test (n = 7).

Project 4:

We have initiated a broad-ranging rational drug discovery effort aimed at developing novel neuroprotective agents for the treatment of CNS injury. Our initial efforts have involved modifications of the tripeptide thyrotropin-releasing hormones (TRH), which we and others have demonstrated has substantial neuroprotective effects in CNS trauma. However, TRH and related TRH analogs have other physiological actions that may reduce their effectiveness as treatments for brain trauma, including potent endocrine, analeptic, and autonomic effects. Based on extensive prior experience studying structural-activity relationships of TRH and TRH analogs, we have designed a series of novel tripeptides that were aimed at enhancing the neuroprotective effects of TRH while eliminating its other physiological actions. These compounds show substantial neuroprotective effects *in vivo* and *in vitro*, as well as cognitive-enhancing actions. Particularly interesting are two novel structures : a diketopiperizine (35b) and a compound that joins a tripeptide to a diketopiperizine (57a). These drugs show significant neuroprotective effects following mechanical trauma *in vitro* and in rodent models of traumatic brain injury. (Fig. 8-10)

In addition, 35b and another tripeptide (53a) show significant cognitive-enhancing effects with regard to spatial learning and memory in mice when the drugs are administered more than one month after trauma. Mechanism studies suggest that these compounds work through multifactorial mechanisms, including inhibition of glutamate toxicity and reduction of apoptosis. Moreover, 35b and 37a show none of the other physiological effects of TRH and, therefore are likely to be both better tolerated and more effective in the treatment of clinical neurotrauma.

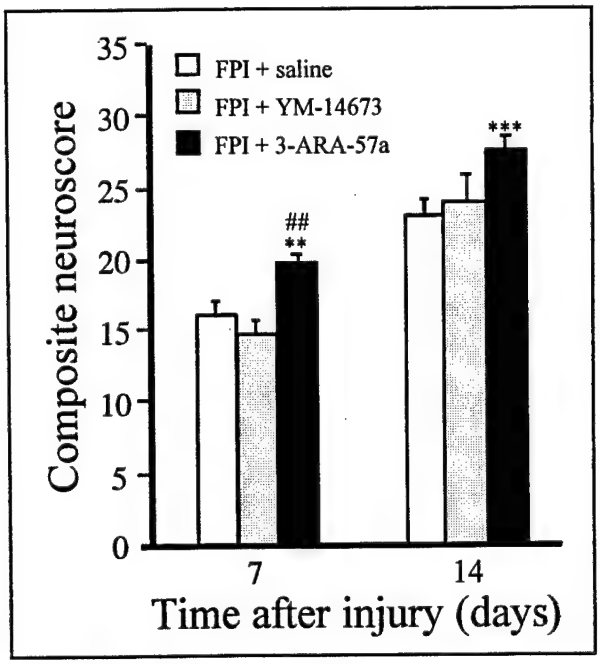

Figure 8. Recovery of neurological function following moderate fluid percussion injury (FPI) in the rat. Results are expressed as mean (± SEM) for each treatment group. ** $p < 0.01$, *** $p < 0.005$ with respect to FPI + Saline; ## $p < 0.001$ with respect to FPI + YM-14673.

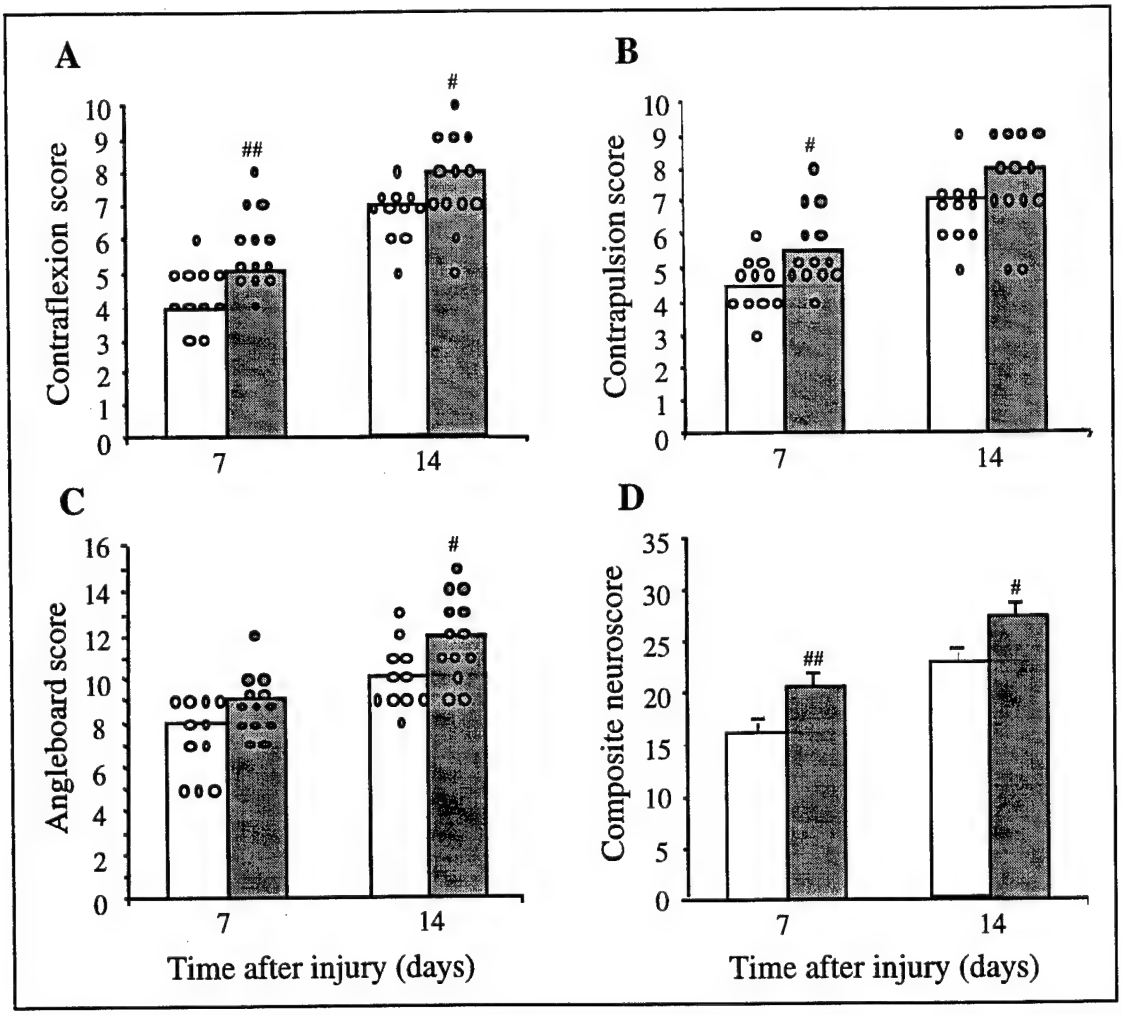

Figure 9. Recovery of neurological function following moderate fluid percussion injury (FPI) in the rat. In panels A,B and C, columns represent median values for each treatment group (open histogram = FPI + saline; shaded histogram = FPI + 2-ARA-53a) for each neurological test score, whereas each dot represents an individual animal score. In panel D, results for the composite score are expressed as mean + SEM. # $p < 0.05$, ## $p < 0.01$ with respect to FPI + saline .

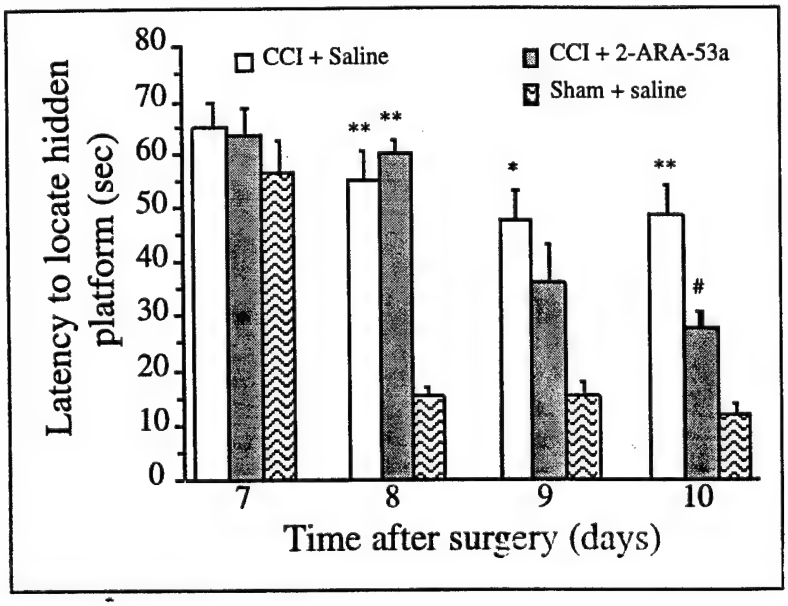

Figure 10. Latency to find the hidden platform in a version of the Morris water maze. Results are expressed as daily means ± SEM for each group over 4 trials. * $p < 0.01$, ** $p < 0.001$ with respect to Sham + saline; # $p < 0.01$, with respect to CCI + saline.

SHERIDAN L. SWOPE, Ph.D.

Neurotransmitter receptors are of primary importance in synaptic transmission and are targets for regulation. Modulation of the function, expression, or density of receptors has a profound effect on synaptic efficacy and thus may mediate plasticity. Accumulating evidence supports a role for phosphorylation in the regulation of synaptic transmission. Protein tyrosine kinases are a unique class of kinases initially found to mediate cell transformation and proliferation. However, protein tyrosine kinases are also involved in differentiated cell function. In fact, many protein tyrosine kinases are most highly expressed in the brain, being present both pre- and postsynaptically, suggesting their importance in the regulation of synaptic activity. Our long-term goal is to study the role of protein tyrosine kinases in synapse formation and function.

Much of the current understanding of synapses originates from studies of the neuromuscular junction (NMJ). The nicotinic acetylcholine receptor (AChR) is the ligand gated ion channel that mediates rapid postsynaptic depolarization at the NMJ. Because of its abundance in the electric organs of *Torpedo californica*, the AChR is the best characterized neurotransmitter receptor and has served as a model to elucidate the structure, function, and modulation of neurotransmitter receptors and ion channels. The AChR is phosphorylated on tyrosine residues both *in vitro* and *in vivo,* and this tyrosine phosphorylation is correlated with a modulation of the rate of receptor desensitization. In addition, tyrosine phosphorylation of the AChR and/or other postsynaptic components is involved in the nerve induced clustering of the AChR during synaptogenesis at the NMJ. Furthermore, protein tyrosine phosphorylation mediates the effect of acetylcholine receptor inducing activity (ARIA) to increase AChR transcription by nuclei underlying the synapse. Our interest has been to identify protein tyrosine kinases that are expressed postsynaptically at the NMJ which function to regulate the AChR.

We have identified two Src like kinases, Fyn and Fyk, that together comprise the predominant protein tyrosine kinase activity in the AChR enriched postsynaptic membrane of *Torpedo* electric organ. Src class kinases are also present in skeletal muscle and brain. Fyn and Fyk associate with the AChR via a binding of their src homology 2 (SH2) domains to the tyrosine phosphorylated δ subunit of the receptor. In addition, Fyn and Fyk phosphorylate the receptor *in vitro*. Other laboratories have demonstrated that Src itself also associates with the AChR of muscle. These initial studies suggest that Src family kinases are important regulators of synaptic function at the NMJ and in the central nervous system.

Over the last year, Dr. Ali Mohamed, a postdoctoral fellow with biochemical and molecular biological experience in the area of protein phosphorylation and Ms Patricia Clutton, a Ph.D. student have continued to be members of the laboratory. In addition, Ms. Anne Miermont, a research assistant, and Dr. Will Rosoff, a postdoctoral fellow with expertise in synaptogenesis, have joined our group. The efforts of these researchers will enable our laboratory to attain its research goals. Extramural funding from the National Institutes of Health, National Institute of Neurological Disorders and Stroke in the form of an R29 or First Award has been successfully extended via a noncompetitive renewal. Furthermore, additional funding through the Muscular Dystrophy Association has been awarded.

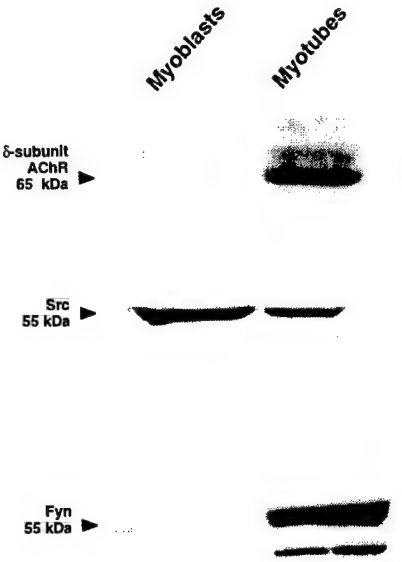

Fig 1. Effect of muscle differentiation on expression of Src class kinases. The C2C12 mouse muscle line was grown in culture and myoblasts or myotubes harvested with 2% SDS lysis buffer. Solubilized proteins (50μg) were resolved by SDS-PAGE and analyzed by Western blotting using antibodies to the AChR δ subunit, Src, or Fyn as indicated. Arrows indicate the position of the AChR δ subunit, Src, or Fyn.

As an established laboratory at the Georgetown Institute of Cognitive and Computation Sciences, the aim of our current research is to continue to test the hypothesis that Src class kinases are involved in synapse formation and function at the NMJ by regulating the AChR. Furthermore, the molecular mechanisms by which these kinases act to regulate synaptic transmission are being investigated.

Clarification of the Mechanisms for Regulation of Src class Kinases at the NMJ

One of our research goals is to identify mechanisms by which Src class kinases are regulated at the NMJ. Prior to innervation, embryonic myoblasts fuse into myotubes. This differentiation process results in an upregulation of AChR expression. Our recent results have demonstrated a specific coregulation of Fyn (Fig 1). During fusion of the C2C12 mouse muscle cells, Fyn was upregulated in concert with the AChR. In contrast, expression of Src was unchanged during differentiation. This specific coregulation of Fyn with the AChR supports the importance of Fyn at the NMJ.

Investigation of the primary extracellular factors that regulate the activity of Src kinases was also initiated. Agrin is the neuron-derived factor that induces AChR phosphorylation and clustering. Our preliminary results indicate that the agrin receptor, MuSK, may be important for regulating Src kinases. Direct *in vitro* binding between MuSK and Src kinases was demonstrated using fusion protein affinity chromatography. MuSK bound to the SH2 domain of Fyn, Fyk, and Src but not Grb2 (Fig 2). This binding was dependent on autophosphorylation of MuSK (data not shown). These results suggested that agrin, acting via MuSK, activates Src class kinases. Presently, this hypothesis is being tested by examining whether treatment of C2C12 myotubes with agrin results in activation of Src and Fyn.

Clarification of the Signal Transduction Cascade Involving Src class kinases

We are also in the process of characterizing the signal transduction pathway(s) by which Src class kinases act to regulate synapse formation and function by asking: what are the identities of cellular components that interact directly with Fyn, Fyk, and Src? These ongoing studies will be performed using coimmunoprecipitation techniques, fusion protein affinity chromatography, and the yeast two-hybrid system. These methods have become generally applicable for the identification of target proteins based on protein-protein interaction including protein kinase substrates.

Using the yeast two-hybrid system, we identified a molecular component of *Torpedo* electric organ that interacts with the unique domain of Fyn. This 13kDa component was homologous to a previously identified mouse sterility factor, Tctex-1 that is a light chain of the cyoplasmic microtuble protein dynein. We tested whether *Torpedo* Tctex-1 was complexed with dynein or cytoskeletal elements of the NMJ including rapsyn and syntrophin. Precipitation of Tctex-1 resulted in specific coprecipitation of the intermediate chain, IC74, of dynein. Further evidence for Tctex-1 being a component of dynein in *Torpedo* electric organ was obtained by immunoprecipitating dynein IC74 and analyzing the precipitate for Tctex-1 by Western blotting . Tctex-1 was specifically coprecipitated with dynein (Fig 3B). These data indicated that Tctex-1 was a component of the molecular motor protein dynein in *Torpedo* electric organ.

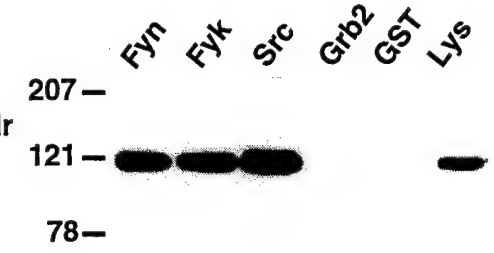

Fig 2. Specificity of MuSK binding to SH2 domains of Src class kinases QT6 cells transfected with myc-tagged *Torpedo* MuSK were treated with 20mM pervanadate, solubilized with 2% SDS lysis buffer, diluted to 2% Triton lysis buffer, and incubated with affinity resin containing the SH2 domain of Fyn, Fyk, Src, or Grb2 or the GST backbone protein. Binding of MuSK was detected by anti-myc Western blotting.

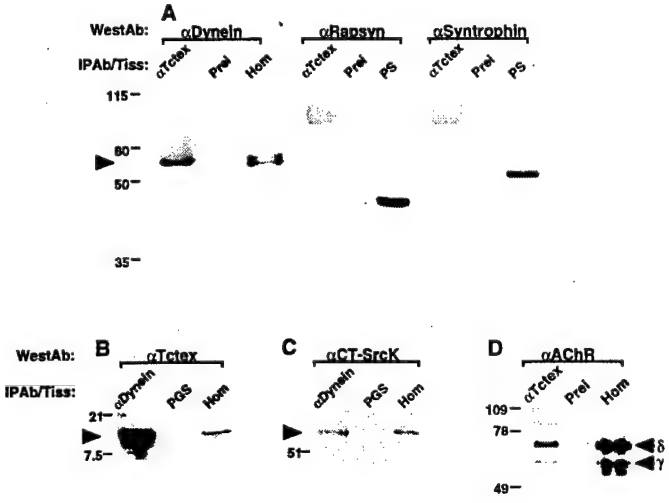

Fig 3 Characterization of a Tctex-1/Dynein complex in *Torpedo* electric organ A. Aliquots of *Torpedo* electric organ homogenate representing 300 μg of protein were solubilized and immunoprecipitated with anti-Tctex-1 (αTctex) or preimmune (Prei) serum. The precipitates and 30 μg of homogenate (Hom) or 0.3 μg of postsynaptic membranes (PS) were resolved by 10% SDS-PAGE and analyzed by Western blotting using an anti-dynein IC74 (αDynein), anti-rapsyn (αRapsyn), or anti-syntrophin (αSyntrophin) antibody. Arrow indicates the position of dynein IC74. B. *Torpedo* electric organ homogenate representing 500 μg of protein was solubilized and immunoprecipitated with anti-dynein IC74 (αDynein) antibody or empty protein G-sepharose (PGS). The precipitates and 30 μg of solubilized homogenate (Hom) were resolved by 15% SDS-PAGE and analyzed by Western blotting using an anti-Tctex-1 antibody (αTctex). Arrow indicates the position of Tctex-1. C. *Torpedo* electric organ homogenate representing 2 mg of protein was solubilized and immunoprecipitated with anti-dynein IC74 (αDynein) antibody or empty protein G-sepharose (PGS). The precipitates and 60 μg of solubilized homogenate (Hom) were resolved by 8% SDS-PAGE and analyzed by Western blotting using an anti-CT-Src kinase antibody (αCT-SrcK). Arrow indicates the position of Src kinases. D. *Torpedo* electric organ homogenate representing 300 μg of protein was solubilized and immunoprecipitated with anti-Tctex-1 (αTctex) or preimmune (Prei) serum. The precipitates and 3.0 μg of solubilized homogenate (Hom) were resolved by 10% SDS-PAGE and analyzed by Western blotting using a monoclonal anti-AChR antibody (88b). Arrows indicate the position of AChR δ and γ subunits. In each panel, molecular weights are indicated to the left.

Association of Src class kinases with the Tctex/dynein complex was also tested. The presently available anti-Fyn antibodies were not useful for directly demonstrating association of Fyn with the Tctex/dynein complex. However, in four experiments, precipitation of dynein from electric organ homogenate resulted in coprecipitation of a Src family kinase as demonstrated by Western analysis with an antibody to the carboxy terminal sequence of Src family kinases (Fig 3C). Library screening as well as PCR analysis have identified Fyn and Fyk as the only Src class kinases in *Torpedo* electric organ . Thus, these data suggested that the Src class kinase associated with the Tctex/dynein complex was Fyn and/or Fyk.

The primary function of the endplate at the NMJ is to mediate synaptic transmission via the activation of the AChR. Since Tctex-1 was detected in postsynaptic membranes, complex formation between the cytoskeletal protein and the AChR was examined. Immunoprecipitation of Tctex-1 resulted in coprecipitation of the AChR (Fig 3D) indicating that the AChR was also contained in a complex with Tctex-1.

The sequence of *Torpedo* Tctex indicated a putative tyrosine phosphorylation site at Tyr4. In fact, a Tctex fusion protein could be phosphorylated on tyrosine residue(s) *in vitro* by immunoprecipitated Fyn. These results suggested that Tctex may be a substrate for Fyn at the NMJ. Anchoring of postsynaptic components at the NMJ by cytoskeletal elements is now believed to involve tyrosine phosphorylation of postsynaptic components. Thus, Fyn may regulate AChR aggregation via an effect on the Tctex cytoskeletal element.

To determine the physiological role of Src class kinases in synapse formation and function, a strategy involving expression of recombinant kinases in a heterologous cell line that expresses the AChR has been developed. Coexpression of Fyn, Fyk, or Src and the endplate specific cytoskeletal protein rapsyn in the Q-F18 cells increased cellular tyrosine phosphorylation (Data not shown). The increase in cellular phosphorylation occurred primarily in the cytoskeletal fraction (Data not shown). These data indicated that rapsyn was able to activate Fyn, Fyk, and Src.

Coexpression of Fyn, Fyk, or Src and rapsyn in the Q-F18 cells also increased phosphorylation of the AChR as demonstrated by phosphorylation state specific antibodies (Fig 5). AChR purified from Q-F18 cells transfected with the kinases and rapsyn were analyzed in parallel for AChR content (Fig 5A) and AChR tyrosine phosphorylation (Fig 5B). Depending on the specific subunit and kinase analyzed, the effect of kinase plus rapsyn was 2-20 fold greater that the effect of rapsyn alone. These results indicated that all three kinases were capable of phosphorylating the AChR. In addition, Fyn-, Fyk-, and Src-mediated AChR phosphorylation occurred only upon expression of rapsyn. These data suggested that the ability of rapsyn to regulate Fyn, Fyk, and Src as shown in Fig 4 resulted in phosphorylation of the AChR by these kinases.

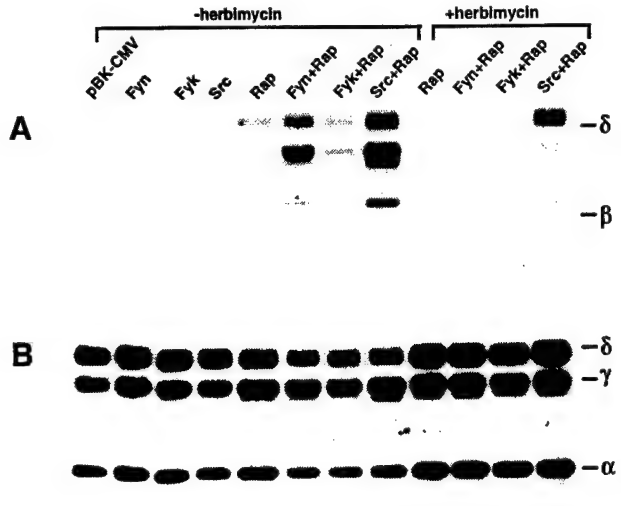

Fig 5. Tyrosine phosphorylation of the AChR β and δ subunit by Src class kinases.
(A) Q-F18 cells were transfected with empty pBK-CMV (pBK-CMV) or expression constructs Fyn pBK-CMV (Fyn), Fyk pBK-CMV (Fyk) or Src pcDNA3 (Src) without or with rapsyn pGW-CMV (Rap) in the absence (-herbimycin) or presence (+herbimycin) 1μM herbimycin A as indicated. After 48 h, cells were solubilized and the AChR purified using acetylcholine-Sepharose affinity chromatography. Aliquots of purified AChR representing approximately equal amounts of receptor, as determined by pilot Western analysis with anti AChR antibody (88b), were resolved by 8% SDS-PAGE and analyzed by Western blotting using mixture of the phosphorylation state specific anti-AChR β subunit (JH1360) and anti-AChR δ subunit (JH1358) antibodies. (B) The blot from A was stripped and reanalyzed by Western blotting using a mixture of anti-AChR γ and δ (88b) and α subunit (109) antibodies. Molecular weight markers, in kilodaltons, are indicated on the left. The positions of AChR α, β, γ, and δ subunits are as indicated.

The physiological relevance of AChR phosphorylation by Src family kinases was examined by testing whether the phosphorylation was associated with anchoring of the receptor to the cytoskeleton. Little or no AChR was associated with the cytoskeleton in control cells or cells expressing Fyn, Fyk, or Src alone as demonstrated by Western analysis using antibodies to the AChR α, γ, and δ subunits (Fig 6A). However, when Fyn, Fyk, and Src were expressed with rapsyn, there was a dramatic increase in the AChR found in the cytoskeletal fraction (Fig 6A). AChR was also detected at the cytoskeleton upon expression of rapsyn alone. However, activation of the coexpressed kinases by rapsyn resulted in greater translocation of the receptor to the cytoskeleton compared to rapsyn alone. Thus, for Fyn, Fyk, or Src plus rapsyn the increase in AChR at the cytoskeleton over the effect of rapsyn alone was 1.9±0.1, 1.7±0.1, and 2.6±0.2 (mean±S.E.M.;n=8) respectively as determined by quantitative scanning densitometry. These data demonstrated that Fyn, Fyk, and

Src could induce anchoring of the AChR to the cytoskeleton in a rapsyn dependent manner. In addition, the rapsyn stimulated effect of Src kinases to increase cytoskeletal anchoring of the receptor was essentially abolished by herbimycin A suggesting that kinase activity was necessary for AChR translocation (Fig 6A). These data indicated an important role for Src kinases in AChR anchoring to the cytoskeleton.

Figure 6. Translocation of AChR to cytoskeleton by rapsyn and Src kinases.
(A) Q-F18 cells were transfected with empty pBK-CMV or expression constructs Fyn pBK-CMV (Fyn), Fyk pBK-CMV (Fyk), or Src pcDNA3 (Src), without or with rapsyn pGW-CMV (Rap) as indicated in the absence (-herbimycin) or presence (+herbimycin) of 1 μM herbimycin A as described under "Experimental Procedures." After 48 h, cells were solubilized in 1% Triton, centrifuged at 15K x g for 10 min, and the Triton insoluble pellet was solubilized in SDS-PAGE sample buffer, sonicated for 30 sec, and centrifuged at 225K x g for 20 min. Aliquots of the solubilized pellets representing 10% of a 100 mm dish were resolved by 8% SDS-PAGE and analyzed by Western blotting using a mixture of anti-AChR γ and δ (88b) and α subunit (109) antibodies. (B) The blot from A was stripped and reanalyzed by Western blotting using the phosphorylation state specific anti-AChR β subunit (JH1360) antibody. The positions of AChR α, β, γ, and δ subunits are indicated.

In summary we have made significant progress in demonstrating that Src class protein tyrosine kinases are involved in the regulation of the AChR of the NMJ. Clarification of these basic molecular processes are relevant to an understanding of synaptic transmission in healthy people as well as those afflicted with neurological and neuromuscular diseases.

PUBLICATIONS FROM THE GICCS FACULTY IN THE LAST YEAR (including abstracts)

DAPHNE BAVELIER, Ph.D.

PUBLICATIONS

Bavelier, D. Corina, D., Jezzard, P., Padmanabhan, S., Clark, V.P., Karni, A., Prinster, A., Braun, A., Lalwani, A., Rauschecker, J., Turner, R. & Neville, H. Sentences Reading: A Functional MRI study at 4T. *Journal of Cognitive Neuroscience,* 9(5), 664-686, 1997.

Neville, H., **Bavelier, D.**, Corina, D., Rauschecker, J., Karni, A., Lalwani, A., Braun, A., Clark, V.P., Jezzard, P., & Turner, R. Cerebral Organization for Language in Deaf and Hearing Subjects: Biological Constraints and Effects of Experience. *Proceedings of the National Academy of Science,* 95(3), 922-929, 1998.

Bavelier, D., Corina, D., Jezzard, P., Clark, V.P., Karni, A., Lalwani, A., Rauschecker, J., Braun, A., Turner, R. & Neville, H. Hemispheric Specialization for English and American Sign Language: Left Invariance, Right Variability. *Neuroreport, 9*, 1998.

Neville, H. & **Bavelier, D.** Neural Organization and Plasticity of Language. *Current Opinions in Neurobiology,* 8(2), 1998.

Bavelier, D., Corina, D. & Neville, H. Brain and Language: A Perspective from Sign Language. *Neuron.* Submitted.

Bavelier, D., Deruelle, C. & Proksch, J. Consistency Effects: The Positivie and the Negative of It. *Perception & Psychophysics.* Submitted.

Book Chapters

Neville, H.J., & **Bavelier, D.** Variability of Developmental Plasticity Within Sensory and Language Systems: Behavioral, ERP and fMRI Studies. In:: Proceedings of the NIMH Conference on Advancing Research on Developmental Plasticity: Integrating the Behavioral Science and Neuroscience of Mental Health. (D. Hann, L. Huffman, I.I. Lederhendler, & D. Meinecke, eds.), Washington, D.C., US Government Printing Office, 1997.

Bavelier, D. Role and Nature of Object Representations in Perceiving and Acting. In:: Fleeting Memories, (Colheart, V., ed.). Boston: MIT Press. (in press)

Neville, H. & **Bavelier, D.** Developmental Specificity in Neurocognitive Development in Humans. In:: The Cognitive Neuroscience, (M. Gazzaniga, ed.) vol. 2. (in preparation)

Conference Abstracts

Newman, A., Corina, C., Tomann, A., **Bavelier, D.**, Braun, A., Clark, V.C., Jezzard, P. & Neville, H. Effects of Age in Acquisition on Cortical Organization for American Sign Language: A Functional Magnetic Resonance (fMRI) Imaging Study. 27th Annual Meeting of the Neuroscience Society, New Orleans, LA, October 1997.

Bavelier, D., Deruelle, C., Klineberg, E. & Proksch, J. Positive and Negative Similarity Effects. 38th Annual Meeting of the Psychonomic Society, Philadelphia, PA, November 1997.

Zemel, R., Behrmann, M., Mozer, M.C., & **Bavelier, D.** Experience-dependent perceptual grouping and object-based attention. 5th Annual Meeting of the Cognitive Neuroscience Society, San Francisco, CA, April 1998.

Bavelier, D. Imaging the Plastic Brain -- Viewing the Functional Anatomy of Cognitive Reorganization. Invited speaker at the 5th Annual Meeting of the Cognitive Neuroscience Society, San Francisco, CA, April 1998.

Tomann, A., Mitchell, T., Neville, H.J., Corina, C., Hutton, C., & **Bavelier, D.** Cortical Reorganization for Motion Processing in Congenitally Deaf Subjects. 5th Annual Meeting of the Cognitive Neuroscience Society, San Francisco, CA, April 1998.

Bavelier, D., Tomann, A., Mitchell, T., Corina, D., Pouget, A., Hutton, C., Liu, G. and Neville, H. Cortical Re-Organization for Visual Functions in Congenitally Deaf Subjects: Part I. Motion Processing. 28th Annual Meeting of the Neuroscience Society, Los Angeles, CA, November 1998.

Mitchell, T., Tomann, A., **Bavelier, D.**, Murray, S., Corina, D., Hutton, C., Liu, G. and Neville, H. Cortical Reorganization for Visual Functions in Congenitally Deaf Subjects: Part II. Object and Face Processing. 28th Annual Meeting of the Neuroscience Society, Los Angeles, CA, November 1998.

GUINEVERE EDEN, D.PHIL.

PUBLICATIONS

Zeffiro, T.A., **Eden, G.F.**, Woods, R.P. & VanMeter, J.W. Intersubject Analysis of fMRI Data Using Spatial Normalization. *Advances in Experimental Medicine Biology*, 413, 235-240, 1997.

Eden, G.F. and Zeffiro, T.A. Neural Mechanisms of Developmental Dyslexia Revealed by Brain Imaging. *Neuron.* (in press)

Eden, G.F., Joseph, J.E., Brown, H.E., Brown, C.P. & Zeffiro, T.A. Utilizing the Hemodynamic Delay and Dispersion to Detect fMRI Signal Change Without Auditory InterferenceL The BIG Technique. *Journal of Magnetic Resonance in Medicine.* (under review)

Book Chapters

Eden, G.F. & Zeffiro, T.A. Functional Magnetic Resonance Imaging. In:: The Foundation and Future of Functional Neuroimaging in Child Psychiatry , (J.M. Rumsey & M. Ernst, eds.). Cambridge University Press. (in press)

Eden, G.F. & Zeffiro, T.A. Functional Neuroimaging in Developmental Dyslexia. In:: Medical Radiology: Diagnostic Imaging and Radiation Oncology, (C. Moonen, Bordeaux, & P.A. Bandettini, eds.), Berlin-Heidelberg: Springer-Verlag. (in press)

Rumsey, J.M. & **Eden, G.F.** Functional Neuroimaging of Developmental Dyslexia: Regional Cerebral Blood Flow in Dyslexic men. In:: Specific Reading Disability: A View of the Spectrum (B. Shapiro, P.J. Accardo & A. J. Capute, eds.), Timonium: York Press, Inc., pp. 35-62, 1997.

Eden, G.F. & Zeffiro, T.A. Looking Beyond the Reading Difficulties in Dyslexia, A Vision Deficit. In:: Biopsychology 98/99, (B.M. Jubilan, ed.),4 ed., pp. 192-196. Guilford: Dushkin/McGraw-Hill, 1998.

Recent Abstracts

Eden, G.F., Joseph, J.E., Brown, C.P. and Zeffiro, T.A. Utilizing the Hemodynamic Lag to Detect fMRI Signal change Without Auditory Interference. *International Society of Magnetic Resonance in Medicine*, Sydney, 1998.

Joseph, J.E., Berger, J.S., Brown, H.E., Zeffiro, T.A. and **Eden, G.F.** Functional Magnetic Resonance Imaging of Silent and Oral Word Reading. *University of Maryland and Georgetown Institute for Cognitive and Computational Sciences Workshop*, Maryland 1998.

Eden, G.F., Joseph, J.E., Brown, H.E., Brown, C.P. and Zeffiro, T.A. fMRI Acquisition Without Auditory Interference: The "Flatcar" Design. *Society for Human Brain Mapping*, 1998.

Joseph, J.E., Zeffiro, T.A. and **Eden, G.F.** Radial Visual Motion Processing in Posterior Parietal Cortex. *Society for Human Brain Mapping*, 1998.

RENÉ ETCHEBERRIGARAY, M.D.

PUBLICATIONS

Gasparini, L., Racchi, M., Binetti, G., Trabucchi, M., Solerte, B., Alkon, D.L., **Etcheberrigaray, R.**, Gibson, G., Blass, J., Paoletti, R. and Govoni, S. Peripheral markers in testing pathophysiological hypotheses and diagnosing Alzheimer's Disease. FASEB J. 12:17-34, 1998.

Allen, J.W. and **Etcheberrigaray, R.** Potassium Channels in Neuropsychiatric Disorders: Potential for Pharmacological Intervention. CNS Drugs, 1998 (in press).

Etcheberrigaray, R., Hirashima, N., Nee, L., Prince, J., Govoni, S., Racchi, M. and Alkon, D.L. Calcium Responses in Fibroblasts from Asymptomatic Members of Alzheimer's Disease Families. Neurobiology of Disease, 1998 (in press).

Bhagavan, S., Ibarreta, D., Ma, D., Kozikowski, A.P. and **Etcheberrigaray, R.** Restoration of TEA-induced Calcium Responses in Fibroblasts from Alzheimer's Disease Patients by a PKC Activator Patients. Neurobiology of Disease, 1998 (under review).

Pascale, A., Bhagavan, S., Neve, R.L., McPhie, D.L. and **Etcheberrigaray, R.** Enhanced IP3 Mediated Calcium Responsiveness in PC12 Cells Expressing the C-100 Fragments of the Amyloid Precursor Protein (in preparation).

Wei, H., Chen, M., **Etcheberrigaray, R.** and Cohan, S.L. Dantrolene Improves EEG Recovery and Reduces CA1 Cell Damage after Ischemia in the Mongolian Gerbil. (in preparation).

Pascale, A. and **Etcheberrigaray, R.** Calcium Alterations in Alzheimer's Disease: Models, Pathophysiology and Therapeutic Opportunities. Pharmacological Research (invited review in preparation).

Abstracts

Bhagavan, S., Ibarreta, D., Kozikowski, A.P. and **Etcheberrigaray, R.** Protein Kinase C Activation Restores TEA-induced Calcium Responses in Fibroblasts from Alzheimer's Disease. 27th Annual Meeting Society for Neuroscience 23:2218, 1997.

Wei, H., Chen, M., **Etcheberrigaray, R.** and Cohan, S.L. Dantrolene Improves EEG Recovery and Inhibits Hippocampal CA1 Neuronal Death After Cerebral Ischemia. 27th Annual Meeting Society for Neuroscience, 23:548, 1997.

Etcheberrigaray, R. Bhagavan, S., Neve, R.L., McPhie, D.L. and Pascale, A. C-100 Enhances IP-3 Mediated Calcium Responsiveness in PC12 Cells. Neurobiology of Aging (6th International Alzheimer's Conference, 1998 (in press).

Pascale, A., Bhagavan,S., Neve, R.L., McPhie, D.L. and **Etcheberrigaray, R.** Enhanced Bradykinin (BK)-induced Ca^{2+} Responses in PC12 Cells Expressing the C-100 Fragment of APP. 28th Annual Meeting Society for Neuroscience, (in press).

Ibarreta, D., Duchen, M., Ma, D., Kozikowski, A.P. and **Etcheberrigaray, R.** Benzolactam (BL) Enhances sAPP secretion in Fibroblasts and in PC12 Cells. 28th Annual Meeting Society for Neuroscience, 1998 (in press).

ALAN I. FADEN, M.D.

PUBLICATIONS

Mukhin, A.G., Ivanova, S.A. and **Faden, A.I.** mGluR modulation of post-traumatic neuronal death: Role of NMDA receptors. *Neuroreport* 8:2561-2566, 1997.

Mukhin, A.G., Ivanova, S.A., Knoblach, S.M. and **Faden, A.I.** New *in vitro* model of traumatic neuronal injury: Evaluation of secondary injury and glutamate receptor mediated neurotoxicity. *J Neurotrauma* 14:651-663, 1997.

Eldadah, B.A.,Yakovlev, A.G. and **Faden, A.I.** The role of Ced-3-related cysteine proteases in apoptosis of cerebellar granule cells. *J Neurosci* 17(16):6105-6113, 1997.

Yakovlev,A.G., Knoblach, S.M., Fan,L., Fox,G.B., Goodnight< R., and **Faden, A.I.** Activation of CPP32-like caspases contributes to neuronal apoptosis and neurological dysfunction after traumatic brain injury. *J Neurosci* 17(19):7415-7424, 1997.

Faden, A.I., Ivanova, S.A., Yakovlev, A.G. and Mukhin, A.G. Neuroprotective effects of group III mGluR in traumatic neuronal injury. *J Neurotrauma* 14(12);885-895, 1997.

Mukhin,A.G., Ivanova, S.A., Allen, J.W. and **Faden, A.I.** Mechanical injury to neuronal/glial cultures in microplates: role of NMDA receptors and pH in secondary neuronal cell death. *J Neurosci Res*, 51:748-758, 1998.

Fox, G.B., Fan, L., LeVasseur, R.A. and **Faden, A.I.** Sustained sensory/motor and cognitive deficits associated with neuronal apoptosis following controlled cortical impact brain injury in the mouse. *J Neurotrauma.* (in press).

Books

Sharpe, V.A. and **Faden, A.I.** Medical Harm: Historical, Conceptual and Ethical Dimensions of Iatrogenic Illness. Cambridge University Press: Cambridge, UK, 1998.

Book Chapters

FADEN, A.I. Therapeutic approaches to spinal cord injury. *In*:: Seil, F.J. (Ed.), Lippincott-Raven Publishers: Philadelphia, Vol. 72; Ch. 35, pp. 377-386, 1997.

Vink,R., McIntosh, T.K. and **Faden, A.I.** Brain injury: metabolic aspects using magnetic resonance. *In*:: Encyclopedia of Neuroscience on CD ROM, 2nd ed.(G. Adelman and B. Smith, eds.). Elsevier: New York, 1997.

Yakovlev, A. and **Faden, A.I.** Traumatic brain injury regulates expression of Ced-related genes modulating neuronal apoptosis. *In*:: Neurotraumatology: Biomechanic Aspects, Cytologic and Molecular Mechanisms. Schmidt-Römhild, Lübeck, pp. 107-120, 1997.

Faden, A.I. Iatrogenic illness: an overview with particular reference to neurologic complications. *In* : Neurologic Clinics. W.B. Saunders Company: Philadelphia, Vol. 16(1), pp. 1-8, 1998.

DR. RHONDA B. FRIEDMAN, Ph.D.

PUBLICATIONS

Glosser, G., **Friedman, R.B.**, Kohn, S.E., Sands, L. and Grugan, P. Repetition of Single Words and Nonwords in Alzheimer's Disease. *Cortex*, 1997, 33, 653-666.

Glosser, G., **Friedman, R.B.**, Kohn, S.L. and Sands, L. Nonword Spelling in Patients with Probable Alzheimer's Disease. *Brain and Language*. (in press).

Glosser, G., **Friedman, R.B.**, Grugan, P., Lee, J.H. and Grossman, M. Lexical Semantic and Associative Priming in Alzheimer's Disease. *Neuropsyhchology*, 12(2), 213-224, 1998.

Glosser, G., **Friedman, R.B.** Can Treatment for Pure Alexia Improve Letter-By-Letter Reading Speed Without Sacrificing Accuracy? (Submitted)

Abstracts

Glosser, G., **Friedman, R.B.**, Kohn, S.E. and Sands, L. Nonword Spelling in Patients with Alzheimer's Disease. Presented at the Academy of Aphasia Meeting. *Abstract: Brain and Language*, 1997, 60(1), 134-137, Philadelphia, 1997.

Friedman, R.B. and Lott, S.N. Treatment for Pure Alexia Employing Two Distinct Reading Mechanisms. Presented at the Academy of Aphasia Meeting. *Abstract: Brain and Language*, 1997, 60(1), 118-120, Philadelphia, 1997.

Glosser, G., Grugan, P.K. and **Friedman, R.B.** Comparison of Reading and Spelling in Patients with Probable Alzheimer's Disease. Presented at the Annual Meeting of the International Neuropsyhcological Society, Hawaii. *Abstract: JINS, 1998, 4,1*, February 1998.

Friedman, R.B. and Lott, S.N. Using Models of Memory to Predict Generalization Effects in Treatment for Alexia. Presented at the Annnual meeting of the International Neuropsychological Society, Hawaii. *Abstract: JINS, 1998, 4,68.*, February 1998.

Book Chapters

Friedman, R.B. and Glosser, G. Aphasia, Alexia and Agraphia. In:: Encyclopedia of Mental Health, (Friedman, H.S., ed). San Diego: Academic Press, 1998, pp. 137-148.

GEOFFREY GOODHILL, PH.D.

PUBLICATIONS

Articles -Peer Reviewed

Goodhill, G.J. Diffusion in Axon Guidance. *European Journal of Neuroscience*, 9, 1414-1421, 1997.

Goodhill, G.J. & Sejnowski, T.J. A Unifying Objective Function for Topographic Mappings. *Neural Computation*, 1291-1304, 1997.

Goodhill, G.J. Stimulating Issues in Cortical Map Development. *Trends in Neurosciences*, 20, 375-376, 1997.

Goodhill, G.J. A Mathematical Model of Axon Guidance by Diffusable Factors. *Advances in Neural Information Processing Systems*, 10, M.I. Jordan, M.J. Kearns & S.A. Solla, eds. MIT Press, 1998, in press.

Goodhill, G.J. Gradients for Retinotectal Mapping. *Advances in Neural Information Processing Systems*, 10, M.I. Jordan, M.J. Kearns & S.A. Jolla, eds. MIT Press, 1998. (in press).

Goodhill, G.J. & Baier, H. Axon Guidance: Stretching Gradients to the Limit. *Neural Computation,*, 10, 521-527, 1998.

Goodhill, G.J. Mathematical Guidance for Axons. *Trends in Neuroscience*, to appear June 1998.

Articles - Non Peer-Reviewed

Goodhill, G.J. Book review of "Neural Organization: Structure, Function and Dynamics" by M.A. Arbib, P. Erdi & J. Szentagothai, MIT Press, 1998. *Neuron*, to appear May 1998.

Book Chapters

Goodhill, G.J. & Sejnowski, T.J. Objective Functions for Topography: A Comparison of Optimal Maps. In: Proceedings of the Fourth Neural Computation and Psychology Workshop: Connectionist Representattions. John A. Bullinaria, David G. Glasspool & George Houghton, eds. London: Springer-Verlag, 1997.

Abstracts

Goodhill, G.J. Theoretical Model of Axon Guidance by a Target-Derived Diffusible Factor. *Society for Neuroscience Abstracts*, 23, 1957.

JAGMEET KANWAL, Ph.D.

PUBLICATIONS

Kamada, K., Pekar, J. and **Kanwal, J.S.** Anatomical and Functional Analysis of the Auditory Cortex in Awake Mustached Bats Using Magnetic Resonance Imaging (in preparation).

Shimoawa, T., Kanou, M., **Kanwal, J.S.** and Suga, N. Sparsely Correlated Activity Between Spatially Segregated Delay-Tuned Neurons in the Auditory Cortex of Mustached Bats (in preparation).

Kanwal, J.S. and Suga, N. Excitatory, Facilitatory and Inhibitory Frequency Tuning of Combination-Sensitive Neurons in the Auditory Cortex of the Mustached Bat. *Jneurophysiol.* , 1997 (to be resubmitted).

Kanwal, J.S. and Esser, K.H. Response Properties of Auditory Neurons in the Frontal Cortex of the Mustached Bat (in preparation).

Kanwal, J.S. Processing Species-Specific Calls by Combination-Sensitive Neurons in an Echolocating Bat. In: Causal Mechanism of Animal Communication (Hauser, M.D. and Konishi, M., eds.), in press.

Kanwal, J.S. Charting Speech with Bats But Without Maps. *Brain Behav. Sci.* , 1997. (in press).

Esser, K-H., Condon, C.J., Suga, N., and **Kanwal, J.S.** Syntax Processing By Auditory Cortical Neurons in the FM-FM area of the Mustached Bat, *Pteronotus Parnellii. Proc. Natl. Acad. Sci.* 94:14019-14024, 1997.

Kanwal, J.S. and Finger, T.E. Parallel Medullary Gustatospinal Pathways in a Catfish: Possible Neural Substrates for Taste-Mediated Food Search. *Jneurosci.* 17:48873-4885, 1997.

Academic Conferences

Kanwal, J.S., Peng, J.P., and Esser K.-H. Convergent and Separate Processing of Communication and Echolocations Sounds in a Bat's Cortex. *SONAR Conference Abstract,* 1998 (in press).

Stotltz, B., Chhina, G.S., and **Kanwal, J.S.** Monaural Presentation of Music Improves Performance on a Tactile Pattern Matching Task in Humans. *Soc. for Neurosci. abstract,* #192.1, p. 494, 1997.

Gupta, P., Dietz, N. and **Kanwal, J.S.** Vocal Communication and Stereotypic Social Behavior Patterns in the Mustached Bat, *Pteronotus Parnellii.* Midwinter Meeting of the *Assoc. Res. in Otolaryngol,* 19:456, 1998.

Kamada, K.K., Chew, B.G., Qiu, H.H., Pekar,J., and **Kanwal, J.S.** Magnetic Resonance Imaging of the Auditory Cortex of Awake Mustached Bats. Meeting of the *Assoc. Res. in Otolaryngol.*,19:456, 1998.

Condon, C.J., **Kanwal, J.S.**, and Suga, N. Responses of Neurons in the Ventroposterior Auditory Cortex of the Mustached Bat to Communication Calls. Midwinter Meeting of the *Assoc. for Res. in Otolaryngol.*, 20, 1997.

DAE-SHIK KIM, Ph.D.

PUBLICATIONS

Miyashita, M., **Dae-Shik Kim**, & Tanaka, S. Cortical Directional Selectivity Without Directional Experience. *NeuroReport*, 8, 1187-1191, 1997.

Schmidt, K.E., **Dae-Shik Kim**, Singer, W. Bonhoeffer, T. & Loewel, S. Functional Specificity of Long-Range Intrinsic and Interhemispheric Connections in the Visual Cortex of Strabismic Cats. *Jneurosci*, 17(14), 5480-5492, 1997.

Goedecke, I. **Dae-Shik Kim**, Bonhoeffer, T. & Singer, W. Development of Orientation Preference Maps in Kitten Visual Cortex. *Europ. J. Neurosci.*, 9, 1754-1762, 1997.

Toth, L.J., **Dae-Shik Kim**, Rao, S.C. & Sur, M. Integration of Local Inputs in Visual Cortex. *Cerebral Cortex*, 7, 703-710. COVER STORY, 1997.

Somers, D.C., Todorov, E.V., Siapas, A.G., Toth, L.J., **Dae-Shik Kim** & Sur, M. A Local Circuit Approach to Understanding Integration of Long-Range Inputs to Primary Visual Cortex. *Cerebral Cortex* (in press). COVER STORY.

Loewel, S., Schmidt, K.E., **Dae-Shik Kim**, Wolf, F., Hoffstuemmer, F., Singer, W. & Bonhoeffer, T. The Layout of Orientation and Ocular Dominance Domains in Area 17 of Strabismic Cats. *European Journal of Neuroscience*, (in press).

Conference Abstracts

Dae-Shik Kim, Ohki, K., Matsuda, Y., Ajima, A., Saito, T. & Tanaka, S. Topological Constraints on Multiple Functional Maps. *Soc. Neurosci. Abstr.*, 920.9, 1997.

Tanaka, S. & **Dae-Shik Kim** Neurotrophic Influence on Synaptic Plasticity and Functional Map Formation. *Soc. Neurosci. Abstr.*, 1997.

Miyashita, M., **Dae-Shik Kim** & Tanaka, S. Self-Organized Hierarchical Network Model for the Emergence of Simple and Complex Cells. *Soc. Neurosci. Abstr.*, 1997.

Ohki, K., Matsuda, Y., Ajima, A., Saito, T., **Dae-Shik Kim**, & Tanaka, S. Differential Organization of Direction Maps in Cat Areas 17, 18m and across 17/18 Transition Zone. *Soc. Neurosci. Abstr.*,1997.

Ajima, A., Ohki, K., Matsuda, Y., Tanaka, S. & **Dae-Shik Kim**. Effect of Stimulus Timing for Cortical Information Integration: An Optical Imaging Study in Rat Barrrel Cortex. *Soc. Neurosci*, 1997.

Dae-Shik Kim, Tian, B. Qui, H.H., O'Reilly, M.P., Malonek, D., Jezzard, P., Rauschecker, J.P., & Pekar, J.J. Magnetic Resonance Imaging of Stimulus-Induced Activation in Cat Visual Cortex. Abstract accepted for the 1998 Annual Meeting of the International Society for Magnetic Resonance in Medicine, p. 514, 1998.

Dae-Shik Kim, Qui, H.H., Tian, B., Rauschecker, J.P., Pekar, J.J. Magnetic Resonance Imaging of Iso-Orientation Domains in Cat Visual Cortex. *Soc. Neurosci. Abstr.*, 1998 (in press).

Tian,B., **Dae-Shik Kim**, Rauschecker, J.P. Optical Imaging of Functional Organization in Cat Auditory Cortex. *Soc. Neurosci. Abstr.* (in press).

ALAN P. KOZIKOWSKI, Ph.D.

PUBLICATIONS

Raves, M., Harel, M., Pang, Y.P., Silman, I., **Kozikowski, A.P.**, and Sussman, J.L. 3D Structure of Acetylcholinesterase Complexed with the Nootropic Alkaloid (-)-Huperzine A. *Nature Structure Biology*, 4, 57-63, 1997.

Kozikowski, A.P., Simoni, D., Roberti, M., Manferdini, M., Du, P. and Johnson, K.M. Synthesis and Biological Evaluation of the 8-Oxa Analogues of Norcocaine; Molecular Modeling Studies of the Interaction of Cocaine and OXa-Norcocaine to a Pseudoreceptor Support Binding of Cocaine in its Neutral Form. *J.Med. Chem.*, submitted, 1998.

Tückmantel, W. , **Kozikowski, A.P.**, Pshenichkin, S., and Wroblewski, J.T. Synthesis and Biology of the 1-Benzyl Derivative of APDC - An Apparent mGluR6 Selective Ligand. *Bioorg. Med. Chem. Lett.*, 7, 601-606, 1997.

Ma, D., Tian, H., Sun, H., **Kozikowski, A.P.**, Pshenichkin, S., and Wroblewski, J.T. Synthesis and Biological Activity of Cyclic Analogues of MPPG and MCPG as Metabotropic Receptor Antagonists. *Bioorg. Med. Chem. Lett.*, 7, 1195-1198, 1997.

Kozikowski, A.P., Araldi, L. and Ball, R.G. Dipolar Cycloaddition Route to Diverse Analogues of Cocain, the 6- and 7-Substituted 3-Phenyltropanes. *J. Org. Chem.*, 62, 503-509, 1997.

Hart, D.J., Li, J., Wu, W.-L., and **Kozikowski, A.P.** Applications of Organosulfur Chemistry to Organic Synthesis: Total Synthesis of (+)-Himbeline and (+)-Himbacine. *J.Org. Chem.*, 62, 5023-5033, 1997.

Kozikowski, A.P., Wang, S., Ma, D., Yao, J., Ahmad, S., Glazer, R.I., Bogi, K., Acs, P., Modarres, S., Lewin, N.E. and Blumber, P.M. Modeling, Chemistry, and Biology of the Benzolactam Analogues of ILV 2. Identification of the Binding Site of the Benzolactams in the CDRD2 Activator-Binding Domain of PKCδ and Discovery of an ILV Analogue of Improved Isozyme Selectivity. *J. Med. Chem.*, 40, 1316-1326, 1997.

Saiah, M.K. Eddine, Avery, M.A., Williamson, J.S., and **Kozikowski, A.P.** Comparative Molecular Field Analysis of Cocaine Analogs. New Highly Predictive Binding and Uptake Models of Cocaine Recognition Sites at the Dopamine Transporter. *J. Med. Chem.*, submitted.

Wilcox, R.A., Fauq, A., **Kozikowski, A.P.**, and Nahorski, S.R. Defining the Minimal Structural Requirements for Partial Agonism at the Type I *m y o*-Inositol 1,4,5,-Triphosphate Receptor. *FEBS Lett.*, 402,241-245, 1997.

Yeats, L.C., Gallegos, A., **Kozikowski, A.P.** and Powis, G. Downregulation of the Expression of the p110 catalytic, and p85 and p55 Regulatory Subunits of Phosphatidylinositol 3-kinase during HT-29 Colon Cancer Cell Anchorage-Independent Growth. *Cancer Research*, submitted.

Kozikowski, A.P., Kotoula, M., Ma, D., Boujrad, N., Tückmantel, W., and Papadopoulos, V. Synthesis and Biology of a 7-Nitro-2,1,3-Benzoxadiazol-4-yl (NBD) Derivative of 2-Phenylindole-3-acetamide: A Fluorescent Probe for the Peripheral-type Benzodiazepine Receptor. *J. Med. Chem.*, 40,2435-2439, 1997.

McKinney, M. and **Kozikowski, A.P.** Pharmacologic Studies of Himbacine and Huperzine A: Potential Use in Cholinergic Replacement Therapy. *Herbal Medicines for Neuropsychiatric Diseases*, 1997.

Kozikowski, A.P., Steensman D., Araldi, G.L., Wang, S., Pshenichkin, S., Surina, E. and Wroblewski, J. Synthesis and Biology of the Conformationally Restricted ACPD Analogue, 2-Aminobicyclo[2.1.1]hexane-2,5-dicarboxylic Acid (ABH_6D); a Potent mGluR Ligand. *J. Med. Chem.*, 41, 1641-1650, 1998.

Smith, M.P., George, C. and **Kozikowski, A.P.** The Synthesis of Tricyclic Cocaine Analogs via the 1,3-Dipolar Cycloadditon of Oxidopyridinium Betaines. *Tetrahedron Lett.*, 39, 197-200, 1998.

Araldi, G.L., Prakash, K.R.C., George, C. and **Kozikowski, A.P.** An Enantioselective Synthesis of 2-alkyl-3-phenyltropanes by an Asymmetric 1,3-Dipolar Cycloaddtion Reaction. *J. Chem. Soc., Chem. Commun.*, 1875-1876, 1997.

Kozikowski, A.P., Qiao, L., Tückmantel, W. and Powis, G. Synthesis of 1D-3-Deoxy-and 2,3-Dideoxyphosphatidylinositol. *Tetrahedron*, 44, 14903-14914, 1997.

Kozikowski, A.P., Steensman, D., Varasi, M., Pshenichkin, S., Surina, E. and Wroblewski, J.T. α-Substituted Quisqualic Acid Analogs: New Matabotropic Glutamate Receptor Group II Selective Antagonists. *Bioorg. Med. Chem. Lett.*, 8, 447-452, 1998.

Bhagavan, S., Ibarreta, D., **Kozikowski, A.P.**, and Etcheberrigaray, R. Restoration of TEA-Induced Responses in Fibroblasts from Alzheimer's Disease Patients by a PKC Activator. *Neurobiology of Aging*, (submitted).

Qiao, L., Wang, S., George, C., Lewin, N.E., Blumberg, P.M. and **Kozikowski, A.P.** Structure-based Design of a New Class of PKC Modulators; Use of SmI_2 promoted Ring Closure in the Enantioselective Assembly of Pyrrolidones. *J. Amer. Chem. Soc.* (in press).

Prakash, K.R.C., Araldi, G.L., Smith, M.P., Zhang, M., Johnson, K.M., and **Kozikowski, A.P.** Synthesis and Biological Activity of New 6- and 7-substituted 2β-butyl-3-phenyltropanes as Ligands for the DAT. *Med. Chem. Res.* (in press).

Kozikowski, A.P., Araldi, G.L., Flippen-Anderson, J., George, C., Pshenichkin, S., Surina, E. and Wroblewski, J. Synthesis and Metabotropic Glutamate Receptor Activity of a 2-aminobicyclo[3.2.0]heptane-2,5-dicarboxylic acid, A Molecule Possessing an Extended Glutamate Conformation. *Bioorg. Med. Chem. Lett.*, 8, 925-930, 1998.

Kozikowski, A.P., Araldi, G.L., Boja, J., Johnson, K.M., Flippen-Anderson, J.L., George, C., and Saiah, E. Chemistry and Pharmacology of the Piperidine Based Analogs of Cocaine - Identification of Potent DAT Inhibitors Lacking the Tropane Skeleton. *J. Med. Chem.* (in press).

Qiao, L., **Kozikowski, A.P.**, Olivera, A. and Spiegel, S. Synthesis and Evaluation of a Photolyzable Derivative of Sphingosine 1-phosphate -- Caged SPP. *Bioorg. Med. Chem. Lett.*, 8, 711-714, 1998.

Kozikowski, A.P., Araldi, G.L., Prakash, K.R.C., Zhang, M. and Johnson, K.M. Synthesis and biological Properties of New 2β-alkyl and 2β-aryl-3-(substituted phenyl)tropane Derivatives: Stereochemical Effect of C-3 on Affinity and Selectivity for Neuronal Dopamine and Serotonin Transporters. *J. Med. Chem.* (submitted).

Kozikowski, A.P., Prakash, K.R.C., Saxena, A. and Doctor, B.P. Synthesis and Biological Activity of an Optically Pure 10-Spirocycloprpyl Analog of Huperzine A. *J. Chem. Soc., Chem. Commun.* (in press).

Qiao, L., Nan, F., **Kozikowski, A.P.**, Kunkel, M., Gallegos, A. and Powis, G. 3-Deoxy-D-Myo-Inositiol 1-Phosphonate, and Ether lipid Analogs as Inhibitors of Phosphatidylinositol-3-kinase Signaling and Cancer Cell Growth. *J. Med. Chem.* (submitted).

Campiani, G., **Kozikowski, A.P.**, Wang, S., Nacci, V., Saxena, A. and Doctor, B.P. Synthesis and Anticholinesterase Activity of Hyperzine A Analogues Containing Phenol and Catechol Replacements for the Pyridone Ring. *Bioorg. Med. Chem. Lett.* (in press).

Smith, M.P., Johnson, K.M., Zhang, M., Flippen-Anderson, J.L. and **Kozikowski, A.P.** Tuning the Selectivity of Monamine Transporter Inhibitors by the Stereochemistry of the Nitrogen Lone Pair. *J. Amer. Chem. Soc.* (submitted).

GUOYING LIU, Ph.D

PUBLICATIONS

Liu, G., Lantos, G., Shafer, V., Knuth, K. and Vaughan, H. Cortical Auditory and Phonetic Processing: an fMRI Study. *NeuroImage* 5(187) 1997.

Lantos, G., **Liu, G.**, Shafer, V., Knuth, K. and Vaughan, H. Tonotopic Organization of Primary Auditory Cortex: An fMRI Study. *NeuroImage*, 5(618) 1997.

Abstracts

Liu, G., Lantos, G., Nagel, R.L. and Fabry, M.E. Detection of Hypoxia in Sickle Cell Anemia by Susceptibility Effects Using Magnetic Resonance Imaging. *Proceedings International Society for Magnetic Resonance in Medicine.* 1(586), 1997.

Tomann, A., Mitchell, T., Neville, H.J., Corina, D., Hutton, C., **Liu, G.**, Bavelier, D. Cortical Reorganization for Motion Processing in Congenitally Deaf Subjects. *Cognitive Neuroscience Society*, 1998.

Bavelier, D., Tomann, A., Mitchell, T., Corina, D., Pouget, A., Hutton, C., **Liu, G.** and Neville, H.J. Cortical Re-Organization for Visual Functions in Congenitally Deaf Subjects: Part I. Motion Processing. *Society for Neuroscience*, 1998.

Mitchell, T., Tomann, A., Bavelier, D., Murray, S., Corina, D., Hutton, C., **Liu, G.** and Neville, H.J. Cortical Re-Organization for Visual Functions in Congenitally Deaf Subjects: Part II. Object and Face Processing. *Society for Neuroscience*, 1998.

JAMES J. PEKAR, Ph.D.

PUBLICATIONS

McLaughlin, A.C., **Pekar, J.**, Santha, A.K.S. and Frank, J.A. Effect of Magnetization Transfer on the Measurement of Cerebral Blood Flow Using Arterial Spin Tagging Approaches. *Magnetic Resonance in Medicine*, 37:501-510, 1997.

Abstracts

Chew, B.G.M., Albensi, B.C., Mattingly, M.O. and **Pekar, J.J.** High Resolution in vivo Brain MRI with Minimally Invasive Techniques. *Proceedings 38th Annual Experimental NMR Conference*, Orlando, FL, p. 67, 1997.

Wessinger, C.M., Tian, B., Japikse, K.C., Ghosh, S., VanMeter, J.W., Platenberg, R.C., **Pekar, J.**, and Rauschecker, J.P. Processing of Complex Sounds in Human Auditory Cortex. *Association for Research in Otolaryngology*, 20:27, 1997.

Albensi, B.C., Knoblach, S.M., Chew, B.G.M., Faden, A.I. and **Pekar, J.J.** Temporal Evaluation of in vivo Traumatic Brain Injury (TBI) Using Multi-Modal MRI. Abstracts, *Soceity for Neuroscience 27th Annual Meeting*, New Orleans, October 1997.

Wessinger, C.M., Tian, B., VanMeter, J.W., Platenberg, R.C., **Pekar, J.**, Rauschecker, J.P. Hierarchical Processing within Human Auditory Cortex Examined with fMRI. Abstracts, *Society for Neuroscience 27th Annual meeting*, New Orleans, October 1997.

Kamada, K., Chew, B.G., Qiu, H.H., **Pekar, J.** and Kanwal, J.S. Magnetic Resonance Imaging of the Auditory Cortex in Awake Mustached Bats. Abstracts, *Association for Research in Otolaryngology Annual Meeting*, 1998.

Kim, D.S., Tian, B., Qiu, H.H., O'Reilly, M.P., Malonek, D., Jezzard, P., Rauschecker, J.P. & **Pekar, J.J.** Magnetic Resonance Imaging of Stimulus-Motion-Induced Activation in Cat Visual Cortex. Proceedingsm *Annual Meeting of the International Society for Magnetic Resonance in Medicine*, Sydney, Australia, p. 514, 1998.

Albensi, B.C., Knoblach, S., Chew, B.G.M., O'Reilly, M.P., Faden, A.I. and **Pekar, J.J.** Serial Magnetic Resonance Imaging of a Rodent Model of Neuroinjury. Proceedings, *Annual Meeting of the International Society for Magnetic Resonance in Medicine,* Sydney, Australia, p. 1183, 1998.

Wessinger, C.M., Tian, B., VanMeter, J.W., Platenberg, R.C., **Pekar, J.J.** and Rauschecker, J.P. Processing of Complex Sounds in Human Auditory Cortex Examined wtih Functional Magnetic Resonance Imaging. Proceedings, *Annual Meeting of the International Society for Magnetic Resonance in Medicine,* Sydney, Australia, p. 1530, 1998.

Kim, D.-S., Qiu, H.H., Tian, B., Rauschecker, J.P. and **Pekar, J.J.** Magnetic Resonance Imaging of Iso-Orientation Domains in Cat Visual Cortex. *Society for Neuroscience Annual Meeting*, submitted, 1998.

In Preparation

Albensi, B.C., Knoblach, S.M., Chew, B.G.M., O'Reilly, M.P., Faden, A.I. and **Pekar, J.J.** Temporal Evaluation of in vivo Traumatic Brain Injury (TBI) Using Multi-Modal MRI. (Manuscript in preparation).

Kim, D.-S., Qiu, H.H., Tian, B., Rauschecker, J.P. and **Pekar, J.J.** Magnetic Resonance Imaging of Iso-Orientation Domains in Cat Visual Cortex. (Manuscript in preparation).

Kamada, K., **Pekar, J.** and Kanwal, J.S. Magnetic Resonance Imaging of Auditory Cortex in the Mustached Bat. (Manuscript in preparation).

Wessinger, Tian, B., VanMeter, Platenberg, R.C., **Pekar, J.** & Rauschecker, J.P. Hierarchical Processing of Pure-tones and Band-Passed Noise Bursts in Human Auditory Cortex. (Manuscript in preparation).

ALEXANDRE POUGET, Ph.D.

PUBLICATIONS

Abstracts

Deneve, S. and **Pouget, A**. Neuronal Object-Centered Representations: Map or Gain Modulation? *Society for Neuroscience Abstracts*, New Orleans, 1997.

Pouget, A. and Ducom, J.C. Noise Reduction, Discrimination and Adaptation in Cortical Circuits. *Society for Neuroscience Abstracts*, San Francisco, 1998.

Deneve, S. and **Pouget, A.** Neural Basis of Object-Centered Representations and Implications for Hemineglect. *Society for Cognitive Neuroscience Abstracts*, San Francisco, 1998.

Book Chapters

Pouget, A. and Sejnowski, T.J. Lesion in a Basis Function Model of Spaatial Representations: Comparison with Hemineglect. In:: Parietal Lobe Contribution in Orientation in 3D Space. (Thier, P. and Karnath, H.O. eds.). Springer Verlag, 1997.

Pouget, A. and Sejnowksi, T.J. A New View of Hemineglect Based on the Response Properties of Parietal Neurons. In: What are the Parietal and Hippocampal Contributions to Spatial Cognition. (Burgess, N. Jeffery, K.J. and O'Keefe, J. Philosophical Transactions of the Royal Society: Series B 352, 1397-1543, 1997.

Pouget, A. and Sejnowski, T.J. A New View of Hemineglect Based on the Response Properties of Parietal Neurons. Philosophical Transactions: Biological Cortex. (Neill Burgess, Kathryn, J., and O'Keefe, John, eds.) *Oxford University Press.*. (in press).

Pouget, A. and Driver, J. Visual Neglect. In: MIT Encyclopedia of Cognitive Sciences (Wilson, R. and Keil, F., eds.), 2nd Edition. Arbib, M.A. (ed). Boston: MIT Press. (in preparation).

Pouget, A. and Latham, P. Dynamical Remappingi In the *Hamdb og Arbib, (eds.) Boston, MIT Press.* (in prepartaion).

Pouget, A. and Latham, P. Reading ou Population Codes. In: The Handbook of Brain Theory and Neural Networks. (in preparation).

Refereed Conference Proceedings

Pouget, A. and Zhang, K. Statistically Efficient Estimation Using Cortical Lateral Connections. *Advances in Neural Information Processing Systems* (Mozer, M.C., Jordan, M.I. and Petsche, T., eds.), 9. MIT Press, Cambridge, MA, 1997.

Gray, M.S., **Pouget, A.**, Zemel, R.S., Nowlan, S.J., and Sejnowski, T.J. Selective Integration: A Model for Disparity Integration. *Advances in Neural Information Processing Systems* (Mozer, M.C., Jordan, M.I. and Petsche, T., eds.). 9. MIT Press, Cambridge, MA, 1997.

Zemel, R.S., Dayan, P., and **Pouget, A.** Population Code Representations of Probability Density Functions. *Advances in Neural Information Processing Systems* (Mozer, M.C., Jordan, M.I. and Petsche, T., eds.). 9. MIT Press, Cambridge, MA, 1997.

Deneve, S. and **Pouget, A.**, Neural Basis of Object-Centered Representations. *Advances in Neural Information Processing Systems*. (Jordan, M.I., Kearns, M.J., and Solla, S., eds.) 10. MIT Press, Cambridge, MA (in press).

Deneve, S., **Pouget, A.** and Latham, P. Heeger's Normalization, Line Attractor Network and Ideal Observers. *Advances in Neural Information Processing Systems.* 11 (submitted).

Research Articles

Pouget, A., and Sejnowski, T.J. Spatial Transformations in the Parietal Cortex Using Basis Functions. *Jounrnal of Cognitive Neuroscience,* 9(2):222-237, 1997.

Cai, R.H., **Pouget, A.**, Schlag-Rey, M. and Schlag, J. Perceived Geometrical Relationships Affected by Eye Movement Signals. *Nature*, 386:601-603, 1997.

Pouget, A., Zhang, K., Deneve, S., and Latham, P.E. Statistically Efficient Estimation Using Population Code. *Neural Computation*, 10:373-401, 1998.

Zemel, R.S., Dayan, P. and **Pouget, A.** Probabilistic Interpretation of Population Code. *Neural Computation,* 10:403-430, 1998.

Schlag, J., **Pouget, A.**, Schlag-Rey, M. and Saderghpour, S. Interaction Between Natural and Electrically Evoked Saccades. III. Is the Compensation by Collicular Stimulation Due to a Feedback Integrator Not Yet Reset? *Journal of Neurophysiology*, 79:903-910, 1998.

Bremmer, F., **Pouget, A.** and Hoffmann, K. Eye Position Effects in Monkey Cortex. III. Representation of Gaze Direction at the Population Level. *European Journal of Neuroscience,* 10(1):153-160, 1998.

Gray, M.S., **Pouget, A.**, Zemel, R.S., Nowlan, S.J. and Sejnowski, T.J. Reliable Disparity Estimation Through Selective Integration. *Visual Neuroscience*, in press.

Pouget, A., Deneve, S., Ducom, J.C. and Latham, P.E. Narrow vs. Wide Tuning CurvesL What's Best for a Population Code? *Neural Computation* (submitted).

Pouget, A. and Sejnowski, T.J. Hemineglect in a Basis Function Model of Parietal Cortex. (in preparation).

Pouget, A., Deneve,S., Ducom, J.C. and Latham, P.E. Statistical Constraints on Computing and Transmitting Population Codes. (in preparation).

Driver, J. and **Pouget, A.** Object-Centered or Relative Neglect? (in preparation).

JOSEF P. RAUSCHECKER, Ph.D., D.Sc.

PUBLICATIONS

Rauschecker, J.P., Tian, B., Pons, T., Mishkin, M. Serial and Parallel Processing in Rhesus Monkey Auditory Cortex. *J. Comp. Neurol.*, 382, 89-103, 1997.

Bavelier, D., Corina, D., Clark, V.P., Dale, A., Jezzard, P., Prinster, A., Karni, A., Lalwani, A., **Rauschecker, J.,**, Turner, R. and Neville, H. Sentence Reading: a 4T fMRI Study of Cortical Regions Active During an English Reading Task. *Journal of Cognitive Neuroscience*, 9, 664-686, 1997.

Grady, C.L., VanMeter, J.W., Maisog, J.M., Pietrini, P., Krasuski, J. and **Rauschecker, J.P.** Attention-related Modulation of Activity in Primary and Secondary Auditory Cortex. *Neuroreport* 8, 2511-2516, 1997.

Jezzard, P., **Rauschecker, J.P.** and Malonek, D. An in vivo Model for Functional MRI in Cat Visual Cortex. *Magnetic Resonance in Medicine*, 38, 699-705, 1997.

Rauschecker, J.P. Processing of Complex Sounds in the Auditory Cortex of Cat, Monkey, and Man. *Acta Otolaryngologica*, 532, 34-38, 1997.

Neville, H.J., Bavelier, D., Corina, D., **Rauschecker, J.P.**, Karni, A., Lalwani, A., Braun, A., Clark, V., Jezzard, P., Turner, R. Cerebral Organization for Language in Deaf and Hearing Subjects: Biological Constraints and Effects of Experience. *Proc. Natl. Acad. Sci.* , USA 95, 922-929, 1998.

Rauschecker, J.P. Parallel Processing in the Auditory Cortex of Primates. *Audiology and Neuro-Otology*, 3, 86-103, 1998.

Tian, B. and **Rauschecker, J.P.** Processing of Frequency-Modulated Sounds in the Cat's Posterior Auditory Field. *J. Neurophysiol.* (in press).

Bavelier, D., Corina, D., Jezzard, P., Clark, V., Karni, A., Lalwani, A., **Rauschecker, J.P.**, Braun, A., Turner, R. and Neville, H.J. Hemispheric Specialization for English and ASL: left invariance - right variability. *Neuroreport* . (in press).

Rauschecker, J.P. Cortical Processing of Complex Sounds. *Current Opinion in Neurobiology* (in press).

Rauschecker, J.P. Auditory Physiology. Invited contribution. *MIT Encyclopedia of Cognitive Science*. (in press).

Rauschecker, J.P. Auditory Cortical Plasticity. Invited review, *Trends in Neurosciences* . (in press).

Abstracts

Rauschecker, J.P. Parallel Processing of Complex Sounds in Primate Auditory Cortex. *proc. Int. Union Physiol. Sci.* 33,L081.04, 1997.

Middlebrooks, J.C., Kaas, J.H., **Rauschecker, J.P.** and Schreiner, C.E. Symposiuym: Auditory Cortex-Common Themes and Specialization for Hearing. *Soc. Neurosci.* Abstr. 23, 1937, 1997.

Tian, B., Fritz, J., Ojima, H., Mishkin, M. and **Rauschecker, J.P.** Hierarchical Processing of Monkey Calls Within Different Areas of Auditory Cortex in the Macaque. *Soc. Neurosci.* Abstr 23, 2073, 1997.

Wessinger, C.M., Tian, B., VanMeter, J.W., Platenberg, R.C., Pekar, J. and **Rauschecker, J.P.** Hierarchical Processing within Human Auditory Cortex Examined with fMRI. *Soc. Neurosci.* 23, 2073, 1997.

Romanski, L.M., Goldman-RTakic, P.S., Tian, B., Fritz, J., Ojima, H. and **Rauschecker, J.P.** Projections from Physiologically Defined Regions of the Auditory Association Belt and Parabelt Cortical Regions of the Superior Temporal Gyrus Target Specific Prefrontal Regions in the Primate. *Soc. Neurosci.* Abstr. 23, 2073, 1997.

Malonek, D., **Rauschecker, J.P.**, Grinvald, A. and Jezzard, P. fMRI and Optical Intrinsic Signals in Cat Visual Cortex: Differences in Response Dynamics. *Soc. Neurosci.* Abstr. 23, 2262, 1997.

Tian, B., Malonek, D. and **Rauschecker, J.P.** Optical Imaging of Activity Patterns in Cat Auditory Cortex Evoked by Tones and Complex Sounds. *Assoc. Res. Otolaryngol.*Abstr 21 (in press).

Zhenochin, S., Fritz, J., Tian, B., Ojima, H. and Rauschecker, J.P. Thalamo-Cortical Projections Underlying Differential Responsiveness in the Lateral Belt Areas of Rhesus Monkey Auditory Cortex. *Assoc. Res. Otolaryngol.* Abstr 21 (in press).

Wessinger, C.M., Tian, B., VanMeter, J.W., Platenberg, R.C., Pekar, J.J. and **Rauschecker, J.P.** Processing of Complex Sounds in Human Auditory Cortex Examined with Functional Magnetic Resonance Imaging. *Proc. Int. Soc. Mag. Res. Med.*, 1530, 1998.

Kim, D.-S., Tian, B., Qiu, H.H., O'Reilly, M.P., Malonek, D., Jezzard, P., **Rauschecker, J.P.**, and Pekar, J.J. Magnetic Resonance Imaging of Stimulus-Motion-Induced Activation in Cat Visual Cortex. *Proc. Int. Soc. mag. Res. Med.*, 514, 1998.

Fritz,J. Tian, B., and **Rauschecker, J.P.** Optical Imaging of Functional Maps in Cat Auditory Cortex. *Soc. Neurosci.* Abstr. 24 (in press).

Tian, B., Kim, D.-S. and **Rauschecker, J.P.** Optical Imaging of Functional Maps in Cat Auditory Cortex. *Soc. Neurosci.* Abstr. 24. (in press).

Wessinger, C.M., Van Lare, J.E., Tian, B., VanMeter, J.W., Pekar, J., **Rauschecker, J.P.** Activation Within Human Auditory Cortex Correlated With Stimulus Complexity. *Soc. Neurosci.*Abstr. 24. (in press).

Bushara, K.O., Weeks, R., Ishii, K., Catalan, M., Cohen, L.G., **Rauschecker, J.P.** and Hallett, M. Modality-Specific Frontal and Parietal Areas for Auditory and Visual Space Perception in Humans. *Soc. Neurosci.* Abstr. 24 (in press).

SHERIDAN SWOPE, Ph.D.

PUBLICATIONS

Swope, S.L., Moss, S.J., Raymond, L.A. and Huganir, R.L. Regulation of Ligandgated Ion Channels by Protein Phosphorylation. In:: Advances in Second Messengers and Phosphoproteins, (D. Armstrong and S. Rossie, eds.). (in press).

Mohamed, A. and **Swope, S.L.** Phosphorylation and Cytoskeletal Translocation of the Acetylcholine Receptor by Src Kinasses; Dependence on Rapsyn. *J. Biol. Chem.* (submitted).

Mou, T. , Fung, E., and **Swope, S.L.** Identification of the Dynein Molecular Motor Component Tctex of *Torpedo* Electric Organ as a Putative Fyn Substrate. (In prep. for Febs Lett., 1998).

Mohamed, A. and **Swope, S.L.** Phosphorylation and Cytoskeletal Translocation of the Acetylcholine Receptor by Src Kinases; Dependence on Rapsyn. *Abstract, 28th Annual Meeting, Society for Neuroscience* (in press).

Mou, T., Fung, E., and **Swope, S.L.** Identification of a *Torpedo* Electric Organ Component that Interacts with the Fyn Protein Tyrosine Kinase. *Abstract, 27th Annual Meeting, Society for Neuroscience,* No. 277.11, p.701, 1997.

MICHAEL ULLMAN, Ph.D.

PUBLICATIONS

Ullman, M.T. Acceptability Ratings of Regular and Irregular Past Tense Forms: Evidence for a Dual-System Model of Language from Word Frequency and Phonological Similarity Effects. *Language and Cognitive Processes* (in press).

Ullman, M.T., Love, T., Swinney, D. and Hickok, G. A Double Dissociation Between Anterior and Posterior Aphasia: Words Linked to Left Posterior Regions, Rules to Left Frontal Regions. *Brain and Language* (in press).

Ullman, M.T. Evidence that Lexical Memory is Part of the Temporal Lobe Declarative Memory, and tha Grammatical Rules are Processed by the Frontal/Basal-Ganglia Procedural System. *Brain and Language.* (in press).

Ullman, M.T. and Gopnik, M. Inflectional Morphology in a Family with Inherited Specific Language Impairment. *Applied Psycholinguistics.* (in press).

van der Lely, H. and **Ullman, M.T.** Past Tense Morphology in Specifically Language Impaired and Normally Developing Children. *Language and Cognitive Processes* . (submitted).

Abstracts

Ullman, M.T., Yee, E. and Schmahmann, J. Cerebellar Atrophy Leads to a Dissociation Within Language. *Proceedings of the 5th Annual Meeting of the Cognitive Neuroscience Society*, 1998.

Love, T., Hickok, G., Swinney, D. and **Ullman, M.T.** A Double Dissociation Within Language: Evidence from Aphasia. *Proceedings of the 5th Annual Meeting of the Cognitive Neuroscience Society*, 1998.

Newman, A., **Ullman, M.T.** and Neville, H. An ERP Study of English Regular and Irregular Past Tense. *Proceedings of the 5th Annual Meeting of the Cognitive Neuroscience Society*, 1998.

Cappa, S. and **Ullman, M.T.** The Processing of Italian Regular and Irregular Verbal Morphology in Patients with Probable Alzheimer's Disease. *Proceedings of the 5th Annual Meeting of the Cognitive Neuroscience Society*, 1998.

Bergida, R., O'Craven, K. and **Ullman, M.T.** Distinct fMRI Activation Patterns for Regular and Irregular Forms in Frontal and Temporal Lobe Regions. *Proceedings of the 5th Annual Meeting of the Cognitive Neuroscience Society*, 1998.

Ullman, M.T. The Role of Declarative and Procedural Memory in Language. *Brain and Cognition.* Abstract presentation at TENNET, Montreal, Canada, in press.

Ullman, M.T. and Corkin, S. Lexical Memory is Part of Declarative Memory: H.M. is Worse at Irregular than Regular Past Tense and Plural Formation. 27th Annual Meeting of the Society for Neuroscience, New Orleans. *Society for Neuroscience Abstracts,* 23, 1055. Selected for press report by the *Society for Neuroscience*, 1997.

Ullman, M.T., Bergida, R. and O'Craven, K. Distinct fMRI Activation Patterns for Regular and Irregular Past Tense. 3rd Annual Conference on Functional Mapping of the Human Brain, Copenhagen. *NeuroImage*, 5(4), Academic Press, 1997.

SHAOMENG WANG, Ph.D.

PUBLICATIONS

Liu, M. and **Wang, S.** A Monte Carlo Docking Method for the Study of Enzyme-Drug Interactions. *J. Mol. Biol.*, 1998 (in review).

Wu, X.-W. and **Wang, S.** Self-Guided Molecular Dynamics Simulation for Efficient Conformational Search. *J. Physical Chemistry*, 1998 (in review).

Wu, X.-W. and **Wang, S.** A Local Free Energy-Guided Molecular Dynamics Simulation Method for Accelerated Conformational Search. *J. Chemical Physics,* 1998 (in review).

Wang, S. and Johnson, K. Discovery of Cocaine Partial Agonists Through 3D-Database Pharmacophore Searching. *Molecular Pharmacology*, 1998 (in review).

Wang, S., Lewin, N.E., Kozikowski, A.P., Milne, G.W.A. and Blumberg, P.M. Characterization of the Binding of Tumor Promoters Teleocidin and ILV to PKC Through Molecular Modeling and Site-Directed Mutagenesis Studies. *J. Med. Chem*, 1998 (in review).

Yao, Z.-J., Ye, B., Wu, S.-W., **Wang, S.**, Wu, L., Zhang, Z.-Y., Burke Jr., T.R. Structure-Based Design and Synthesis of Small Molecule Protein-Tyrosine Phosphatase 1B Inhibitors. *Bioorganic and Medicinal Chemistry*, 1998 (in press).

Qiao, L., **Wang, S.**, Lewin, N.E., Blumberg, P.M., Kozikowski, A.P. Structure-Based Design of a Novel Class, High Affinity Protein Kinase C Ligands. *J. Am. Chem. Soc.*, 1998 (in press).

Kozikowski, A.P., Steensman, D., Araldi, G.L., Tuckmantel, W., **Wang, S.**, Pshenichkin, S., Surina, E. and Wroblewski, J. Synthesis and Biology of the Conformationally Restricted ACPD Analogue, 2-Aminobicyclo[2.1.1]hexane-2,5-Dicarboxylic Acid-I (ABHxD-I); a potent mGluR agonist. *J.Med. Chem.*, 1998 (in press).

Zhao, H., Neamati, N., **Wang, S.**, Nicklaus, M., Mazumder, A., Pommier, Y., Burke, T.R., Zhao, H., Milne, G.W.A. Discovery of Human Immunodeficiency Virus Type I Integrase Inhibitors by Pharmacophore Searching. *J.Med.Chem.*, 40, 930-936, 1997.

Zhao, H., Neamati, N., Hong, H., **Wang, S.**, Milne, G.W.A., Pommier, Y., Burke Jr., T.R. Hydrazide-Containing Inhibitors of HIV-1 Integrase. *J.Med. Chem.*,40,937-941, 1997.

Neanati, N., Hong, H., Mazumder, A., **Wang, S.**, Sunder, S., Milne, G.W.A., Proksa, B., Pommier, Y. Depsides and Depsidones as Inhibitors of HIV-1 Integrase: Discovery of Novel Inhibitors Through 3D Database Searching. *J. Med. Chem.*, 40,942-951, 1997.

Kozikowski, A.P., **Wang, S.**, Ma, D., Yao, J., Ahmad, S., Glazer, R.I., Bogi,K., Acs. P., Modares, S., Lewin, N.E., and Blumber, P.M. Modeling, Chemistry and Biology of the Benzolactam Analogues of ILV. *J.Med.Chem.*, 40, 1316-1326, 1997.

Yang, D. and **Wang, S.** Small Molecules Targeted at the Growth Factor Receptors as Potential Therapeutics for the Treatment of Breast Cancer. *Current Pharmaceutical Design.*, 3,335-354, 1997.

Yan, X., Day, P., Hollis, T., Monzingo, A.F., Schelp, E., Robertus, J.D., Milne, G.W.A. and **Wang, S.** Recognition and Interactions of Small Rings with a Ricin A Chain Binding Site. *Proteins: Structure, Function and Genetics*, 31,33-41, 1997.

Milne, G.W.A., Nicklaus, M.C.and **Wang, S.** Pharmacophores in Drug Design and Discovery. *Data Management in Computer-Aided Drug Design*, 1997 (in press).

Oligino, L., Sastry, L., Lung, T., Bigelow, J., Cao, T., Burke, T., **Wang, S.**, Kragg, D., Roller, P., and King, C.R. Identification of a Non-Phosphorylated Small Peptide Ligand of the Grb2 SH2 Domain. *J. Biol. Chem.*, 272, 29046, 1997.

Tuckmantel, W., Kozikowski, A.P., **Wang, S.**, Pshenichkin, S. and Wroblewski, J.T. Synthesis, Molecular Modeling, and Biology of the 1-Benzyl Derivatives of APDC--An Apparent mGluR6 Selective Ligand. *Bioorg.Med. Chem. Let.*, 7,601-606, 1997.

Yao, Z.-J., Ye, B., Zhao, h., Yan, X., Wu, L., Barford, D., **Wang, S.**, Zhang, Z.-Y. and Burke Jr., T.R. Structure-Based Design of Small Molecule Protein-Tyrosine Phosphoatase Inhibitors. *Proc.15th Amer. Peptide Symposium* (Tam, J.P. and Kaumaya, P.T.P., eds.), ESCOM/Kluwer Acad. Publishers, Dordecht, The Netherlands, 1997.

Lung, F.-D.T., Sastry, L., **Wang, S.**, Lou, B.-S., Barchi, J.J., King. C.R. and Roller, P.P. Novel Non-Phosphorylated Peptides Binding to the Grb2 SH2 Domain. *Proc. 15th Amer. Peptide Symposium* (Tam, J.P. and Kaumaya, P.T.P., eds.), ESCOM/Kluwer Acad. Publishers, Dordecht, The Netherlands, 1997.

Saxena, A., Kozikowski, A.P., **Wang, S.**, Campiani, G., Qingjie, D. and Doctor, B.P. Characterization of C-10 Substituted Analogues of Huperzine A as Inhibitors of Cholinesterases. *Proc. The 4th International Conference: Progress in Alzheimer's Diseases*, 1997 (in press).

JIAN-YOUNG WU, Ph.D.

PUBLICATIONS

Tsau, Y., Guan, L. and **Wu, J.-Y.** Initiation of Spontaneous Epileptiform Activity in the Neocortical Slice. *J. Neurophysiology*. (in press).

Review Articles and Book Chapters

Wu, J.Y.,Lam, Y.m, Falk, C.X., Cohen, L.B., Fang, J., Loew, L., Prechtl, J., Kleinfield, D. and Tsau, Y. Voltage-Sensitive Dyes for Monitoring Multineuronal Actitivity in the Intact Central Nervous System. *Histochemical J.* 30:169-187 (invited review).

Wu, J.Y., Cohen, L.B. and Falk, C.X. Fast Multisite Optical Measurement of Membrane Potential: With Two Examples. In:: Fluorescent and Luminescent Probes for Biological Activity (W.T. Mason, ed.), Academic Press, 1998 (in press).

Wu, J.Y., Cohen, L.B., Tsau, Y., Zochowski, M. and Falk, C.X. Imaging with Voltage Sensitive Dyes: Spike Signals, Population Signals, and Retrograde Transport. In: Imaging Living Cells (R. Yuste, F. Lanni and A. Konnerth, eds.). Cold Spring Harbor Press, 1998 (in press).

Abstracts

Guan, L., Tsau, Y. and **Wu, J.-Y.** Formation of Epileptic Focus is Suppressed by the Activities from Other Initiation Sites. Abstracts, *Soc. for Neuroscience*, 23:2152, 1997.

Tsau, Y., Guan, L. and **Wu, J.-Y.** Initiation and Propagation of Epileptiform Activity in Neocortical Slices. Abstracts, *Soc. for Neuroscience*, 23:2152, 1997.

Wu, J.-Y., Guan, L. and Tsau, Y. Optical Imaging of Dynamic Neuron Ensembles in Neocortical Slices. Abstracts, *Soc. for Neuroscience*, 23:2097, 1997.

Hahm, J.-O., Tsau, Y., New, K.C., **Wu, J.-Y.**, Martuza, R.L. and Rabkin, S.D. Gene Gransfer in Human and Rat Cortical Slices Using Defective Herpes Simplex Virus (HSV) Vectors. Abstracts, *Soc. for Neuroscience*, 1998 (in press).

Tsau, Y., Guan, L. and **Wu, J.-Y.** Initiation of Spontaneous Epileptiform Events in Neocortical Slices: Dominant Focus. Abstracts, *Soc. for Neuroscience*, 1998 (in press).

Pazdalski, P.S., Tsau, Y. and **Wu, J.-Y.** Light Scattering in Cortical Tissue as an Indicator of Normal and Epileptiform Activity: An In Vitro Study. Abstracts, *Soc. for Neuroscience,* 1998 (in press).

Wu, J.-Y., Tsau, Y. and Guan, L. Spontaneous Initiation of Epileptiform Events in Neocortical Slices. Abstracts, *American Epilepsy Soc.* , 1998 (in press).